Aromatic transformations facilitated by 6–ruthenium complexes

JACK ANDREW PIKE

Aromatic transformations facilitated by η^6–ruthenium complexes

Jack Andrew Pike

A thesis submitted for the degree of Doctor of Philosophy

Department of Chemistry

December 2018

Abstract

The chemistry of η^6-arene metal complexes has been explored for over 60 years and the ability to activate arenes through this complexation has been used extensively in organic synthesis. As a result of binding to the metal, the complexed arene becomes more susceptible to nucleophilic attack and deprotonation of the aromatic and benzylic protons is made more facile. Additionally, binding a metal centre to one face of the arene subsequently has a steric effect on the reactivity, wherein the bound face is blocked from reagents and directs attack to the free face. Over the last 15 years, this area of organometallic chemistry has seen a resurgence of interest due to the catalytic capabilities of these complexes. Through an arene exchange mechanism, arenes can participate in reactions when bound to the metal catalyst, and can then exchange for another equivalent of starting material to facilitate catalytic turnover. This thesis will describe a number of projects that have been developed over three years that uses this methodology to perform transformations which are of significant interest to the scientific community.

Firstly, a trifluoromethylation protocol is described, which uses a $[RuCp]^+$ binding unit to activate a range of electron-deficient arenes towards the nucleophilic attack of commercially available Me_3SiCF_3 (Ruppert's Reagent). A library of complexes exhibit reaction, and a mixture of products are formed *via* S_NAr and *ortho*-addition mechanisms. Following trifluoromethylation, the unbound arenes can be collected in quantitative yield using photolysis and chemical oxidation.

Secondly, a C–H activation and arylation protocol is described, where the same $[RuCp]^+$ binding unit is used to enhance aromatic acidity of a η^6-arene complexes. Through a concerted metalation deprotonation mechanism, a library of complexes can be activated by silver, and consequentially arylated using catalytic palladium chemistry. Following arylation, the bi-aryl arene can be liberated from ruthenium by UV irradiation.

The largest chapter of this thesis describes the catalytic radical hydrodeiodination of aryl iodides *via* an arene exchange mechanism. This reaction uses commercially available materials to achieve deiodination for iodoarenes in high yields and with excellent functional group tolerance and chemoselectivity.

Lastly, the early findings towards tether assisted arene exchange is described. The rates of arene exchange are studied for a library of tethered Cp ruthenium complexes, which show potential for enhanced arene exchange in catalytic reactions.

Declaration

The work described in this thesis was undertaken at the Department of Chemistry, Durham University between October 2014 and June 2018. All of the work reported is my own, except where specifically stated otherwise. No part has previously been submitted for a degree at this or any other university.

Statement of Copyright

Acknowledgements

Mum and Dad,
I cannot begin to explain how grateful I am for everything you have both done for me.
The years you went without so Tom, Hettie and I could succeed have
carved in me values that have made me the man I am today.
You taught me humility, courage, patience and kindness.
All I ever wanted was to make you proud, so this thesis is dedicated to you.

I also want to thank all members of my family for their love and support over the years, in particular to my Grandmothers (Nan Sheep, Nan Video and Nan Pip) for teaching me that there is no substitute for hard work.

I want to thank the friends I have made through Ustinov College, in particular Yan and Jasmine, who have kept me on track through good and bad times.
I would also like to thank friends I made in the department of chemistry, including Andrew, Phil, Akkharadet, Brette and Luke.

Thanks also to members, past and present, of Ustinov College Spin Doctors for an incredible release of stress and competitive energy.

Thank you to Dr Aileen Congreve, Dr Alan Kenwright, Dr Juan Aguilar Malavia, Dr Jackie Mosely, Mr Peter Stokes, Dr David Parker, Dr Emily Unsworth, and Dr Dmitry Yufit for your advice and expertise in analysis.

Thanks go to Dr Luke Wilkinson, Archie McNeillis, Niall O'Driscoll and William Helme to their contributions to the Walton group.

Thank you to the Department of Chemistry, Durham, for funding and opportunities.

Special thanks to Dr James Walton for your guidance and support, and for taking a shot on me. I still remember the first time I walked into your office in the summer of 2015, and I hope you are as proud of our achievements as I am.

And lastly, thank you to Jess.
You showed me what love is and I could not have done this without you.

Abbreviations

Ac	acetate
Ad	adamantyl
Bu	butyl
$CDCl_3$	deuterated chloroform
CD_3OD	deuterated methanol
$CHCl_3$	chloroform
CMD	concerted metalation deprotonation
COD	cyclooctadiene
COSY	correlation spectroscopy
Cp	cyclopentadiene
Cp*	pentamethylcyclopentadiene
d	doublet
DBU	1,8-diazabicyclo[5.4.0]undec-7-ene
DBN	1,5-diazabicyclo[4.3.0]non-5-ene
DCM	dichloromethane
DCE	dichloroethane
dd	doublet of doublets
ddd	doublet of doublets of doublets
DDQ	2,3-dichloro-5,6-dicyano-1,4-benzoquinone
ddt	doublet of doublets of triplets
DMAP	dimethylaminopyridine
DMI	1,3-dimethyl-2-imidazolidinone
DMF	dimethylformamide
DFT	density functional theory

DPPP	1,3-bis(diphenylphosphino)propane
dq	doublet of quartets
dt	doublet of triplets
EDG	electron donating group
ESI	electrospray ionisation
Equiv	equivalent
Et	ethyl
EWG	electron withdrawing group
FG	functional group
High Res	high resolution
HOMO	highest occupied molecular orbital
HPLC	high performance liquid chromatography
In situ	in the original place
LUMO	lowest unoccupied molecular orbital
m	multiplet
m	meta
Mass Spec	mass spectrometry
Me	methyl
MW	microwave
NMR	nuclear magnetic resonance
NOESY	nuclear Overhauser effect spectroscopy
o	ortho
p	para
PET	positron emission tomography
Ph	phenyl

Pr	propyl
q	quartet
qdd	quartet of doublets of doublets
s	singlet
sept.	septet
SET	single electron transfer
S_NAr	nucleophilic aromatic substitution
t	triplet
TBAF	tributylammonium fluoride
TEMPO	2,2,6,6-tetramethyl-1-piperidinyloxy
Tf	triflate
TIPS	triisopropylsilyl ether
tt	triplet of triplets
td	triplet of doublets
tdd	triplet of doublet of doublets
TFA	trifluoroacetic acid
THF	tetrahydrofuran
TMS	trimethylsilane
UV	ultraviolet
δ	delta
η	eta
π	pi
σ	sigma

Contents

1. Introduction

1.1 The Chemistry of Benzene

The transformation and manipulation of aromatic moieties is ubiquitous in chemistry. For hundreds of years, benzene and other aromatic compounds have been extensively studied and their properties and reactivity are of paramount importance in life and nature. The relevance of aromatic chemistry cannot be underestimated; the four compounds shown in Figure 1.1 are among the highest sold pharmaceutical compounds of 2016 and 2017, and each contain a substituted benzene functionality.

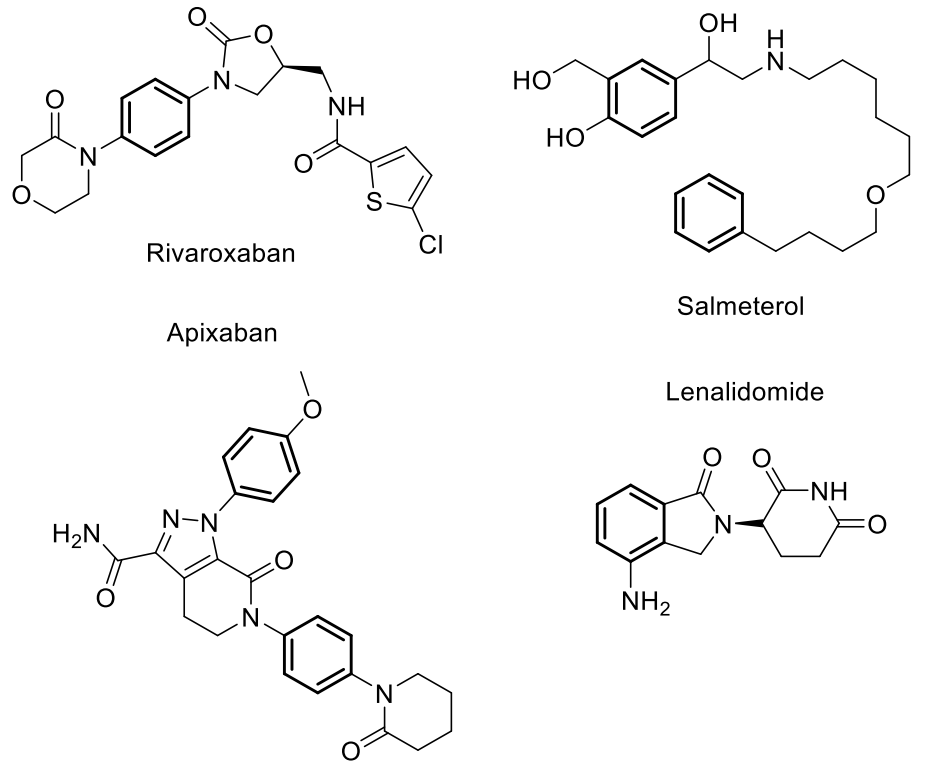

Figure 1.1 *Chemical structure of rivaroxaban (anticoagulant), salmeterol (treatment for asthma), apixaban (anticoagulant) and lenalidomide (treatment of blood cell cancer).*

A common method of transforming the groups around benzene is nucleophilic aromatic substitution (S_NAr). This proceeds by loss of a leaving group from the ring *via* the attack of a nucleophile. The benzene ring is not inherently electrophilic due to the delocalised ring of π electrons and the negative cloud above and below the ring which repels the incoming attack of nucleophiles. Secondly, the bond between the ring and the leaving group must be sufficiently polarised to direct the attack of the nucleophile. To promote the substitution reaction, it is known that an electron withdraw moiety can be incorporated into the structure to increase the polarity of the ring and also stabilise charged

intermediates that exist during the process. Figure 1.2 shows how an electron withdrawing group (EWG) can stabilise the Meisenheimer intermediate formed following attack of a nucleophile.

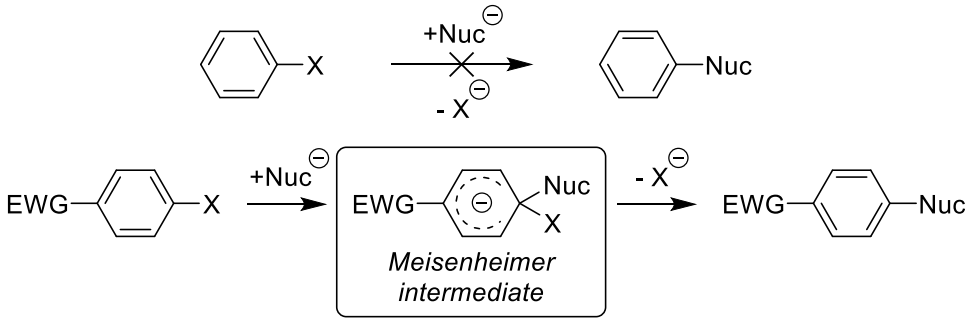

Figure 1.2 *The mechanism of nucleophilic aromatic substitution, facilitated by an electron withdrawing group.*

Although a covalently bound electron withdrawing group will facilitate the above reaction, it may not necessarily be desired in the final structure of the product compound. For example, the nitro group is an excellent functional group for facilitating S_NAr, however reduction of the nitro group to an amine and subsequent removal of the amine add additional steps to the synthetic route. A functionality which allows for ring manipulation that can be selectively bound and removed is attractive synthetically. π-Complexes of metals meet these conditions and have become popular in organic synthesis.

1.2 Properties of Metal-Arene Complexes

It has been known for decades that benzenoid aromatics can form π-complexes with a number of transition metals. Although the very first η^6-arene complex was prepared in 1919, their structure or properties were not fully understood until much later. It was only in 1955 that E. O. Fisher prepared the "sandwich" complex bis(benzene)chromium, $(C_6H_6)_2Cr$.[1] Complexes of this type have received extensive interest regarding their ability to facilitate transformations of the bound arene.

With π-complexation of the arene comes a significant alteration of the physical and chemical properties. The transition metal has a net electron-withdrawing effect on the delocalized π system of the aromatic ring, similar to the covalently bound groups discussed above, and affects its reactivity in a number of ways. The complexed arene becomes more susceptible to nucleophilic substitution reactions, and for the same reasons, is deactivated towards electrophilic substitution. Due to the electron withdrawing

nature of the metal centre, the electron deficient arene is also able to stabilise a negative charge more easily. As a result, deprotonation of the aromatic and benzylic protons is made more facile. Lastly, binding a metal centre to one face of the arene, subsequently has a steric effect on the reactivity, wherein the bound face is blocked from reagents and directs attack to the free face. This enhanced reactivity is illustrated in Figure 1.3.

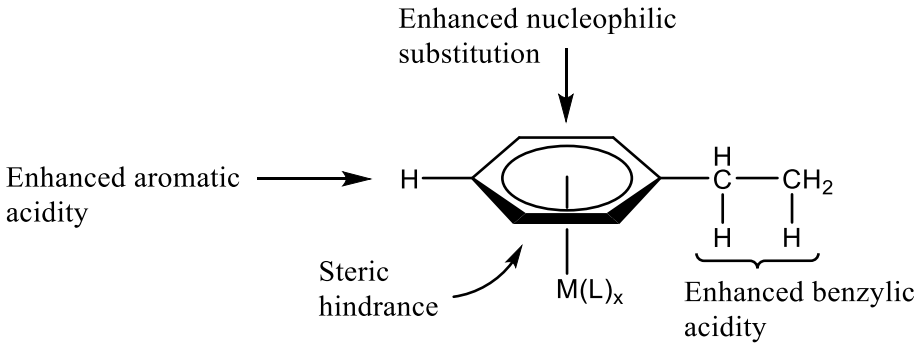

Figure 1.3 *Summation of reactivity of metal bound arenes.*

The bond between η^6 bound arenes and the metal centre is relatively strong. Figure 1.4 shows the molecular orbitals for the π system in benzene along with the metal d orbitals that form bonding interactions.

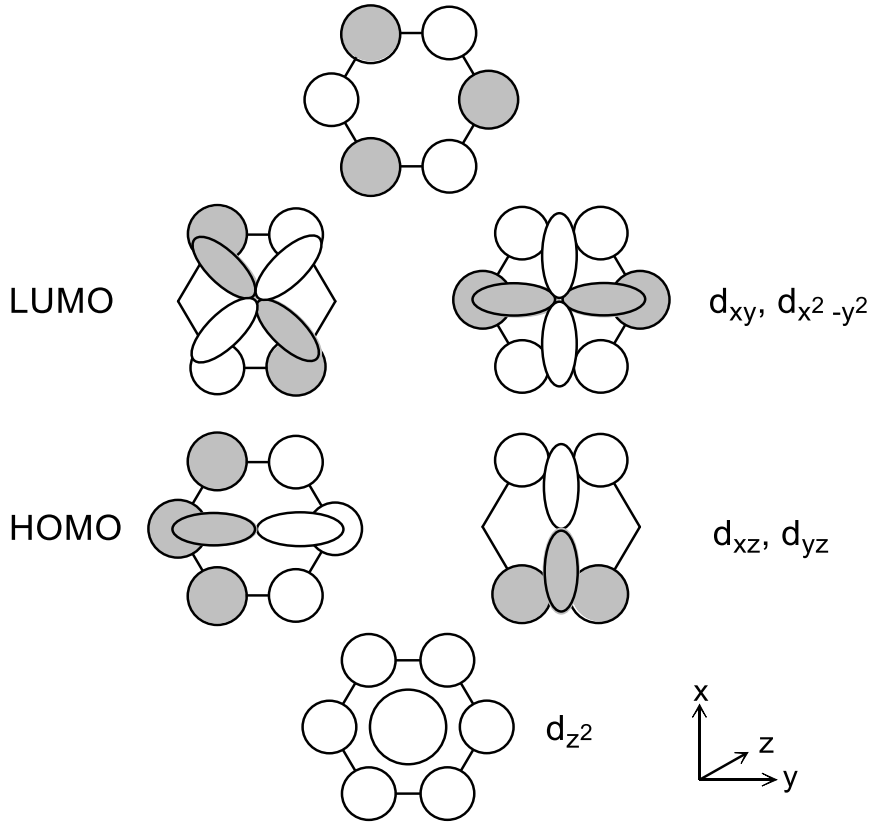

Figure 1.4 *The molecular orbitals, including HOMOs and LUMOs, of the π system in benzene with the metal d orbitals of appropriate symmetry to form bonding interactions.*

The molecular orbital of benzene with no nodes has a strong σ interaction with the d_{z2} orbital. Adjacent to this, π bonds exist between the arene HOMOs and the corresponding d orbitals (d_{xz} and d_{yz}). Finally, the antibonding π*-based LUMOs of the arene can participate in δ-backbonding interactions from the metal also. The combination of these interactions creates a strong bond between the bound arene and the metal.

1.3 Reactivity of Arene π-Complexes

The purpose of this review is to demonstrate the range of π-arene transition metal complexes synthesised and their utility in organic synthesis. To date, a number of reviews have discussed these complexes and their contribution to catalysis.[2,3] Complexes of metals from group 6–9 have been reported in the literature and the chemistry of each group will be summarised in each section herein. Although synthetic examples of η^6-arene complexes of group 10 metals exist, stoichiometric or catalytic reactions on the bound arene have not been reported, likely due to their thermal instability.[4–9] For this reason they will not be discussed.

1.3.1 Reactions Using Chromium and Molybdenum (Group 6)

A range of synthetic methodologies have been developed using tricarbonyl M(0) complexes (where M = Cr, Mo). By taking advantage of the enhanced chemical properties described above, a number of useful organic transformations can be performed on the metal bound arene. These neutral metal tricarbonyl units are by far the most utilised in organic synthesis largely due to their facile synthesis. Generally, [(η^6-arene)$M(CO)_3$] complexes are made via thermolysis of [$M(CO)_6$] with the desired arene, or *via* arene exchange from an existing arene complex.[10] The latter is often required in the case of electron deficient arenes (nitrobenzene, α,α,α-trifluorotoluene, etc.) where direct thermolysis is not possible (Figure 1.5).[11]

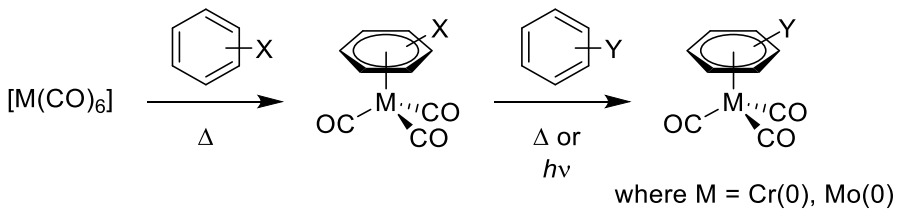

Figure 1.5 *Thermolytic synthesis of [(η^6-arene)$M(CO)_3$] and synthesis via arene exchange*

Chromium has been used extensively in the latter half of the last century to facilitate arene transformations activated by π-complexation, and a plethora of different reactions have been demonstrated exploiting the different ways that the arenes are activated. In 1980, Semmelhack *et al*. reported nucleophilic addition to styrene-derived ligands bound η^6 to $Cr(CO)_3$ (**1.1**, Figure 1.6).[12] The scope of this reaction was of interest to Semmelhack and co-workers since previous β-addition reactions to η^6-styrene complexes resulted in poor yields.

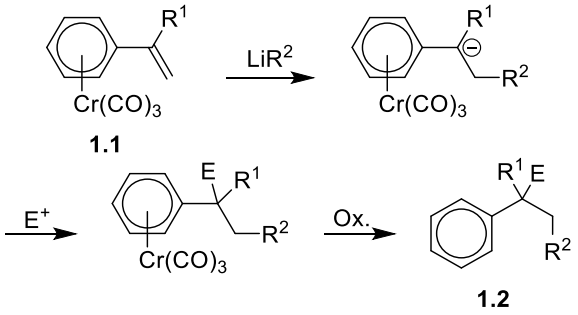

Figure 1.6 *General reaction sequence for the nucleophilic addition to styrene ligands.*

The reaction proceeds firstly with anti-Markovnikov nucleophilic attack at the styrene to give the negatively charged intermediate, which is stabilised by the electron withdrawing effect of the bound metal fragment. Addition of an electrophile followed by oxidation to remove the metal gave the respective racemic substituted phenyl alkane **1.2**. The conversion achieved moderate to high yields with a variety of ligands, lithiated alkyl nucleophiles and trapping electrophiles, demonstrating a facile and interesting method to form two new C–C bonds.

Substitution of aryl halides is commonplace for a number of organic processes, and in 1983 Houghton *et al*. reported the rapid intramolecular nucleophilic substitution of fluoro-arenes when bound to chromium to prepare the heterocycle chroman.[13] By simply treating the arene-bound complex **1.3** with base, the deprotonated primary alcohol attacks the ring to form the metal bound heterocycle **1.4**, which, when oxidised with iodine, gives the free arene **1.5** in a 75% yield (Figure 1.7).

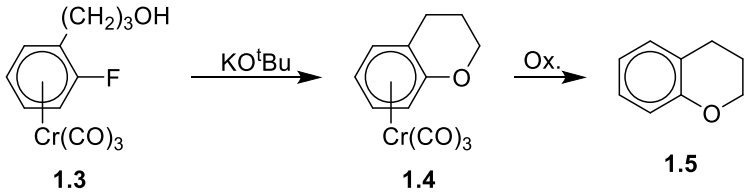

Figure 1.7 *Reaction pathway for the preparation of chroman, modified from Houghton et al.*[13]

A further development in the reactivity of these chromium tricarbonyl aryl halide complexes is the use of additional metals to facilitate bimetallic catalysis. In 1999, Bräse reported intramolecular cyclisation of allyl ether chloroarenes using both chromium and palladium.[14] The electron withdrawing nature of the metal tricarbonyl fragment is utilised to promote the Heck reaction catalysed by palladium to cyclise allyl ethers intramolecularly (Figure 1.8). Following the formation of the (η^6-arene)chromium complex **1.6**, the bound arene was subjected to catalytic palladium conditions for the intramolecular Heck coupling reaction to give heterocycle **1.7**.

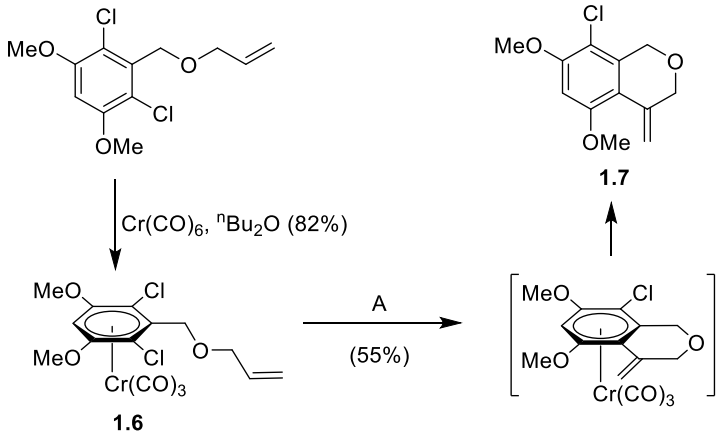

Figure 1.8 *Reaction pathway for bimetallic Heck cyclisation reported by Bräse.*[14] *(A) $Pd(OAc)_2$ (5 mol%), PPh_3 (10 mol%), NEt_3, DMF, 80°C, 24 h.*

A more recent example of a bimetallic system comes from Larrosa and co-workers, whereby a palladium cross coupling reaction via C–H activation is promoted by the fluoroarene substrate being bound η^6 to tricarbonyl chromium.[15] Excellent yields were achieved for the palladium catalysed direct arylation of a number of fluoroarene complexes (**1.8**) and iodoarenes (Figure 1.9). The $Cr(CO)_3$ fragment is used to increase the acidity of the aryl protons and facilitate the reaction.

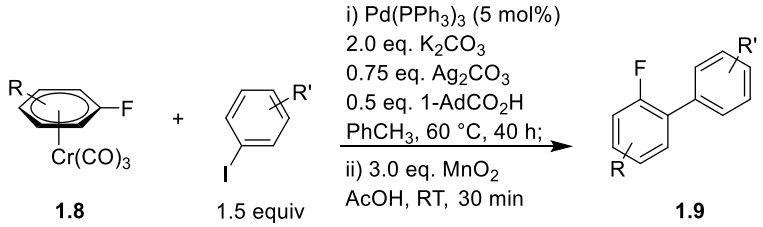

Figure 1.9 *Reaction pathway of C–H activation and reductive coupling of chromium bound fluorobenzenes and aryl iodides, modified from Larrosa et al.*[15]

An arene transformation not yet mentioned in this review is dehalogenation, which is an important pathway for the disposal of environmentally damaging polyhalo-aromatic hydrocarbons. In the 1980s, Heppert *et al.* reported a $Cr(CO)_3$-mediated reductive

dehalogenation of a number of aryl halides.[16] Discovered through serendipity, the group was attempting the S_NAr of Cr-bound aryl chlorides, **1.10**, using a nucleophilic FeCp carbonyl species (Figure 1.10). Substitution was observed (**1.11**), but the additional reductive dehalogenation pathway to complex **1.12** was observed also and further probed. They found that more electron deficient arenes preferred dehalogenation over substitution, and that I >> Cl > F was favoured.[17] It was from these trends that the authors concluded the transformation likely occurred *via* a SET (single electron transfer) mechanism and the hydrogen extracted following loss of the halogen is provided by the reaction solvent.

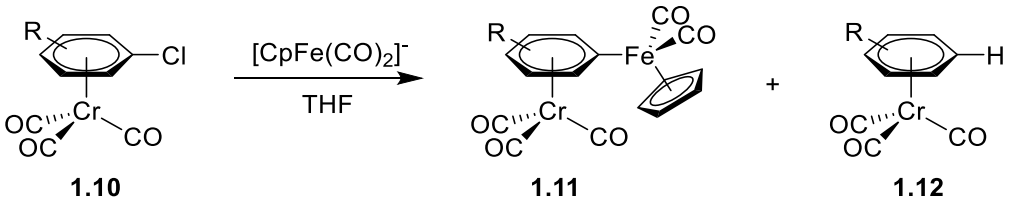

1.10 **1.11** **1.12**

Figure 1.10 *$[Cr(CO)_3]$ mediated dehalogenation using $[FeCp(CO)_2]^-$ as a nucleophilic complex*

In the case of molybdenum, the direct complexation of arenes from $Mo(CO)_6$ is more difficult and more limited than chromium. Achieving higher yields is inhibited by the requirement of long reaction times at high temperatures and the much higher sensitivity to oxygen. Despite the Mo-arene bonding being stronger than the Cr-arene bond,[18,19] the arene is much more labile when bound to molybdenum, and this ease of arene exchange has been manipulated synthetically. Even without the aid of a Lewis acid catalyst, rates of exchange in Mo-arene complexes at 60 °C are comparable to the analogous Cr complexes at 150 °C, and this property has enabled the preparation of a much greater range of complexes.[11]

It is likely that the challenging synthesis and the lability of the bound arene has hindered the development of molybdenum-based transformation strategies to the same extent as chromium. A noteworthy example however was reported by Kündig *et al.* where *trans*-addition across a double bond achieved two new carbon substituents implemented into $[(\eta^6\text{-benzene})Mo(CO)_3]$ system **1.13** (Figure 1.11).[20] Initial nucleophilic addition of lithium dithiane results in the expected formation of an anionic Meisenheimer type intermediate complex **1.14**. Electrophilic addition proceeds with the introduction of allyl and crotyl bromides, producing the η^3-allyl/η^5-cyclohexadienyl intermediate complexes **1.15**, which when allowed to react under CO atmosphere liberate the allyl cyclohexadiene product **1.16**. This reaction pathway not only shows an interesting pathway to

dearomatisation of benzene by forming two new C–C bonds, but also demonstrates the viability of using Mo-arene complexes for stereoselective aromatic transformations.

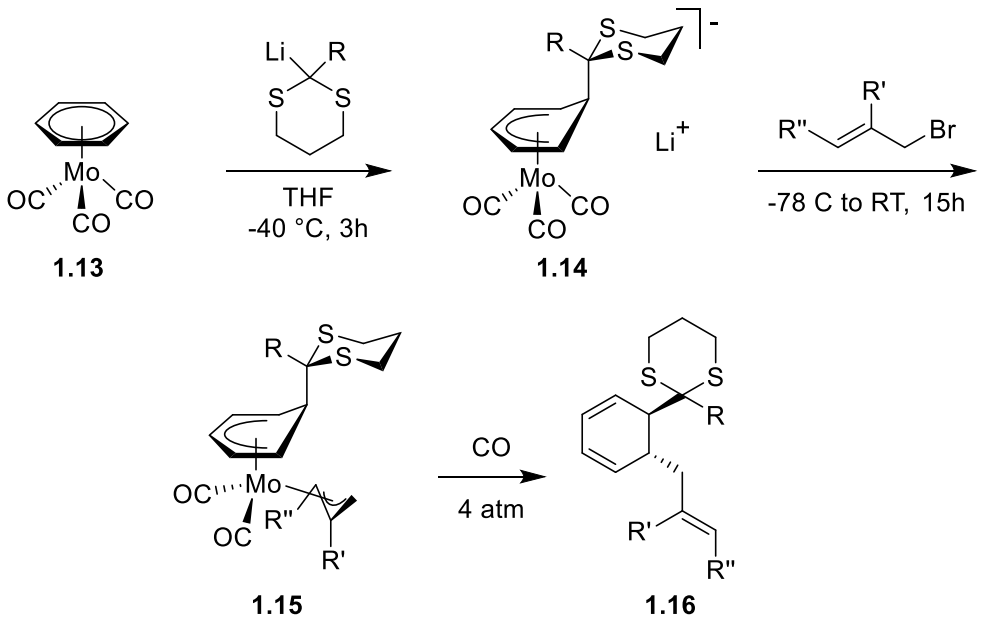

Figure 1.11 *trans-addition of two carbon substituents across a benzene double bond in [(η^6-benzene)Mo(CO)$_3$].*

1.3.2 Reactions Using Manganese, Rhenium and Technetium (Group 7)

In a similar fashion to the chromium and molybdenum examples discussed above, complexes of [(η^6-arene)Mn(CO)$_3$]$^+$ can be prepared through thermolysis of [Mn(CO)$_5$]$^+$ or by photolysis of an existing arene complex. However, in the case of manganese, strongly electron deficient arenes and aryl halides are not able to make stable complexes. Arene complexes of manganese have been utilised for nucleophilic substitution reactions on the bound ring, and the Pearson group have extensively developed synthesis of aryl ethers with amino acid side chains using cationic tricarbonyl manganese(I) bound to aryl chloride substrates (**1.18**).[21–24] These transformations were studied for the synthesis of the 14-membered cyclic peptide model of ristocetin A, a glycopeptide antibiotic (Figure 1.12) .[23,24]

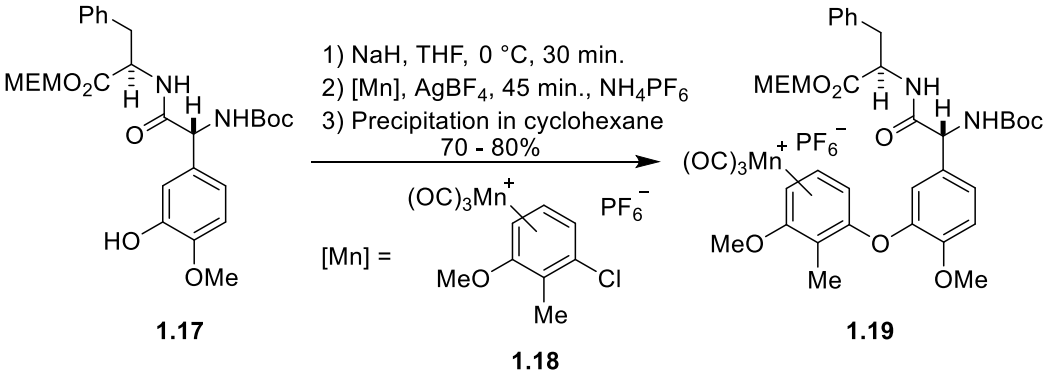

Figure 1.12 *The synthesis of aryl ether using aryl chloride manganese substrate, modified from Pearson et al.*[24]

The enhanced susceptibility for nucleophilic attack into the aromatic system does not limit the reactivity to simply substitutions. When nucleophiles attack the aromatic system, cyclohexadienyl Meisenheimer intermediate complexes can then be introduced to other reagents for further transformations. The reactivity of these intermediates has been studied in depth with a range of d^6 metal complexes.[25] An example of this kind of study with manganese was conducted in 1982 by Sweigart *et al*. where benzene tricarbonyl manganese complex **1.20** treated with an alkyl Grignard reagent allowed the isolation of the subsequent Meisenheimer intermediate complex **1.21** (Figure 1.13).[26]

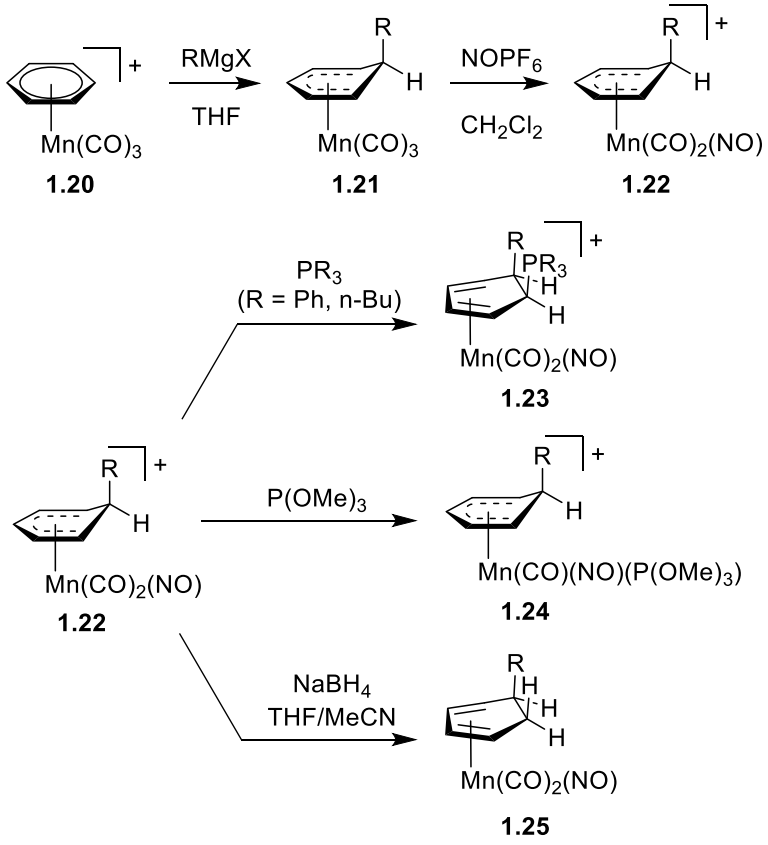

Figure 1.13 *Formation and reactivity of manganese Meisenheimer intermediate* ***1.22****.*

In order to reactivate the ring for a second nucleophilic attack, it is necessary to substitute one CO for NO^+ so as to increase the electron withdrawing effect of the metal fragment and to add charge to the complex (**1.22**). It is notable that only trace amounts of the analogous chromium complex could be synthesised.[27] The reactivated intermediate can then be transformed into a number of cyclohexadiene complexes using the appropriate reagents.

The few known examples of rhenium arene complexes exist in the form of bis-arene sandwich complexes. $[Re(\eta^6\text{-arene})_2]^+$ complexes can be prepared from perrhenate salts by reduction using Zn and $AlCl_3$ while using the arene of choice as solvent (benzene, mesitylene and naphthalene).[28] While only hydrocarbon arenes are tolerated in the reaction, the naphthalene sandwiches have a degree of lability which was exploited by Alberto *et al.* to synthesise asymmetric sandwiches $[Re(\eta^6\text{-}C_6H_6)(\eta^6\text{-}C_{10}H_8)]^+$ which can then further react with Lewis basic ligands to generate benzene bound piano stool complexes ($[(\eta^6\text{-arene})ML_3]$).[29] These benzene piano stools proved stubborn to exhibit any arene exchange behaviour, either by thermolysis or photolysis, and so their inherent stability showed promise for biological applications. Complexes of ^{99}Tc with analogous structures have been reported, but their use in synthesis and catalysis is likely limited due to their radioactivity and short half-lives.[29–31]

1.3.3 Reactions Using Iron and Ruthenium (Group 8)

Arene complexes of the group 8 metals are commonly found the in the form of $[(\eta^6\text{-arene})M(\eta^5\text{-cyclopentadienyl})]^+$ (where M = Fe, Ru,). In the case of $[FeCp]^+$ π-complexes, ferrocene is often used as a starting material, where treatment with a strong Lewis acid in the presence of the desired arene will yield the sandwich complex (Figure 1.14).[32]

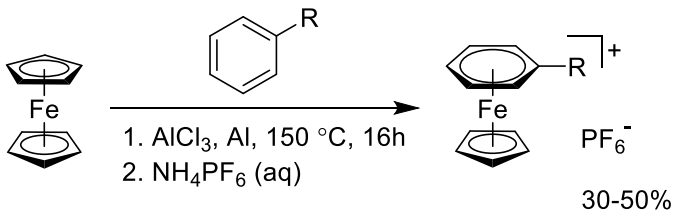

Figure 1.14 *Synthesis of $[(\eta^6\text{-arene})FeCp]PF_6$ from ferrocene*

This can be a difficult reaction, and harsh conditions are required due to ferrocenes high stability of heat. As with examples mentioned earlier, this route of direct arene

complexation will not tolerate electron deficient arenes and the use of Lewis acids can be challenging when using alkyl substituted arenes, as competing Friedel-Crafts reactions can occur. Complexes of more electron deficient arenes can be achieved through photolysis of existing π-arene complexes.

A recent report from Driess *et al.* shows an interesting solution to the inert nature of ferrocene by symmetrically functionalising the two Cp rings of the complex with coordinating bulky silyl ligands (Figure 1.15). This 1,1-bis(silylenyl)-substituted ferrocene **1.26** can then chelate to another iron(II) ion which can form π-complexes much more readily.[33]

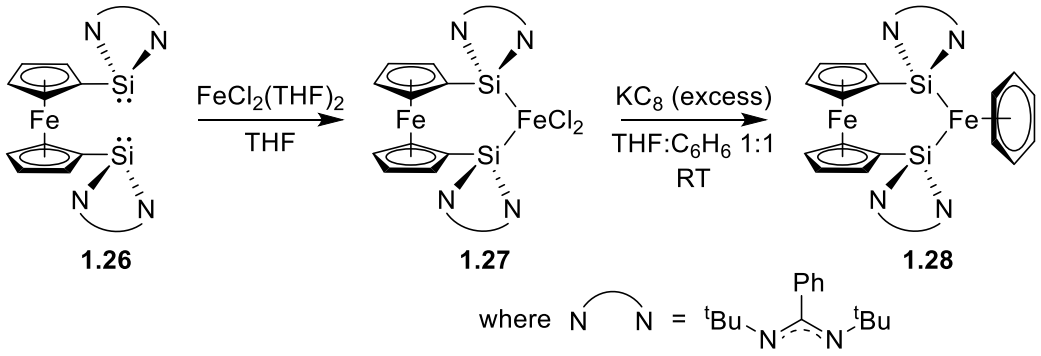

Figure 1.15 *Synthesis of an $Fe^0(\eta^6$-benzene) complex* ***1.28*** *from $FeCl_2$ and a disilenylferrocene ligand.*

Complexes of ruthenium can be made with much more synthetic ease, and commonly follow one of two routes. The simplest route is reacting commercially available piano stool complex $[RuCp(MeCN)_3]PF_6$ with the desired arene in a non-coordinating, non-aromatic solvent. This relatively mild method is often very high yielding and will tolerate electron-deficient arenes unlike the majority of direct synthetic pathways discussed so far.[34,35] The other commonly-used route is to react chloro-bridging arene-bound ruthenium dimer **1.29** in the presence of donor ligands or Cp type anions.[36–38] This reaction is carried out under mild conditions using polar solvents and is usually a high yielding route to complexes of the form $[(\eta^6$-arene$)RuL_2Cl]^{n+}$ and $[(\eta^6$-arene$)RuCp]^+$ (Figure 1.16). A small number of dimers differing in bound arene (benzene, *p*-cymene, *p*-xylene, etc.) are commercially available, but the arene can be exchanged thermolytically or photolytically following the formation of the monomeric Ru species.

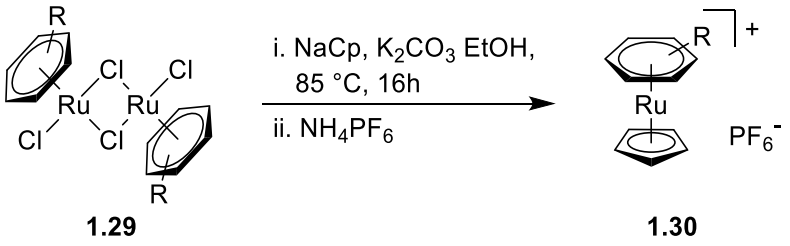

1.29 **1.30**

Figure 1.16 *Thermolytic synthesis of [(η^6-arene)RuCp]$^+$ complexes from chloro-bridging arene bound ruthenium dimers.*

Similar transformations of η^6-bound arenes to that already mentioned can be achieved with Fe(II) and Ru(II) scaffolds. In 1991, Woodgate *et al*. reported double nucleophilic aromatic substitution of 1,2-dichlorobenzenes with substituted 1,2-benzenediols to synthesise an array of dibenzo[*b,e*][1,4]dioxin derivatives (**1.32**).[39] The bischloride arene bound η^6 to a cationic [FeCp]$^+$ fragment **1.31** is activated firstly towards intermolecular nucleophilic substitution, followed rapidly by intramolecular substitution by the second alcohol to form the heterocyclic product (see Figure 1.17).

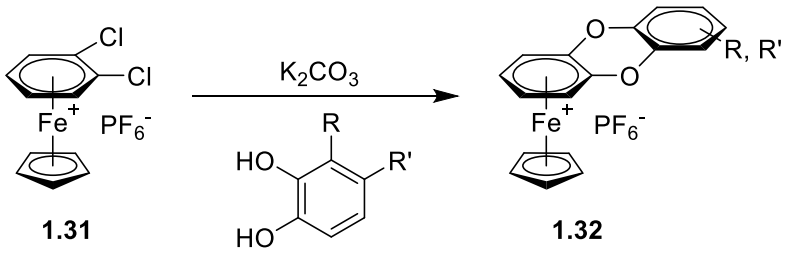

1.31 **1.32**

Figure 1.17 *Double nucleophilic aromatic substitution between η^6-1,2-dichlorobenzene and substituted 1,2-benzenediols.*

At the same time Pearson was working on the aryl manganese complexes mentioned earlier, a study was conducted on similar iron and ruthenium complexes.[22] A number of reactions were reported between [(1,3-dichlorobenzene)MCp]$^+PF_6^-$ complexes (**1.33**, M = Fe(II), Ru(II)) and sodium phenoxide nucleophiles that showed very high selectivity towards monosubstitution when one equivalent of nucleophile is used. A limitation to the arene-manganese complexes studied was only mono-chlorosubstitution was possible, but with iron and ruthenium a number of nucleophiles are able to perform sequential substitution of both chlorides when excess nucleophile is used (Figure 1.18).

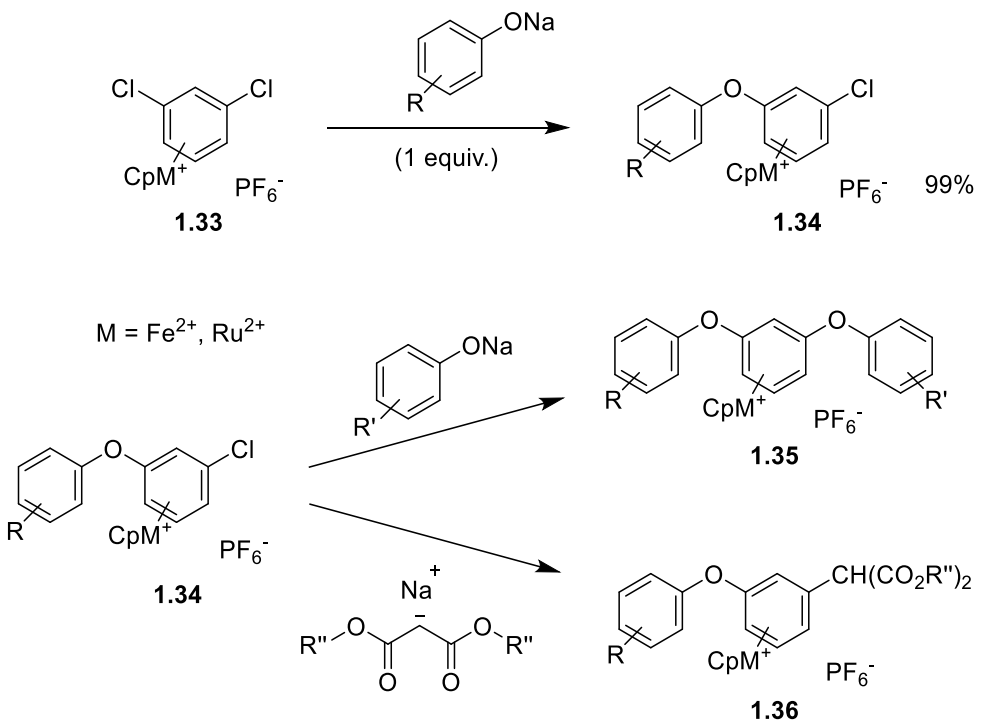

Figure 1.18 *Sequential substitution of 1,3-dichlorobenzene facilitated by iron and ruthenium Cp scaffolds.*

Recently, ruthenium π-complexes were shown to improve the compatibility of arene florination using PhenoFluor. Fluorination reactions with ^{18}F are developed for the application of positron emission tomography (PET). Due to the prevalence of fluorine in pharmaceuticals, ^{18}F is an attractive tracer for studying drug disposition and biochemical interactions in humans. ^{18}F deoxyfluorination of free arenes using PhenoFluor has been demonstrated with electron deficient substrates,[40] but the scope of this reaction has been expanded through ring activation *via* coordination of the $[RuCp]^+$ unit (Figure 1.19).[41]

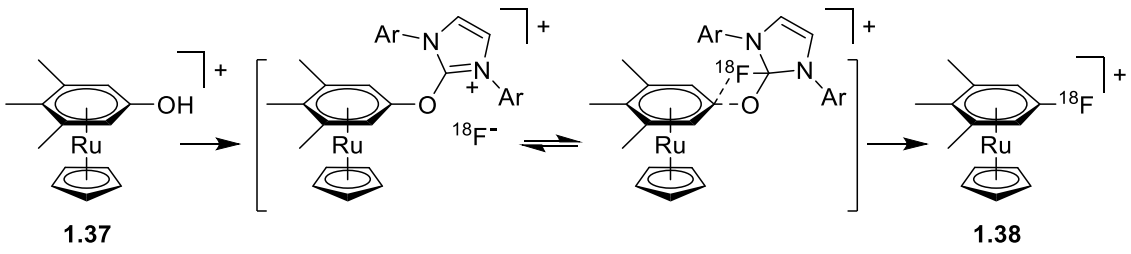

Figure 1.19 *Ruthenium mediated deoxyfluorination using PhenoFluor*

The Ru-mediated procedure reduces side products, increasing yields of fluorinated arenes and also reduces the processes air and water instability.

1.3.4 Reactions Using Cobalt, Rhodium and Iridium (Group 9)

Arene complexes of cobalt are commonly seen in one of two forms. Cobalt complex [(η^3-cyclooctenyl)Co(η^2,η^2-COD)] (**1.39**, where COD = cyclooctadiene) can be reacted using the desired arene as solvent, under a hydrogen atmosphere, to facilitate complexation (**1.40**, Figure 1.20). It is found that more electron-rich arenes tend to be higher yielding.[42]

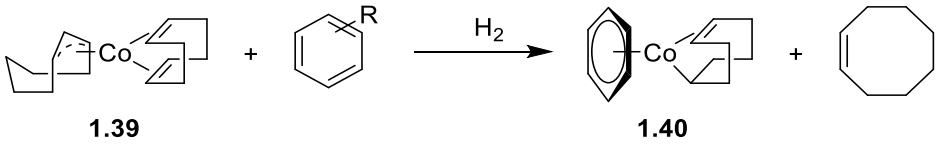

1.39 **1.40**

Figure 1.20 *Synthesis of {(η^6-arene)cobalt}$^+$complexes by hydrogenation of alkenyl ligands.*

Cobalt complexes exhibiting a tetramethylcyclobutadienyl (Cb*) moiety are also popular, as this ligand is substitutionally inert and forms the metal fragment [CoCb*] which is isolobal to [FeCp]$^+$.[43]

Rhodium and iridium share similar chemistry to one another and can form arene complexes [(η^6-arene)M(PR_3)$_2$]$^+$ by reacting the desired arene with metal dimer [(PR_3)$_2$M]$_2$(μ-X)$_2$ (where X is a halide and M is Rh, Ir) under mild conditions.[44,45] Previously discussed within the reactivity of chromium was the synthesis of chroman via intramolecular S_NAr conducted by Houghton *et al*. This synthesis was further developed by the group into a catalytic cyclisation using [(η^6-benzene)rhodium(III)(η^5-C_5EtMe_4)]$^{2+}$ **1.41** as a precatalyst.[46] The crucial part to make this reaction catalytic was the ability to interchange the bound arene between cyclised product complex **1.44** and starting substrate complex **1.43**. The free metal fragment **1.42** is stabilised by weakly coordinating ligands whilst not bound to an aromatic ring (Figure 1.21).

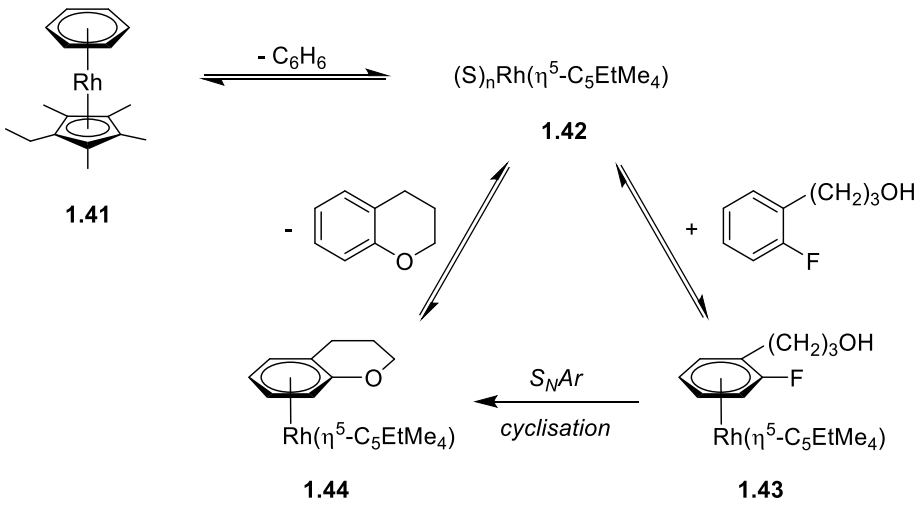

Figure 1.21 *Catalytic Catalytic cyclisation of fluoro-aryl alcohols (solvent used: 17% (v/v) solution of acetone in nitromethane). All complexes have a charge of 2+ and S = σ-bonded ligand, e.g. solvent or alcohol of substrate.*[46]

The rhodium centre also activates the aryl fluoride further such that the neutral alcohol can perform the substitution. In the previous case with chromium, additional base was required for anionic alkoxide attack. This is the first appearance in the report of a catalytic arene transformation with respect to the activating transition metal. The mechanism and role of metal fragments in catalysis will be discussed in greater detail later in this review.

A recent report from Ritter *et al.* demonstrates the use of an $[IrCp]^{2+}$ unit for the C–H activation of benzene to from phenols (Figure 1.22).[47] Addition of $NaClO_2$ converts the benzene-bound complex **1.45** directly to the η^5-phenoxo complex **1.46** in high yields under mild conditions. This intermediate is then subjected to strong acid to protonate and dissociate the arene. While not a catalytic process, the group were able to demonstrate recyclability of the transition metal by salvaging the iridium as the tris acetonitrile piano stool complex.

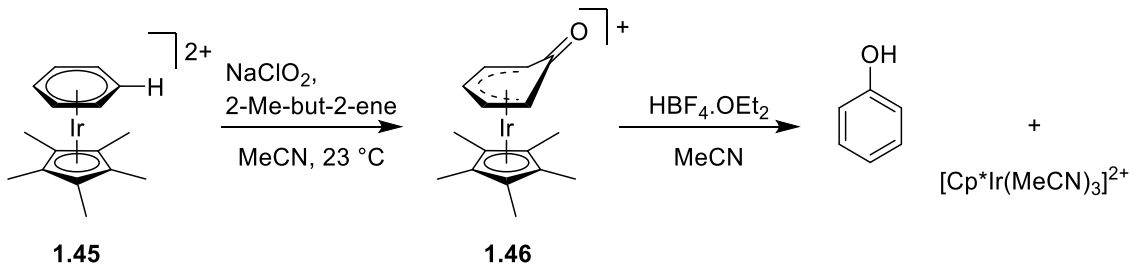

Figure 1.22 *Synthesis of phenols via C–H activation mediate by* $[IrCp]^{2+}$ *fragment.*

1.4 Arene Exchange

There is a recurring drawback for the majority of the reactions involving arenes π-complexed to metal fragments, and this is dissociation of the arene from the metal. In most cases oxidation or photolysis is used to remove a stoichiometric amount of metal from the desired product, which is not only wasteful in terms of atom economy and material cost, but also adds another synthetic step to the procedure. For these reasons, it is much sought after to find systems where the product arene and the substrate arene are free to exchange on the metal fragment and therefore create a catalytic process.

1.4.1 Arene Exchange Mechanism

Semmelhack proposed a simple catalytic cycle to describe the nucleophilic aromatic substitution reaction, where nucleophilic aromatic substitution mediated by the metal fragment is subsequently followed by arene exchange (Figure 1.23).[48]

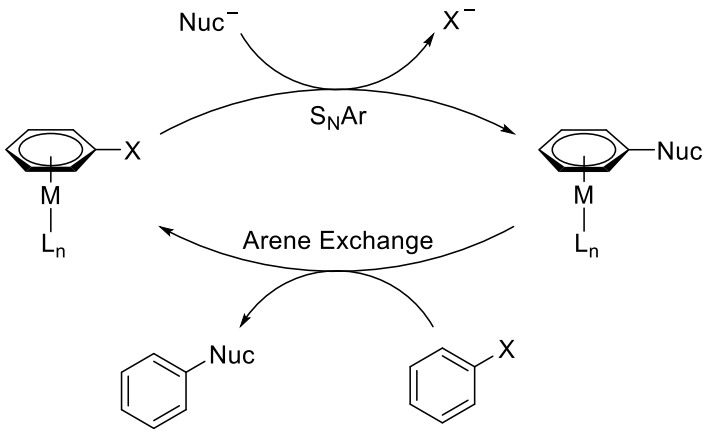

Figure 1.23 *General cycle for catalytic S_NAr of metal-bound arene complexes, modified from Semmelhack et al.*[48]

Extensive kinetic work from Traylor and co-workers during the 1980s established the stepwise "unzipping" mechanism for the exchange of η^6-arene metal complexes, which is shown in Figure 1.24.[49–51]

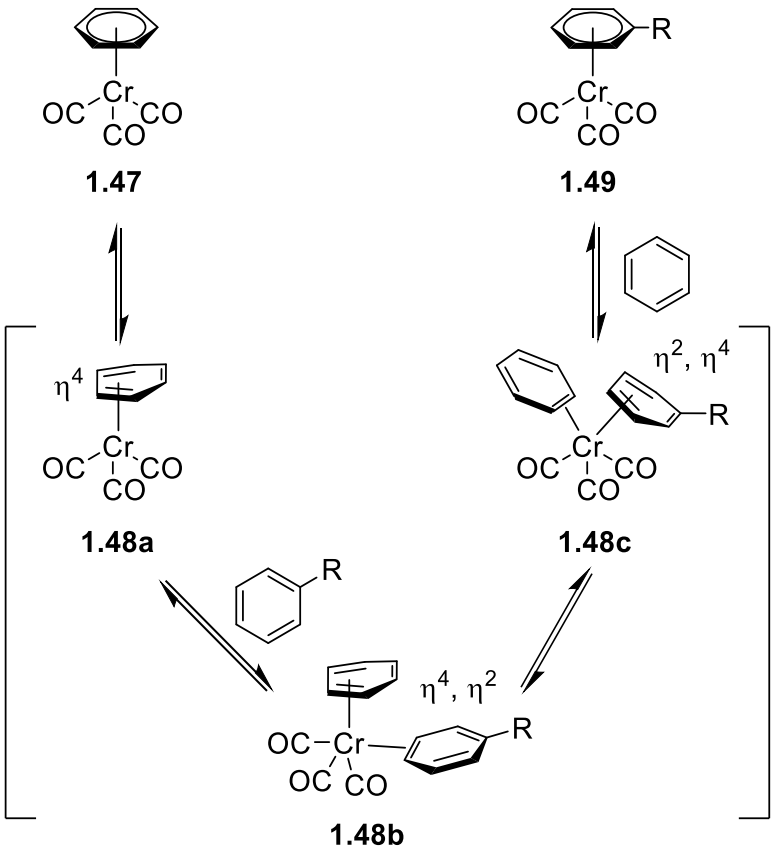

Figure 1.24 *The "unzipping" mechanism of arene exchange on a $Cr(CO)_3$ metal fragment.*[49–51]

The first step is the shift of the bound arene from η^6-complex **1.47** to η^4-complex **1.48a**, which is rate limiting. This is due to the destabilisation of the complex associated with losing electron donation, and in the Figure above, the chromium complex changes from having 18 valence electrons to 16. This intermediate with a free coordination site can now accept donation from an incoming free arene to make the η^4, η^2 intermediate **1.48b**. It has been shown that carrying out exchange reactions in coordinating solvents can stabilise the intermediate by coordinating to the metal and restoring the electron count to 18.[38,48] The following step is the binding substitution of each arene; the originally bound arene shifts from η^4 to η^2, and vice versa for the approaching arene to form intermediate **1.48c**. The final step sees the originally bound arene leave and the approaching arene bind η^6 to the metal fragment to give complex **1.49**. This process of arene exchange has been studied to afford arene transformations that are catalytic with regards to the metal fragment.[52,53]

1.4.2 Dependence on Incoming and Outgoing Arene

The rate in which arenes will exchange to and from a complex depends on a number of factors, one of which is the particular arenes participating in the exchange. In general,

arenes that are more electron rich will bind more strongly than electron deficient ones. The trend in Figure 1.25 shows the relative order of thermodynamic stabilities from highest to lowest of [(η^6-arene)$Cr(CO)_3$] complexes and the rate of exchange follows the same pattern, where electron rich arenes exchange far more slowly than electron deficient ones.[54,55]

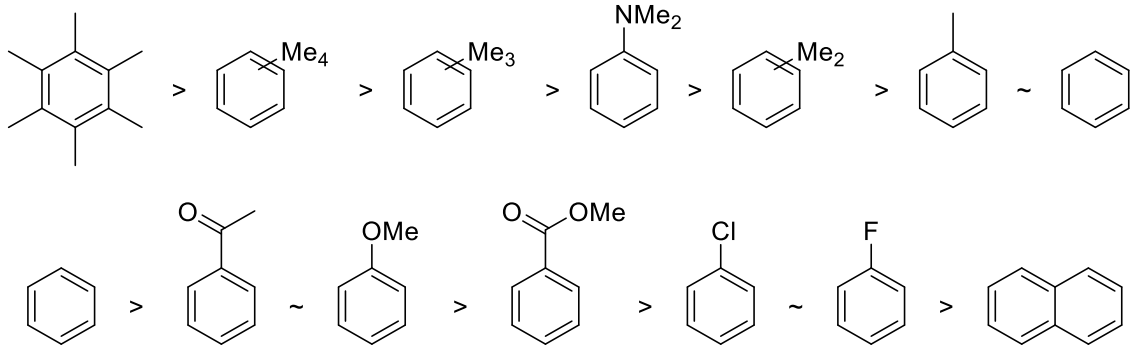

Figure 1.25 *Order of stabilities in [(η^6-arene)$Cr(CO)_3$] complexes.*

In the case of catalysed arene exchange (i.e. coordinating solvent is used, etc.), the rate becomes independent of the incoming arene.[56] However, when exchange is not catalysed, incoming arenes with a greater electron density on the ring are able to exchange faster, as they have a great binding ability to assist with the zipping/unzipping mechanism. With this in mind, the mechanism shown in Figure 1.26, with two possible pathways, is in better agreement with what is observed experimentally. In both pathways, a haptotropic shift of the outgoing arene from η^6 to η^4 is the rate determining step. However, in pathway A, a catalysing molecule (i.e. solvent) assists in the lowering of the activation barrier and increases rate of exchange, whereas in pathway B, only the incoming arene can assist in the lowering of this barrier. The coexistence of these two pathways rationalises the observed dependence on the electronic properties of the incoming arene and its effect on the rate of exchange.

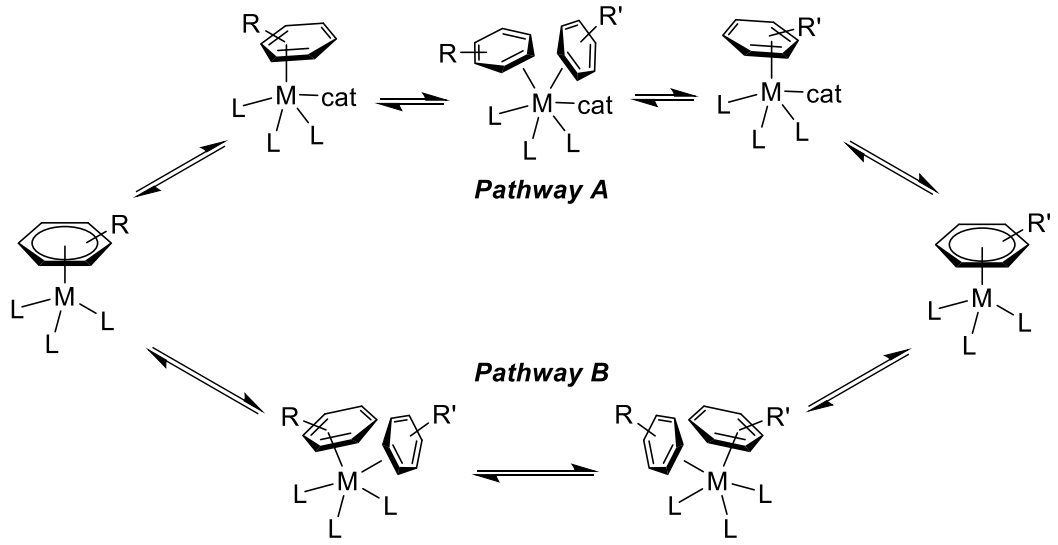

Figure 1.26 *Mechanism of arene exchange. cat = catalysing ligand (i.e. solvent etc.).*

1.4.3 Tether-Accelerated Arene Exchange

As mentioned above, the process of arene exchange can be catalysed by the use of coordinating solvent molecules to lower the barrier of the rate limiting haptotropic shift. In order to more effectively utilise the coordination of assisting ligands, a number of tethered arene-metal complexes have been developed with the hypothesis that intramolecular coordination should further decrease the energy barrier of arene exchange. The first reported example of tether-assisted arene-exchange was a chromium carbonyl complex with methylacrylate as a multidentate ligand which could change its hapticity during arene exchange (**1.50a** and **1.50b**, Figure 1.27).[57] The ability of the carbonyl group of methylacrylate to coordinate during the η^6 to η^4 transition of the outgoing arene allowed the complex to exchange at room temperature at the same rate the analogous $[Cr(CO)_3]$ complex would at 170 °C.[50]

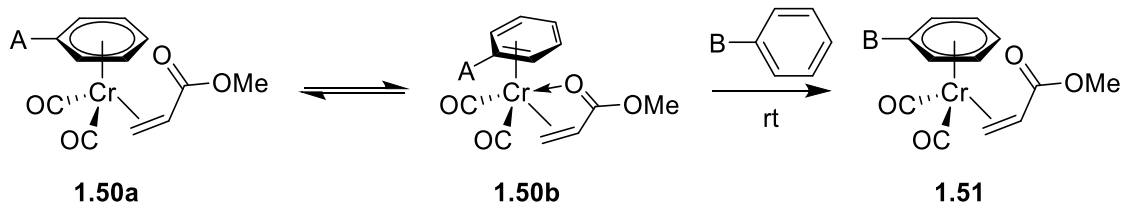

Figure 1.27 *Tethered chromium carbonyl complex with methylacrylate as a catalysing coordinating ligand.*

Semmelhack later demonstrated the use of another tethered chromium complex to assist arene exchange, and extensively studied the kinetic effect that a variety of functional groups had to the rate of exchange.[48,58] A series of functionalised tris(pyrrole)phosphine

ligands were synthesised and the degree to which they increased the rate of arene exchange in [(η^6-arene)$Cr(CO)_2L$] complexes (**1.52a**) was measured (Table 1.1). A clear correlation was observed between the donating ability of each ligand and the increase in rate of arene exchange.

Table 1.1 *Tethered chromium carbonyl complex with functionalised tris(pyrrole)phosphine as a catalysing coordinating ligand, with the exchange half-life of each complex.*

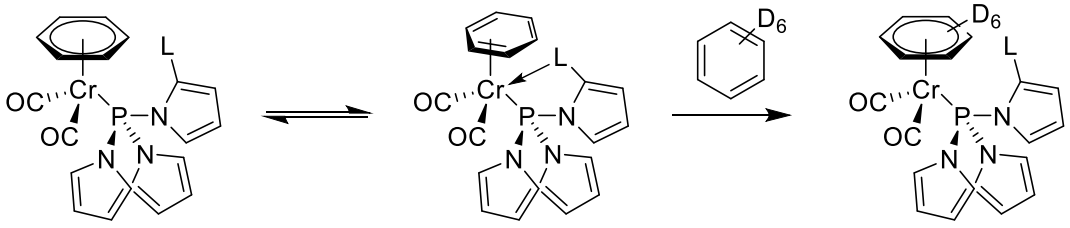

1.52a **1.52b** **1.53**

Coordinating functional group, L	Temp (°C)	Exchange half-live (h)	Coordinating functional group, L	Temp (°C)	Exchange half-live (h)
$–CO_2Me$	70	0.5	$–CO_2Me$	23	115
–SMe	70	8.7	$–CONMe_2$	22	9
–SPh	70	30.6	–2-Py	22	8
$–SF_3$	70	>150			

Recent work from Walton *et al.* reported tether-assisted arene exchange for ruthenium complexes, where a series of tethered $[RuCpL]^+$ complexes (where CpL is a Cp ring bearing a coordinating functional group) were compared to see how the rate of exchange was accelerated (Figure 1.28).[59]

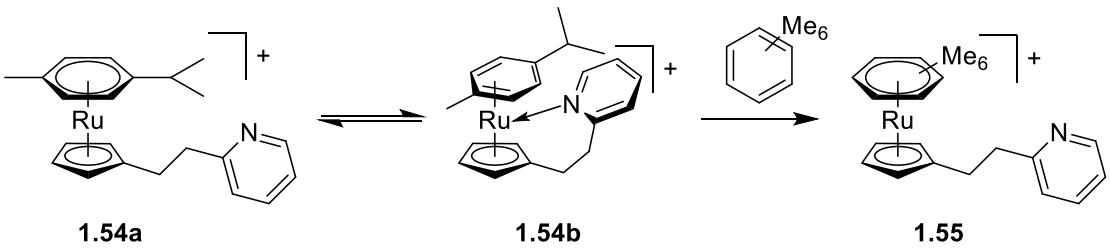

1.54a **1.54b** **1.55**

Figure 1.28 *Tethered ruthenium Cp complex with pyridine functionalisation which catalyse arene exchange.*

This study showed a similar conclusion to Semmelhack's work, where the donating ability of the Cp arm mirrored the rate of arene exchange and, again, a pyridine ligand (complex **1.54a**) was the highest performing coordinating tether.

1.4.4 Photocatalytic Arene Exchange

The use of UV light to liberate η^6-bound arenes from metals has been discussed above and has been frequently utilised to prepare complexes of electron deficient arenes. In a similar fashion to the mechanism discussed in section 1.4.2, depending on the particular chemical environment, photolysis and subsequent liberation of the bound arene will result in the newly available coordination sites being occupied by solvent molecules or available incoming arenes. Photolysis in this fashion has been frequently reported for $[FeCp]^+$ and $[RuCp]^+$ systems, and can follow an arene exchange procedure or solvation procedure depending on conditions.[60,61] Woodgate *et al.* published the $[RuCp]^+$ mediated S_NAr of chlorobenzene (complex **1.56**) with morpholine and used UV irradiation (Rayonet photoreactor at 300nm) to liberate the *N*-aryl-morpholine product in the presence of acetonitrile to collect the free arene product and the trisacetonitrile piano stool ruthenium complex in quantitative yields (Figure 1.29).[62]

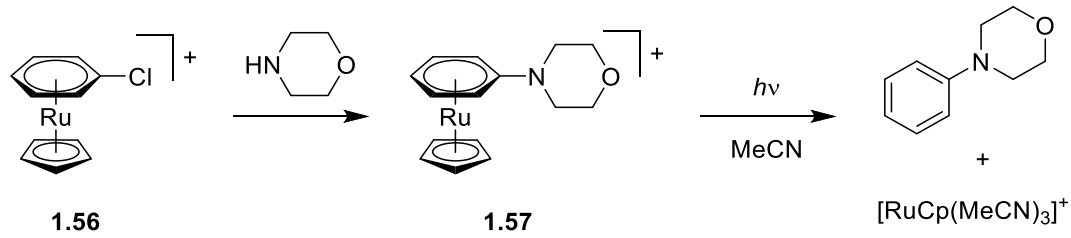

Figure 1.29 *Photolysis used to liberate the product of S_NAr*

By irradiating the complex in a coordinating solvent like acetonitrile, the free metal centre is solvated as the arene is liberated. Analogous reactions with $[FeCp]^+$ have been reported, but require much lower temperatures due to the instability of the consequent solvated iron complex.[63] However, if a non-coordinated solvent is used (i.e. CH_2Cl_2) with an excess of another arene, photocatalysed arene exchange can be achieved. In this process, interestingly, the reactivity of iron and ruthenium differ quite significantly. While it has been reported that $[(\eta^6$-*p*-xylene)$FeCp]^+$, in the presence of C_6Me_6, will undergo complete arene exchange using only bright sunlight in 5 hours, the analogous Ru complex exhibits no reaction under the same conditions.[64]

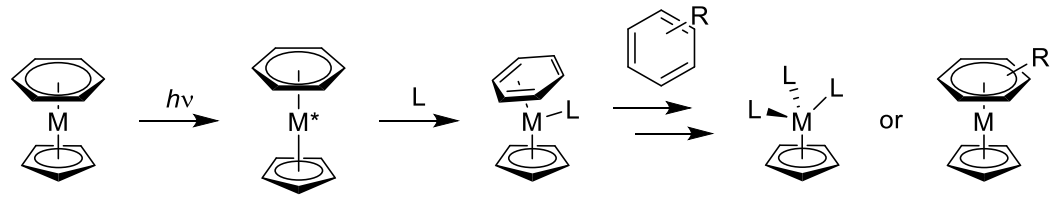

Figure 1.30 *Mechanism of photocatalytic arene exchange in [(η^6-arene)MCp]$^+$ complexes (where M = Fe, Ru).*

The proposed mechanism for the photolysis of [(η^6-arene)MCp]$^+$ complexes (where M = Fe, Ru) is through a metal-centred photoexcited state. The promotion of an electron from the metal-centred d(z^2) orbital to a metal-centred d(xz) or d(yz) orbital leads to bond elongation of the metal arene bond and depopulation of the d(z^2) orbital (Figure 1.30). This opens the metal centre to nucleophilic attack from solvent molecules or incoming arenes, depending on the reaction conditions, and leads to an η^4-arene intermediate. This intermediate can then rapidly liberate the outgoing arene and in the presence of coordinating solvent or arene, will become fully solvated or proceed with arene exchange respectively.

1.5 Metal Arene complexes in Catalysis

As mentioned previously, a frequent limitation to this chemistry is the stoichiometric use of transition metal. Attempts have been made to tackle this drawback *via* catalytic transformations through the arene exchange mechanism discussed above. Catalysis *via* this mechanism is challenging, as properties that enhance the reactivity of the bound arene disfavour exchange. A strong metal-arene bond and subsequently large electron-withdrawing effect maximises the activation of the ring, but this complex will exhibit sluggish arene exchange, and vice versa (Figure 1.31).

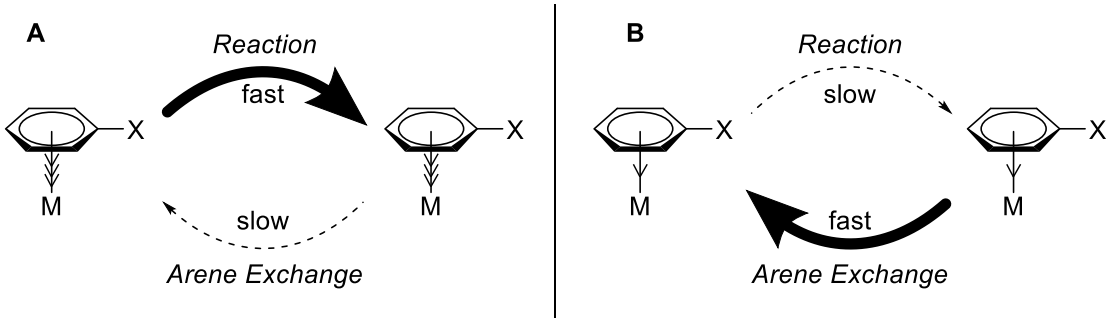

Figure 1.31 *Effect on rate of reaction and arene exchange depending on electronic of metal fragment*

In order for catalysis to be achieved, strategies must balance sufficient activation of the substrate arene with reasonable rates of exchange. To date, there has only been a relatively few reported examples of catalytic reactions with regards to a bound metal fragment. The first of its kind was the rhodium-catalysed cyclisation, via intramolecular S_NAr, of aryl fluorides report by Houghton, which was discussed in section 1.3.4 (Figure 1.21).[46] The reaction had a narrow scope and required 23% catalyst loading, but pioneered both intra- and intermolecular catalytic transformations through an η^6-arene intermediate.

It was not until 20 years later that another example of catalysis was reported by Hartwig, who reported anti-Markovnikov addition of nucleophiles to styrene derivatives catalysed *via* η^6-arene ruthenium complex **1.58** (Figure 1.32).[65] Regioselectivity for the beta position was optimised to 96% by tuning multidentate phosphine ligands and the reaction tolerated a range of styrenes and secondary amines. In a later study, the suggested mechanism goes *via* η^6-arene intermediates where nucleophilic attack at the alpha carbon, stabilised by the net withdrawing metal fragment, is followed by arene exchange.[66] Shibata was more recently able to demonstrate the analogous reaction enantioselectively using chiral BINAP-phosphine ligands, albeit with lower converstions.[67]

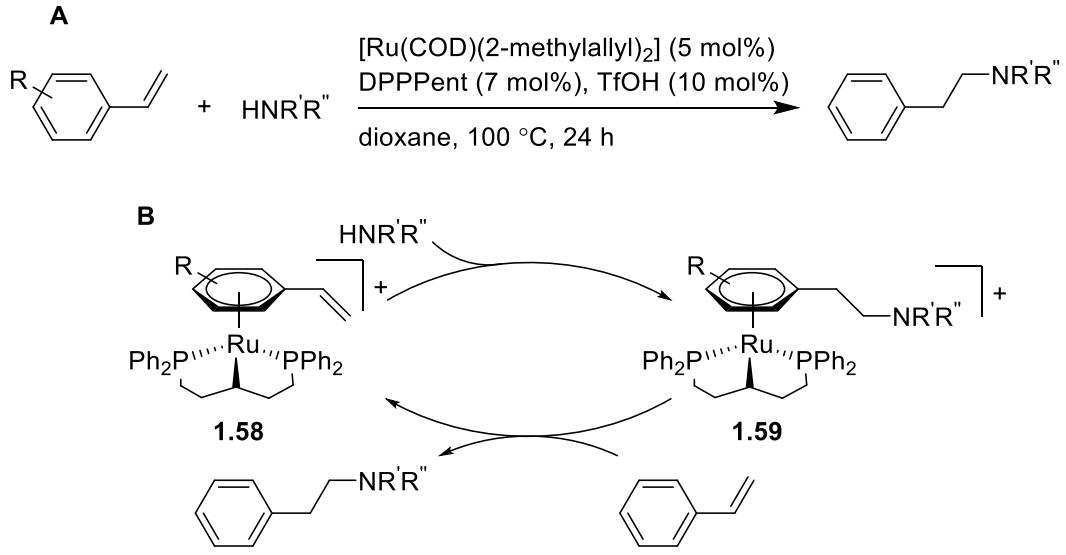

Figure 1.32 *Anti-Markovnikov addition of nucleophiles to styrene derivatives catalysed via an η^6-arene ruthenium complex.*

Around the same time, Rodgers reported a photocatalysed Bergman cycloaromatisation using $[(MeCN)_3MCp^*]^+$ (where M = Fe or Ru).[68] Previous work required stoichiometric amounts of transition metal, however with constant irradiation catalytic turnover was achieved (Figure 1.33).[69] The resting state of the catalyst is the product bound complex **1.60**, which when irradiated liberates the product and solvates the $[MCp]^+$ fragment

(**1.61**). The turnover number of 3.3 for this reaction is poor, but this is the first and currently the only example of photocatalysis *via* an η^6-arene intermediate. This chemistry is entirely unexplored but shows promise for catalytic arene transformations under mild conditions.

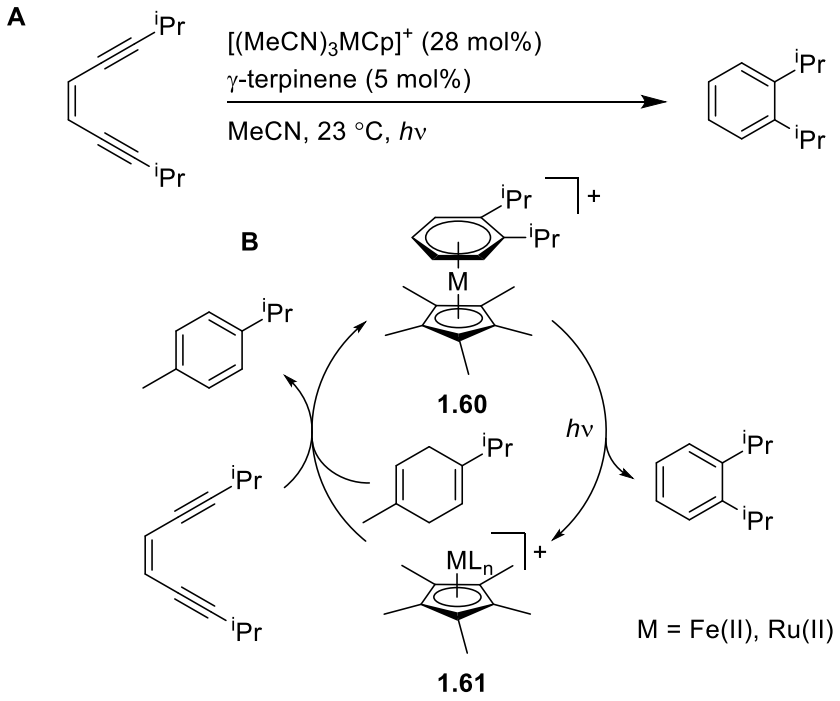

Figure 1.33 *Photocatalytic cycloaromatization via π-arene metal intermediates.*

In 2010, Shibata used a similar ruthenium DPPPent complex to Hartwig for the catalytic S_NAr of unactivated fluorobenzenes with a number of nucleophilic secondary amines (see Figure 1.34).[70] A number of cyclic and acyclic amines proceeded in reaction with *p*-fluorotoluene, alongside a scope of unactivated fluorobenzenes tolerating S_NAr with morpholine, all achieving good to moderate yields.

A noteworthy result is the successful reaction which proceeds between morpholine and 4-dimethylamino-fluorobenzene. Substitution still occurs despite the NMe_2 group being a strong electron donating group, albeit in low yields, which further demonstrates the strong electron-withdrawing capacity of the ruthenium metal fragment in complex **1.62**.

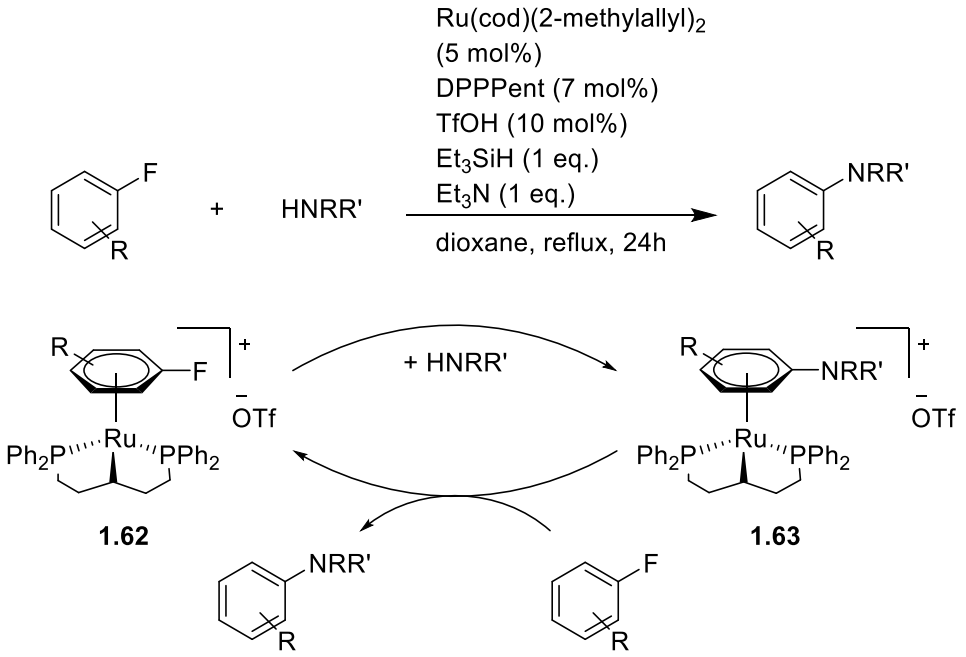

Figure 1.34 *General procedure for catalytic S_NAr of substituted fluorobenzenes reported by Shibata.*[70]

In the following year Shibata published work which showed that by tuning the ligands on the ruthenium catalyst, the yields of substitution could be improved.[71] Using electron poor monodentate phosphine ligands, like tris(*p*-fluoro)phenylphosphine, lead to higher catalytic conversions due to a more electropositive metal centre binding to the substrate (Figure 1.35).

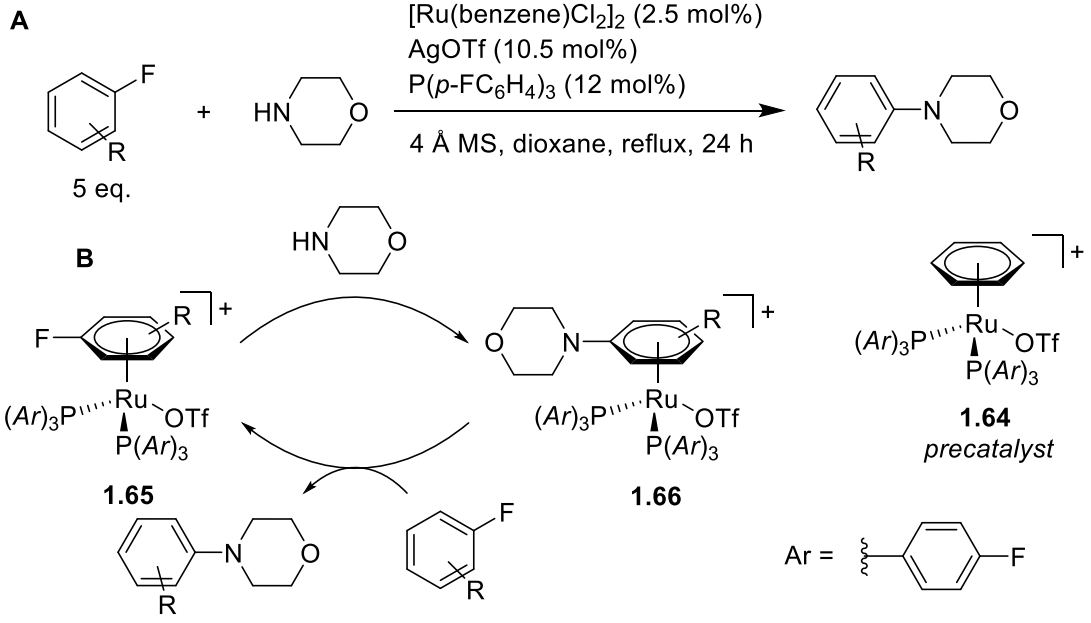

Figure 1.35 *The reaction of substituted fluorobenzenes and morpholine with ruthenium catalyst.*[71]

Only a small number of secondary amines were tested as nucleophiles, which reacted with *p*-fluorotoluene in moderate to good yields. Morpholine, however, was able to react with a variety of electron rich fluoroarenes (*via* complex **1.65**), again with good to moderate conversion.

In 2011, Tsuchimoto reported the first main group metal catalysed S_NAr *via* a π-arene intermediate.[72] The group proposed that the η^5-thiophene intermediate **1.67** was responsible for the activation toward nucleophilic attack, as evidenced by deuteration experiments and the fact that electron deficient thiophenes, unable to form the intermediate π-complex, would not undergo reaction (Figure 1.36).

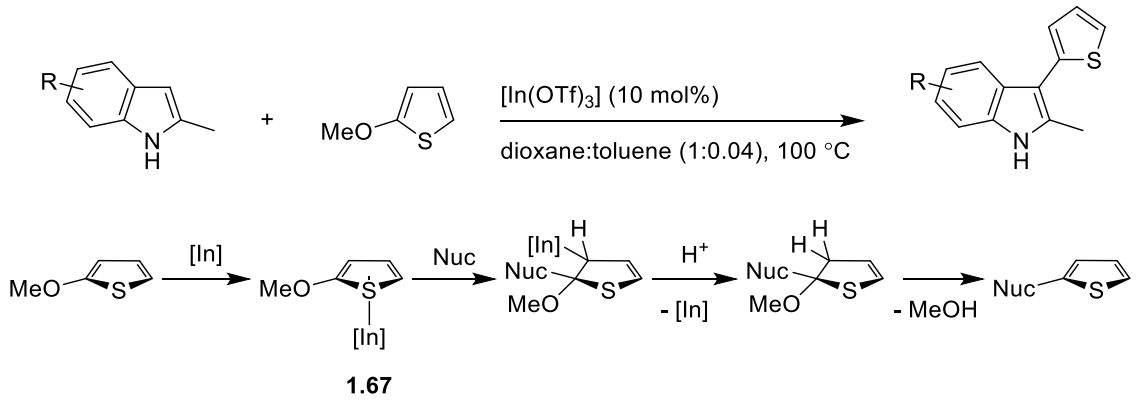

Figure 1.36 *In-catalysed S_NAr of methoxythiophenes via a π-arene intermediate.*

A following study published recently in 2018 showed how this method could tolerate a wide range of nucleophiles including alcohol, amines and sulfur-derived nucleophiles, and the electrophile scope was also expanded to include heterocyclic thianaphthenes.[73]

Also in 2011, Hartwig published the nickel-catalysed hydrogenolysis of aryl ethers.[74] Hydrogenolysis was achieved at 100 °C and 1 bar H_2, significantly lower than typical conditions (>250 °C and >30 bar H_2), and tolerated both electron rich and poor substrates. It was not until 2017 that a mechanism of action was reported, which postulated an η^6-arene intermediate which would undergo oxidative addition of the C–O bond of the ethers across nickel (**1.70**, Figure 1.37).[75]

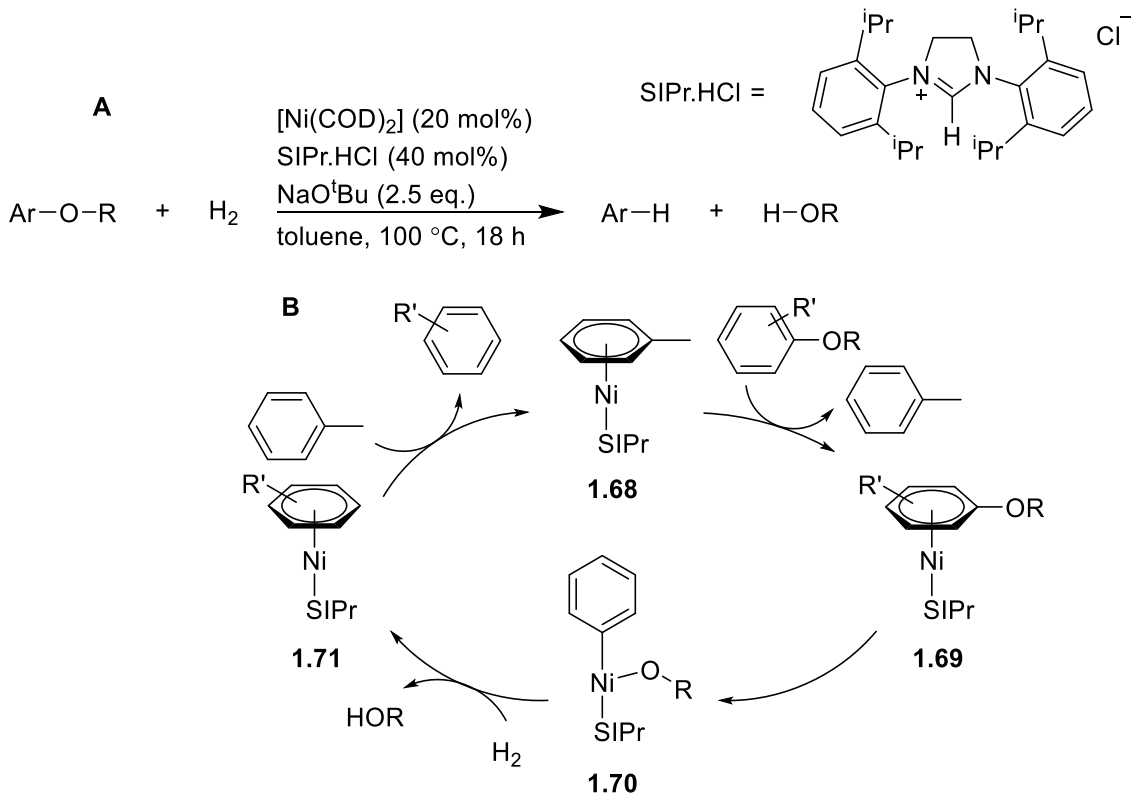

Figure 1.37 *Mechanism for catalytic hydrogenolysis of aryl ethers.*

Between Hartwig reporting the initial reaction and the later proposed mechanism, Wang *et al.* published a catalytic amination of aryl fluorides which underwent analogous reactivity.[76] Using [Ni(COD)$_2$] as precatalyst and a similar *N*-heterocyclic carbene ligand formed the η^6-arene intermediate and consequently facilitated the oxidative addition of the C–F bond. Though lower catalyst loading was needed, the reaction would only tolerate secondary amines at this stage. It was not until Sawamura *et al.* later introduced a bulky bis-phosphine ligand that catalyst loading was dropped further and the scope was extended to primary amines.[77]

Shortly after Wang's initial report of Ni-catalysed amination of fluorobenzenes, Arnold and Bergman reported a niobium catalysed hydrodefluorination which followed a similar mechanism (Figure 1.38).[78] The oxidative addition step from η^6-intermediate **1.73** to η^1-intermediate **1.74** similar to that proposed by Hartwig was confirmed by DFT calculations and proceeds *via* a bimetallic arene bridged inverted sandwich complex which has been found to exist in previous work from the group.[78]

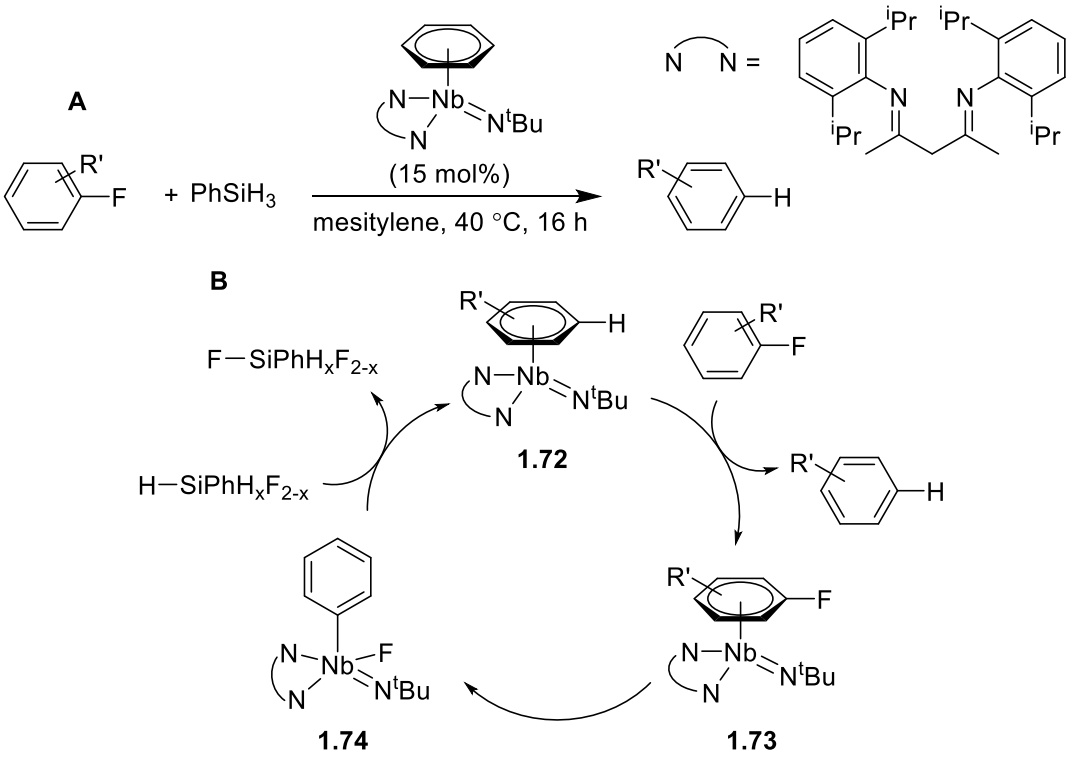

Figure 1.38 *Nb-catalysed hydrodefluorination of arylfluorides.*

In the following year, an example of catalytic S_NAr was reported by Walton and Williams, which showed that the commercially available complex [(*p*-cymene)RuCp]PF_6 (**1.75**) could be used as a precatalyst to facilitate the S_NAr reaction of *p*-chlorotoluene and morpholine.[38] A high yield of 90% was achieved for the reaction, albeit using high temperatures and long reaction times (Figure 1.39).

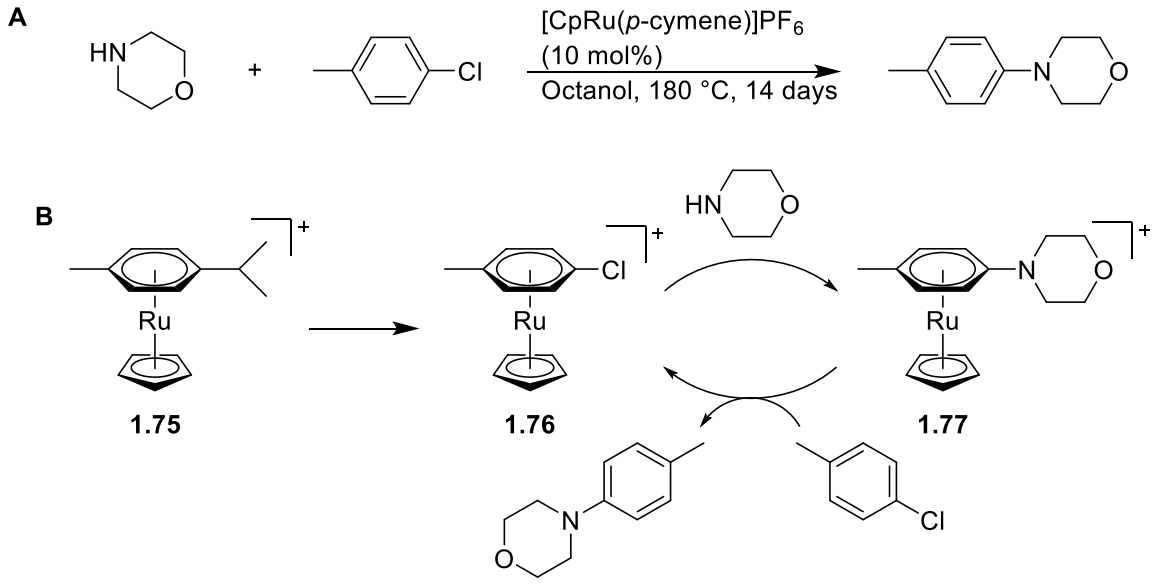

Figure 1.39 *The reaction of p-chlorotoluene and morpholine with cationic ruthenium Cp catalyst*

Successful conversion was observed in coordinating solvents like octanol, cyclohexanone and DMI, whereas no reaction occurred when the non-coordinating solvent *p*-xylene was used, illustrating the effect of coordinating solvents in the arene exchange mechanism.

Soon after, Grushin reported a similar $[RuCp]^+$ system to Walton and Williams to catalyse the fluorination of halobenzenes.[79] A Cp* ruthenium naphthalene precatalyst **1.78** was used to catalyse the S_NAr reaction of chloro-, bromo- and iodobenzene and nucleophilic fluoride (Figure 1.40).

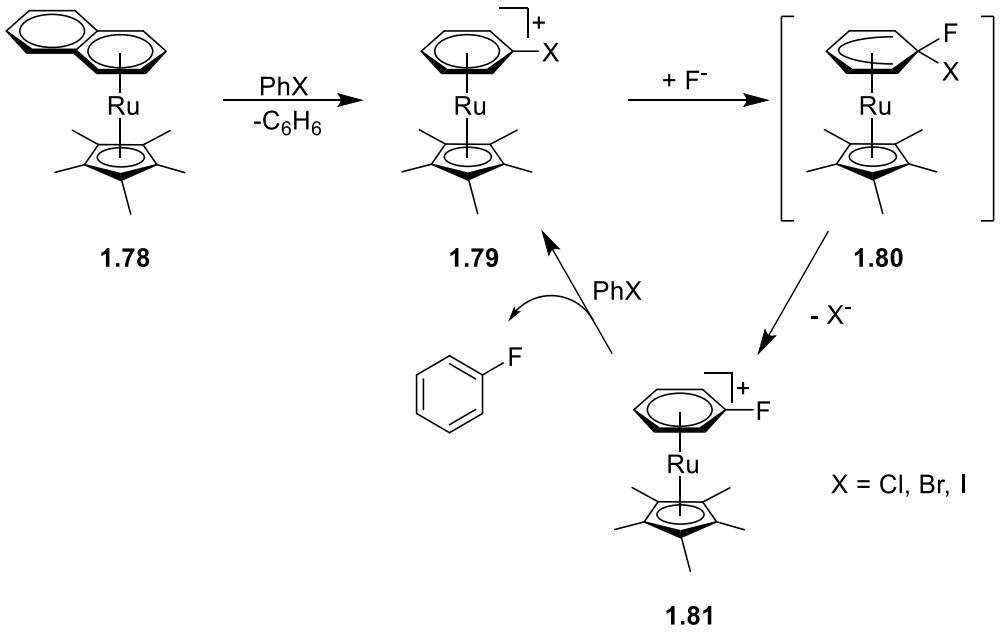

Figure 1.40 *General reaction pathway for catalytic fluorination of haloarenes reported by Grushin.*[79]

Unsurprisingly, the yields for the reaction of chlorobenzene was faster than that of bromo-and iodobenzene. The reaction between *p*-chlorotoluene and CsF saw exclusively *p*-fluorotoluene, confirming an S_NAr mechanism, *via* intermediate **1.80**, rather than an aryne mechanism, and accounts for the impressive regio- and chemoselectivity of the reaction. The most recent example of catalysis was reported in 2016 by Matsuzaka, where stilbene derivatives were formed in good yields from toluene and benzaldehydes.[80] The activation of toluene through π-complexation (**1.82**) enables deprotonation at the benzylic position, which then acts as a nucleophile (Figure 1.41).

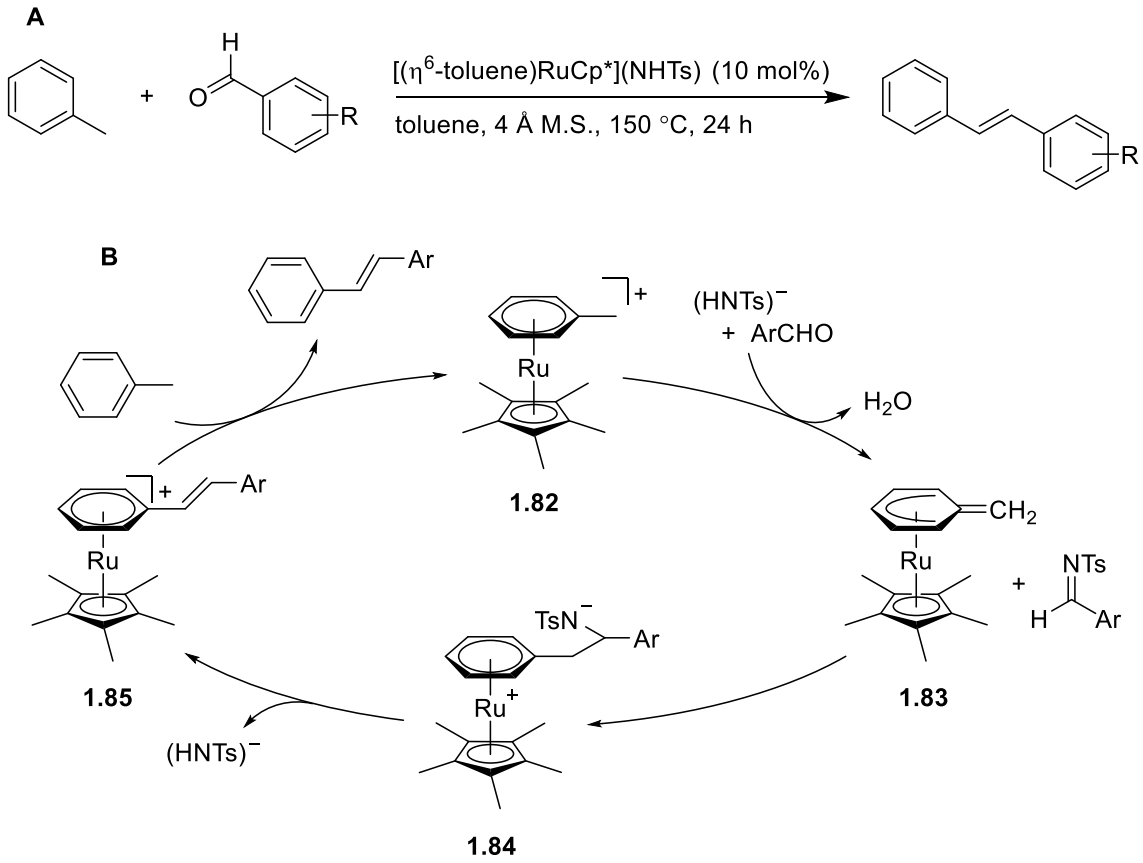

Figure 1.41 *Ru-catalysed benzylic functionalisation of π-coordinate toluene.*

The aromatic aldehydes have been electrophilically activated by imine formation with the $(NHTs)^-$ counterion, which is a crucial step in the reaction, indicated by the lack of reactivity when Cl^- and TfO^- counterions were used. The publication does not determine the rate limiting step of this catalytic cycles, however there is evidence to suggest that this step is the arene exchange which completes the cycle. Excellent yields are recorded using the $[RuCp^*]^+$ fragment, and reduced conversion is seen when the more electron deficient $[RuCp]^+$ fragment is used, which is indicative of an arene exchange pathway.

1.6 Project Aims

As shown, activation of arenes through π-coordination has been used as a powerful technique for synthetic chemists for several decades. More recently, the development of catalytic processes *via* η^6-arene intermediates has emerged. Excluding Houghton's report using rhodium in 1984, all examples of catalytic arene transformations have been published in the last fifteen years, demonstrating a resurgence in this field of organometallic chemistry in catalysis. The aims of this project are to create new reactions facilitated by η^6-arene intermediates and also to translate both new and existing

stoichiometric transformations into catalytic reactions. Based on modern synthetic challenges, the following specific reactions were to be explored:

a. Develop a trifluoromethylation protocol using a nucleophilic source of CF_3 and electrophilically activated $[(\eta^6\text{-arene})RuCp]^+$ complexes
    i. Prepare initial $[(\eta^6\text{-arene})RuCp]^+$ complex for trifluoromethylation based on literature precedent
    ii. Test complex for trifluoromethylation and optimise reaction conditions
    iii. Synthesise a library of $[(\eta^6\text{-arene})RuCp]^+$ complexes and test under optimised conditions
    iv. Develop a catalytic procedure for trifluoromethylation
b. Develop a C–H activation protocol using activated $[(\eta^6\text{-arene})RuCp]^+$ complexes
    i. Prepare initial $[(\eta^6\text{-arene})RuCp]^+$ complex for C–H activation based on literature precedent
    ii. Develop optimised conditions for C–H activation and reductive coupling of prepared complexes using Pd chemistry
    iii. Synthesise a library of $[(\eta^6\text{-arene})RuCp]^+$ complexes and test under optimised conditions
    iv. Develop a C–H activation procedure catalytic to ruthenium
c. Determine the effect of tethered catalysts on the rate of arene exchange
    i. Prepare a library of tethered $[RuCp]^+$ complexes
    ii. Measure their rates of arene exchange compared to unfunctionalised Cp
    iii. Test top performing catalysts in the groups understood catalytic reactions

The following chapters describe how a number of η^6-arene ruthenium cyclopentadienyl intermediates have developed a range of new reactions. *Chapter 2* discusses a novel trifluoromethylation reaction mediated by $[RuCp]^+$ and *Chapter 3* will discuss a C–H activation protocol also mediated by the same metal fragment. The focus of *Chapter 4* is the development of a catalytic hydrodeiodination reaction involving $[(\eta^6\text{-arene})RuCp]^+$ intermediates discovered serendipitously, followed by *Chapter 5* which is the early steps of a kinetic study of a number of tethered $[RuCp]^+$ units designed to increase the rate of arene exchange. The work described in *Chapters 2* and *3* have been published since the preparation of this thesis, while *Chapters 4* and *5* contain work currently unpublished.[81,82]

2. Nucleophilic trifluoromethylation of electron-deficient arenes

2.1 Introduction

2.1.1 Chemistry of trifluoromethyl groups

The C–F bond has been an intense area of interest, particularly its role in pharmaceuticals,[83,84] agrochemicals,[85] and materials.[86] Unique properties arise from organic molecules containing fluorine as a result of its small atomic radius and electronegativity, causing high polarity within the compounds.[87] For the same reasons, CF_3 groups have a similar effect to fluorine when incorporated into organic molecules. The CF_3 functional group has the same electronegativity as chlorine and a similar van der Waals radius to an isopropyl group.[88] Such properties are utilised in medicinal chemistry, where incorporation of fluorine into pharmaceuticals improves the candidate molecule's bioavailability, lipophilicity and metabolic stability.[83] So it comes as no surprise that currently around 25% of all pharmaceuticals and 30% of all applied agrochemicals contain at least one fluorine or trifluoromethyl substituent.[89] Figure 2.1 demonstrates a small sample of aryl-trifluoromethylated compounds used commercially that are more effective than their non-fluorinated analogues.

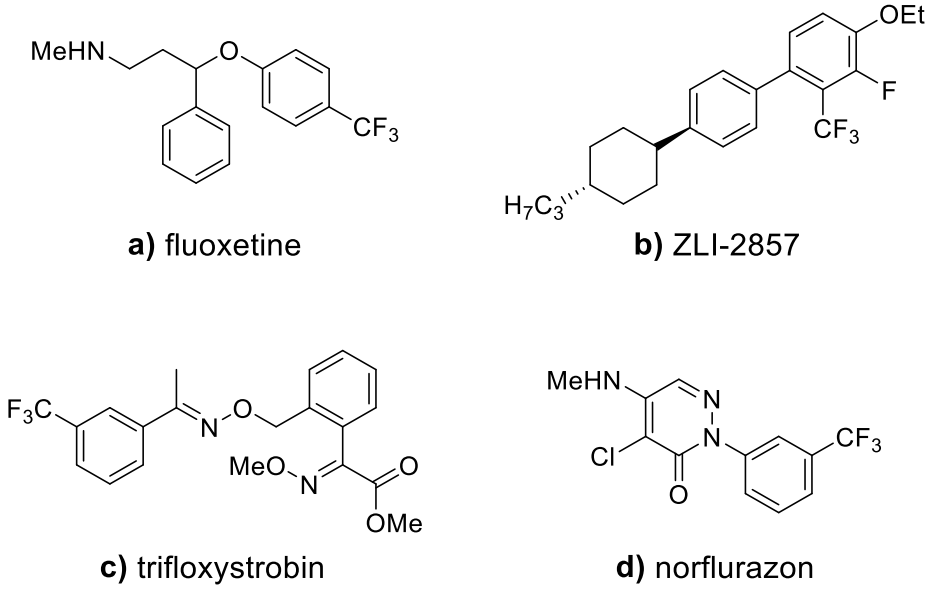

Figure 2.1 *a) Fluoxetine (Prozac), one of the most widely sold antidepressants[90] b) ZLI-2857, a fluorinated component of liquid-crystal mixtures in LCD screens[91] c) trifloxystrobin, a top-selling fungicide[92] d) norflurazon, a bleaching herbicide inhibiting carotinoid synthesis.[85]*

Methodology to install CF_3 substituents into organic frameworks has been intensely studied and the mechanism in which they are incorporated can be broken down into three classes; electrophilic trifluoromethylation, direct free radical trifluoromethylation and nucleophilic trifluoromethylation. These three procedures will be briefly reviewed herein.

2.1.2 Electrophilic Trifluoromethylating Agents

Considering the properties of the C–F bond, the idea of a positively charged source of a perfluoroalkyl group seems unconventional. However electrophilic trifluoromethylation is a well-studied and successful area of fluorine chemistry. The first electrophilic source of CF_3 was reported by Yagupolskii and co-workers in 1984, where it was found that a diaryl(trifluoromethyl)sulfonium salt was able to successfully add CF_3 groups to aryl sulfoxides (**2.1**, Figure 2.2A). *p*-Nitro-thiophenolate reacts with the sulfonium salt to give the corresponding trifluoromethylated sulfide in a modest yield of 65%.[93] It was suggested that the electrophilicity of the salt was restricted by electron donating substituents on the arenes which stabilise the positive charge on the sulfur.

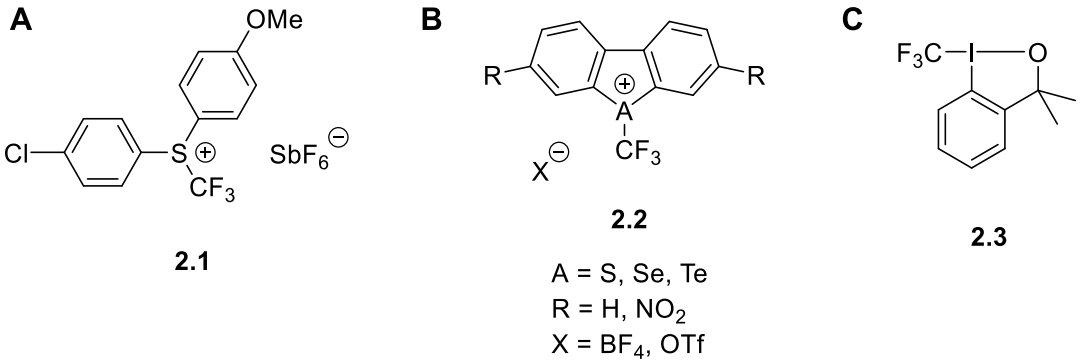

***Figure 2.2 A** Yagupolskii's reagent. **B** Umemoto type reagents. **C** Togni's reagent*

Umemoto and co-workers developed a family of (trifluoromethyl)dibenzoheterocyclic salts wherein their electrophilicity could be tuned with electron-withdrawing and electron-donating groups on the arene rings.[94–96] By nitrating the arenes, the electrophilicity of the reagent could be increased through increasing the positive charge on the sulfur (**2.2**, Figure 2.2B).[94] As a result, much better reactivity was observed with a greater scope of nucleophiles.[96]

Another known class of electrophilic CF_3 reagents uses hypervalent iodine. Attempts were made by Yagupolskii and Umemoto to synthesise iodonium salts capable of supplying electrophilic CF_3 but their efforts were unsuccessful.[97–99] Togni and co-workers

were the first to publish successful trifluoromethylation whereby CF_3 was covalently bound to iodine. Togni's reagent (**2.3**, Figure 2.2C) is made in an easy one-pot synthesis by firstly substituting the chlorinated derivative with an acetoxy group, followed by CF_3^-, provided by treatment with Me_3SiCF_3 (Ruppert's reagent).[100] **2.3** is able to react with an impressively large nucleophile scope, including aromatic and aliphatic thiols, β-keto esters, α-nitro esters and aryl- and alkylphosphines.

Electrophilic trifluoromethylation has become a powerful tool for synthetically incorporating CF_3 groups into organic compounds, and a recent review from Shibata summarises the recent advances in the area.[101]

2.1.3 Direct Free Radical Trifluoromethylating Agents

Direct free radical trifluoromethylation is a more modern reaction compared to electrophilic and nucleophilic, but since the first reported example by Langlois and co-workers in 1991, the area has become a powerful tool for adding CF_3 groups to arenes and heteroarenes.[102] Pioneering work from Langlois showed how sodium trifluoromethanesulfinate (Langlois' reagent) **2.4** and t-butyl hydroperoxide, with catalytic Cu(II), could trifluoromethylate electron-rich aromatic compounds. 20 years later, a powerful procedure published by MacMillan showed that under mild visible-light irradiation, ruthenium and iridium photoredox catalysts were able to directly trifluoromethylate an impressive array of inactivated arenes and 5- and 6-atom heterocycles (Figure 2.3).[103]

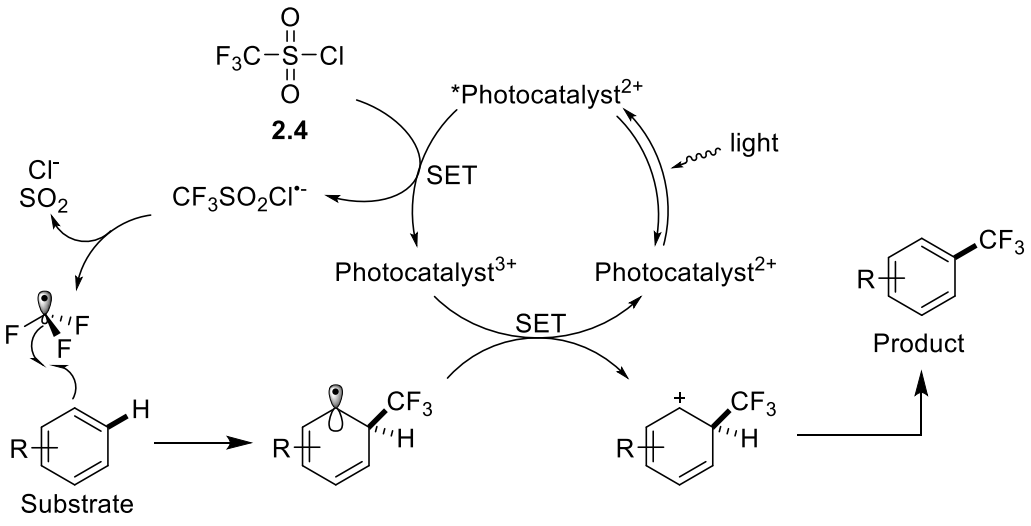

Figure 2.3 *Mechanism for MacMillan's direct trifluoromethylation of aryl C-H bonds via photoredox catalysis.*[103]

Once the photocatalyst was initiated *via* excitation, a single electron transfer process creates a CF_3 radical from triflyl chloride. Once this free radical has directly reacted with the aromatic substrate, another single electron transfer produces the product and regenerates the ground state photocatalyst and completes the cycle.

Concerns grew regarding the use of these methodologies for the production of pharmaceuticals, agrochemicals and materials due to the difficult removal of residual metal from reaction mixtures. Therefore, mild, environmentally safe transition-metal-free methodologies became highly sought after. Around the same time MacMillan published his findings, a transition-metal-free method for trifluoromethylation of heterocycles was published by Baran and co-workers, using similar conditions to Langlois' original report.[104] Monitoring the reaction of arene substrate, sodium trifluoromethanesulfinate and t-butyl hydroperoxide in DCM:H_2O (2.5:1) using calorimetric analysis showed that a large amount of heat was produced at the start of the reaction, but a very small amount of arene product was being produced.

This was attributed to side reactions occurring between the sulfinate and hydroperoxide, which explained the large excess of these reagents required in previous work.[102] It was found that, rather unconventionally, that if the reaction mixture was not stirred, a much greater yield of arene product was obtained, although longer reaction times were required. By keeping the reaction mixture still, the substrate and hydroperoxide would remain in the organic layer and the sulfinate in the aqueous, significantly reducing side reactions between the reagents. This mild, air-stable, transition-metal-free procedure was successful for a large range of heterocycles and had a wide functional group tolerance.

A very recent example of a transition-metal-free system is from Li and co-workers, employing sodium triflinate as the source of the CF_3 motif. By dissolving the reagents in acetone and irradiated with UV light, direct radical trifluoromethylation of a number of electron-rich arenes was achieved.[105] The photo-induced catalysis is initiated by exciting acetone to a n, π^* triplet-excited state ketone, which can then further react with triflinate to create the electron deficient CF_3 radical capable of reaction with substrate arenes. As already mentioned, the arenes used for the scope of this reaction are highly electron-rich, which demonstrates a limitation to this pathway. Nonetheless it is an interesting example of metal-free catalysis with industrial potential for pharmaceuticals, supported by the gram-scale reaction capability and tolerance towards a number of biologically active substrates, all achieving modest yields.

2.1.4 Nucleophilic Trifluoromethylating Agents

Incorporation of CF_3 moieties into organic molecules *via* a negatively charged CF_3 nucleophile seems a most sensible pathway considering the polarity of the C-F bond. One of the most well-known sources of nucleophilic perfluoroalkyl groups are organosilicon reagents, which have been comprehensively reviewed by Prakash and Yudin.[106] Since its first use in the early '80s, trimethyl(trifluoromethyl)silane (TMS-CF_3, Ruppert-Prakash reagent) has been an essential synthetic agent for the trifluoromethylation of organic compounds. Prakash first used the reagent for the trifluoromethylation of aldehydes and ketones into the corresponding alcohol, and this work spurred a succession of similar reactions to be reported.[107]

In 1990, it was shown by Bardin and co-workers that activated aromatics could react with Ruppert's reagent *via* S_NAr (Figure 2.4).[108] Perfluorination is required to sufficiently activate the arene towards nucleophilic attack by CF_3^-, generated *in situ* from TMS-CF_3. Using this method, substitution of fluoride and nitro groups was achieved.

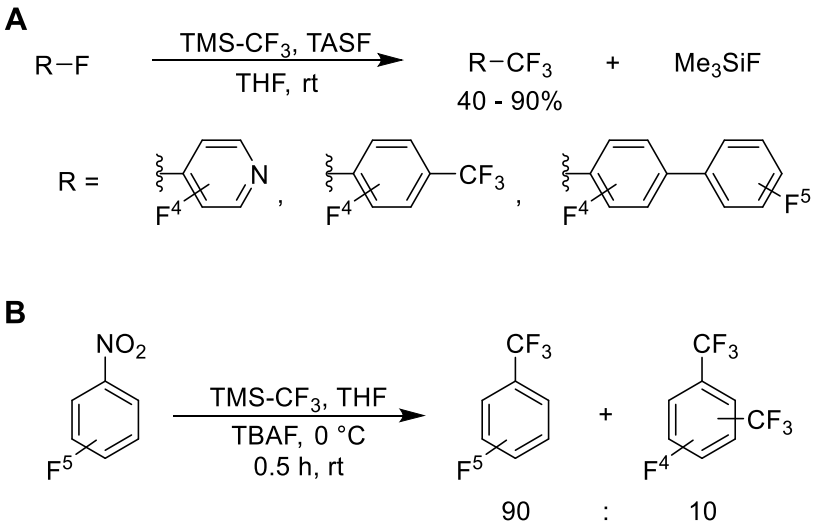

Figure 2.4 *S_NAr reactions of perfluorinated aromatics, modified from Bardin.*[108] ***A*** *Substitution of fluoride for CF_3 for a number of arenes.* ***B*** *Substitution of NO_2 for CF_3, where a side product is bis-substitution.*

A limitation of Ruppert's reagent is the difficultly in controlling its reactivity. The compound is a volatile liquid that is also moisture and air sensitive. A number of successful cases have shown how using copper to mediate reactions with Ruppert's reagent can improve reactivity and reactions proceed with less functionalised arenes.[109–112] A recent publication from Gooßen and co-workers synthesised a number of potassium borate salts (**2.5**) that were novel sources of nucleophilic CF_3 and were able to

react with a variety of electron-rich and electron-poor aryl iodides to afford trifluoromethylated arenes in very good yields (Figure 2.5).[111] These salts were synthesised to near quantitative yields and were air and moisture stable for easy laboratory storage. This reaction required a catalytic amount of Cu(I) and 1,10-phenanthraline which, once bound to the CF_3 moiety, transformed the aryl iodide substrate *via* a concerted σ-bond metathesis mechanism.

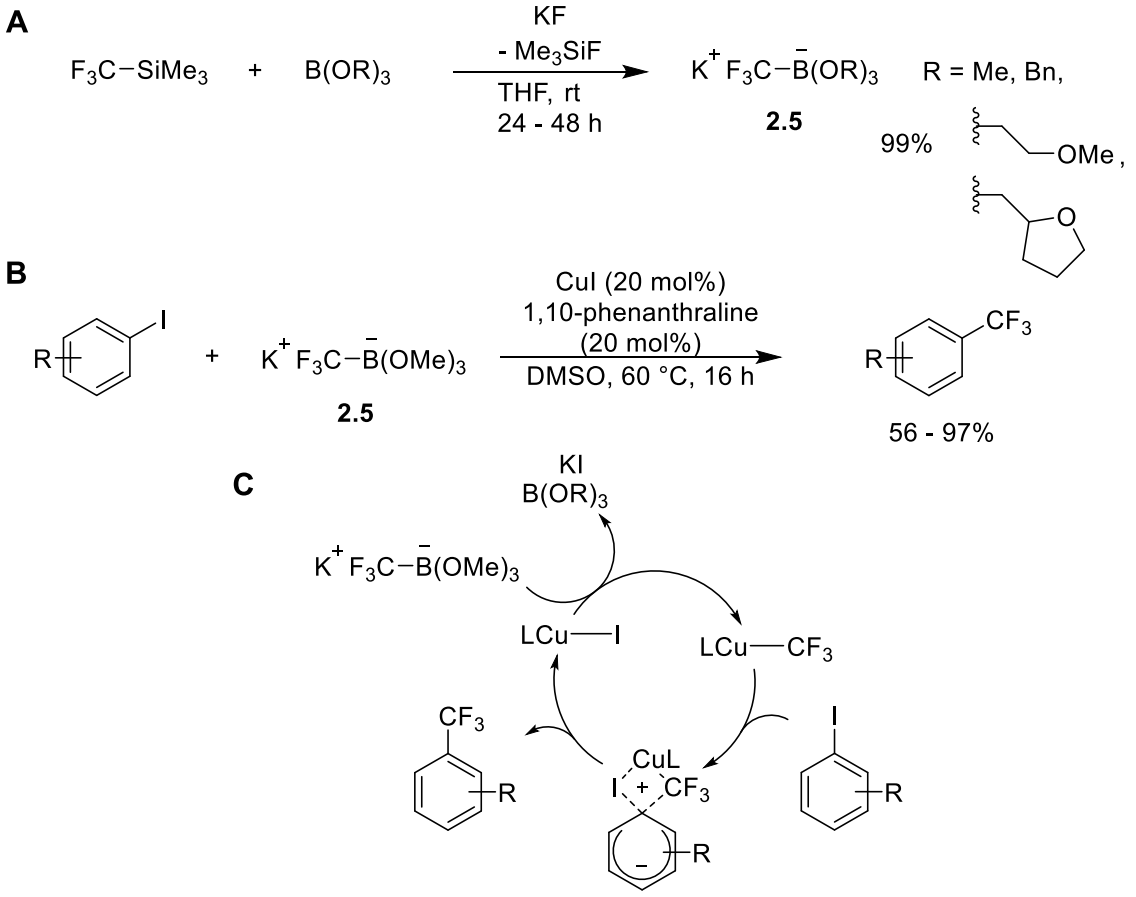

Figure 2.5 A *Reaction pathway for the synthesis of potassium (trifluoromethyl)borate salts.* ***B*** *Reaction pathway for the trifluoromethylation of aryl iodides with borate salt and catalytic copper.* ***C*** *Catalytic cycle for the trifluoromethylation reaction, modified from Gooßen.*[111]

Although the examples described for the three classes of trifluoromethylation reaction are successful, creating new methodologies and discovering mechanistic insight into existing ones remains a challenge for today's scientific community.

The Walton group recently showed the catalytic S_NAr of unactivated aryl chlorides (i.e. those without electron withdrawing substituents), mediated by transient η^6-coordination to $[CpRu]^+$.[38] The π-complexation of an arene to a transition metal increases its reactivity towards nucleophilic attack,[26,113–115] resulting in efficient S_NAr. Following the success of this reaction, we hypothesised that the electron-withdrawing effect of π-complexation could allow for trifluoromethylation of arenes with nucleophilic CF_3. This would

overcome the limitations of current nucleophilic trifluoromethylations, which require highly electron-deficient perfluorinated arene substrates (e.g. $C_6F_5NO_2$).[108] This chapter describes the successful reaction of the nucleophilic Me_3SiCF_3 reagent towards $[(\eta^6\text{-arene})RuCp]^+$ π-complexes, producing a single regioisomer of trifluoromethylated products. Importantly, we also show the ability to recover the activating transition metal complex, $[CpRu(NCMe)_3]^+$, by photolysis. This process holds potential for the late-stage trifluoromethylation of electron-deficient arenes and could have significant impact upon the pharmaceutical and agrochemicals industry.

During the preparation of the manuscript for this project, Yagupolskii reported similar reactivity with $(\eta^6\text{-arene})Cr(CO)_3$ complexes.[115] Trifluoromethylation progressed using Ruppert-Prakash reagent and $[Me_4N]F$ with a series of chromium complexes of relatively electron rich arenes in good yields (Figure 2.6).

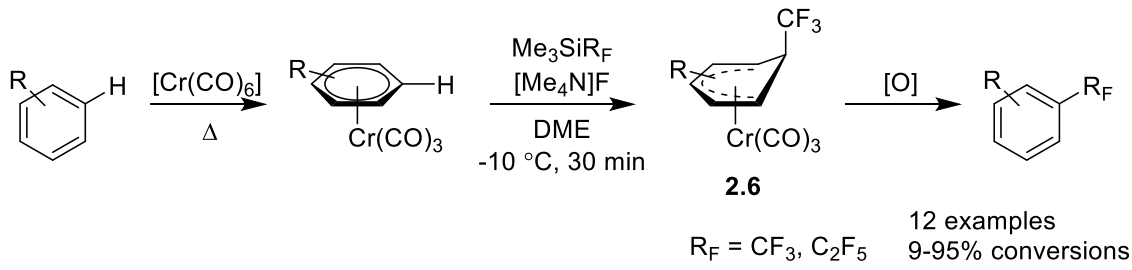

Figure 2.6 *Nucleophilic trifluoromethylation of aromatic compounds via $(\eta^6$-arene)$Cr(CO)_3$ complexes.*

The oxidation of the various Meisenheimer complexes **2.6** required differing reagents, including iodine, 1,4-benzoquinone and cerium ammonium nitrate (CAN), which liberated the free arene in high yields but decomposed the chromium.

2.2 Results and Discussion

2.2.1 Synthesis of initial π-complex $[(\eta^6$-nitrobenzene)RuCp]PF_6

To determine firstly whether trifluoromethylation is feasible, the sandwich complex $[(\eta^6$-nitrobenzene)RuCp]PF_6 (**2.8**) was synthesised. Synthesis was achieved through heating $[CpRu(NCMe)_3]PF_6$ (**2.7**) and the corresponding arene at reflux in 1,2-dichloroethane to give the η^6-bound arene complex in high yield following recrystallisation from $MeCN/Et_2O$ (93%, Figure 2.7A). Confirmation of successful complexation to the metal was provided by multinuclear NMR spectroscopy, mass

spectrometry and elemental analysis. In addition, it was possible to obtain single crystals of a suitable quality for X-ray diffraction studies for complex **2.8** by layering a concentrated acetone solution with diethyl ether (Figure 2.7B). Complex **2.8** displays the expected pseudo-linear geometry about the Ru centre. The Ru–C6(plane) distance (1.711(3) Å) and Ru–C5(plane) distance (1.819(3) Å) are in agreement with structures of other similar sandwich complexes.[79] For crystal and structural refinement data, see *Appendix*.

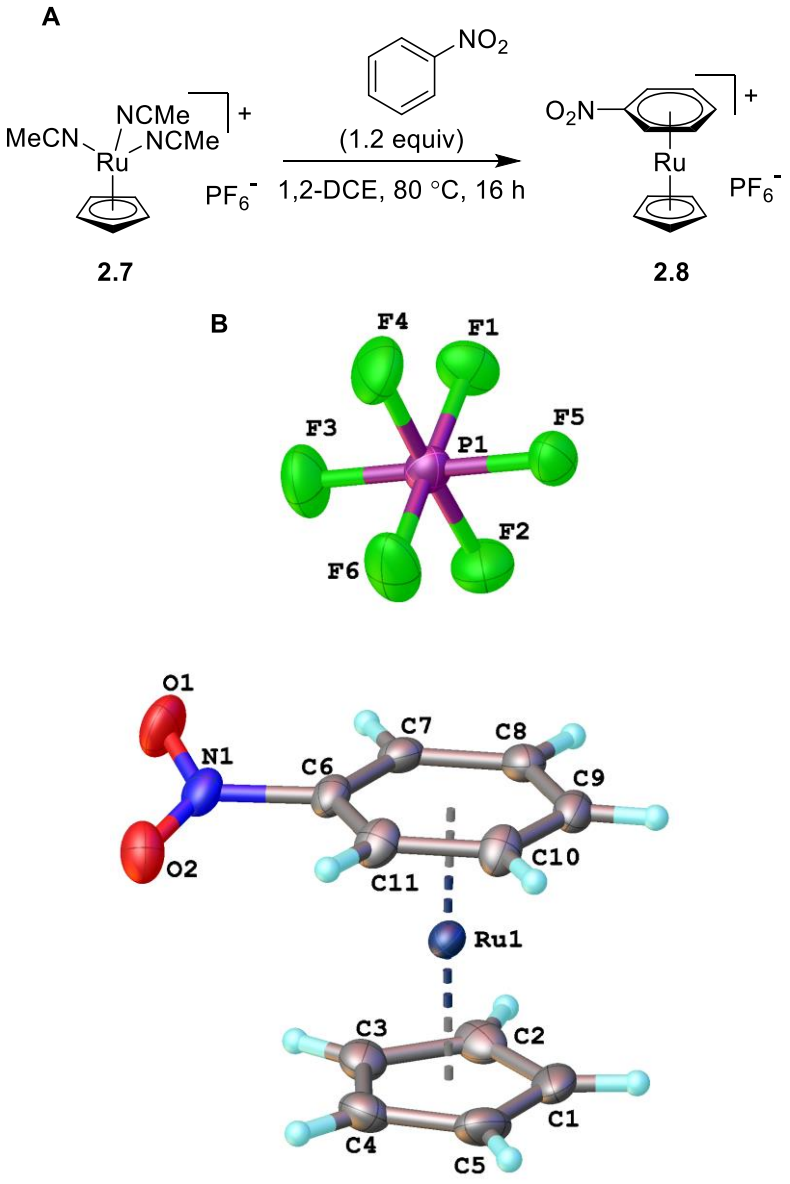

Figure 2.7 A *Synthesis and* ***B*** *molecular structure of [(η^6-nitrobenzene)RuCp]PF_6* ***(2.8)****; thermal ellipsoids are drawn at 50% probability level.*

2.2.2 Optimisation of trifluoromethylation reaction

In an attempt to achieve aryl trifluoromethylation, complex **2.8** was treated with Me_3SiCF_3 under similar conditions to those used by Bardin *et al.* previously for the substitution of pentafluoro-nitrobenzene (Table 2.1).[108] In order to activate Me_3SiCF_3 as a nucleophilic source of CF_3, a stoichiometric amount of F^- is required. Initial investigations using tetrabutylammonium fluoride (TBAF) as the source of F^- and anhydrous DMF as solvent resulted in low reaction conversions, likely due to water in the TBAF solution. However, when anhydrous KF was employed as the fluoride salt, the trifluoromethylation proceeded smoothly. Monitoring the reaction *in situ* by mass spectrometry showed complete consumption of starting material after 8 hours. ^{1}H- and ^{19}F-NMR spectroscopy of the reaction mixture prior to purification showed a mixture of two compounds.

Table 2.1 *Trifluoromethylation of complex **2.8** with Me_3SiCF_3. Conditions: starting material (0.2 mmol), Me_3SiCF_3 (1.1 equiv.), fluoride salt (1.1 equiv.). Conversions determined by ^{1}H-NMR, using α,α,α-trifluorotoluene as internal standard.*

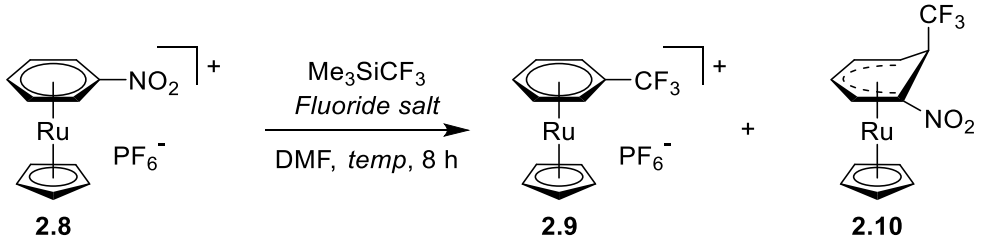

2.8 **2.9** **2.10**

Entry	Fluoride salt	Temp (°C)	Conv. (%)	Product ratio (**2.9**:**2.10**)
1	TBAF	25	0	-
2	KF	25	28	50:50
3	KF	0	64	50:50
4	KF	40	19	50:50
5[a]	KF	0	51	50:50

[a] Reaction was carried out in MeCN.

The two species were isolated by column chromatography and fully characterised. One of these species was confirmed to be the complex [(η^6-α,α,α-trifluorotoluene)RuCp]PF_6 (**2.9**), the product of nitro substitution by CF_3, *via* an S_NAr mechanism. To validate the formation of this complex, spectral comparison was carried out with a sample of [(η^6-α,α,α-trifluorotoluene)RuCp]PF_6 prepared by reaction between trifluoromethyl-benzene and [$(MeCN)_3$RuCp]PF_6.

The second species obtained from the crude reaction mixture was the Meisenheimer complex [(η^5-1-nitro-2-trifluoromethylcyclohexadienyl)RuCp] (**2.10**). This species is formed by the nucleophilic addition of ''CF_3^-'' to the carbon *ortho* to the aryl nitro group (mechanism and resonance forms in Figure 2.8). Notably, no *para*-directed addition was observed. This could be due to the inductive electron withdrawing effect of the nitro group making the ortho positions more electropositive and therefore a more likely site of nucleophilic attack.

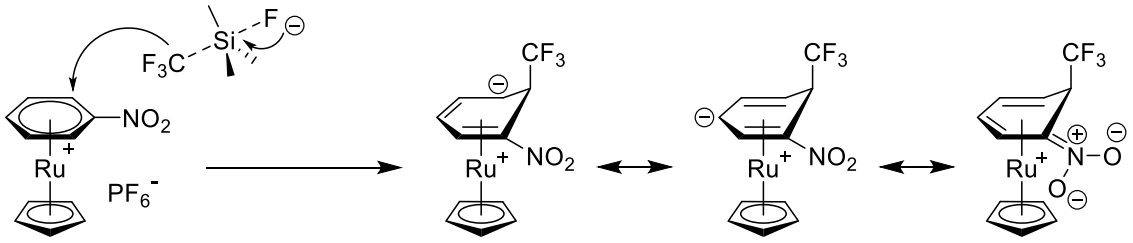

Figure 2.8 *Mechanism for the ortho addition of CF_3^- and the resonance forms of Meisenheimer complex* ***2.10***

Similar nucleophilic addition reactions have been observed for related η^6-arene transition metal complexes.[26,27,116,117] Multinuclear NMR, $HRMS^+$ and IR spectroscopy data were used to assign the Meisenheimer intermediate and confirmed the intact nitro group in the complex. Based on the ^{1}H-NMR coupling constants, the product of the exo-addition of the CF_3 moiety is exclusively observed. This is likely due to the steric bulk of the ruthenium metal centre and Cp ring restricting the endo attack of ''CF_3^-''. Figure 2.9 shows the shift assignment for the protons within the 6-membered ring, which additionally all shared correlation in COSY-NMR.

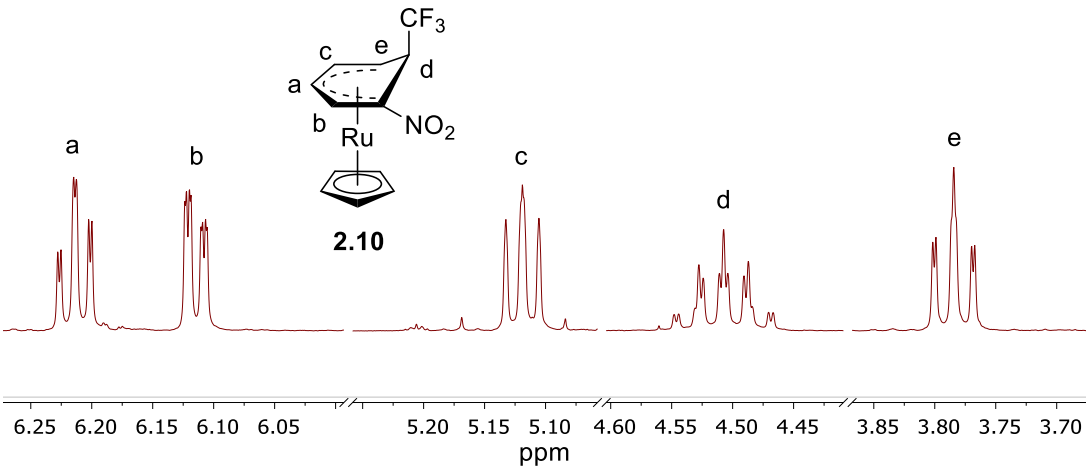

Figure 2.9 *^{1}H-NMR spectrum of Meisenheimer complex* ***2.10****. ($CO(CD_3)_2$, 298 K, 400 MHz).*

The significantly lower chemical shifts of these peaks are indicative of the broken aromaticity, and the introduction of fluorine brings about increased complexity in

splitting patterns. In particular, resonance ***d*** in Figure 2.9, which corresponds to the proton closest to the CF_3 group, appears as a quartet of doublets of doublets. This is due to $^3J_{H\text{-}F}$ coupling to the three fluorine atoms and two independent proton couplings ($^3J_{H\text{-}H}$ and $^4J_{H\text{-}H}$) to protons ***e*** and ***c*** respectively. Identifying this proton was imperative to the successful assignment of the compound, as this set a reference to follow with regards to following correlation in the COSY NMR. Linear correlation from resonance to resonance was observed in the COSY NMR which allowed assignment of the four remaining cyclohexadienyl protons. It is also worth considering that the sample of this complex collected would be a racemic mixture of two enantiomeric complexes, where the exo-addition occurs at the ortho carbon either side of the nitro group.

Under the initial conditions described above, analysis of the ^{1}H- and ^{19}F-NMR spectra suggests an approximate 1:1 ratio between complexes **2.9** and **2.10**. In an attempt to shift the ratio in which the two complexes are produced and probe if any thermodynamic or kinetic preference exists for either complex, the reaction was repeated using similar conditions at a variety of temperatures (Table 2.1, entries 2–4). While the product ratio was unaffected by the change in reaction temperature, it was found that lower temperatures increased the overall reaction yield, suggesting decreased reagent decomposition at lower temperature. This ratio of 1:1 is an interesting result, however. Should there be no favourability toward S_NAr or *ortho*-addition, one might expect a 1:2 ration respectively, as the number of addition sites is twice as many as substitution. In the case of this reaction then, there could be additional factors dictating how the reaction proceeds and further research is required to identify the nature of this selectivity.

2.2.3 Decomplexation of trifluoromethylated products

Following successful instalment of trifluoromethyl groups into $[(\eta^6\text{-arene})RuCp]^+$ complexes, the potential to liberate the functionalised arenes from their Ru complexes was investigated. Complex **2.9** was dissolved in deuterated acetonitrile and subjected to ultraviolet irradiation (Figure 2.10A). Photolysis was monitored by ^{1}H-NMR and revealed 90% decomplexation of α,α,α-trifluorotoluene **2.11** after 8 h irradiation (365 nm), along with an equimolar quantity of $[CpRu(NCCD_3)_3]^+$.

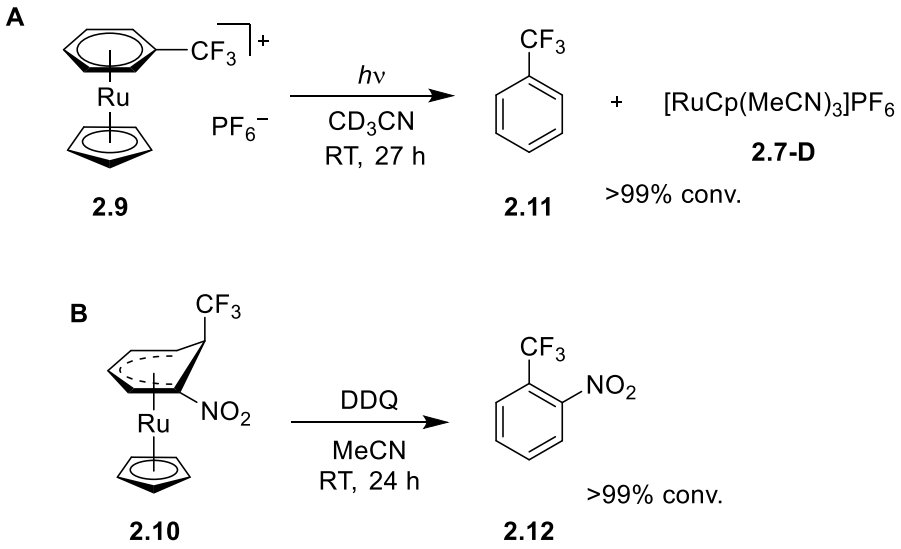

Figure 2.10 *Liberation of trifluoromethylated arene products by* ***A*** *Photolysis and* ***B*** *oxidation.*

This Ru species is the MeCN-d_3 analogue of the Ru complex used to synthesise complex **2.8**, highlighting the ability to recycle the activating Ru complex. After 27 h, quantitative conversion had been achieved (Figure 2.11). In the figure, the empty and filled squares correspond to the aromatic *ortho*-protons of the bound arene and liberated arene respectively. The empty and filled circles correspond to the bound Cp ligand of the arene sandwich complex and the trisacetonitrile piano-stool complex respectively.

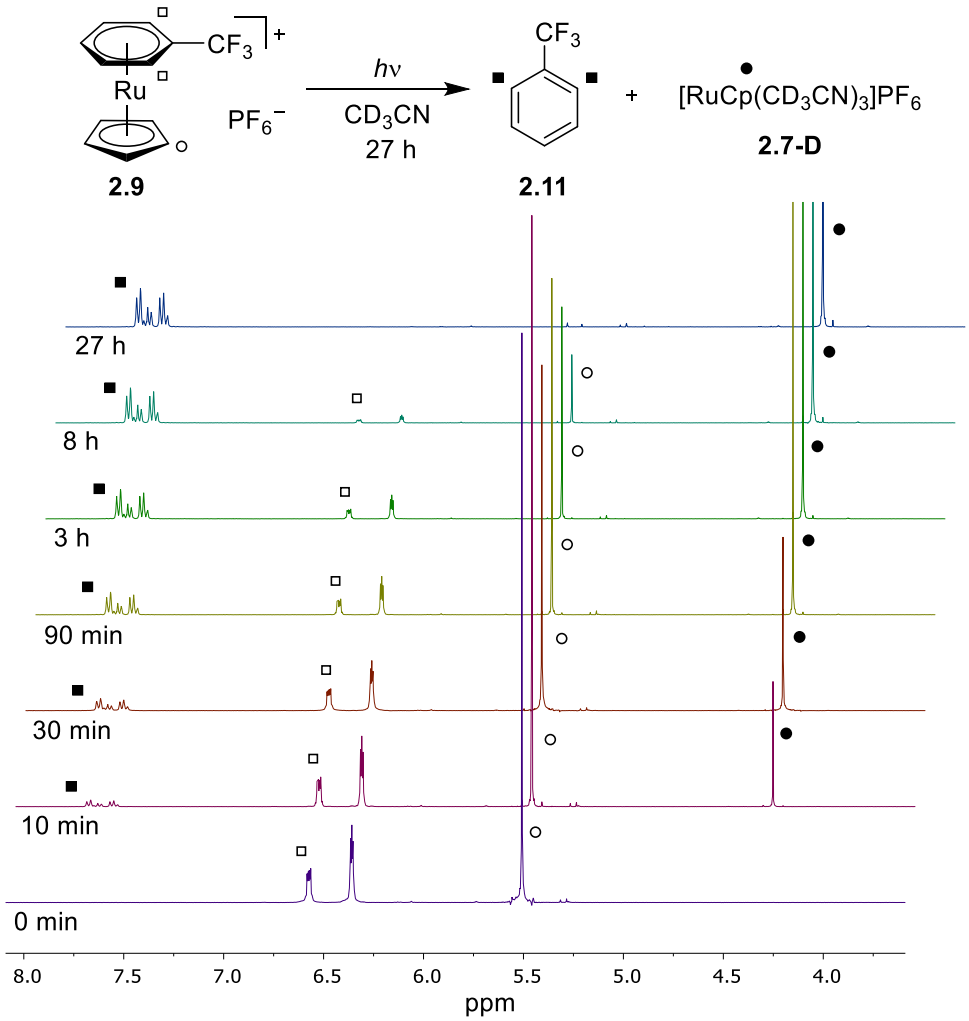

Figure 2.11 *Stacked ^{1}H-NMR spectra (CD_3CN, 298 K, 400 MHz) for the photolysis of complex* ***2.9****.*

We hypothesised that oxidation of the Meisenheimer complex **2.10** would lead to a disubstitued η^6-coordinated aromatic complex. A range of oxidising agents showed no reactivity with **2.10**, including trityl chloride (Ph_3CCl), trityl tetrafluoroborate (Ph_3CBF_4) and pentachlorophosphate (PCl_5), while reaction with nitrosyl tetrafluoroborate ($NOBF_4$) gave a mixture of unassignable products. Treatment of **3** with 2,3-dichloro-5,6-dicyano-1,4-benzoquinone (DDQ), however, led to successful oxidation and decomplexation to give quantitative conversion to the unbound arene, 1-nitro-2-trifluoromethylbenzene **2.12** (Scheme 2.10B).

Overall this reaction is a regioselective, mild C–H activation and trifluoromethylation of nitrobenzene. Importantly, when unbound nitrobenzene is treated under the same trifluoromethylation conditions, no reaction is observed, confirming the importance of the $[CpRu]^+$ fragment, which is essential to facilitate both the S_NAr reaction and the ortho addition reaction.

2.2.4 Exploring the scope of the trifluoromethylation protocol

To determine the versatility of our trifluoromethylation method, a selection of alternative arenes were investigated under the optimised reaction conditions (Table 2.2). Several Ru complexes were synthesised, incorporating η^6-bound substituted arenes, including 4-nitrotoluene, cyanobenzene, benzoic acid, 4-chlorotoluene, fluorobenzene and trifluoromethylbenzene.

Table 2.2 *Trifluoromethylation of various Ru complexes with Me_3SiCF_3. Conditions: starting material (0.2 mmol), Me_3SiCF_3 (1.1 equiv.), KF (1.1 equiv.). Conversions determined by ^{1}H-NMR, using α,α,α-trifluorotoluene as internal standard.*

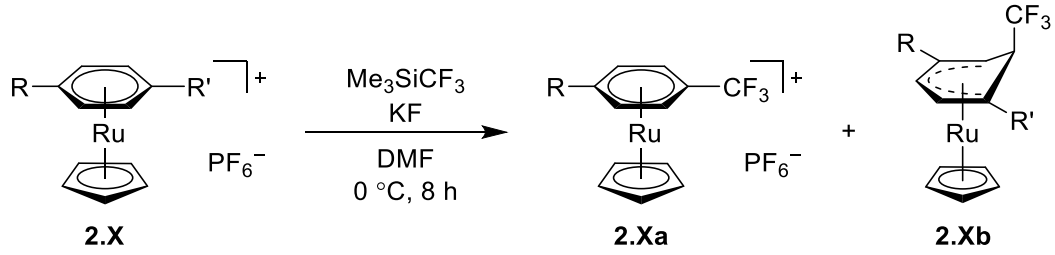

X	R	R'	Conv. (%)	Product ratio (a:b)
13	CH_3	NO_2	61	50:50
14	H	CN	26	0:100
15	CH_3	Cl	12	0:100
16	H	CH_3	10	0:100
9	H	CF_3	0	-
17	H	CO_2H	0	-
18	H	H	22[a]	0:100
19	H	F	0[b]	-

[a] Carried out at 40 °C. [b] Reaction with fluorobenzene complex resulted in slow hydrolysis and formation of bound phenol complex.

Each new complex was subjected to the trifluoromethylation conditions. Reaction of [(η^6-4-nitrotoluene)RuCp]PF_6 **2.13** gave a 1:1 mixture of substitution product (**2.13a**, R = CH_3) and Meisenheimer complex (**2.13b**, R = CH_3, X = NO_2). The observation that the substitution product is a single regioisomer provides confirmation of an S_NAr mechanism, in which initial attack of the CF_3 moiety occurs at the nitro-bound carbon. Reaction with the cyanobenzene complex **14** gave exclusively the Meisenheimer complex (**2.14b**, R = H, X = CN). The absence of any substitution product is consistent with the poorer leaving group ability of the cyano group. This highlights the potential for a selective C–H activation and trifluoromethylation and also demonstrates the versatility of

the mild activation protocol. Exclusive formation of the Meisenheimer intermediate was also observed for 4-chlorotoluene- and toluene-bound complexes, albeit in low conversion (Table 2.2, **2.15b** and **2.16b**). The benzene complex reacted to give 22% conversion to the Meisenheimer complex, but required heating at 40 °C to ensure solubility of the starting complex. No reaction was observed with the other arene complexes tested, with the exception of the fluorobenzene complex, which undergoes slow hydrolysis to the phenol complex.

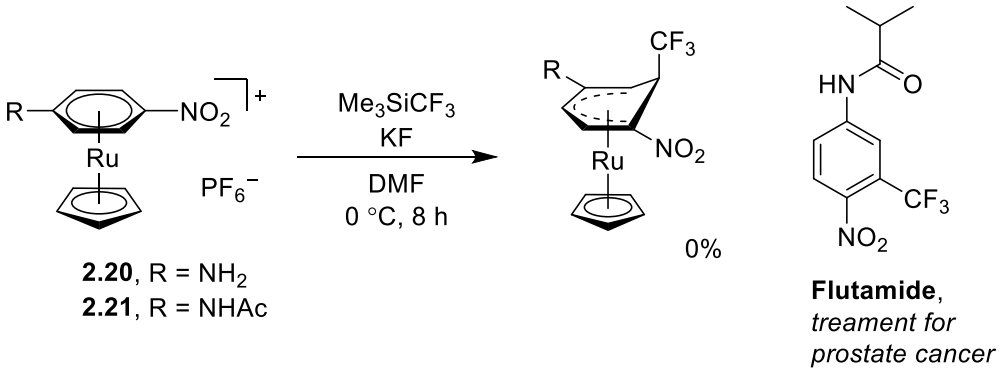

Figure 2.12 *Attempt at late-stage trifluoromethylation towards the synthesis of flutamide.*

Flutamide is currently used to treat prostate cancer, and this transformation seemed a promising late stage trifluoromethylation technique towards the synthesis of this compound. In an attempt to scope the pharmaceutical applicability of this reaction, complexes **2.20** and **2.21** were tested under the optimised conditions. These complexes were synthesised using the standard procedure of heating the free arenes, 4-nitroaniline and 4-nitroacetanilide, with $[Ru(NCMe)_3Cp]PF_6$. Unfortunately, no reaction with Me_3SiCF_3 was observed for both complexes, likely due to the electron donating nature of the bound amine and amide groups reducing the electrophilicity of the ring. Further development of the reaction conditions is required in order to achieve a process towards the synthesis of flutamide, but this method shows promise for the late-stage installation of CF_3 groups into arenes.

2.3 Conclusions

In summary, this chapter presents the trifluoromethylation of a number of electron deficient arenes using Me_3SiCF_3, facilitated by η^6-coordination to $[CpRu]^+$. Under the optimised reaction conditions, nitrobenzene is converted to two products in a 1:1 ratio; the product of an S_NAr reaction to give complex **2.9**, and an ortho-addition reaction to

give Meisenheimer complex **2.10**. The substitution product, trifluoromethylbenzene **2.11**, is isolated by photolysis, with recovery of the $[RuCp]^+$ activating group. The C–H activation product, trifluoromethyl-nitrobenzene **2.12**, can also be isolated following oxidation of the Meisenheimer intermediate with DDQ. The trifluoromethylation proceeds under very mild conditions and liberation of the bound arenes from their corresponding complexes is high yielding. To our knowledge, this method of trifluoromethylation of arenes using Me_3SiCF_3 facilitated by the η^6-binding to a Ru metal fragment is the first of its kind and could be applied to the late-stage functionalisation of pharmaceuticals and agrochemicals. Furthermore, the ability to produce 1,2-substituted trifluoro-nitroarenes may lead to compounds with enhanced efficacy.

3. C–H activation of π-arene ruthenium complexes

3.1 Introduction

3.1.1 C–H activation in organic synthesis

The activation of C–H bonds in organic chemistry is a highly desirable method of manipulating chemical structures. Typical formation of new C–C or C–heteroatom bonds derives from two compatible functional groups which when reacted together create a new structure in the compound. However, there are a number of attractive benefits if these bonds can be made using C–H bonds as one or both of these functional groups. Firstly, any preparation of common bond forming functional groups (halides, esters, aldehydes, amines, etc.) is circumvented which improves the step economy of the bond forming step. Similarly, without the traditional functional groups, the reaction will be more atom economic with regards to the by-products. The field of C–H activation is enormous and hundreds of publications are released annually on this topic. In this brief review, the challenges facing C–H activation will be described and, in particular, efforts to functionalise arenes through C–H activation.

3.1.2 Challenges in C–H activation

Successful C–H functionalisation holds a number of challenges. Due to the inertness of C–H bonds, reaction conditions for the bond-cleavage are typically very harsh, which limits the scope of functionalisation reactions and functional group tolerance. Reactions must also be site- and stereoselective so that bond formation is predictable and precise. C–H bonds are typically very abundant in the majority of molecules, so organic chemists must design sophisticated systems to target accurately the point at which functionality is to be installed within these molecules. In 2011, Gutekunst and Baran wrote a critical review discussing a historical collection of C–H functionalisation strategies that exemplify the efficacy of C–H activation in total synthesis.[118] Since then, review journals have dedicated entire issues to pay tribute to this colossal field and how it has transformed organic synthesis.[119,120] With a focus on the project to which this chapter is dedicated, the discussion herein will contain only examples of arene functionalisation.

3.1.3 Arene activation towards C–H activation

The C–H activation of arenes is well researched due to the abundance of the benzene group in pharmaceuticals, agrochemicals and materials. However, for the vast majority of

C(sp^2)–H activation procedures, only a specific range of substrates can facilitate reactions. These substrates fall into three categories; arenes which incorporate a directing group into their structure, arenes which are inherently electron-rich and, lastly, arenes that are electron-deficient.

3.1.3.1 Arene activation using a directing group

This strategy uses a directing group designed into the structure of the substrate which anchors a transition metal catalyst into position for C–H activation (Figure 3.1). A coordinating functionality, typically amido and pyridine moieties, will bind to the transition metal and create proximity between the metal and C–H bond target, which can then react to form a cyclometalated intermediate. Activation of this kind commonly takes place *ortho* to the directing group,[121–123] however examples of *meta* and *para* directed C–H activation have also been published.[124–127]

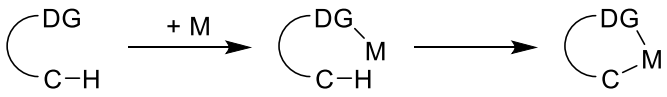

Figure 3.1 *General pathway for transition metal mediated C–H activation via directing group.*

Following the activation of the C–H bond, substitution of the metal creates new C–C, C–N and C–O bonds. The most utilised transition metal for these types of transformations is palladium,[122,128] which has been extensively studied over the last few decades.[129,130] A recent report from Yu *et al.* showed *ortho*-C–H functionalisation of benzaldehydes using transient directing groups.[131] One issue with directing groups is removal of the particular functional group used to facilitate the C–H bond, should it not be present in the desired final structure. This publication shows how this is circumvented using a catalytic amount of 2-methylalanine, which forms a transient imino acid in the reaction and directs the C–H activation (**3.1**, Figure 3.2). The use of transient directing groups in synthesis *via* C–H activation was recently reviewed by Gandeepan and Ackermann.[132]

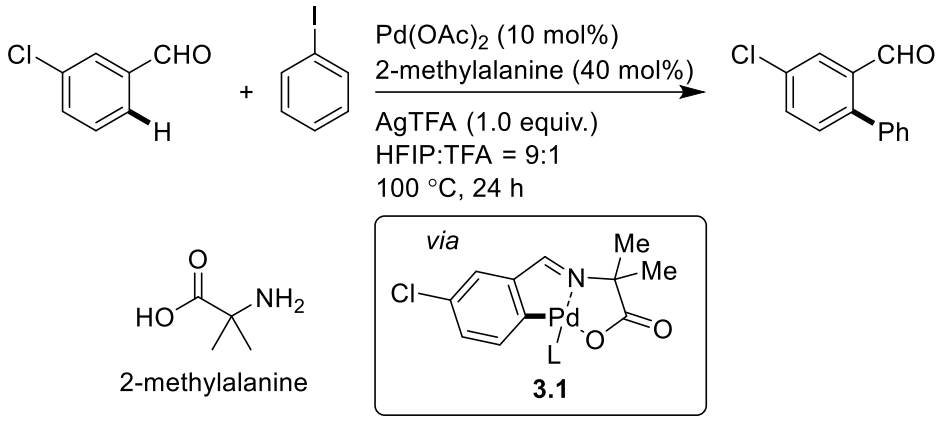

Figure 3.2 *ortho-C–H Arylation of benzaldehydes using cat. Pd and 2-methylalinine as a transient directing group.*

While palladium is commonplace for this type of activation, examples using other metals have been reported, including Ru,[121] Rh[123] and Ir.[125,133] A recent publication from the Glorius group describes the rhodium catalysed *ortho* C–H activation to synthesise 1-aminoindolines (Figure 3.3).[123] In the catalytic cycle, the Boc-bound nitrogen coordinates to the Rh metal and orchestrates the C–H activation to form the 5-membered cyclometalated intermediate. This intermediate then reacts with the chosen alkene substrate through coordination then insertion to create the new C–C bond.

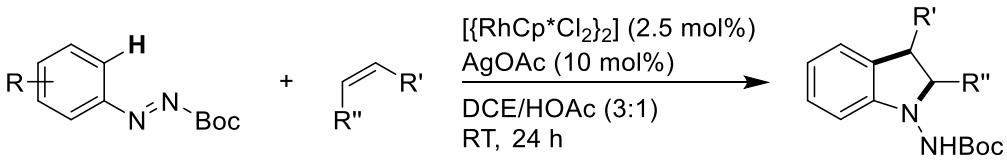

Figure 3.3 *Rhodium-catalysed synthesis of 1-aminoindolines from aryl-substituted diazenecarboxylates and alkenes.*

3.1.3.2 Arene activation of electron-rich arenes

In the case of electron-rich arenes, is it possible to directly activate C–H bonds through electrophilic metalation. Aromatic heterocycles hold an inherent electronic selectivity toward specific C–H bonds due to their structure. This allows regioselective activation without the need for directing groups. A number of excellent reviews have been written to discuss direct arylation of a range of heteroaromatic compounds.[134–136] These reviews highlight the in-built regioselectivity achieved for C–H activation protocols due to the electronic bias of the heterocycles. An example from the Sames group shows how indoles hold an intrinsic selectivity for the C2 position, and the phosphate free arylation reaction is able to synthesise a host of arylated indoles in moderate to good yields (Figure 3.4).[137]

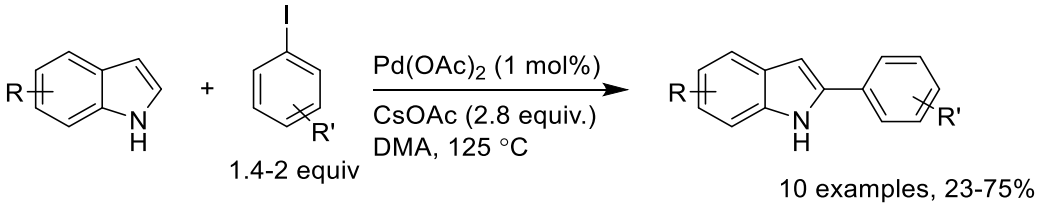

Figure 3.4 *Phosphine-free palladium-catalysed C–H bind arylation of free (N–H)-indoles.*

A report in 2008 from Rossi *et al.* showed how 1-methyl-1*H*-imidazoles can be selectively arylated at the C5 position of the imidazole using a palladium catalyst (Figure 3.5).[138]

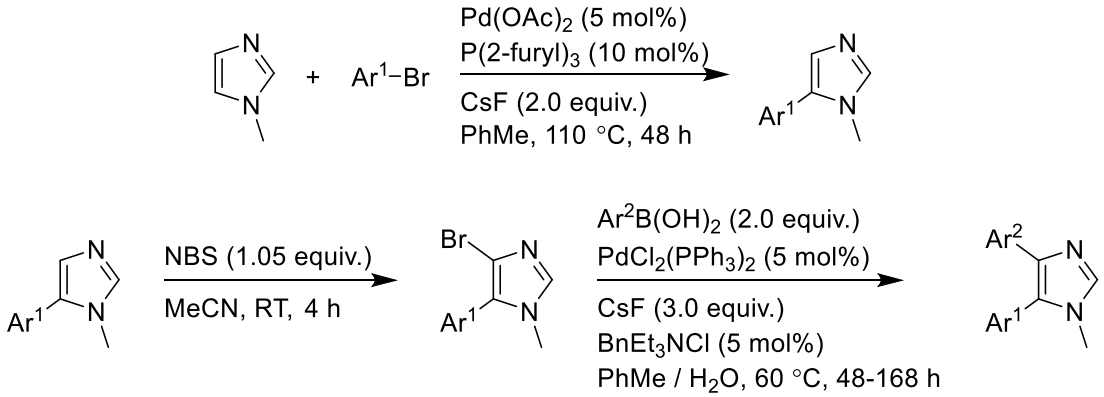

Figure 3.5 *Regioselective synthesis of 4,5-diaryl-1-methyl-1H-imidazoles by Pd-catalysed direct C-5 arylation of 1-methyl-1h-imidazole with aryl bromides.*

Following the initial arylation at C5, bromination at C4 using N-bromosuccinimide and sequential Pd-catalysed arylation with aryl boronic acids affords a library of 4,5-diaryl-1-methyl-1H-imidazoles. The development of this general procedure using commercially available materials allows access to electron-rich and electron-deficient arene bearing imidazoles with high yields and high regioselectivity. Two of the products prepared in this study were also found to have excellent cytotoxicity against human tumour cells lines.

3.1.3.3 Arene activation of electron-deficient arenes

Lastly, electron-deficient aromatics which bear a sufficiently acidic proton can also be directly activated. This mechanism was discovered and developed by Fagnou, with the first report being published in 2006, which demonstrated the palladium-catalysed direct arylation of perfluorobenzenes (Figure 3.6).[139]

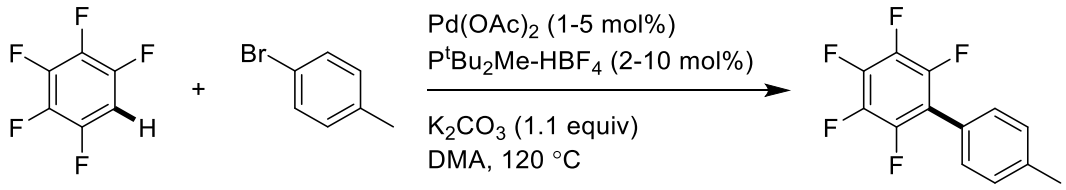

Figure 3.6 *Catalytic intermolecular direct arylation of perfluorobenzene.*

This seminal paper showed a direct trend between reactivity and arene acidity, which was demonstrated in two ways. Firstly, the reaction showed decreasing yields as fluorine atoms were removed from the substrates, indicating that the acidity is vital to the C–H activation. Also, in substrates with more than one chemically distinct C–H bond, activation would preferentially occur at the more acidic position, *ortho* to a fluorine atom. Computational studies suggested that there was no interaction between the fluorine atoms and the palladium, and so a concerted metalation reaction mechanism was suggested. This concerted metalation-deprotonation mechanism has been further developed over the last decade, as will be discussed below.

3.1.4 Concerted Metalation-Deprotonation (CMD) mechanism

Exploration into the CMD mechanism continued in the Fagnou group, and in 2008 it reported further analysis of the mechanism across a broad range of aromatic substrates.[140] Using both experimental and DFT results, they concluded that energetic costs and gains associated with arene distortion and bringing the two compounds together have a profound effect on the formation of the CMD transition state **3.2** (Figure 3.7).

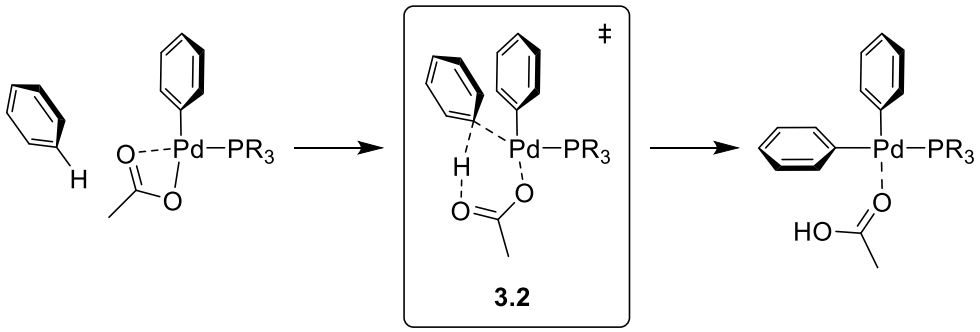

Figure 3.7 *Formation of CMD transition state to form C–H activated arene-Pd complex.*

It was also found that in computational simulation, proton abstraction to the acetate ion *via* this transition state gave results most consistent with experimental data and the lowest energy-barrier.[139] Although this work from Fagnou pioneered a new mechanism for direct arene activation, it still relied on sufficient activation from covalently bound electron-

withdrawing groups to mediate reactivity. More electron-rich arenes like benzene failed to be activated under these conditions *via* a CMD mechanism.[140] In 2013 however, Larrosa *et al.* was the first group to achieve C–H activation of more electron-rich arenes by activating the arenes *via* π-complexation. As already discussed, arenes that are bound in an η^6-fashion to transition metals have increased aromatic proton acidity due to the net electron-withdrawing effect of the bound metal. Larrosa was able to perform C–H activation on a number of [(η^6-arene)$Cr(CO)_3$)] complexes to give the arylated products through a CMD mechanism (Figure 3.8).[15]

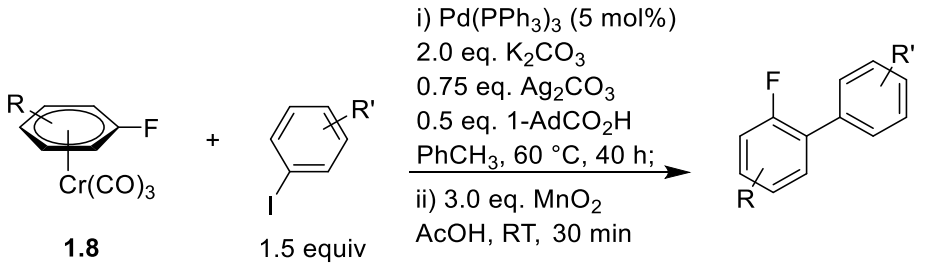

Figure 3.8 *Pd-catalysed direct arylation of [(η^6-fluoroarene)$Cr(CO)_3$)] complexes with iodoarenes.*

Reaction proceeded for a range of [(η^6-fluoroarene)$Cr(CO)_3$)] complexes with a range of iodoarenes, but a limitation of this protocol was that a covalently bound fluorine atom was required to generate good yields from the reaction. The analogous reaction with [(η^6-benzene)$Cr(CO)_3$)] achieved a yield of 42%, showing a potential for a broader scope of aromatic C–H activation through π-complexation. Four years later, in 2017, Larrosa further developed this procedure and designed a route to medium sized bi-aryl rings using similar arene activation (Figure 3.9).[141]

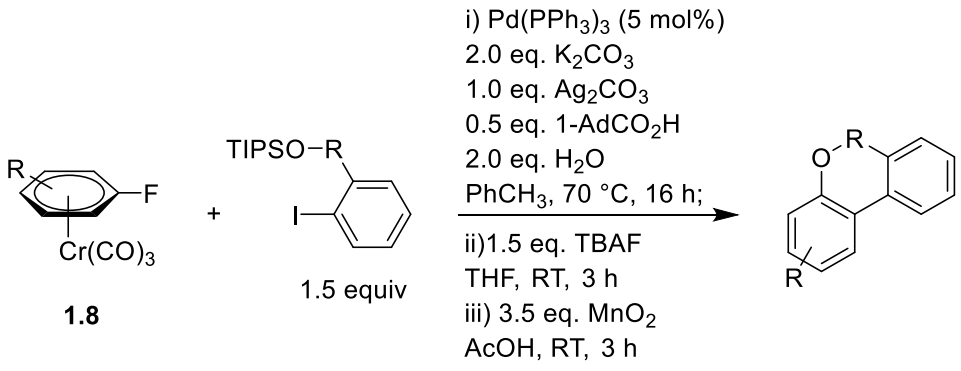

Figure 3.9 *Direct arylation-cyclisation reaction for the construction of medium-sized rings.*

Firstly, the [(η^6-arene)$Cr(CO)_3$)] complexes undergo arylation using Pd-catalysis with an iodoarene bearing a triisopropylsilyl ether (TIPS) protected alcohol substituent. Then, reaction with TBAF deprotects the alcohol and causes the intramolecular cyclisation *via* S_NAr. However, limitations to the work from Larrosa is the wasteful use of stoichiometric

amounts of chromium and excess of manganese. The Walton group envisions that a $[RuCp]^+$ binding unit can facilitate analogous reactivity to the chromium complexes developed by Larrosa, while having the potential for catalytic turnover. This chapter will describe the stoichiometric C–H activation of $[(\eta^6\text{-arene})\ RuCp]PF_6$ complexes and steps towards a catalytic process *via* an arene exchange mechanism.

3.2 Results and Discussion

3.2.1 Synthesis of initial π-complex $[(\eta^6\text{-}o\text{-fluorotoluene})RuCp]PF_6$

Investigation began with the C–H activation of *ortho*-fluorotoluene through η^6-binding to $[RuCp]^+$. Through similar chemistry described in *Chapter 2*, complex **3.3** was synthesised by reacting the unbound arene with commercially available piano stool complex $[RuCp(MeCN)_3]PF_6$ **2.7**. The complexation was confirmed by multinuclear NMR, high-resolution mass spectrometry and C,H,N elemental analysis. The NMR spectrum in Figure 3.10 shows the shifts for the four ring protons, the Cp ring and the methyl group of complex **3.3**. The aromatic protons appear at lower frequency, indicative of η^6-binding, and the shift at 2.52 ppm for the methyl group is a narrow doublet due to long range couple to the adjacent fluorine atom (J = 1.5 Hz).

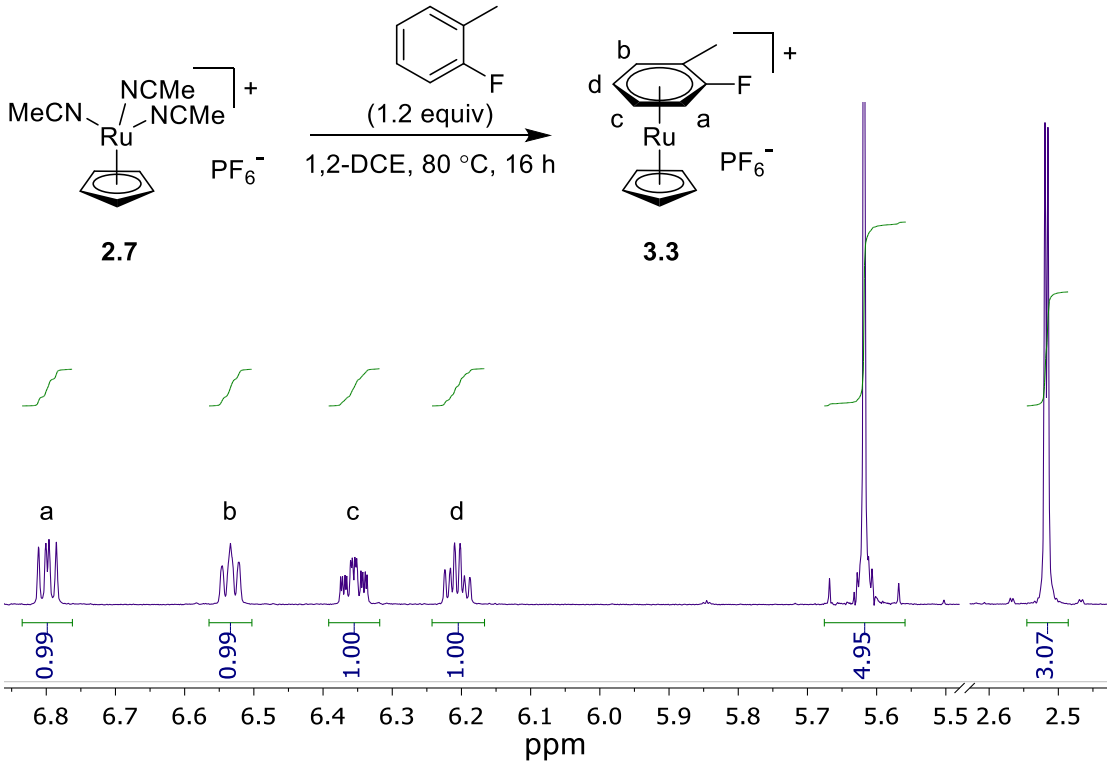

Figure 3.10 *Synthesis of $[(\eta^6\text{-}o\text{-fluorotoluene})RuCp]PF_6$* ***3.3*** *and its ^{1}H-NMR spectrum ($CO(CD_3)_2$, 298 K, 400 MHz).*

3.2.2 Optimisation of C–H activation reaction *conducted by Dr Luke Wilkinson*

With this complex in hand, extensive experimentation began to determine the best reaction conditions to achieve C–H activation. Optimisation studies for the sources of palladium and silver, phosphine ligand and carboxylic acid were undertaken, as well as establishing the optimal stoichiometries of each reagent (Table 3.1). In addition to that shown below, screens for base, solvent and temperature were also performed to determine optimal conditions for the reaction.[82]

Table 3.1 *Establishing optimised reaction conditions for the C–H activation of complex* ***3.3*** *and coupling to 4-iodoanisole.*[a]

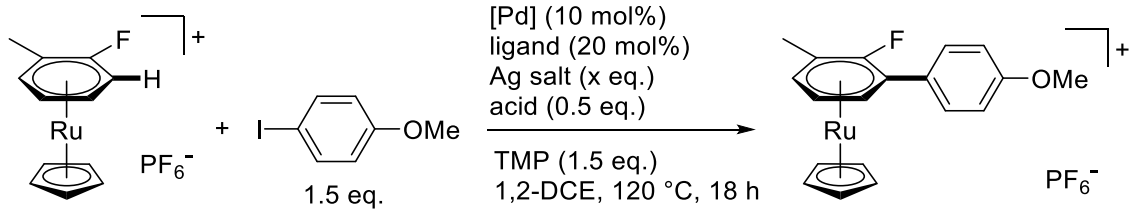

3.3 **3.4**

Entry	[Pd]	ligand	acid	Ag salt (equiv)	Conversion (%)
1	$PdCl_2$		1-$AdCO_2H$	Ag_2CO_3 (0.75)	30
2	$PdCl_2$	dppe	1-$AdCO_2H$	Ag_2CO_3 (0.75)	51
3	$Pd_2(dba)_3$		1-$AdCO_2H$	Ag_2CO_3 (0.75)	10
4	$Pd_2(dba)_3$	dppe	1-$AdCO_2H$	Ag_2CO_3 (0.75)	34
5	$Pd_2(dba)_3$	DavePhos	1-$AdCO_2H$	Ag_2CO_3 (0.75)	28
6	$Pd(OAc)_2$		1-$AdCO_2H$	Ag_2CO_3 (0.75)	16
7	$Pd(OAc)_2$	SPhos	1-$AdCO_2H$	Ag_2CO_3 (0.75)	49
8	$Pd(OAc)_2$	DavePhos	1-$AdCO_2H$	Ag_2CO_3 (0.75)	69
9	$Pd(OAc)_2$	DavePhos		Ag_2CO_3 (0.75)	8
10	$Pd(OAc)_2$	DavePhos	PivCO_2H	Ag_2CO_3 (0.75)	17
11	$Pd(OAc)_2$	DavePhos	1-$AdCO_2H$		0
12	$Pd(OAc)_2$	DavePhos	1-$AdCO_2H$	AgOTf (1.50)	2
13	$Pd(OAc)_2$	DavePhos	1-$AdCO_2H$	Ag_2O (0.75)	22
14	$Pd(OAc)_2$	DavePhos	1-$AdCO_2H$	Ag_2CO_3 (0.50)	29
15	$Pd(OAc)_2$	DavePhos	1-$AdCO_2H$	Ag_2CO_3 (1.00)	74
16	**$Pd(OAc)_2$**	**DavePhos**	**1-$AdCO_2H$**	**Ag_2CO_3 (2.00)**	**83**

[a]Reaction optimisation carried out by Dr Luke A. Wilkinson. Conversions to **3.4** were determined by ^{1}H- and ^{19}F-NMR against an internal standard.

Although C–H activation was observed without the use of phosphine ligands, regardless of initial Pd species (entries 1, 3 and 6), the use of these ligands significantly increased the conversion to the coupled complex. The carboxylic acid was also imperative to the reaction, as conversion decreased dramatically when no acid was added (entry 9). 1-Adamantanecarboxylic acid was the best performing (entry 8) and its role will be discussed in more detail later in this chapter. Lastly, an exploration of a number of silver salts found Ag_2CO_3 gave the highest conversion, but using two equivalents achieved 83%, which established the optimised conditions for this process.

Any study following this reaction optimisation was conducted by the PhD candidate.

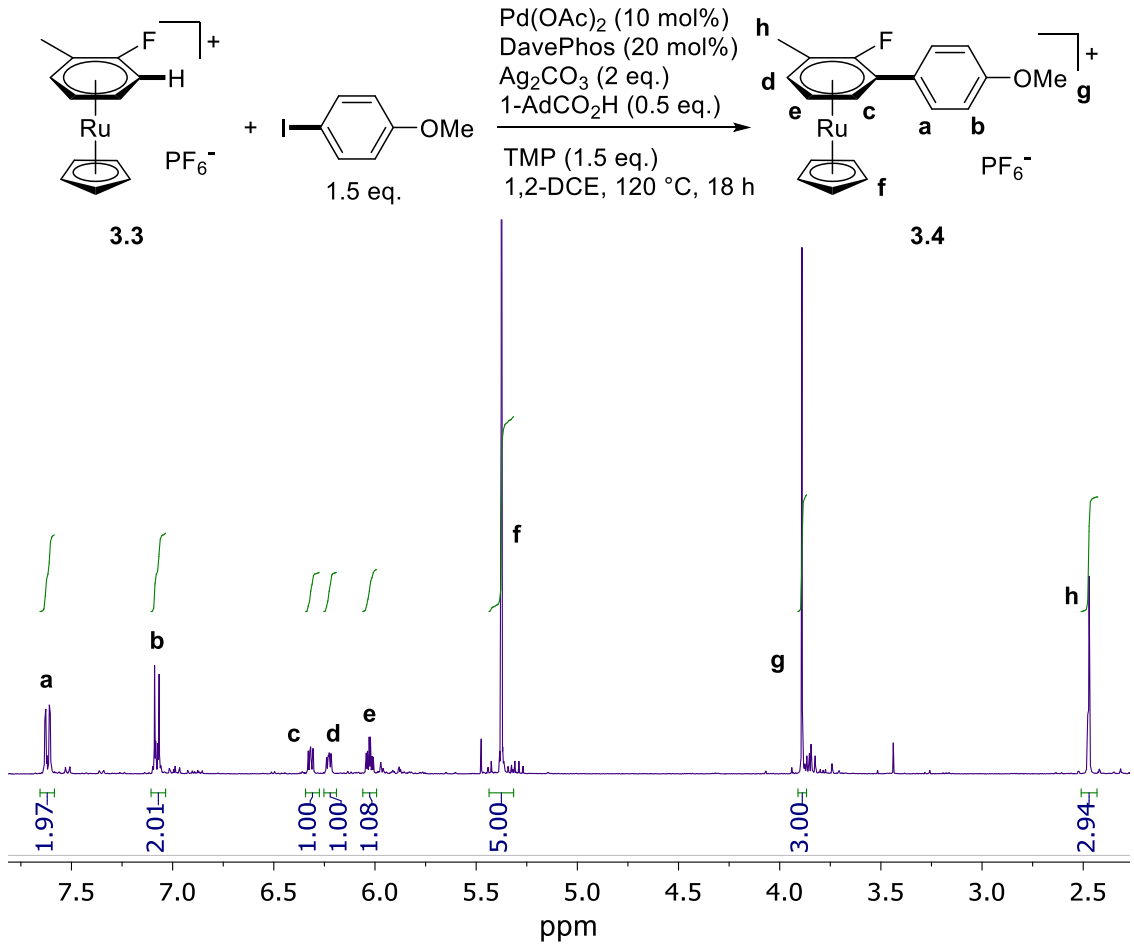

Figure 3.11 *C–H activation under optimised conditions to synthesis complex* ***3.4*** *and its* ^{1}*H-NMR spectrum (*CD_3CN*, 298 K, 400 MHz).*

With optimised conditions in hand, a larger scale reaction using 100 mg of starting complex was carried out. The resulting coupled complex **3.4** was isolated by flash column chromatography and fully characterised by ^{1}H- and ^{13}C-NMR and high-resolution mass spectrometry. Analysis of the proton NMR spectrum strongly supported the formation of complex **3.4** (Figure 3.11). The number of metal-bound aromatic protons, indicative of

η^6-binding due to their lower ppm as discussed above, had reduced from four to three when compared to starting material **3.3**. Two new shifts in the free-aromatic region had appeared, along with the appearance of a new methoxy-group shift at 3.89 ppm, which correspond to the coupled aryl moiety. This combined with the observed m/z spectroscopy ion corresponding to $[M\text{-}PF_6]^+$ for complex **3.4**, which displays a ruthenium isotope pattern, confirmed the successful synthesis of the complex.

3.2.3 Exploring the scope of the C–H activation reaction

To explore the scope of the C–H activation protocol under optimised conditions, a number of aryl halides were tested with complex **3.3**, alongside a library of $[(\eta^6\text{-arene})RuCp]^+$ complexes tested with 4-iodoanisole (Table 3.2). The synthesis of the tested complexes is shown in Table 3.3. Firstly, other halo-anisoles were tested, and while 4-bromoanisole successfully coupled to complex **3.3**, no reaction was observed with 4-chloroanisole (**3.4b** and **3.4c**). The trend of ArI > ArBr > ArCl is consistent with an oxidative addition mechanism of aryl halides to Pd species, which follows the bond dissociation energy of the C–X bond.[142,143] Next, a number of iodo-arenes were tested under optimised conditions and achieved conversions ranging from 0-83%. More electron-rich aryl iodides tended to react more successfully (**3.5**, **3.6**, **3.8** and **3.9**), while electron poor substrates gave lower conversions (**3.7**). In the case of complex **3.8**, only 11% conversion was observed, likely due to the steric bulk restricting coupling. Electron-deficient arenes tend to undergo oxidative addition more readily, so a plausible explanation to the conversions observed is that more electron-rich Pd–Ar species can transmetalate more efficiently. A proposed mechanism of the reaction will be discussed in more detail later.

Next, a library of $[(\eta^6\text{-arene})RuCp]^+$ complexes were reacted with 4-iodoanisole. The reaction with fluorobenzene complex gave good conversion to the mono-substituted product, with a small amount of disubstituted product observed where both *ortho* C–H bonds are activated (**3.10**). No reaction was observed for nitro- and chloro-complexes (**3.11** and **3.13**), but C–H activation was achieved for the CF_3 complex (**3.12**). A very encouraging result was the successful activation of benzene and *p*-cymene complexes, albeit at low conversions (16% and 20% for **3.14** and **3.15** respectively). As discussed above, the C–H activation of arenes typically requires covalently-bound directing or activating groups, so to see the successful activation of these covalently-unactivated

arenes with this protocol is very promising. The isolated yields shown in Table 3.2 are low due to the scale of the reactions, where just 15 mg of starting complex was used.

Table 3.2 *C–H activation between various [(η⁶-arene)RuCp]⁺ complexes and aryl halides under optimised reaction conditions.*[a]

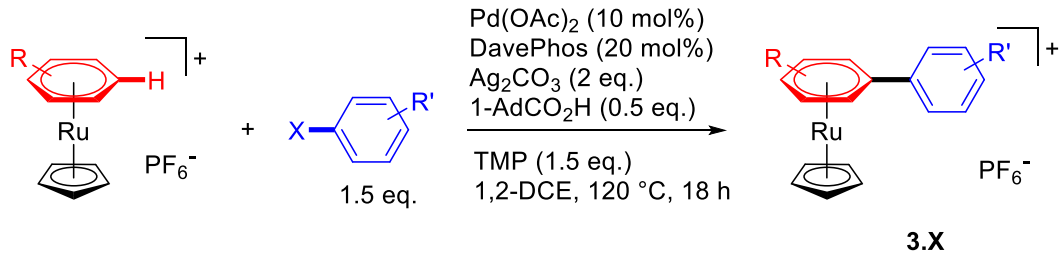

3.X

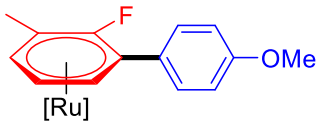

3.4a, 83% (33%)

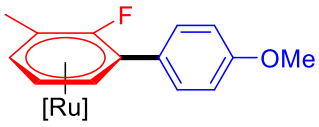

3.4b, 52% (29%)[b]

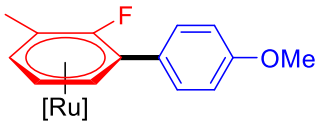

3.4c, 0%[c]

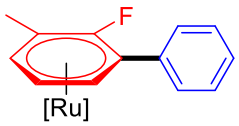

3.5, 68% (15%)

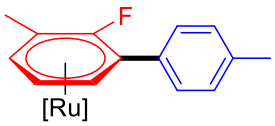

3.6, 61% (8%)

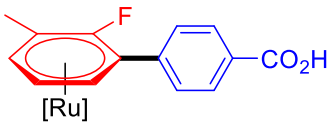

3.7, 6%

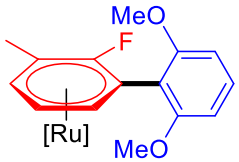

3.8, 11%

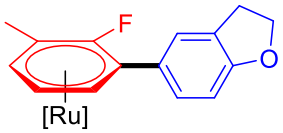

3.9, 54% (5%)

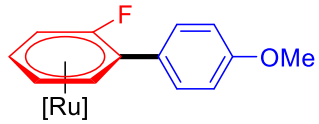

3.10, 60% (10%)[d]

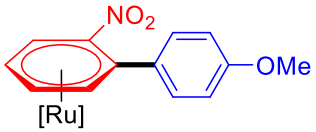

3.11, 0%

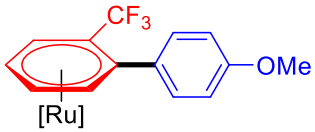

3.12, 10%

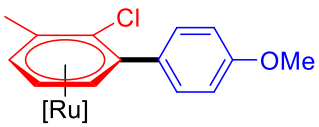

3.13, 0%

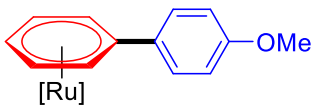

3.14, 16%

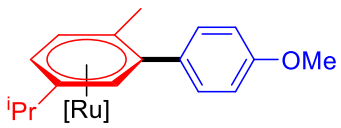

3.15, 20%

[a]Conversions were determined by ^{1}H- and ^{19}F-NMR against an internal standard. Isolated yields are given in parentheses. Reactions with conversions less than 20% were not isolated. [b]4-Bromoanisole used as substrate. [c]4-Chloroanisole used as substrate. [d]Reaction of fluorobenzene complex gave an additional 5% formation of disubstituted product.

Table 3.3 *Synthesis of [(η⁶-arene)RuCp]PF₆ complexes for C–H activation.*

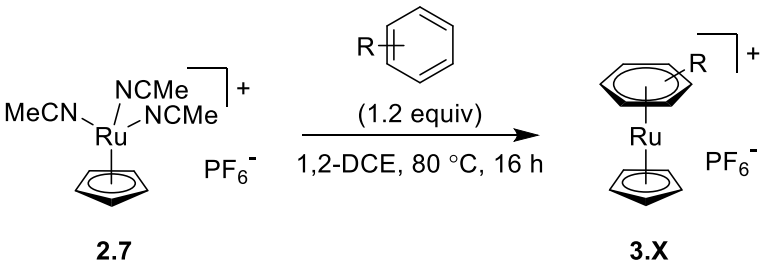

2.7 **3.X**

Compound	Arene	Yield
3.3	*o*-fluorotoluene	90%
2.19	fluorobenzene	82%
2.8	nitrobenzene	93%
2.9	α,α,α-trifluorotoluene	91%
3.16	*o*-chlorotoluene	97%
3.17	*p*-cymene	94%

3.2.4 Recovery of $[(MeCN)_3RuCp]^+$ following C–H activation

To demonstrate the recyclability of the ruthenium metal, the biaryl complex **3.4** was irradiated under UV light in an attempt to liberate the biaryl ligand *via* photolysis. *In situ* NMR studies of complex **3.4**, dissolved in deuterated acetonitrile and irradiated under UV light (365 nm, 36 W), showed the liberation of the arene ligand and the consequential formation of metal complex $[RuCp(MeCN)_3]PF_6$ **2.7**. After two hours of irradiation, 87% of the biaryl product had been liberated from the η^6-bound $[RuCp]^+$ unit, and quantitative photolysis was observed after 6 hours (Figure 3.12).

During the photolysis of complex **3.4**, a number of noteworthy observations can be seen in the ^{1}H-NMR spectra. The pair of shifts corresponding to the free anisole-arene aromatic protons and the methyl group protons of the metal bound arene undergo small shifts to lower ppm. This is due to the electron withdrawing effect of the $[RuCp]^+$ fragment being removed, so these protons are now more shielded. The aromatic protons of the metal-bound ring exhibit a large shift to higher ppm due to the liberation of the $[RuCp]^+$ and the rings aromaticity being reinstated. Lastly, the disappearance and reappearance of Cp peaks for complexes **3.4** and **2.7** respectively shows the formation of the trisacetonitrile piano stool biproduct. The formation of this biproduct is reassuring, as this complex is used to synthesise all the $[(\eta^6\text{-arene})RuCp]^+$ complexes shown in this project, and shows promise for a one-pot C–H activation protocol catalytic in ruthenium.

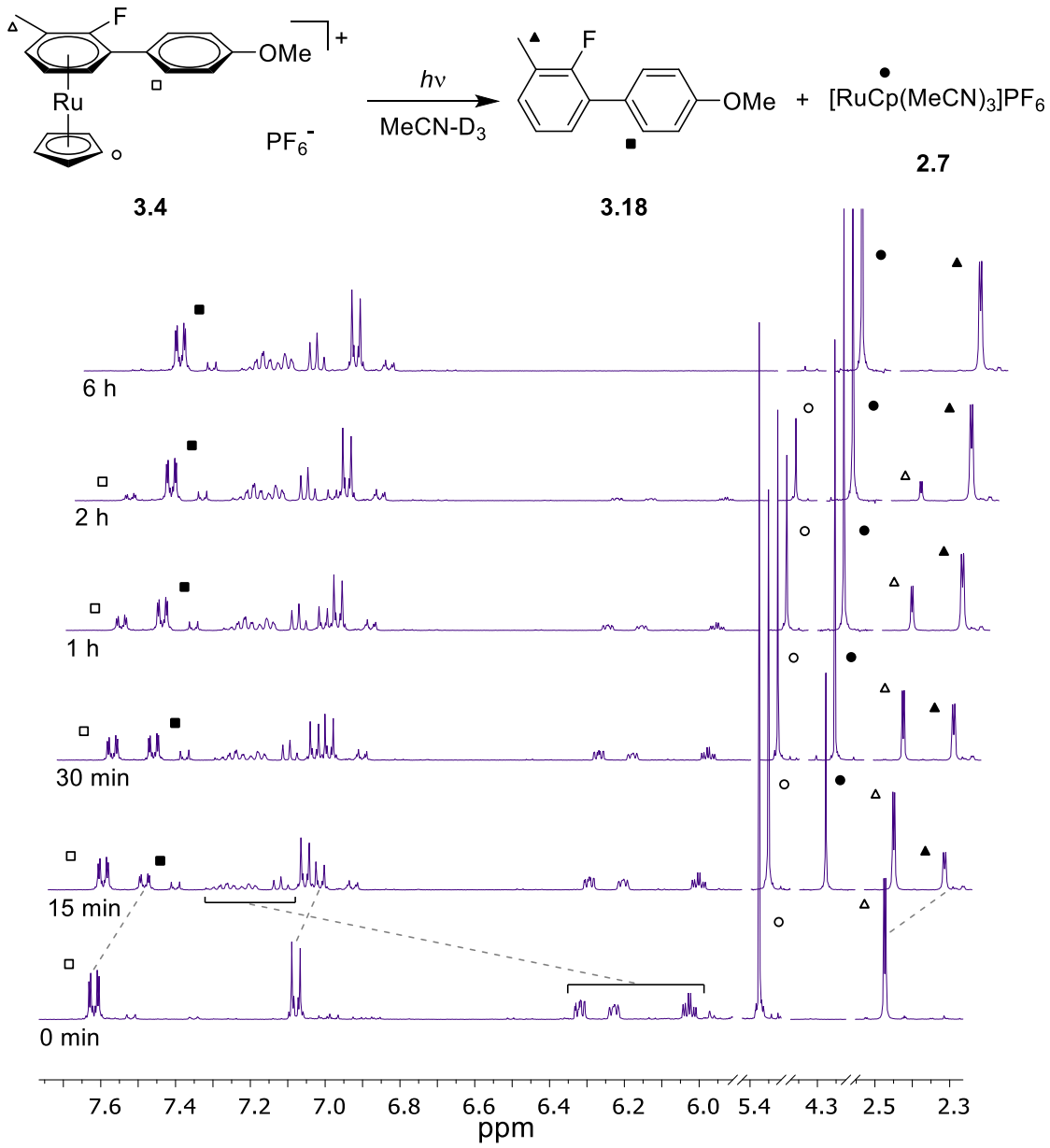

Figure 3.12 *Stacked ^{1}H-NMR spectra (CD_3CN, 298 K, 400 MHz) for the photolysis of complex* ***3.4****.*

3.2.5 Investigating the mechanism of the C–H activation reaction

We wished to probe the mechanism of this arylation to more thoroughly understand the role of the palladium and silver in the reaction. As discussed above, the first example of C–H activation of this nature with electron-deficient arenes was reported from Fagnou *et al.*, where catalytic direct arylation of perfluorobenzene was described.[144] This followed the CMD mechanism, and the palladium was responsible for the initial activation of the aromatic C–H bond. Previous work has used silver salts to scavenge halide ions made as a result of the Pd-catalysed coupling reactions. However, in more recent studies, the role

of silver has been shown to be influential in the C–H activation process.[145,146] Pertinent to the chemistry in this chapter, a recent publication from Larrosa reported the C–H activation of (η^6-arene)$Cr(CO)_3$ is likely to be silver-mediated rather than palladium.[147] With similar questions in mind, the mechanism of this C–H activation protocol was interrogated.

It is already known that silver must play a vital role in this process, as reactivity is switched off entirely without it (Table 3.1, entry 11). In an attempt to further understand the role silver holds in the mechanism of this process, *o*-fluorotoluene complex **3.3** was subjected to the optimised reaction conditions with 10 equivalents of D_2O and no palladium metal.

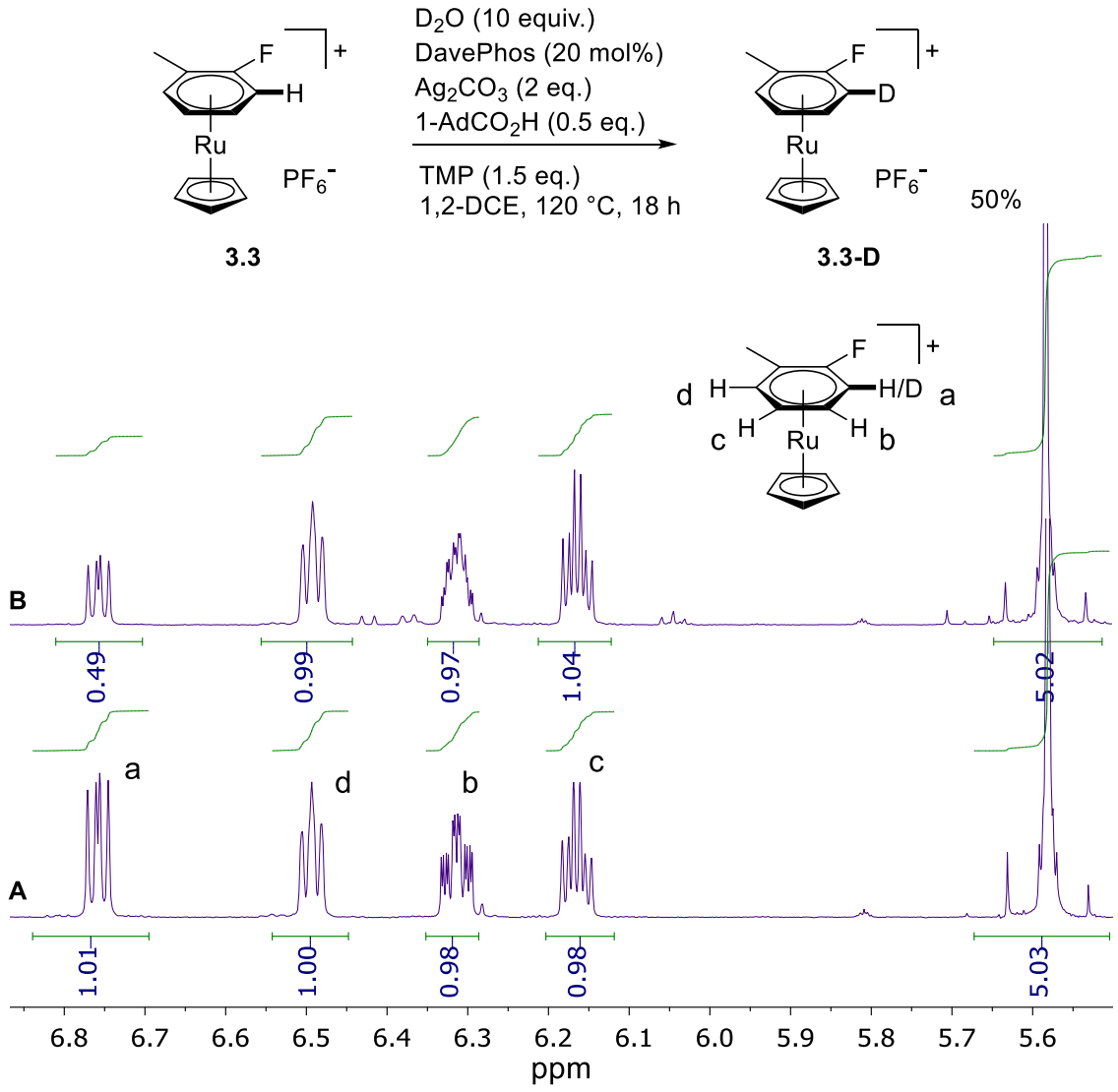

Figure 3.13 *Ag-catalysed H/D exchange experiment and ^{1}H-NMR Spectra of complexes **3.3** (A) and **3.3-D** (B) (MeCN-D_3, 298 K, 400 MHz).*

After reaction for 18 hours, analysis of the four aromatic proton shifts of the complex showed that peak **a**, corresponding to the proton *ortho* to fluorine, had decreased in intensity by 50% relative to the three other environments (Figure 3.13). In addition, the splitting pattern of proton **b**, the proton *meta* to fluorine and *ortho* to the position of C–H activation, had become much more complex. Both of these observations suggest deuteration at the **a** position on the arene at a conversion of 50%. A new species was also observed in the ^{19}F-NMR, which existed in a 1:1 ratio with the starting material. The result of this deuteration experiment suggests that it is silver which mediates the C–H activation of the ruthenium complex, similar to the results previously reported by Larrosa. Following this result, the mechanism in Figure 3.14 was proposed for the C–H activation of [(η^6-arene)RuCp]$^+$ complexes.

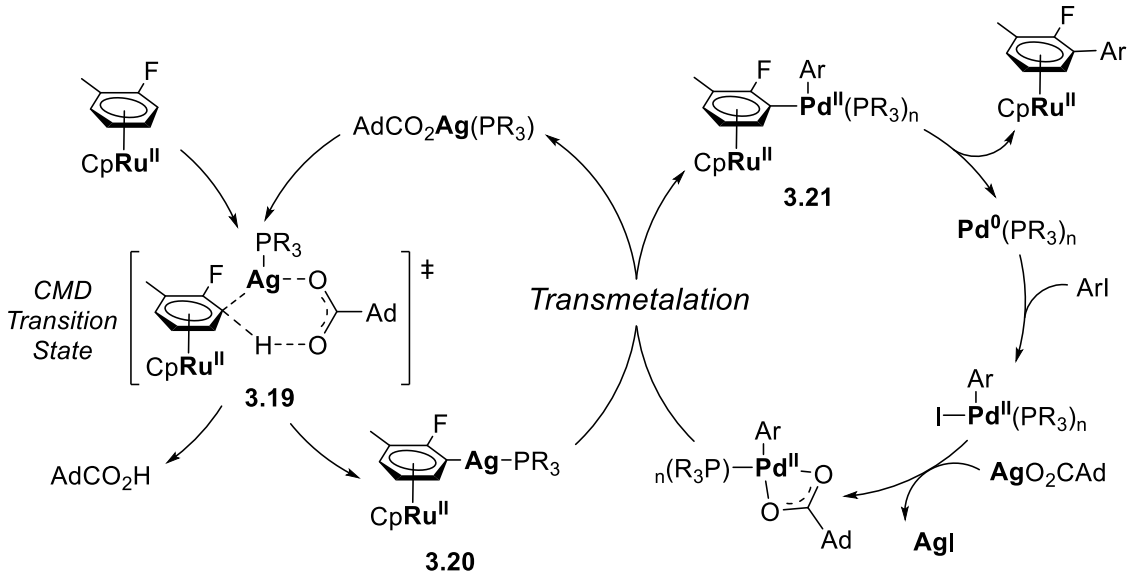

Figure 3.14 *Proposed Concerted Metalation-Deprotonation (CMD) mechanism, via Ag$^+$ mediated C–H activation.*

The first step of the mechanism is the concerted metalation-deprotonation of the ruthenium complex, mediated by silver, to intermediate **3.20**, *via* transition state **3.19**. Due to the net electron-withdrawing effect of the [RuCp]$^+$ unit, the arene is sufficiently activated towards C–H activation due to the increased aromatic acidity. Previous work has shown the conjugate base of the carboxylic acid and phosphine ligand are essential for this transition step, in particular how the acid assisted in the deprotonation of the substrate.[146–148] The reaction does still proceed in the absence of carboxylic acid (Table 3.1, entry 9), most likely due to the abundance of carboxylate ions present in the reaction system (AcO^-, Ag_2CO_3). Following C–H activation, the (η^6-arene)RuCp fragment transmetalates from silver to palladium to form complex **3.21**, which reductively

eliminates the coupled arene product complex. Considering the proposed mechanism above, it is also clear why increasing the stoichiometry of silver during optimisation improved the conversion. Ag^+ will inevitably be consumed through precipitation of AgI salts as a result of the aryl iodide substrates adding to palladium. However, the deuteration experiments have shown the importance of Ag for the C–H activation of the ruthenium complex, and therefore increased abundance will improve the efficiency of this step.

3.3 Conclusions

In summary, a new C–H activation process has been developed, mediated by the η^6-binding of ruthenium. The net electron-withdrawing effect of the $[RuCp]^+$ fragment increases the acidity of the aromatic protons, and enables a C–H activation reaction that does not proceed without complexation. The process allowed a number of different iodoarenes to form biaryl products, and through our optimised conditions it was possible to activated the simplest of arenes, benzene. This is an exciting prospect, as arene C–H activation of this type typically requires some form of covalently bound activating group. Experimental data collected shows strong agreement with the proposed concerted metalation-deprotonation mechanism, where initial C–H activation is mediated by silver, and the reductive coupling of the arene units follows a transmetalation step. Photolysis experiments showed that the coupled biaryl ligand can be liberated quantitatively under mild conditions, and that complete recoverability of the ruthenium metal is possible through the formation of the piano-stool complex $[RuCp(MeCN)_3]PF_6$. This shows great promise for a reaction catalytic in Ru, which shall be discussed in the future work section of this thesis.

4. Catalytic hydrodeiodination of arenes *via* η^6-intermediates

4.1 Introduction

4.1.1 Organohalides and their role in society

Organic halides have widespread usage and versatility as chemical reagents, solvents and intermediates in organic synthesis. Halogenated molecules, both man-made and created in nature, have had a significant impact on societies, in positive and negative ways.[149] Figure 5.1 shows a very small number of examples that demonstrate the plethora of applications, and problems, that these compounds are associated with.

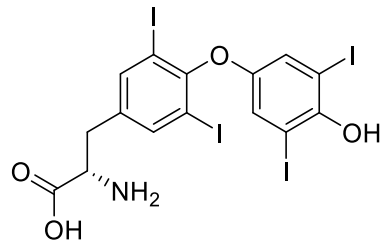

Thyroxin

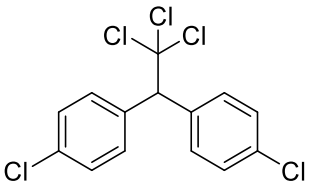

Dichlorodiphenyltrichloroethane (DDT)

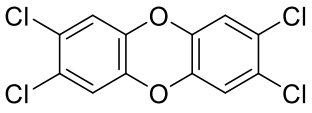

2,3,7,8-tetrachlorodibenzo-*p*-dioxin
(2,3,7,8-TCDD)

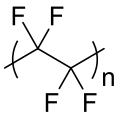

Polytetrafluoroethylene
(PTFE, Teflon)

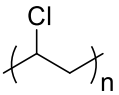

Polyvinyl chloride
(PVC)

Figure 4.1 *Chemical structure of thyroxin (thyroid hormone), dichlorodiphenyltrichloroethane (DDT, insecticide), 2,3,7,8-tetrachlorodibenzo-p-dioxin (2,3,7,8-TCDD, combustion by-product), polytetrafluoroethylene (PTFE, non-stick Teflon coatings) and polyvinyl chloride (PVC, plastic).*

Thyroxin is a hormone made in the thyroid gland and is one of the few naturally occurring compounds synthesised in the human body which contains a halogen.[150] DDT used as an insecticide has saved millions of lives between 1939 to 1972, due to its control of malaria-carrying mosquitos.[151] The uses and application of PVC expanded immensely due to its water and fire resistance and versatility with its physical properties. However, despite the widespread use of these halogenated materials, a vast majority of them are listed as pollutants. DDT is very resistant to biodegradation, and while it has low toxicity to humans, its toxicity to birds and aquatic life led to its ban in 1972. The monomer used to synthesise PVC, vinyl chloride, has been linked to rare forms of liver disease.[149]

Possibly the most shocking of this group is 2,3,7,8-TCDD. Dibenzo-*p*-dioxins and dibenzofurans like this are by products of combusting chemical waste, with this particular example in Figure 5.1 being 100,000 more toxic than sodium cyanide.[152] In the interest of safety and environmental preservation, the dehalogenation of organic matter has become an important field of study for industry, academia and governments. One of the most studied methods of reducing the C-X bond involves the replacement of the halogen with hydrogen *via* hydrogenolysis or hydrodehalogenation. In this brief introduction, reported examples of metal-mediated methods for hydrodehalogenation will be discussed.

4.1.2 Metal-mediated hydrodehalogenation

4.1.2.1 Group I and II (alkaline- and earth-) metals

Examples of dehalogenation mediated by lithium,[153,154] sodium,[155,156] potassium,[157,158] magnesium[159,160] and calcium[161,162] have been reported. With lithium in particular, Yus developed a system consisting of lithium as an electron source and a catalytic amount of an arene (usually naphthalene or 4,4'-di-*tert*-butylbiphenyl (DTBB)) to give organolithium intermediates under mild conditions. Upon work up with water or deuterium oxide the resulting lithiated compounds would give the reduced products. This method was very versatile, with examples reported for alkyl, aryl, vinyl and polymeric organic chlorides (Figure 4.2).[163–167]

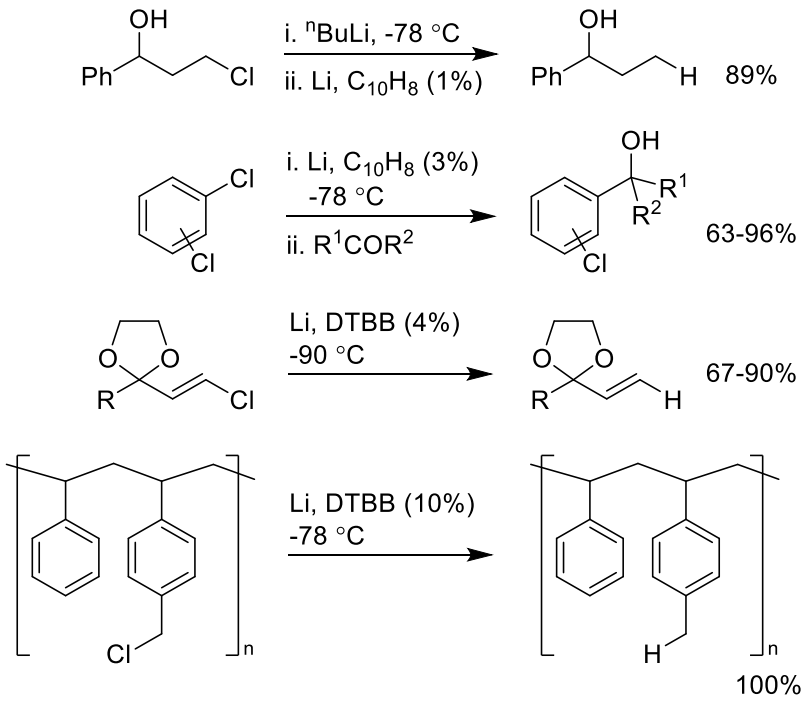

Figure 4.2 *Reduction of organic chlorides with the Li-arene system reported by Yus.*

4.1.2.2 Transition Metals

Although a broad range of transition metals have been reported to facilitate hydrodehalogenation reactions, which have been extensively reviewed, palladium is the most utilised metal for this type of reaction.[149] One of the first examples of using palladium to remove halogens was report by Heck in 1977 for the palladium-catalysed reduction of halo- and nitroaromatic compounds.[168] The reaction tolerated a number of functional groups and was able to remove iodide, bromide and chloride from arenes. Many examples of hydrodehalogenation catalysed by homogeneous and heterogeneous forms of palladium have followed this first report. A study published in 2010 from Ramanathan and Jimenez showed an interesting synthetic pathway, using halogens as blocking groups for aromatic chemistry.[169]

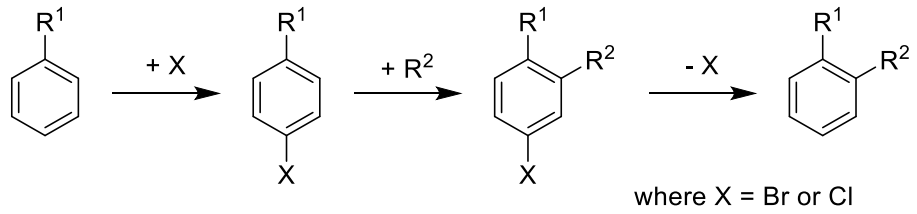

Figure 4.3 *Regioselective synthesis at the ortho-position,*

Installing a halide in the *para*-position allowed regioselective synthesis at the *ortho*-position of the arenes. These arenes could then be subjected to hydrodehalogenation using 10 wt% palladium-on-carbon and atmospheric pressure of hydrogen to give the bis-substituted products.

More recently in 2017, Chelucci *et al.* reported the room temperature hydrodehalogenation of halogenated heteropentalenes.[170]

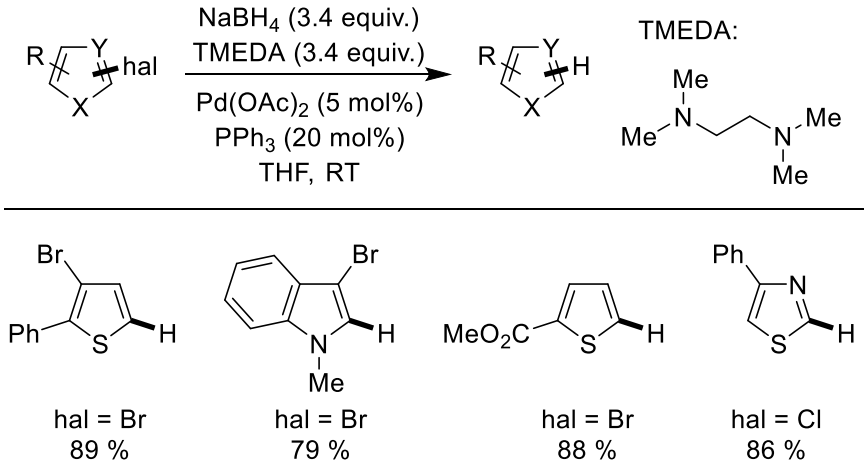

Figure 4.4 *Palladium catalysed reductive dehalogenation of heterocyclic halides.*

Using $NaBH_4$ and N,N,N',N'-tetramethylethylenediamine (TMEDA) in combination as a source of hydride, this palladium catalysed process was highly efficient at hydrodehalogenating bromo- and chloro-heterocycles. The reaction showed excellent regio- and chemoselectivity and uses the inexpensive catalyst $Pd(OAc)_2/PPh_3$.

Reported cases of dehalogenation *via* η^6-intermediates are rare. Already discussed in *Chapter 1* is the dehalogenation of [(η^6-haloarene)$Cr(CO)_3$] complexes using a nucleophilic FeCp carbonyl species reported by Heppert (Figure 4.5).[16]

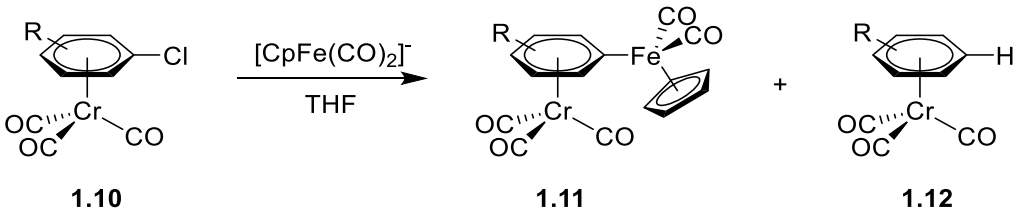

Figure 4.5 *[$Cr(CO)_3$] mediated dehalogenation using [$FeCp(CO)_2$]⁻ as a nucleophile complex*

A later example from Rose *et al.* demonstrated the reaction between superhydride Et_3BHLi and a number of [(η^6-haloarene)$Cr(CO)_3$] complexes (Figure 4.6).[171,172] The reaction is thought to go *via* a Meisenheimer intermediate, where hydride attacks at a *meta*-position to the halide.

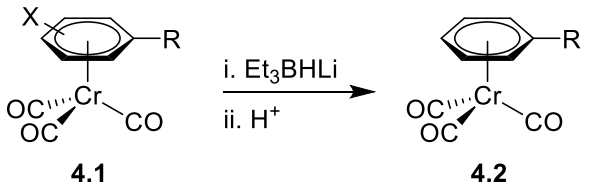

R = Me, $SiMe_3$, Si^iPr_3
X = *o*-Cl, *p*-Cl,
o-F, *p*-F

Figure 4.6 *Hydrodehalogenated [(η^6-arene)$Cr(CO)_3$] complexes via nucleophilic attack from superhydride Et_3BHLi.*

Evidence to support this mechanism came when reaction with deuterated Et_3BDLi gave product complexes deuterated at this *meta*-position only, and that the halide must be eliminated from the Meisenheimer complex *via* a *tele-meta* substitution pathway. The group concluded that this could have great potential in selective deuteration of aromatic compounds towards specific labelled substrates in biochemical applications.

4.1.3 Serendipitous project discovery

One project being explored within the Walton group is the optimisation of the catalytic S_NAr of aryl chlorides published by the group in 2015.[38] Work carried out by Archibald McNeillis (MChem project student) used microwave heating to drastically reduce reaction times from 14 days to 36 hours to achieve the same conversions. With optimised conditions in hand, he set out to explore the scope of the reaction. To see if haloarenes other than chlorides would demonstrate similar reactivity, *p*-halotoluene substrates (where halo = F, Cl, Br, I) were tested. While good to moderate yields were recorded for fluoro- and bromotoluene, no substitution was observed for iodotoluene (Figure 4.7). When the product mixture was analysed by ^{1}H-NMR, chemical shifts in agreement with toluene were observed instead.

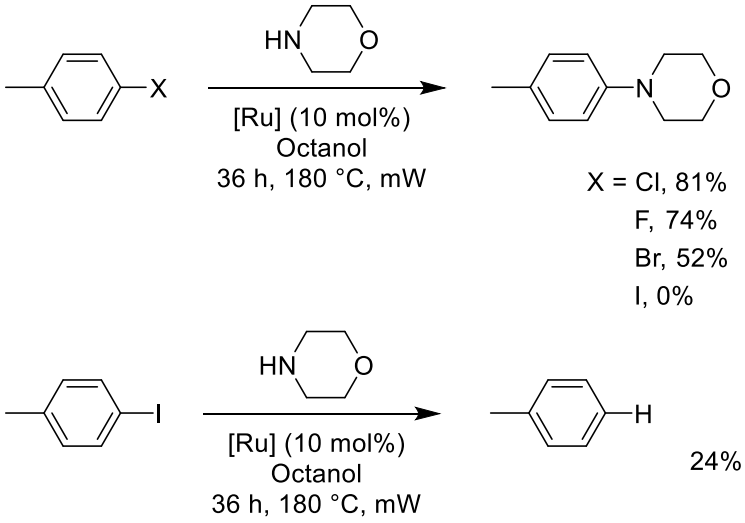

Figure 4.7 *Exploring the scope of ruthenium catalysed S_NAr of aryl halides and discovery of deiodination. [Ru] = $[RuCp(MeCN)_3]PF_6$*

All reagents were analysis for possible contamination of toluene but none was found, indicating clearly that toluene was being produced as a product of this reaction. The group recognised that this transformation could be mechanistically interesting and industrially applicable, and so proceeded to develop this reaction further.

4.1.4 Radical hydrodeiodination with alcoholate as organic chain reductant

In recent literature, there is an example of hydrodehalogenation which is particularly important to this project. In 2016, Studer reported a metal-free radical deiodination which proceeded through electron catalysis and used an alcoholate as an organic chain reductant (Figure 4.8).[173]

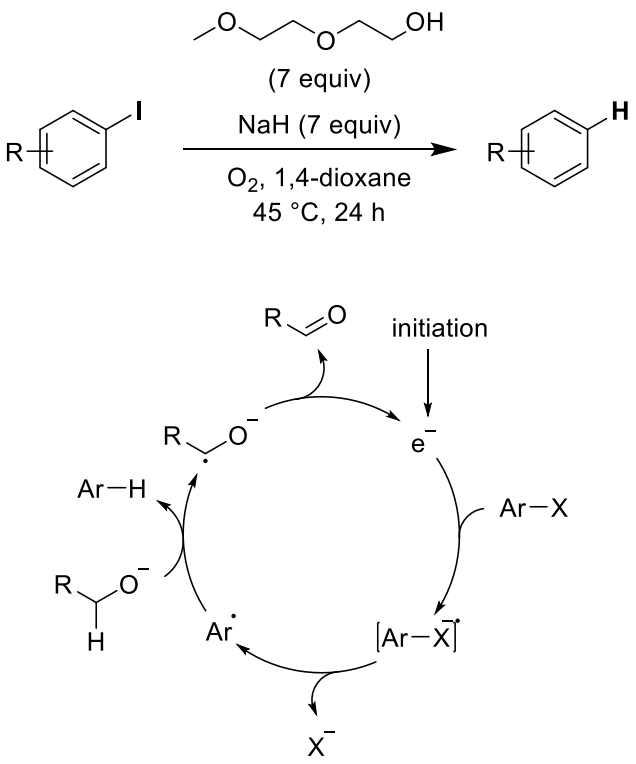

Figure 4.8 *Radical Hydrodeiodination of aryl iodides with an alcoholate as organic chain reductant through electron catalysis.*

Although Figure 4.8 only shows aryl iodides, the reaction was capable of deiodinating alkenyl, alkynyl and alkyl substrate under the same conditions. In this paper, the authors discuss the activation of alcohols toward H-donation through deprotonation. Utilising this strategy, NaH was used as base to activate 2-(2-methoxyethoxy)ethyl alcohol, which acts as an excellent H-donor and consequential single-electron transfer reagent for further organoiodide reductions. The overall result is a catalytic cycle of efficient single-electron transfers producing deiodinated substrates with the alcohol oxidising to an aldehyde as a by-product. This reaction is high yielding for a number of substrates and operates under mild conditions at low temperatures. Drawbacks to this reaction are the scope is limited to electron-rich substrates and a large excess of base and H-donor reagent are required. The significance of this study to the project presented in this chapter will be discussed later in the mechanistic examination section.

4.2 Results and Discussion

4.2.1 Initial reaction development and optimisation

Upon discovery of the deiodination reaction, development of an optimised procedure followed. Initial investigations were carried out with a screen of different bases being tested (Table 4.1). Conversions were calculated by comparing ^{1}H-NMR resonance integrals of starting material to product.

Table 4.1 *Catalytic hydrodeiodination of 4-iodotoluene using bases at varying times.*

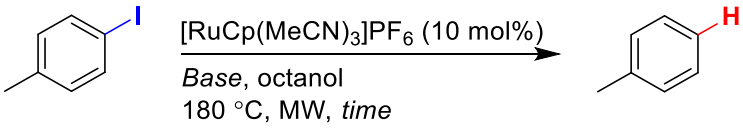

Entry	Base	Time (h)	Conv. (%)
1	Morpholine	18	24
2	DBU	18	100
3	DBU	6	100
4	DBU	3	97
5	DBN	3	95
6	DABCO	3	67

It was initially predicted that this process might occur *via* an ionic mechanism, so for that reason a range of known non-nucleophilic bases were tested. Promisingly, reaction with 1,8-diazabicyclo[5.4.0]undec-7-ene (DBU) gave quantitative conversion to the deiodinated arene after 18 hours (entry 2). Screening the reaction time showed that excellent conversion was still achieved after just three hours (entry 3 and 4). Other non-nucleophilic bases were tested under the new reaction time, but those tested did not outperform DBU.

Following this, the temperature was varied to determine whether reaction was observed at lower temperatures (Table 4.2). It was found that reducing the temperature of the reaction switched off reactivity entirely (entry 1). The harsh conditions required for arene exchange were discussed in *Chapter 1*, and the fact that such high temperatures are required for this reaction to proceed suggests an arene exchange mechanism could be occurring here. Using conventional heating rather than microwave gave a slightly lower yield, but required much longer reaction times. (entry 4).

Table 4.2 *Catalytic hydrodeiodination of 4-iodotoluene at varying temperatures.*

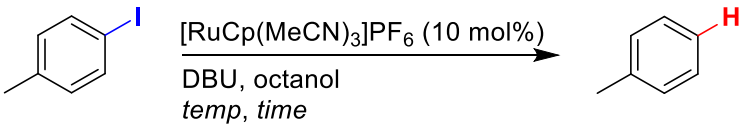

Entry	Temperature (°C)	Time (h)	Heating method	Conv. (%)
1	120	3	MW	0
2	150	3	MW	79
3	180	3	MW	97
4	180	18	Conventional	84

This is likely due to how the microwave in our laboratory records temperature, in that an infrared sensor records the temperature of the outside of the glass vial. The inside of the vial and the reaction mixture could potentially be higher, which would account for the higher conversion and shorter reaction time.

To further optimise this procedure, a series of solvents were tested with the best conditions recorded so far (Table 4.3).

Table 4.3 *Catalytic hydrodeiodination of 4-iodotoluene using a number of solvents.*

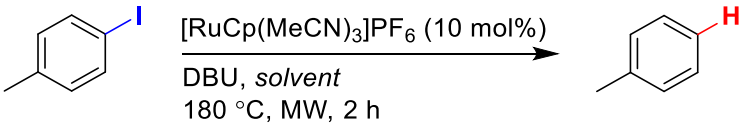

Entry	Solvent	Conv. (%)
1	cyclohexanone	34
2	diglyme	48
3	DMA	71
4	octanol	74

With the theory that the reaction could be following an arene exchange mechanism, a number of high boiling point coordinating solvents were tested for the deiodination. As the reaction with octanol for three hours was close to quantitative, the solvent screen was run for two hours so a better comparison of each solvent's performance could be measured. As expected, conversion was observed with the use of each solvent tested. DMA gave a closely comparable conversion (entry 3) but, again, no solvent outperformed octanol (entry 4).

Lastly, the catalyst loading was explored to determine what effect the amount of ruthenium used in the reaction had on the conversion and reaction time (Table 4.4).

Table 4.4 *Catalytic hydrodeiodination of 4-iodotoluene under varying catalyst loadings and reaction times.*

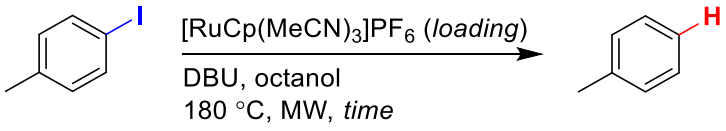

Entry	Catalyst loading (mol%)	Time	Conv. (%)
1	10	3	97
2	1	6	50
3	1	12	87
4	1	18	98

Entry 1 in Table 4.4 shows the optimised conditions with 10 mol% loading of ruthenium catalyst. It was found that with 1 mol% loading over 6, 12 and 18 hours the conversions achieved were 50, 87 and 98 respectively (entries 2, 3 and 4). This was a promising result in two ways, as the lower catalyst loading shows a significantly better atom economy for the process. A more in-depth discussion on the mechanism of this reaction will appear later in section 4.2.3.

4.2.2 Exploring the scope of hydrodeiodination

With optimised conditions now in hand, the scope of the hydrodeiodination was explored (Table 4.5). Reactions undertaken proceeded with excellent chemoselectivity and functional group tolerance. Firstly, excellent yields were still observed when differing regioisomers of iodotoluene were tested (**4.3**). In addition, more steric bulk and congestion around the arene and the iodine atom had little effect on the conversions recorded, with the deiodination of 2-iodomesitylene achieving quantitative conversion (**4.7**). 4-Iodoboronic acid was tested, as it was envisioned that should this group be tolerated in the reaction, further chemistry (e.g. palladium coupling chemistry, etc.) could then be applied to the product. Although the compound was successfully deiodinated, unfortunately the boronic acid was also exchanged for hydrogen during the reaction to yield benzene as the only product (**4.9**).

Table 4.5 *Catalytic hydrodeiodination of aryl iodides under optimised conditions.*[a]

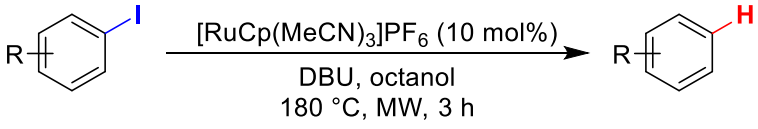

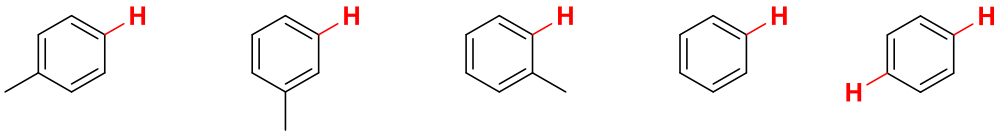

4.3*p*, 97% (74%) **4.3*m*** 92% (99%) **4.3*o*** 89% (73%) **4.4** 81% (52%) **4.4'** 88% (61%)[b]

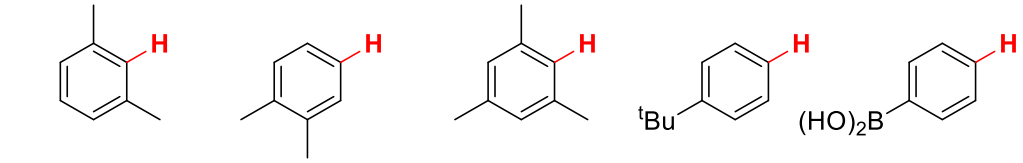

4.5 90% (95%) **4.6** 94% (66%) **4.7** >99% (93%) **4.8** 89% (53%) **4.9** 90% (46%)[c]

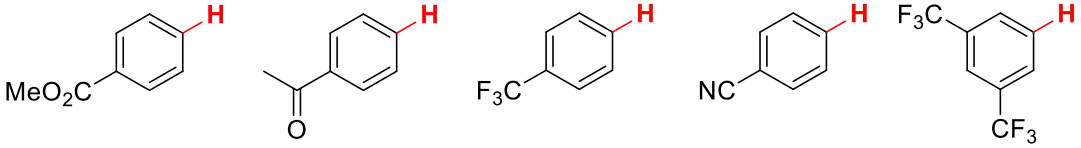

4.10 95% (92%) **4.11** 94% (68%) **4.12** 96% (75%) **4.13** 95% (55%) **4.14** 99% (77%)

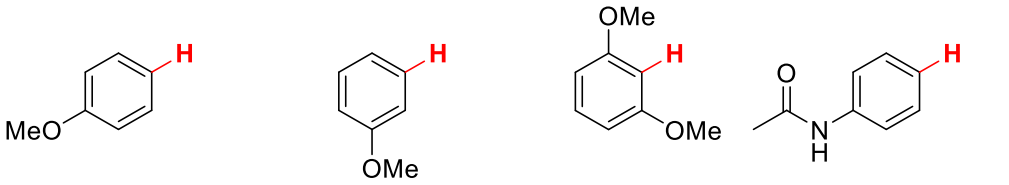

4.15*p* >99% (62%) **4.15*m*** >99% (59%) **4.16** 90% (67%) **4.17** 99% (65%)

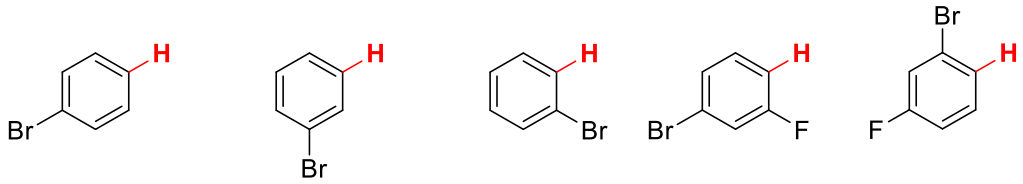

4.18*p* 90% (67%) **4.18*m*** 90% (57%) **4.18*o*** 89% (72%) **4.19** 93% (71%) **4.19'** 92% (65%)

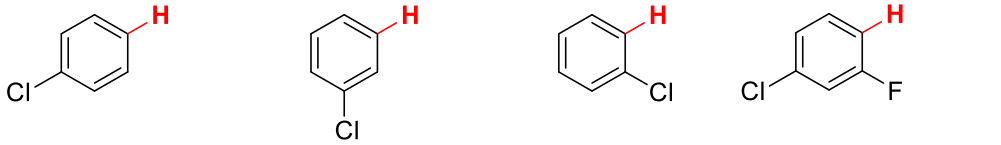

4.20*p* 95% (78%) **4.20*m*** 97% (84%) **4.20*o*** 96% (84%) **4.21** 92% (76%)

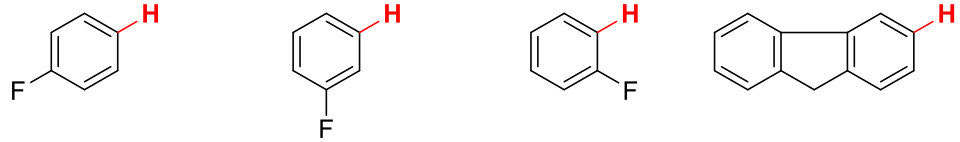

4.22*p* 90% (56%) **4.22*m*** 94% (52%) **4.22*o*** 94% (60%) **4.23** >99% (>99%)[d]

[a]Conditions: starting material (100 mg), DBU (1 equiv.), [Ru] (0.1 equiv.) and octanol (1 mL). Conversions were determined by ^{1}H-NMR integral comparisons between starting material and product and by GC-MS, which in all cases were in agreement within <4%. Yields given in parentheses were determined by ^{1}H-NMR against a known amount of intenal standard spiked into NMR solvent (DMF in $CDCl_3$). [b]Two equivalents of DBU was used to deiodinated at both positions. [c]Starting material was converted entirely to benzene with a conversion of 90%. [d]Reaction with 2-iodofluorene was conducted at gram scale and the yield in parentheses is isolated yield following column chromatography.

Initially when testing 1,4-diiodobenzene (**4.4'**), optimised conditions were maintained and 1 equivalent of base was used in regards to the moles of starting material. The results of this reaction gave a mixture of products identified as starting material 1,4-diiodobenzene, iodobenzene and benzene, in a ratio of approximately 17:65:17 respectively. This strongly indicated the need for a stoichiometric amount of base in regards to the moles of iodine removed.

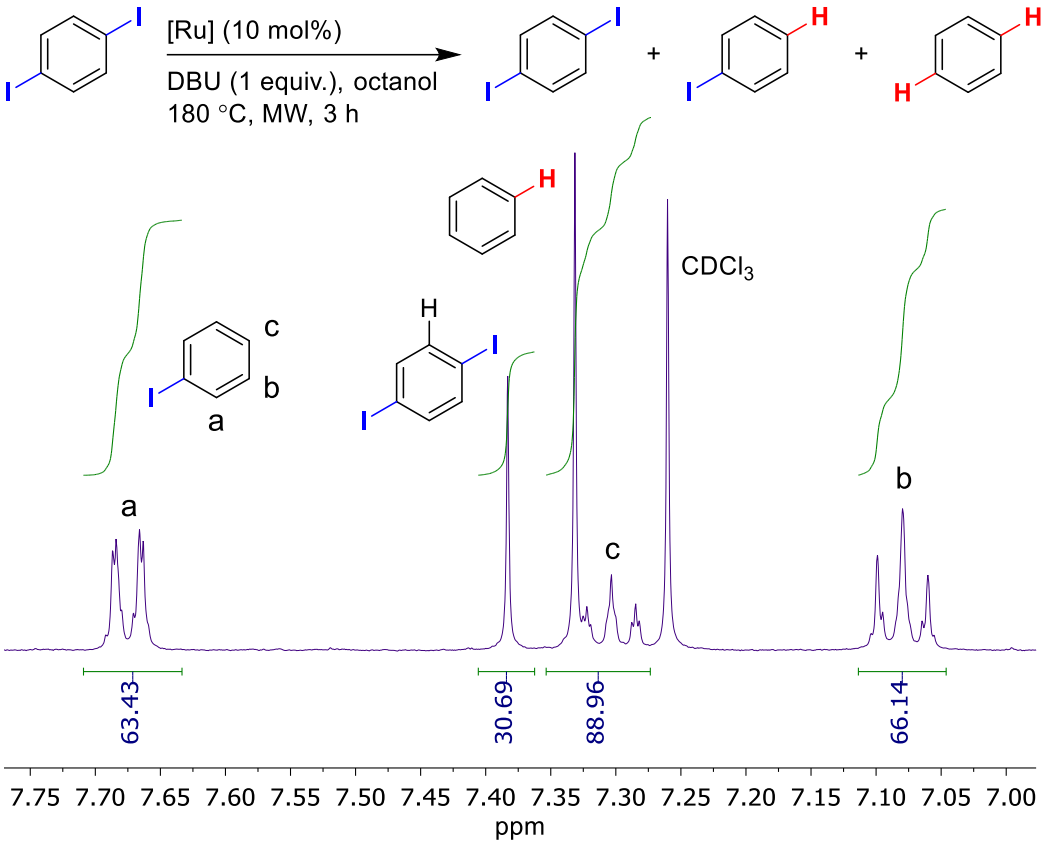

Figure 4.9 *Reaction of 1,4-diiodobenzene under optimised conditions with 1 equivalent of DBU ($CDCl_3$, 298 K, 400 MHz). [Ru] = $[RuCp(MeCN)_3]PF_6$*

Encouragingly, when the reaction was repeated with two equivalents of DBU with respect to the starting material, a conversion of 88% was observed, with the remaining 11% existing as iodobenzene.

A variety of electron-withdrawing and donating groups were tested under the optimised conditions, many of which were tolerated in the reaction and maintained excellent yields. Of the more electron-deficient arenes, those holding groups including CF_3, cyano and aldehydes all proceeded in deiodination in excellent yields (**4.12**, **4.14**, **4.13** and **4.11** respectively). Nitro groups were not tolerated under the optimised conditions and were

found to reduce to amines, a reaction that shall be discussed in the future work section of this thesis.

More electron riches arenes bearing groups including esters, ethers and amides were deiodinated with similarly excellent yields (**4.10**, **4.15**, **4.16** and **4.17**). Reactions with different regioisomers of iodophenol did not exhibit reaction, however. A plausible explanation for this could be deprotonation of the alcohols by DBU base which deactivates the catalysts, which has been shown in other reactions with η^6-complexes.[79] Also, reactions with regioisomers of iodoaniline showed products that were not a result of deiodination alone and could not be identified. Further study into the identification of these products is ongoing.

Lastly, other halogenated arenes were tested to determine the chemoselectivity of the reaction. The reaction was found to be extremely selective to iodine, with all regioisomers of bromoiodobenzene (**4.18**), chloroiodobenzene (**4.20**) and fluoroiodobenzene (**4.22**) showing removal of iodine only. Entries **4.19**, **4.19'** and **4.21** which contained a mixture of different halogens on the same aromatic ring all exhibited the same high selectivity and excellent yields.

Although the conversions for all tested substrates were very high, yields recorded for some substrates were much lower. Due to the scale of the scope reactions and the volatility of the products, isolation was deemed too difficult. Instead, yields were recorded *via* crude ^{1}H-NMR integral comparison by accurately spiking a known amount of DMF into $CDCl_3$ (1 μL/1 mL). With some of the substrates tested, the lower boiling point products, like benzene and toluene, seemed to show the biggest deviation, whereas higher boiling point products like mesitylene saw agreeable measurements. Following this, 2-iodofluorene was tested due to its high boiling point and stability. The reaction was conducted at a one gram scale, and under the optimised conditions, a quantitative yield was isolated following column chromatography post-reaction (**4.23**).

4.2.3 Exploring the mechanism of the catalytic hydrodeiodination

A rigorous study of this reaction is required for an arene exchange mechanism like that shown in Figure 4.10 to be suggested. This section will describe the experiments designed to determine the mechanism occurring in this process.

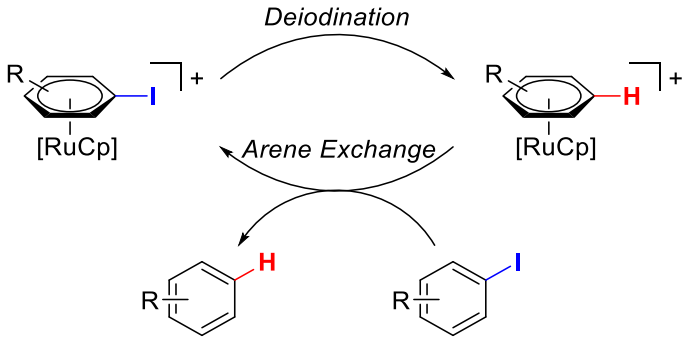

Figure 4.10 *General mechanism for catalytic hydrodeiodination via arene exchange.*

4.2.3.1 Establishing a reaction *via* an η⁶-intermediate

To begin, the possibility of the reaction proceeding *via* an η⁶-intermediated was evaluated. Repeating the reaction under optimised conditions but in the absence of ruthenium complex showed no reaction after 24 hours (Figure 4.11) which demonstrates the significance of the metal.

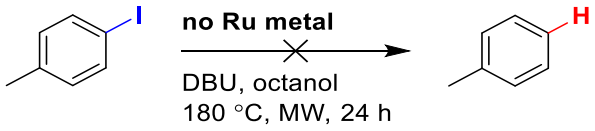

Figure 4.11 *Reaction with 4-iodotoluene under optimised conditions in the absence of ruthenium gave no reaction.*

To gather further evidence to support the existence of η⁶-intermediates during the mechanism, a number of experiments were designed. Firstly, should the reaction occur *via* an intermediate of this kind, the deiodination of the Ru-bound arene complex should be feasible. To attempt this, complex **4.24** was synthesised by reacting the commercially available starting material $[RuCp(MeCN)_3]PF_6$ (**2.7**) with 4-iodotoluene (Figure 4.12). This complex was fully characterized by multinuclear NMR, mass spectrometry, and C,H,N elemental analysis.

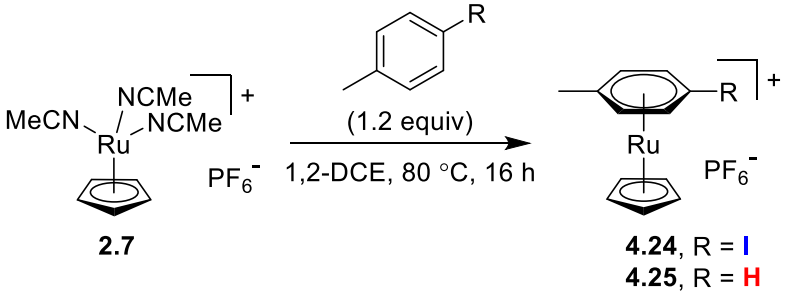

Figure 4.12 *Synthesis of [(η⁶-arene)RuCp]PF_6 complexes (**4.24** and **4.25**)*

With this complex in hand, the stoichiometric deiodination of 4-iodotoluene with respect to ruthenium was attempted. Similar conditions to the optimised procedure above were used, but anticipating a much faster reaction, the reaction was run for a shorter time of 30 minutes. After 30 minutes, an aliquot of the crude reaction mixture was taken for ^{1}H-NMR analysis (Figure 4.13). The spectrum showed that no starting material remained, but a number of products were present. Included in these products was unbound toluene and a mixture of peaks in the metal-bound arene region.

HRMS$^+$ showed the existence of an ion with m/z equal to that of [(η^6-toluene)RuCp]$^+$. In order to make a comparison by NMR spectroscopy, the complex [(η^6-toluene)RuCp]PF_6 was made *via* the same method outlined above in Figure 4.12. When comparing the NMR spectra of this complex with the spectra of the crude reaction mixture, clear similarities were observed, with the Cp singlets appearing at the same chemical shift, and the aromatic protons appearing at a similar ppm with similar peak shape. The majority of the crude aliquot taken from the reaction mixture is octanol, which will have an effect on the exact chemical shifts of species in the sample, and also the resolution of said peaks. This set of broad peaks also integrated equally to the Cp singlet (5:5). A plausible explanation for the observation of free toluene could be the decomposition of the product complex **4.25**, or exchange of the arene from this complex by other coordinating compounds (e.g. octanol, etc.) The multiplet at 5.8 is believed to correspond to one of the alkene protons of 1-octene, which is produced by the elimination of water from octanol solvent at high temperatures. With these observations, it seems the stoichiometric deiodination reaction results in a mixture of toluene-bound [RuCp]$^+$ complex and free toluene, which supports the proposal of a mechanism *via* η^6-intermediates.

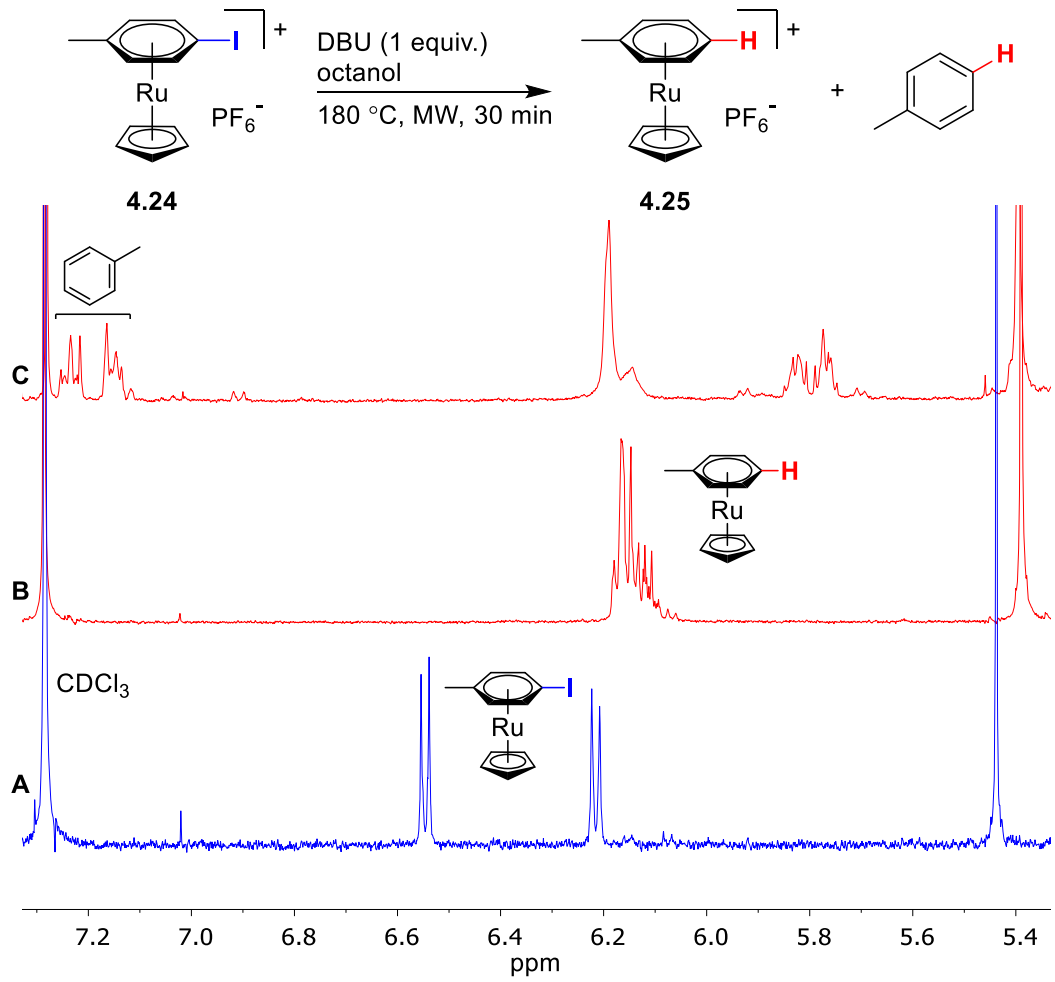

Figure 4.13 *Reaction with [(η⁶-4-iodotoluene)RuCp]PF₆ under optimised conditions with ¹H-NMR spectra (CDCl₃, 298 K, 400 MHz) showing:* ***A*** *[(η⁶-4-iodotoluene)RuCp]PF₆ complex (**4.24**),* ***B*** *[(η⁶-toluene)RuCp]PF₆ complex (**4.25**), and* ***C*** *crude aliquot taken from the reaction mixture.*

Secondly, if this reaction does proceed *via* an arene exchange mechanism, it is likely that the rate determining step is the exchange of toluene product arene with starting material 4-iodotoluene. This also suggests the resting state in the catalytic cycle would be complex **4.25**. Using this complex as the catalyst, 4-iodotoluene was reacted under optimised conditions, and almost quantitative conversion to toluene was observed, showing no change in reactivity or conversion (Figure 4.14).

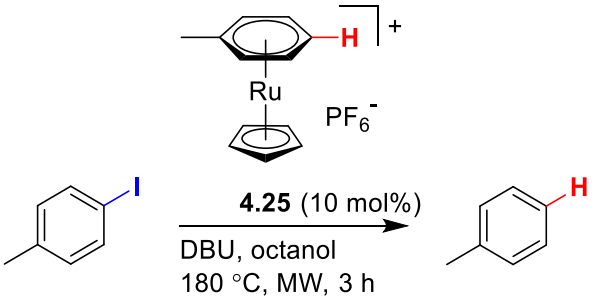

Figure 4.14 *Reaction with 4-iodotoluene under optimised conditions using [(η⁶-toluene)RuCp]PF₆ (**4.25**) as catalyst.*

The catalytic compatibility of this complex provides more evidence to support an arene exchange mechanism.

Considering the speed of this reaction, it was envisioned that exchange of the toluene bound complex must be relatively fast. To test this, an arene exchange experiment with hexamethylbenzene were conducted to measure the rate of exchange from complex **4.25**.

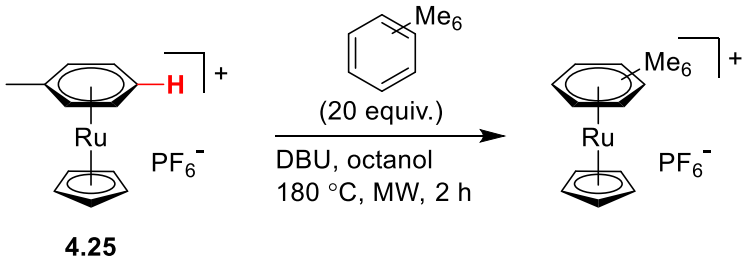

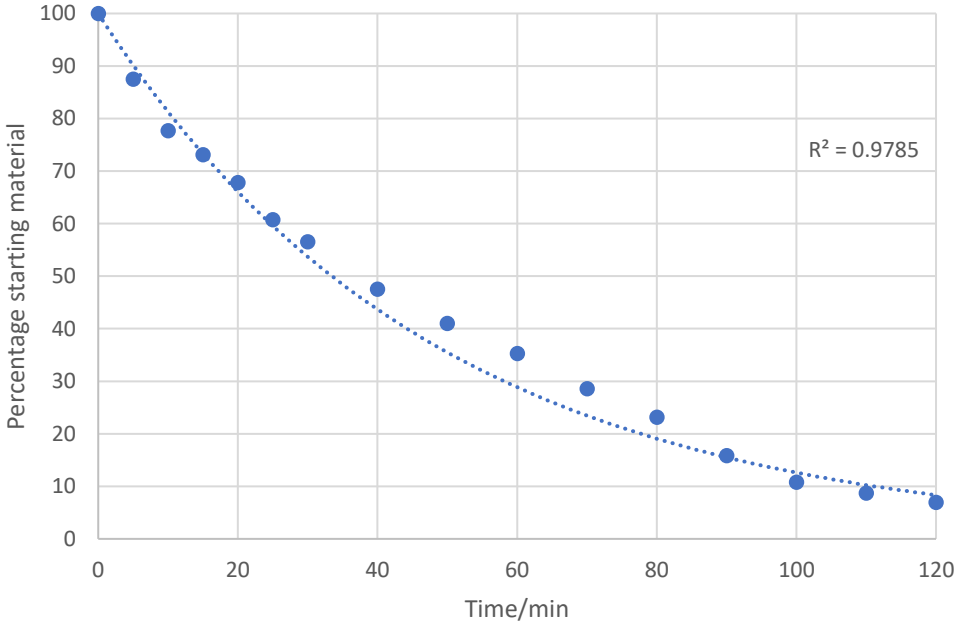

Figure 4.15 *Arene exchange of [(η⁶-toluene)RuCp]PF₆ (**4.25**) with hexamethylbenzene.*

The arene exchange process is reversible. However, using an excess of an electron rich arene like hexamethylbenzene, which will form a strong metal-arene bond, will reduce the reverse reaction as much as possible. Reacting complex **4.25** under these conditions showed fast exchange compared to similar experiments done by the group,[59] with 50% of the starting material exchanged after 37 minutes. This result was encouraging, as should the rate of exchange be found to be very slow, it is not likely that an arene exchange of this sort would allow the high conversions observed in the reaction after just 3 hours.

4.2.3.2 Establishing a radical hydrodeiodination of iodoarene complexes

When this reaction was first discovered through serendipity, an anionic process was envisioned for the mechanism of the deiodination occurring at the arene. However, similarly discussed above in the introduction of this chapter is the example of radical hydrodeiodination published by Studer which uses electron catalysis. Reviewing this recent study identified a number of similarities between our reaction and Studer's, notably the requirement of base and the formation of aldehyde as a result of alcohol oxidation. With this study in mind, we set about exploring the mechanism of the deiodination occurring herein.

Firstly, the octanal potentially produced by this reaction was monitored by proton NMR *in situ*, to determine if it is made stoichiometrically with regards to the toluene produced (Figure 4.16).

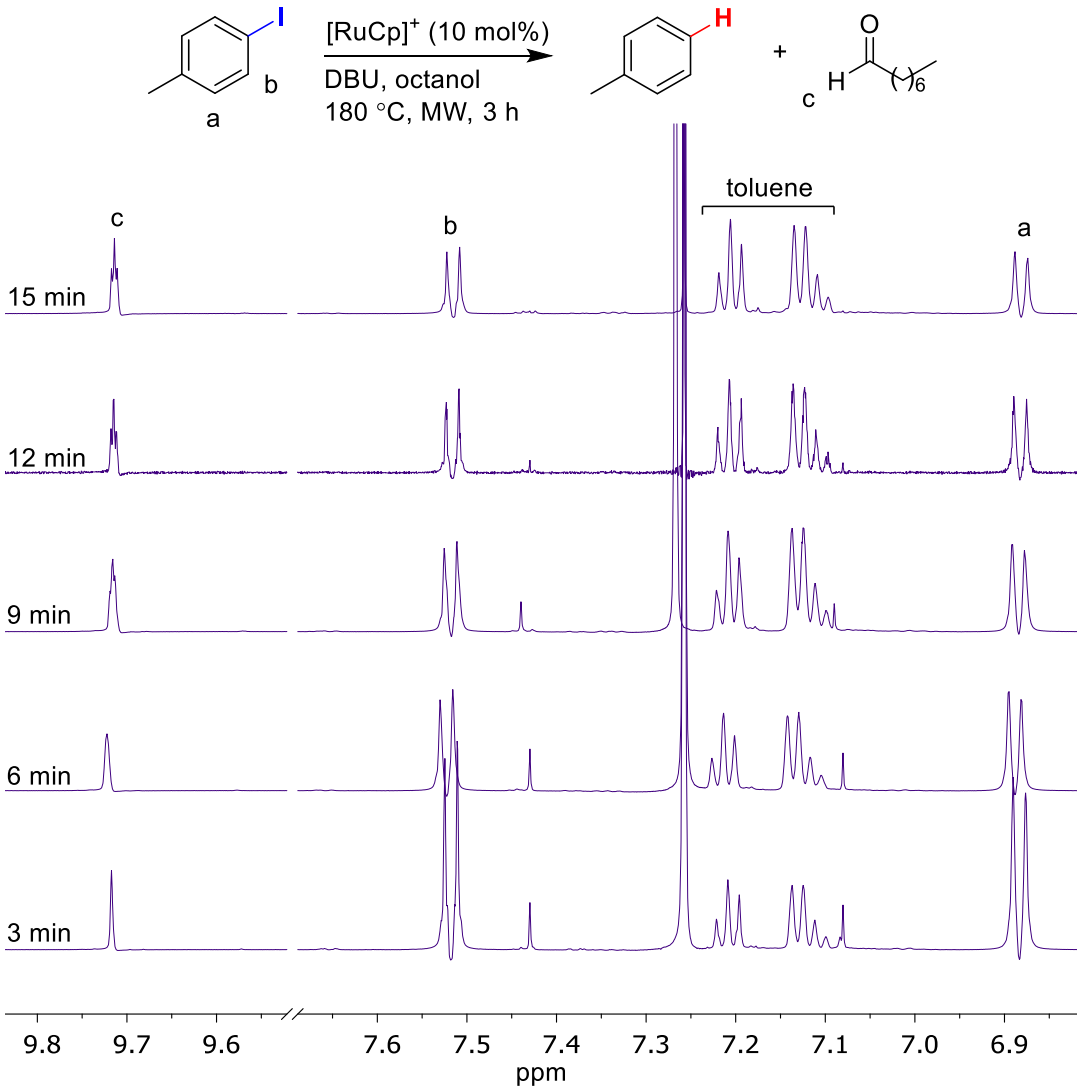

Figure 4.16 *Standard deiodination reaction monitored by in situ proton NMR. These spectra show the chemical shifts for octanal, 4-iodotoluene and toluene.*

An aliquot of crude reaction mixture was taken every 3 minutes for 90 minutes, followed by every 10 minutes until the reaction has progressed for 3 hours. Analysis of the spectra showed that in the initial stages, the rate of production of octanal is proportional to that of toluene. However over longer reaction times the rate decreases and the amount of octanal present reaches a constant, presumably due to its stability under the harsh conditions of the reaction. This result does provide good evidence of the stoichiometric product of octanal as a by-product from the reaction.

Also, to probe this mechanism, control substrates were designed and tested to determine whether a radical reaction could be taking place. These substrates were 1-allyloxy-2-iodobenzene (**4.26**) and 4-(2-iodobenzene)but-1-ene (**4.27**), and their synthesis is described in Figure 4.17.

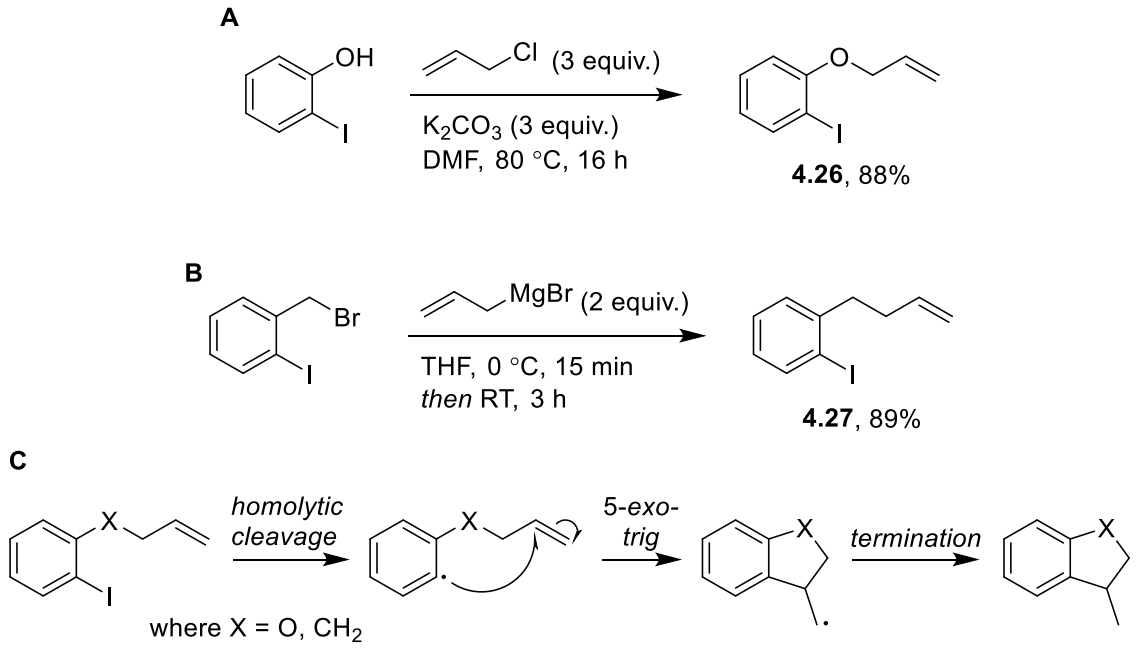

Figure 4.17 A *Synthesis of 1-allyloxy-2-iodobenzene (**4.26**). **B** Synthesis of 4-(2-iodobenzene)but-1-ene (**4.27**). **C** Mechanism for 5-exo-trig radical cyclisation of arene substrates.*

These compounds were chosen to test for a 5-*exo-trig* cyclisation during the reaction, which would provide strong evidence of a radical process occurring (Figure 4.17C).[173] Compounds **4.26** and **4.27** were reacted under the optimised conditions and a crude NMR was taken of the resulting mixture following reaction.

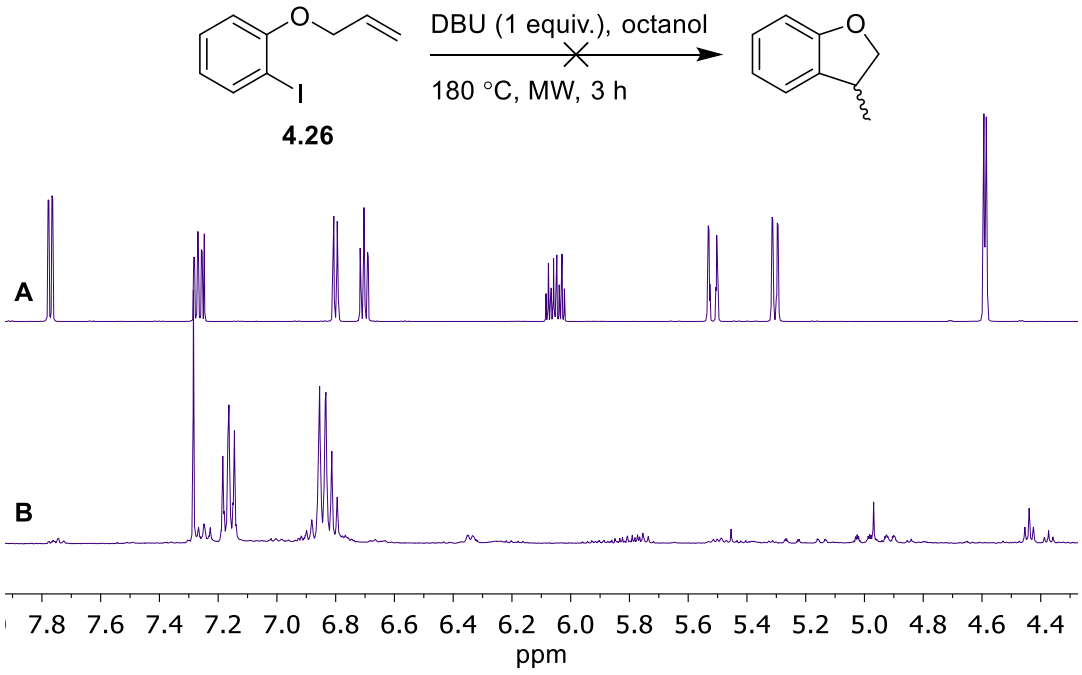

Figure 4.18 *1-Allyloxy-2-iodobenzene (**4.26**) reacted under optimised conditions, with NMR spectra of **A** starting material and **B** the resulting crude reaction mixture ($CDCl_3$, 298 K, 400 MHz).*

Analysis of the NMR showed no starting material remained, and that reaction had produced mostly one single aromatic product that did not contain an alkene environment. The pattern of the chemical shifts (d:t:t, 2:2:1) is in agreement with a monosubstituted aromatic compound, however this compound could not be identified at this point. Importantly, the existence of the product of 5-exo-trig was not observed.

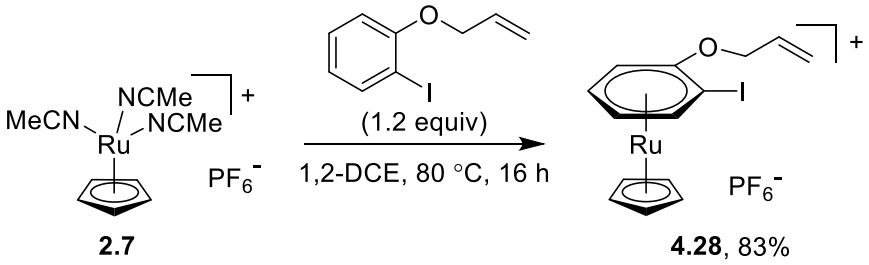

Figure 4.19 *Synthesis of [(η⁶-1-allyloxy-2-iodobenzene)RuCp]PF_6 (**4.28**)*

To further analyse this reaction, [(η⁶-1-allyloxy-2-iodobenzene)RuCp]PF_6 (**4.28**) was synthesised by reacting the free arene with the Ru precursor [RuCp(MeCN)$_3$]PF_6 (**2.7**) (Figure 4.19) and fully characterized by multinuclear NMR, mass spectrometry, and C,H,N elemental analysis. This complex was then subjected to identical deiodination conditions to those for 4-iodotoluene complex **4.24** in Figure 4.12, to determine whether this reaction could occur while bound in an η⁶-intermediate (Figure 4.20).

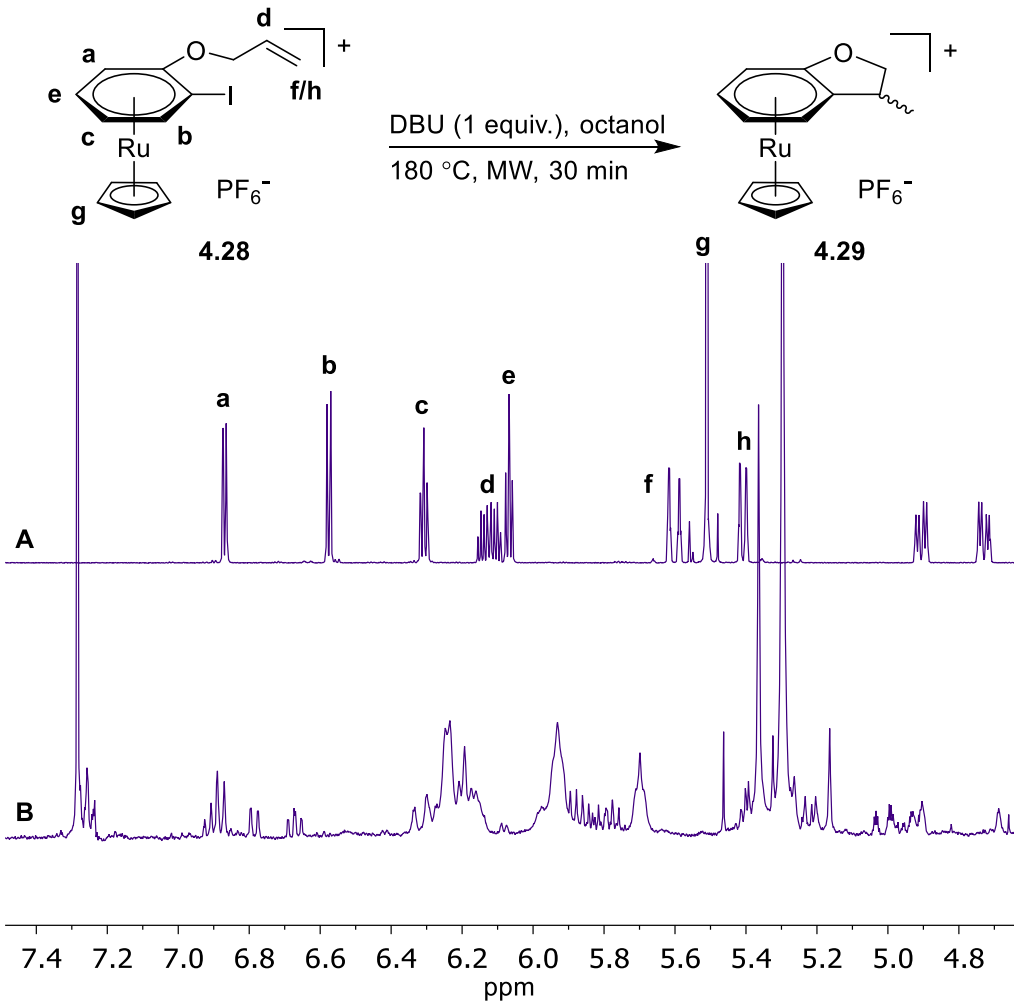

Figure 4.20 *Reaction of **4.28** under deiodination conditions, with **A** the spectrum of starting material ($CO(CD_3)_2$, 298 K, 400 MHz) and **B** the spectrum of the crude mixture following reaction ($CDCl_3$, 298 K, 400 MHz).*

Analysis of the reaction mixture showed a mixture of products and no starting material remained, as confirmed by $HRMS^+$ spectrometry. The predominant mass ion peak observed in the spectrum, with mass-to-charge ratio of 373 *m/z*, is consistent with the complex $[(\eta^6\text{-(octyloxy)benzene})RuCp]^+$. This complex would be the result of substitution of the allyloxy ether with an equivalent of octanol solvent alongside deiodination. With this result, it is also plausible that the monosubstituted compound observed in the catalytic reaction could be (octyloxy)benzene. Overall, due to the apparent instability of this substrate, other compounds were explored to determine a radical process.

Envisioning greater stability, the same tests were conducted on compound **4.27** in an attempt to observed this radical cyclisation. Complex **4.30** was made in a similar fashion to **4.28** by reacting the free arene with $[RuCp(MeCN)_3]PF_6$ (**2.7**) (Figure 4.21) and fully characterized by multinuclear NMR, mass spectrometry, and C,H,N elemental analysis.

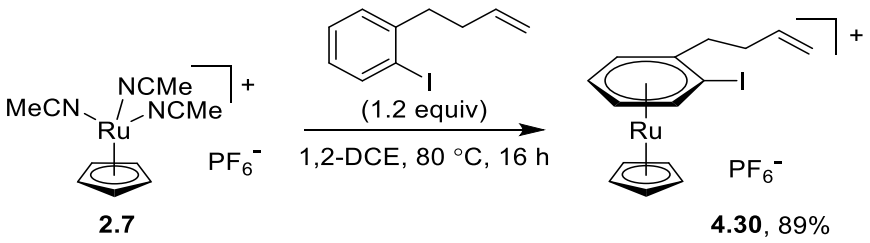

Figure 4.21 *Synthesis of [(η⁶-4-(2-iodobenzene)but-1-ene)RuCp]PF₆ (**4.30**).*

Following their synthesis, the free arene **4.27** and complex **4.30** were subjected to deiodination conditions identical to that described above for the analogous oxygen containing species. The desired products of these reactions were also prepared according to the conditions shown in Figure 4.22 in order to draw comparisons during analysis. 1-Methylindane **4.31** was prepared almost quantitatively by hydrogenolysis of racemic 3-methyl-1-oxoindanone over Pd/C catalyst in ethanol under 3 bar hydrogen. A sample of this was then reacted with $[RuCp(MeCN)_3]PF_6$ (**2.7**) to form the complex $[(\eta^6$-1-methylindane)RuCp$]PF_6$ **4.32**. This complex was fully characterised, but this will be discussed in more detail later in this section.

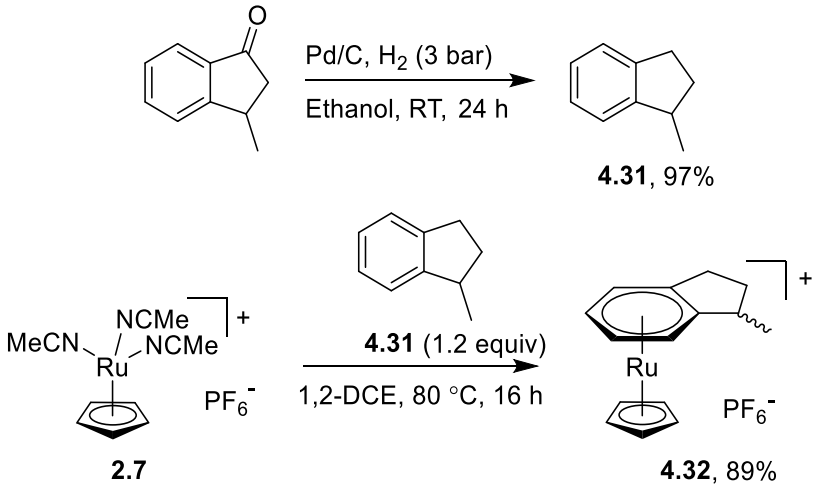

Figure 4.22 *Synthesis of 1-methylindane (**4.40**) and [(η⁶-1-methylindane)RuCp]PF₆ (**4.32**).*

Following the reaction of complex **4.30** under deiodination conditions, a crude sample of the reaction mixture was analysed by NMR spectroscopy and mass spectrometry. The ^{1}H-NMR spectrum of the reaction mixture (Figure 4.23C) was compared to the spectra of the free arene and complex expected to be formed (**4.31** and **4.32** respectively, Figure 4.23A and B). As with previous similar experiments, the amount of octanol in the crude NMR sample increases the difficulty to make accurate comparisons, and the analysis of the stack spectra in Figure 4.23 is not conclusive that this compound has been formed, however it does show the loss of any alkene peaks. Analysis of the reaction mixture by

mass spectrometry did reveal a peak corresponding to a positive ion with mass-to-charge ratio of 299 *m/z*, which is in agreement with the complex [(η⁶-1-methylindane)RuCp]⁺. However, if the starting complex **4.30** had undergone deiodination without the sequential cyclisation, this product would also have this same m/z. Ultimately, drawing strong conclusions from these experiments about a radical mechanism remains a challenge.

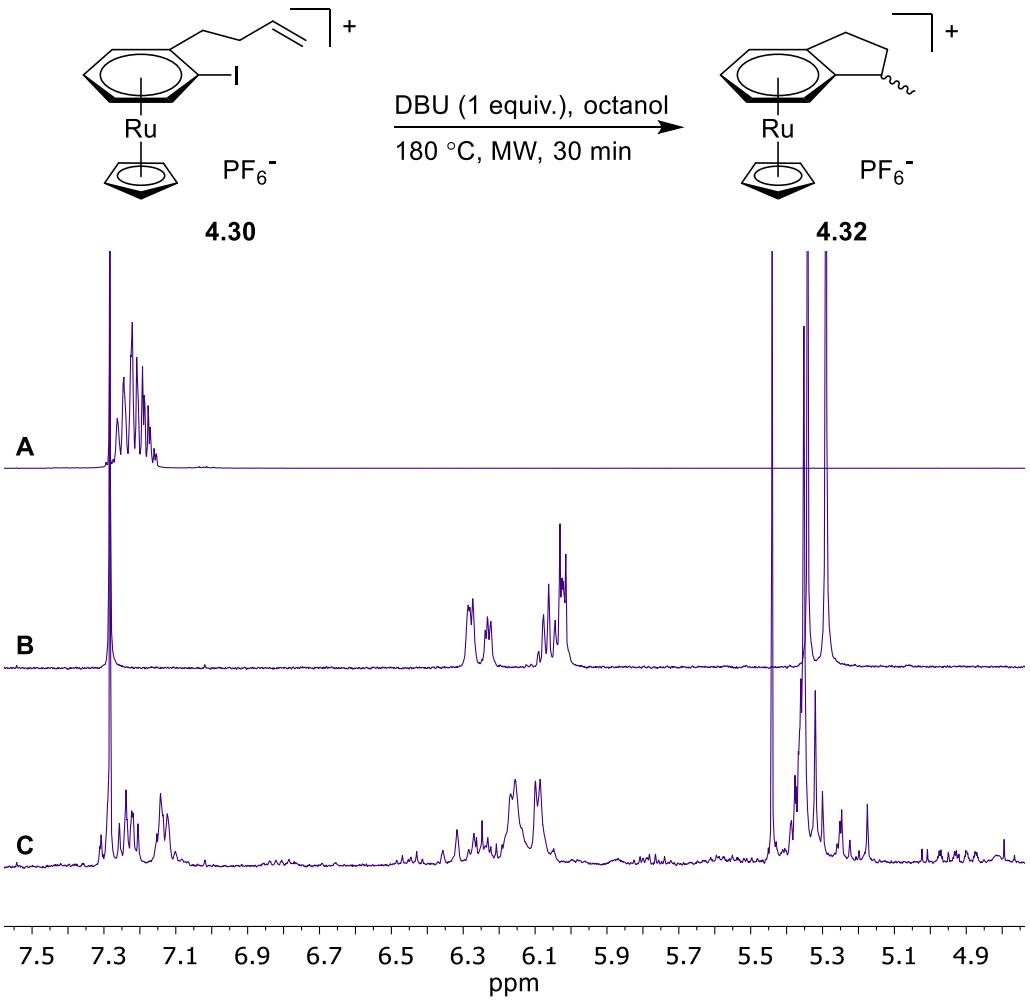

Figure 4.23 *Complex **4.30** subjected to deiodination conditions, with the ^{1}H-NMR spectra of **A** 1-methylindane **4.31**, **B** [(η⁶-1-methylindane)RuCp]PF$_6$ **(4.32)**, and **C** an aliquot of the crude reaction mixture (CDCl$_3$, 298 K, 400 MHz).*

Complex **4.32** was synthesised according to the conditions provided in 4.22, and crude solid collected without further purification was a racemic mixture with two sets of signals. This complex has both stereoisomerism and planar isomerism brought about by the chiral carbon in the 5 membered ring of the bound arene and by the η⁶-binding of the [RuCp]⁺ fragment respectively (Figure 4.24A). Using reverse phase HPLC (see experimental section for details), enantiomeric pairs were isolated. They could then be fully characterized by multinuclear NMR, while mass spectrometry and C,H,N elemental analysis was collected for the racemic solid. In addition, it was possible to obtain single

crystals of a suitable quality for X-ray diffraction studies of **4.32** by layering a concentrated acetone solution with diethyl ether (Figure 4.24B, for crystal and structural refinement data, see *Appendix*). Analysis of these crystals revealed a racemate containing two independent ionic pairs.

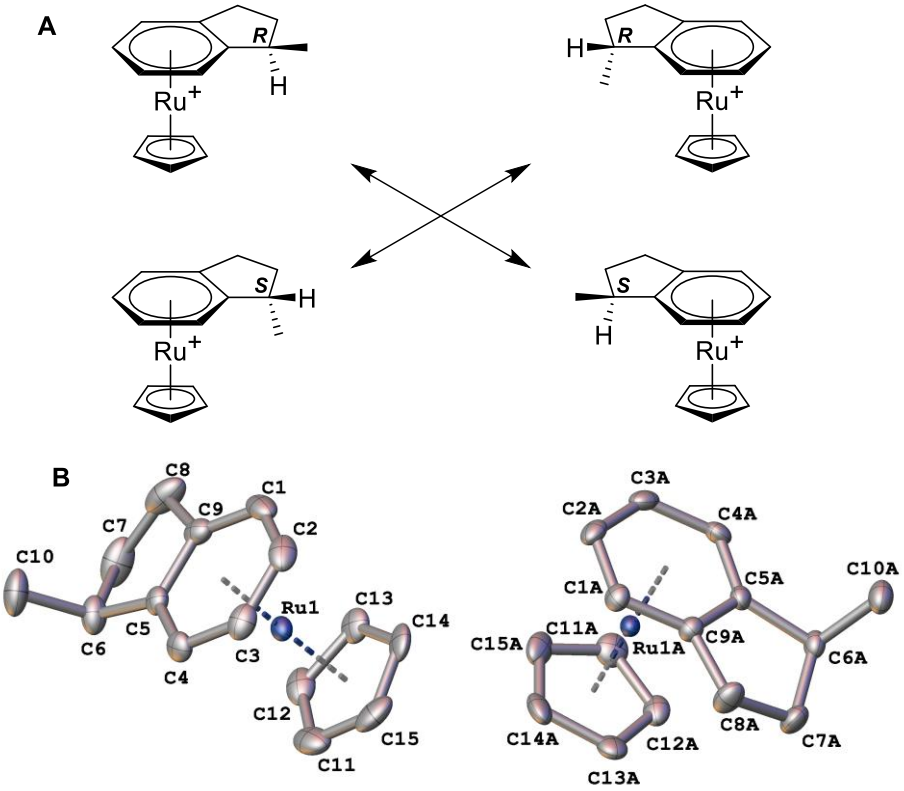

***Figure 2.24 A** The four diastereomers (and enantiomeric pairs) of complex **4.32** and **B** molecular structure of [(η^6-1-methylindane)RuCp]$^+$ (**4.32**); hydrogens have been omitted for clarity and thermal ellipsoids are drawn at 50% probability level.*

Obtaining the absolute configuration was essential for the assignment of the ^{1}H-NMR spectra of this complex. Initially, NOESY was carried out in an attempt to observe correlation between the downward pointing methyl groups and the Cp ring, envisioning the methyl group protons and Cp protons would be close in space. However, upon analysis, no correlation was observed.

The ratio of the two pairs of complexes was also inequivalent, with 3:2 preference observed when synthesised from the racemic starting arene **4.31**. It was envisioned that the more abundant isomer would be the complexes were the methyl group points away from the metal centre, minimising steric clash, and analysis of the proton NMR and molecular structure supported our theory. Analysis of the ^{1}H-NMR spectra from each isolated enantiomeric pair revealed complex coupling patterns for the proton attached to

the same carbon as the methyl group (proton 9, Figure 4.26, see experimental section for full assignment).

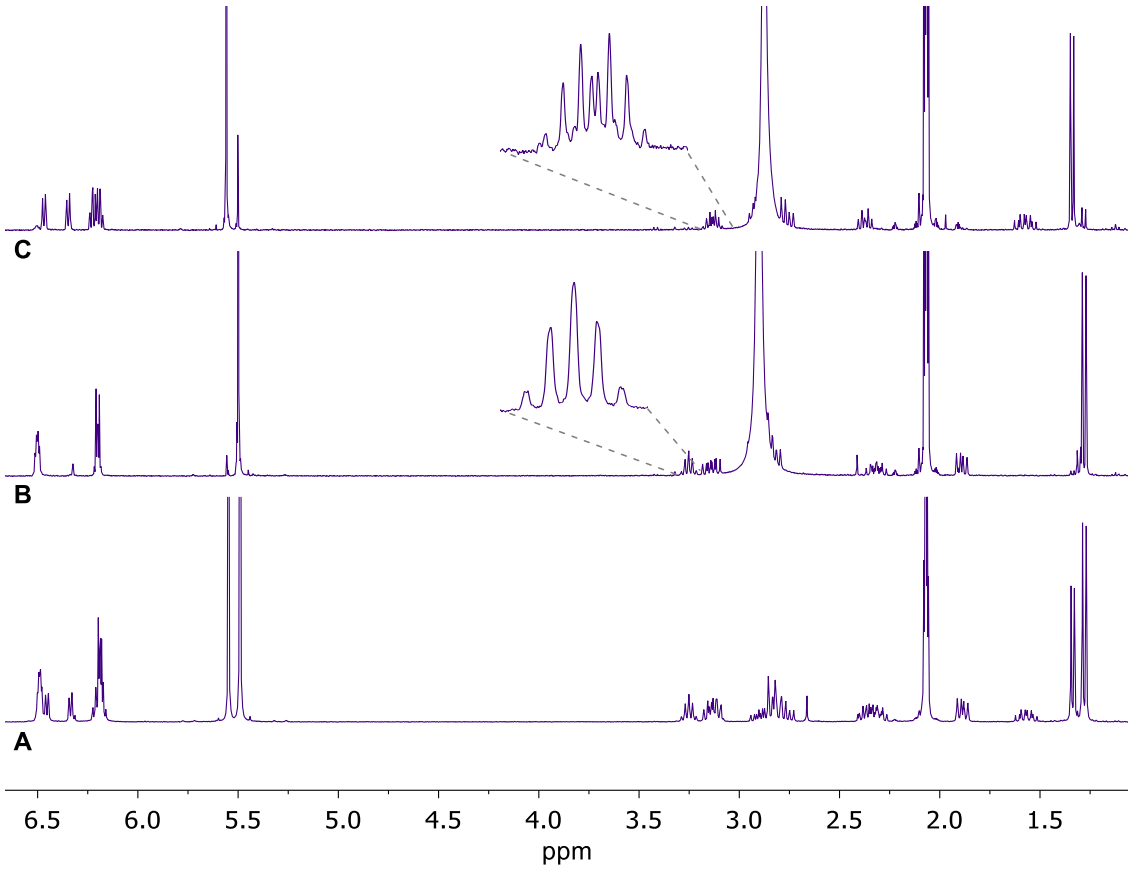

Figure 4.25 *^{1}H-NMR spectra of **A** the mixture of isomers before purification of complex **4.32**, **B** the major isomer and **C** the minor isomer ($CO(CD_3)_2$, 298 K, 400 MHz).*

In the pair of complexes where the methyl group points away from the metal centre, proton 9 does not share the same $^3J_{H\text{-}H}$ coupling to its surrounding 5 protons (10 and 8/8'). The torsion angle between proton 9 and proton 8 is 96.1° (Figure 4.26, see *Appendix* for further details), which according the Karplus equation creates a very small coupling constant, hence the pentet of doublets observed (Figure 4.25B, pd, 7.5 Hz, 1.0 Hz). Making the assumption that the opposing isomer, where the methyl group points toward the ruthenium metal, has the same molecular structure, its proton 9 would couple to 8' very strongly due to the torsion angle of 148.7°. This large coupling constant is observed within the doublet of pentets in the spectrum recorded for the separated isomer (Figure 4.25C, dp, 11.0 Hz, 6.5 Hz).

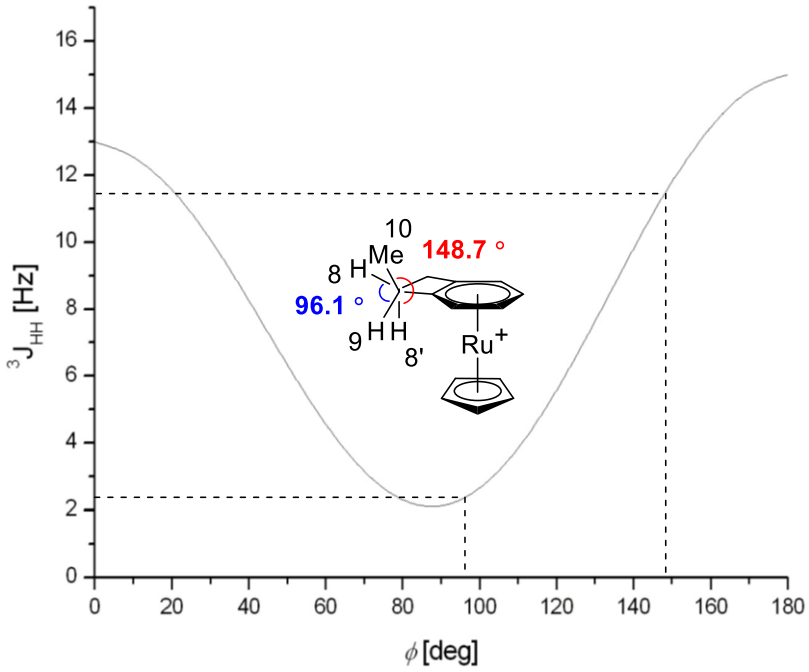

Figure 4.26 *Torsion angles between protons 8 and 9 and methyl group 10 and 8', with their corresponding coupling relationship according to the Karplus equation.*

This analysis strongly supports the assignment of these two complexes and complements our theory regarding the structural preference occurring with the synthesis of complex **4.32**. The significance of this selectivity will be discussed in more detail in the future work section of this thesis.

To further probe the radical nature of this mechanism, a number of radical traps were introduced into the reaction (Figure 4.27). These molecules are known to react very quickly with formed radicals and hinder the normal process of a radical reaction. Therefore, in the instance where reactivity is switch off as a result of their addition, this is typically used to support the existence of a radical mechanism occurring.[174,175]

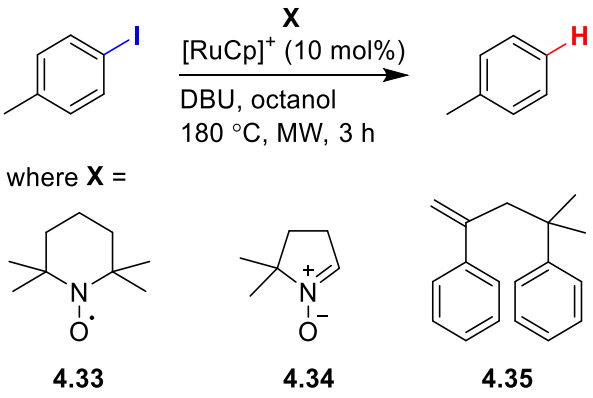

Figure 4.27 *The structure of 2,2,6,6-tetramethyl-1-piperidinyloxy (TEMPO, **4.42**), 5,5-dimethyl-1-pyrroline N-oxide (DMPO, **4.43**) and 2,4-diphenyl-4-methyl-1-pentene (α-methylstyrene dimer (MSD), **4.44**)*

Firstly, the addition of one equivalent of TEMPO **4.33** to the standard reaction resulted in no change in reaction, and almost quantitative yield was recorded. Supportive of a radical process, when two equivalents of **4.33** were added, conversion slowed to 77%. It was also observed that significant amounts of octanal were being produced in these test reactions, likely as a result of TEMPO reacting with the octanol solvent. A similar result was observed in the case of DMPO **4.34**, where the standard reaction with one equivalent of the trap showed no change in conversion and large amounts of octanal are produced. With these results in mind, traps unlikely to react with the solvent were tested.

When 2,4-diphenyl-4-methyl-1-pentene **4.35** is used as a radical trap, it reacts with radicals through an addition-fragmentation reaction according to Figure 4.28. The resulting radicals from the fragmentation deactivate by either combination or disproportionation (styrene and cumene).[176]

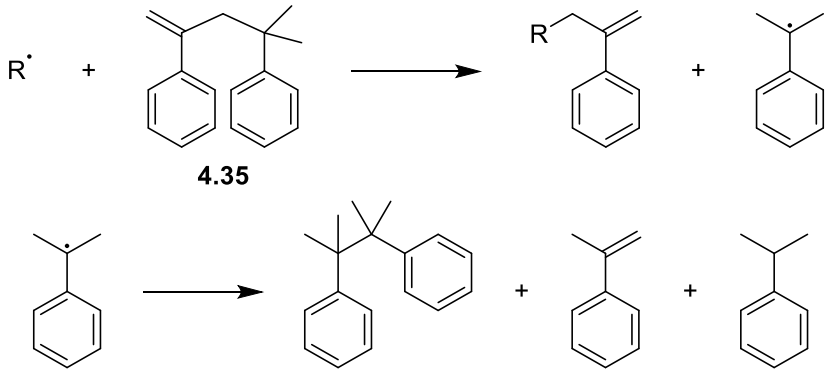

Figure 4.28 *The general reaction of free radicals with MSD and the resulting by-products.*

This molecule was introduced into the standard deiodination reaction, and upon analysis mixed observations were found. An aliquot of the crude reaction mixture was taken and analysed by NMR spectroscopy and mass spectrometry. Although it showed no starting material remained, the ^{1}H-NMR gave a host of unidentifiable shifts. Similarly, the mass spectrum showed a large number of different m/z values, some of which showed evidence of the radical reaction. Although the expected product complex was not observed (complex A, Figure 4.29), [η⁶-arene)RuCp]$^{+}$ complexes of the three by-products of the MSD fragmentation were clearly resolved (complexes B, C and D, Figure 4.29), suggesting the existence of free radicals in this reaction.

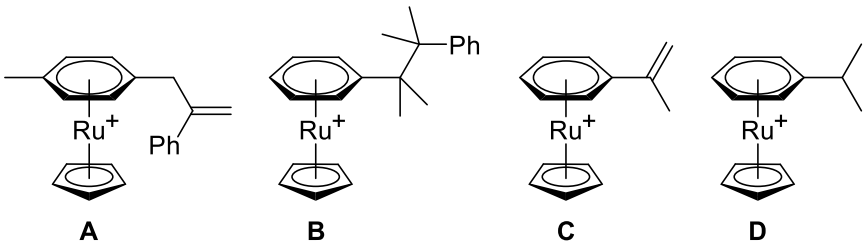

Figure 4.29 *The expected product complex **A** from the reaction with trapping agent MSD, and three observed by-products **B**, **C** and **D**.*

4.2.3.3 Proposed catalytic cycle for the hydrodeiodination

By conducting all the control experiments discussed above, the mechanism shown in Figure 4.30 is proposed for the reaction.

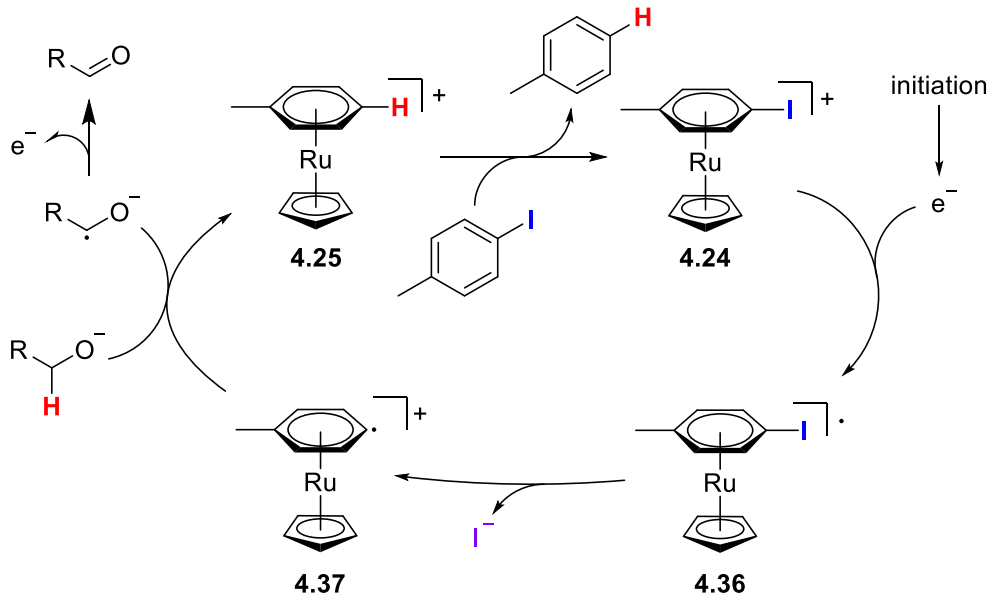

Figure 4.30 *Proposed mechanism for the radical hydrodeiodination of 4-iodotoluene catalysed via [(η^6-arene)RuCp]$^+$ intermediates.*

First an equivalent of 4-iodotoluene binds to the ruthenium metal to form complex **4.24**, which, following an initiation step, becomes a radical anion by receiving an electron. Homolytic cleavage and loss of I^- from this species forms radical carbanion complex **4.37**. This complex reacts with octanol solvent, which has been deprotonated by base, to create the positively charged toluene complex **4.25** and the radical anion form of octanol, which forms octanal following single electron transfer. Lastly, complex **4.25** undergoes arene exchange with another equivalent of 4-iodotoluene, liberating toluene and completing the cycle.

4.3 Conclusions

Presented in this chapter is a novel method for the deiodination of iodoarenes catalysed by ruthenium. This reaction is extremely versatile to a plethora of functional groups and achieves excellent conversions. The reaction exhibited outstanding chemoselectivity towards iodine when tested against other halogens, and was unhindered by sterically bulky substrates, both electron-donating or withdrawing. Optimised conditions were achieved using a loading of 0.1 equivalents of a commercially available source of ruthenium, however excellent reaction was still achieved at 0.01 equivalents. The reaction also occurs at good rate, with some substrates achieving quantitative conversions after just 3 hours, which is unprecedented for a reaction that likely proceeds *via* an arene exchange mechanism.[59,79] A radical mechanism has been proposed for the deiodination, supported by a range of control reactions and literature precedent.[173] Following this work, further study will be conducted into stereoselective radical cyclisations which may proceed *via* a similar mechanism to this reaction, plus catalyst optimisation to achieve conversions under milder conditions. These ideas will be discussed in greater detail in the future work section of this thesis.

5. Tethered [(η^6-arene)RuCp]$^+$ complexes for accelerated arene exchange

5.1 Introduction

Discussed in detail in the introduction of this thesis are the challenges facing arene exchange. The η^6-arene metal bond is relatively strong, therefore sophisticated chemistry is required to lower the barrier for exchanging bound arenes and achieve catalysis *via* these complexes as intermediates. The first advancement in such exchange reactions came from the use of coordinating solvents. The ability of these solvents to coordinate to the ruthenium during the η^6–η^4 slippage of the outgoing arene has a profound effect on recorded rates of exchange.[57–59]

In order to improve the efficacy of this stabilising coordination, complexes were designed which incorporated an intramolecular coordinating tether. The first of its kind was reported by Kündig in 1998, which used a chromium carbonyl complex with methylacrylate as a multidentate ligand which could change its hapticity during arene exchange (**1.50a** and **1.50b**, Figure 5.1).[57] The ability of the carbonyl of methylacrylate to coordinate during the η^6 to η^4 transition of the outgoing arene allowed the complex to exchange at room temperature at the same rate as the analogous [$Cr(CO)_3$] complex would at 170 °C.[50]

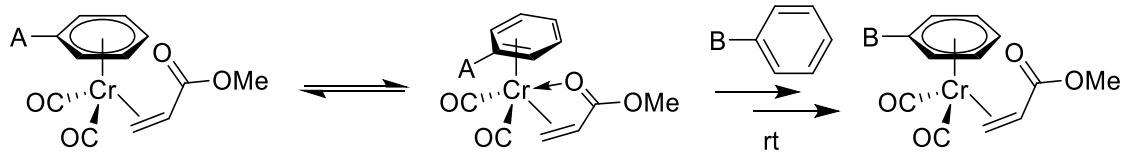

1.50a **1.50b** **1.51**

Figure 5.1 *Tethered chromium carbonyl complex with methylacrylate as a catalysing coordinating ligand.*

Recent work from the Walton group reported tether-assisted arene exchange for ruthenium complexes, where a series of tethered [RuCpL]$^+$ complexes (where CpL is a Cp ring bearing a coordinating functional group) were compared to see how the rate of exchange was accelerated (Figure 5.2).[59] The degree of arene exchange for the below complexes was recorded over 3 and 16 hours in both octanol and cyclohexanone (Table 5.1). All tethered complexes achieved higher rates of exchange than the non-functionalised Cp complex **3.17** in cyclohexanone, but a variance in performance was observed.

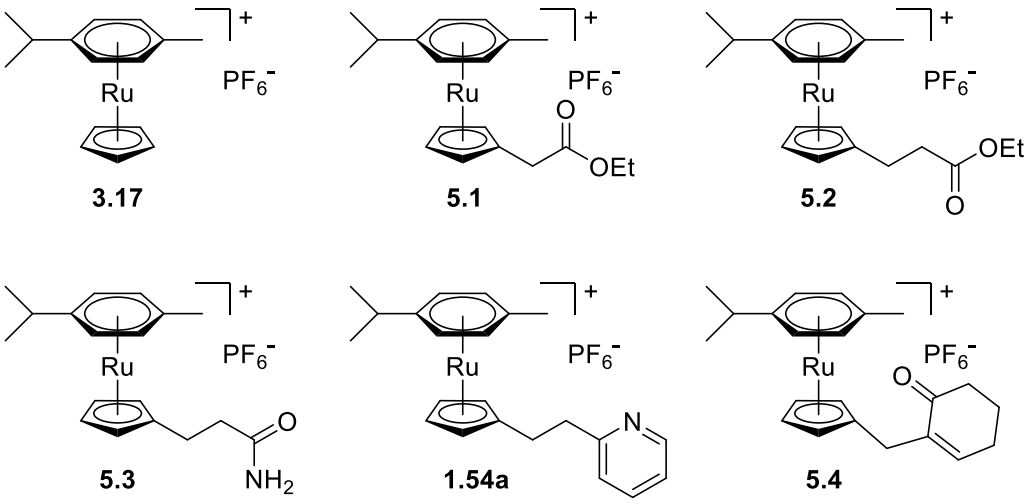

Figure 5.2 *Tethered ruthenium Cp complexes synthesised to improve rates of arene exchange.*

The pyridine tethered complex was the best performing complex, which achieved full conversion after 16 hours in both solvents. Previous work from Semmelhack which describes a number of tethered chromium complexes also found pyridine coordinating complex to perform well.[48]

Table 5.1 *The percentage of arene exchange for tethered ruthenium complexes using either cyclohexanone or 1-octanol as the solvent after 3 and 16 h reaction times.*

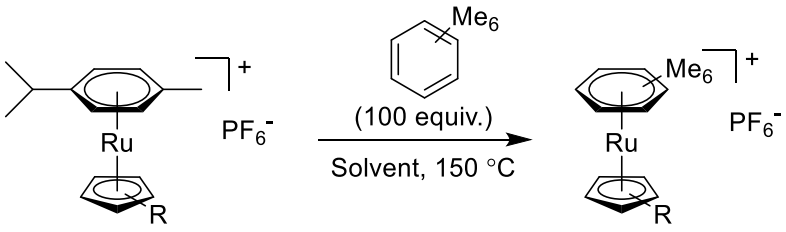

	Arene exchange (%)			
	Cyclohexanone		1-Octanol	
Complex	3 h	16 h	3 h	16 h
3.17	6	38	17	92
5.1	(6)[a]	(50)[a]	(15)[a]	(84)[a]
5.2	9	51	13 (18)[b]	90 (88)[b]
5.3	–[c]	–[c]	(17)[d]	(85)[d]
1.54a	44	100	36	100
5.4	12	50	12	65

[a] Values for decarboxylated **5.1** ([(MeCp)Ru(*p*-cymene)]⁺), which forms under exchange conditions. [b] Values for the octyl ester of **5.2**, which forms in 1-octanol. [c] Complex **5.3** reacts with cyclohexanone, leading to invalid results. [d] Values for the octyl ester of **5.3**, which forms under the exchange conditions.

Complexes **5.2** and **1.54a** were taken forward and tested for their ability to catalyse the S_NAr of aryl chlorides with morpholine. However, despite the enhanced rate of arene exchange, these tethered complexes did not achieve improved catalysis. Similar conversion was observed after 24 hours, however over longer periods (7 days) the non-functionalised $[RuCp]^+$ complex demonstrated the greatest conversion in catalysis. This is likely due to the stability of these complexes, with complex degradation likely to occur over the extended harsh reaction conditions (180 °C, 7 days).[59]

The project reported in this chapter will study a new library of tethered complexes for arene exchange catalysis. By exploring a new range of functionalised tethered complexes, the aim is to discover interactions that will achieve greater rates of arene exchange and that these increased rates will translate to improved catalysis.

5.2 Results and Discussion

5.2.1 Synthesis of tethered cyclopentadienyl complex library

Investigations begin with the synthesis of the library of tethered complexes. Figure 5.3 shows the seven complexes chosen to explore the effect different coordinating functional groups have on the rate of arene exchange in the particular $[RuCp]^+$ system.

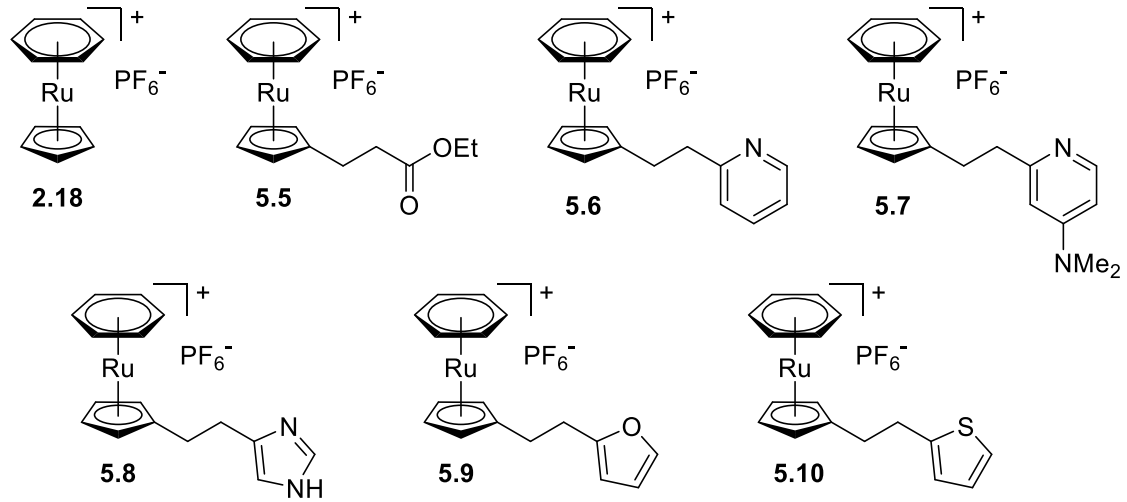

Figure 5.3 *Library of [(η^6-benzene)RuCpL]PF_6 (where L = tethered coordinating functional group) complexes designed to enhance arene exchange.*

The ester and pyridine complexes showed good exchange potential in the previous work by the group, so were included as a comparison with the new complexes (complexes **5.5** and **5.6)**. Complex **5.7** was designed to increase the electron density in the pyridine ring and enhance the donating potential of the pyridine nitrogen. Complexes **5.8**, **5.9** and **5.10**

all have a similar structure, and a comparison will be drawn between the hardness and softness of the coordinating atom.

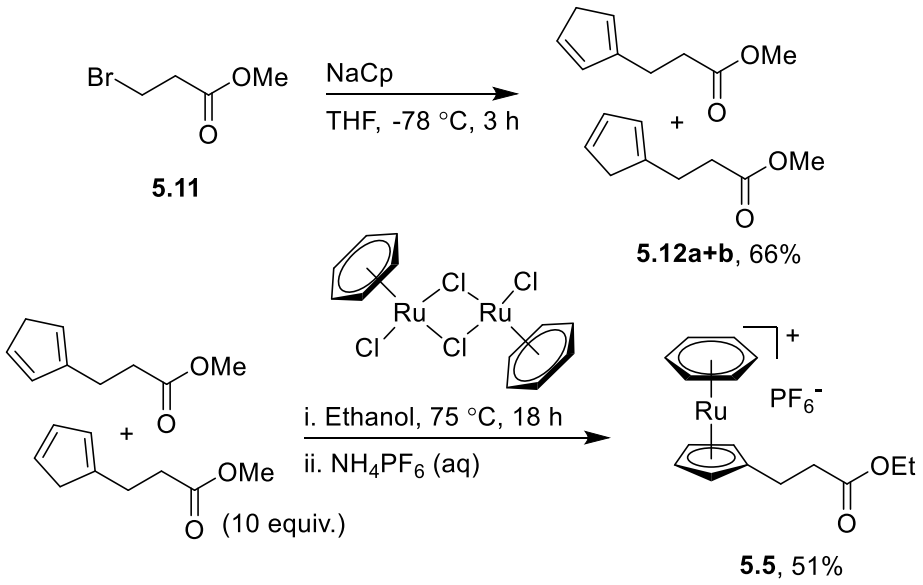

Figure 5.4 *Synthesis of [Ru(η⁶-benzene)(ethyl-3-(η⁵-cyclopentadienyl)propanoate)]PF₆* ***5.5***

Complex **5.5** was synthesised from methyl 3-bromopropionate (**5.11**), which was reacted with NaCp to form the two Cp isomer compounds **5.12a** and **5.12b** in a good yield. Without separation, the mixture of compounds was then reacted with [Ru(η⁶-benzene)Cl_2]$_2$ dimer to give the ester-tethered sandwich complex **5.5** in a moderate yield. The ester changes from methyl to ethyl during this final step due to the ethanol solvent used during complexation (Figure 5.4). Complex **5.5** was fully characterised by multinuclear NMR spectroscopy and high-resolution mass spectrometry.

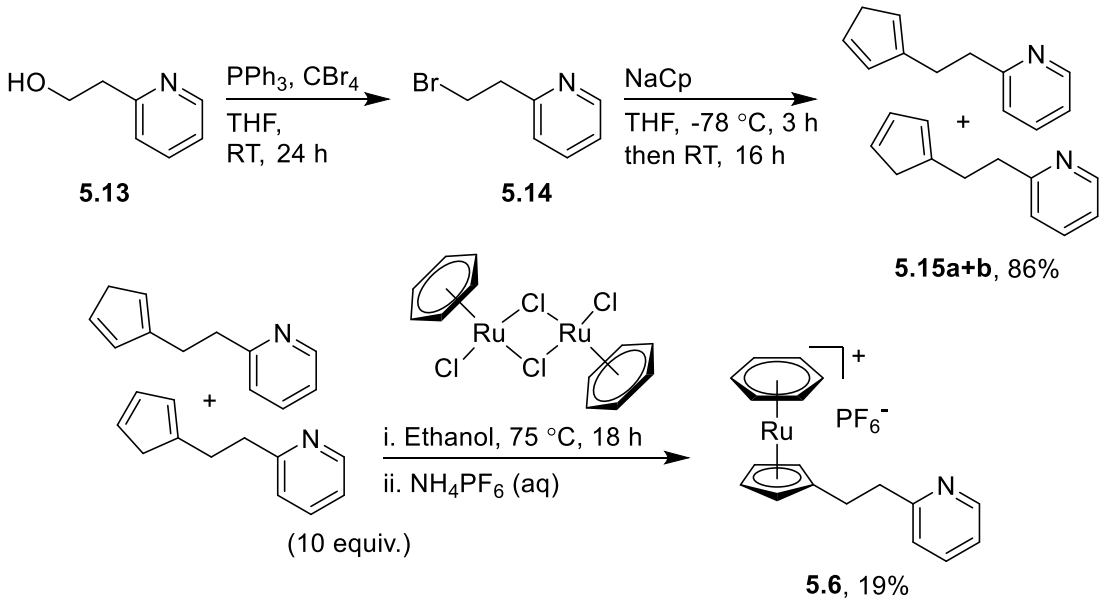

Figure 5.5 *Synthesis of [Ru(η⁶-benzene)(2-[2-(η⁵-cyclopentadienyl)ethyl]pyridine)]PF₆* ***5.6***

Complex **5.6** followed an analogous synthetic route to complex **5.5**, and began with the commercially available 2-pyridineethanol (**5.13,** Figure 5.5). Compound **5.13** was brominated an *via* Appel reaction to form 2-(2-bromoethyl)pyridine (**5.14**). Although **5.14** was initially isolated and characterised, it is susceptible to rapid degradation *via* bromine elimination to form the pyridylalkene. For this reason, subsequent reactions used the crude solution of compound **5.14** in THF following filtration to react immediately with sodium cyclopentadiene to give compound **5.15a** and **5.15b** in excellent yields. Complexation of these two Cp isomers with [Ru(η^6-benzene)Cl_2]$_2$ dimer gave complex **5.6**. Similarly, complex **5.6** was fully characterised by multinuclear NMR spectroscopy and high-resolution mass spectrometry.

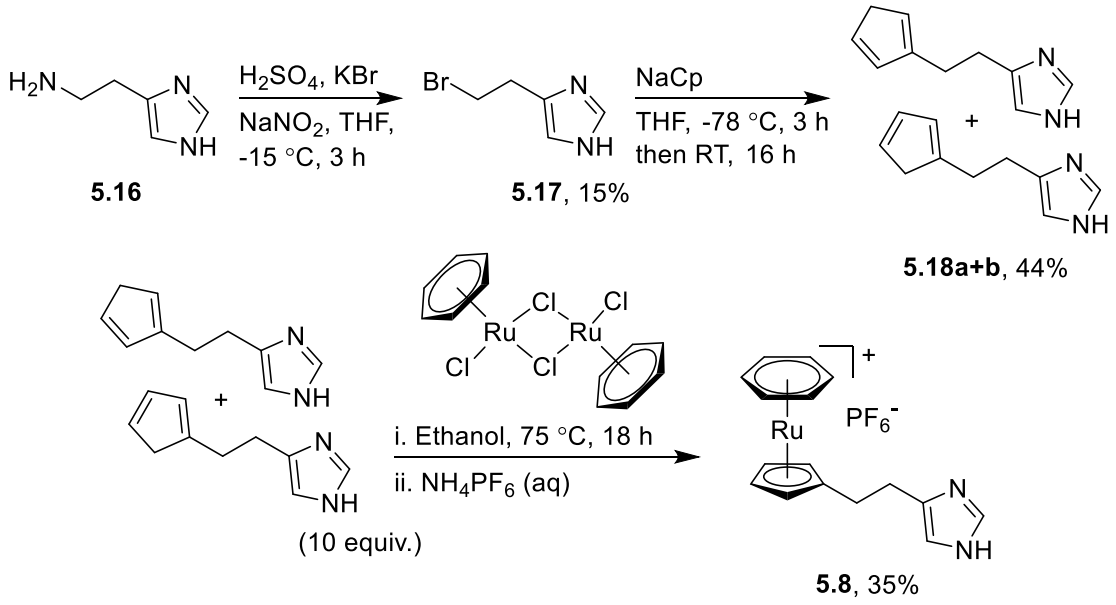

Figure 5.6 *Synthesis of [Ru(η^6-benzene)(4-[2-(η^5-cyclopentadienyl)ethyl]imidazole)]PF_6* ***5.8***

A similar route again was followed for complex **5.8**, highlighted in Figure 5.6. To begin, histamine was brominated to give 4-(2-bromoethyl)imidazole **5.17** in low yields. Compound **5.17** suffered from poor stability, so compounds **5.18a** and **5.18b** were made by reacting the crude reaction solution of **5.17** with sodium cyclopentadienyl, in a similar fashion to pyridine derivatives **5.15a** and **5.15b**. The set of Cp analogues were then reacted with the ruthenium dimer to form sandwich complex **5.8**, which was characterised by NMR spectroscopy and high-resolution mass spectrometry. Although this very challenging synthesis was achieved, the amount of material obtained was insufficient for further analysis. Therefore, complex **5.8** was not including in the exchange analysis which will be discussed later in this chapter.

Complexes **5.9** and **5.10** were synthesised by William Helme (MChem project student), and their synthetic routes will not be discussed in detail. The two complexes were made by following an analogous complexation reaction using the corresponding tethered Cp compounds with the ruthenium dimer, and were fully characterised by multinuclear NMR spectroscopy and high-resolution mass spectrometry.

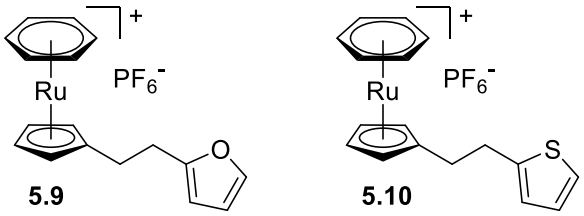

Figure 5.7 *[Ru(η^6-benzene)(2-[2-(η^5-cyclopentadienyl)ethyl]thiophene)]PF_6 (**5.9**) and [Ru(η^6-benzene)(2-[2-(η^5-cyclopentadienyl)ethyl]furan)]PF_6 (**5.10**) synthesised by William Helme.*

Attempts to synthesise complex **5.7** began using 4-(dimethylamino)pyridine (DMAP, **5.19**) as a starting material, with a target to alkylate this reagent and install functionality to which cyclopentadiene could be introduced (Figure 5.8). DMAP was activated using the Lewis acid boron trifluoride (**5.20**), which underwent successful alkylation to form 2-methyl-4-(dimethylamino)pyridine·trifluoroborate (**5.21**) using butyl lithium base and methyl iodide. The following step attempted to remove the BF_3 Lewis acid by heating **5.21** in methanol at reflux. When the product of this reaction was analysed by NMR spectroscopy, the proton NMR spectrum was in agreement with reported literature for compound **5.22**, however impurities containing boron and fluorine were still present, indicated by boron and fluorine NMR spectra. Attempts at purification *via* column chromatography resulted in collecting compound **5.21** only, suggesting the Lewis acid recombines with the pyridine during chromatography. Similar results were found when **5.21** was stirred at high temperatures in water.

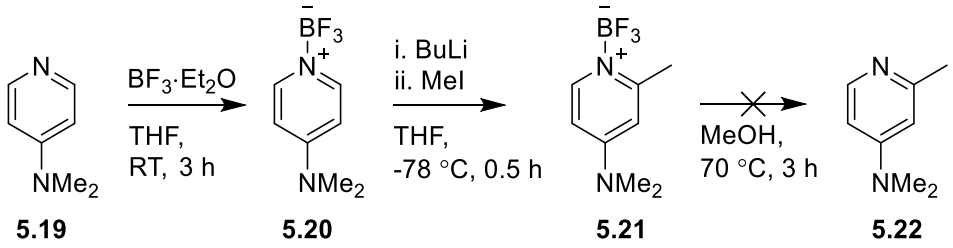

Figure 5.8 *Synthetic route toward 2-methyl-4-(dimethylamino)pyridine (**5.22**) from 4-(dimethylamino)pyridine (**5.19**).*

Compound **5.21** was subjected to reaction with paraformaldehyde in an attempt to further alkylate the pyridine. The crude product mixture of this reaction was analysed by ^{1}H-NMR spectroscopy. Two triplets, which integrate 1:1 and correlate to each other in COSY-NMR, were observed at 3.95 ppm and 2.88 ppm and could potentially correspond to the CH_2–CH_2 chain in compound **5.23** (Figure 5.9). However, this species was not able to be isolated, and therefore could not be confirmed. It is likely that with BF_3 still attached, competition to deprotonate at the methyl group or the 6-position of the pyridine ring hinders the reaction progressing to one product. Due to the difficulty of this particular route, other starting materials were explored.

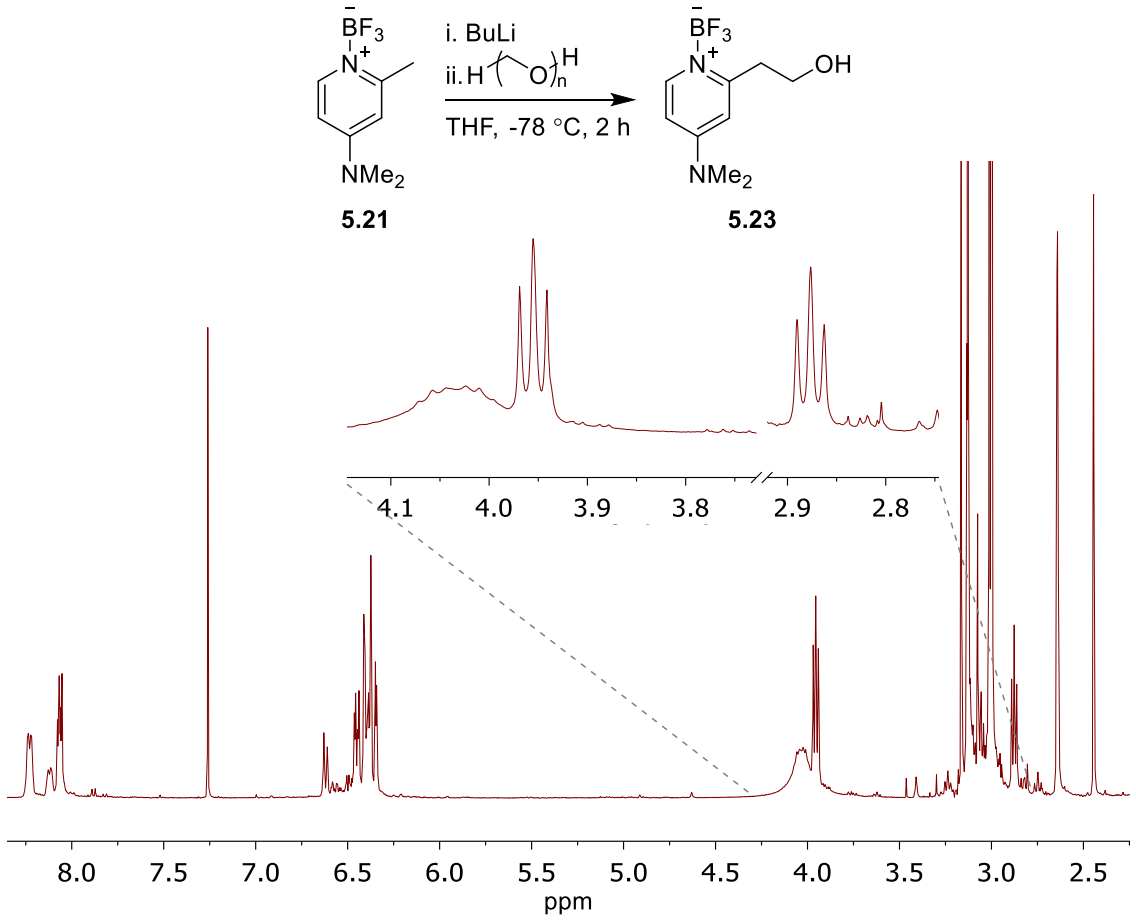

Figure 5.9 *Attempted hydroxyalkylation of 2-methyl-4-(dimethylamino)pyridine·trifluoroborate (**5.21**) with the ^{1}H-NMR spectrum of crude reaction mixture.*

To avoid activation by a Lewis acid, the starting material 2-bromo-4-aminopyridine (**5.24**) was selected. This compound was selected due to the 2-position on the pyridine ring being pre-functionalised and therefore suitable for the synthetic route envisioned. Firstly, compound **5.24** was methylated using sodium hydride and methyl iodide to form 2-bromo-4-dimethylaminopyridine (**5.25**, Figure 5.10).

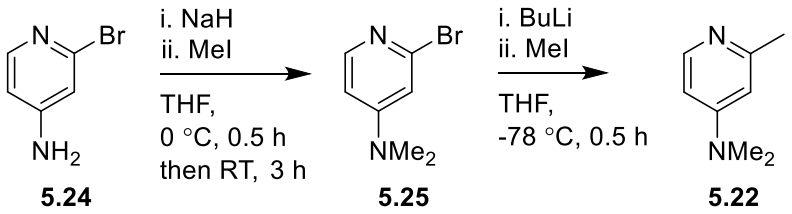

Figure 5.10 *Synthetic route toward 2-methyl-4-(dimethylamino)pyridine (**5.22**) from 2-bromo-4-aminopyridine (**5.24**).*

Compound **5.25** was then subjected to methylation conditions using butyl lithium and methyl iodide to form 2-methyl-4-(dimethylamino)pyridine (**5.22**). Confirmation of successful synthesis was obtained from the additional singlet observed at 2.43 ppm in the ^{1}H-NMR spectrum corresponding to the methyl group. Due to time restrictions of the project, synthesis towards complex **5.7** progressed no further than this point. However, plans for a complete synthesis will be described in the future work section of this thesis.

5.2.2 Arene exchange of tethered cyclopentadienyl complexes

With five of the seven complexes in hand, the rate of arene exchange was studied for the tethered complex library (Figure 5.11). The complexes were reacted with hexamethylbenzene over three and a half hours, with aliquots of the reaction solution being taken every 15 minutes and analysed by mass spectrometry (for complexes **5.9** and **5.10**, aliquots were taken every 15 minutes for 90 minutes, followed by every 30 minutes for a total reaction time of three and a half hours. These results were collected by William Helme). As outlined in *Chapter 4*, arene exchange is a dynamic reversible process, but by using an excess of a strongly electron-rich arene, this experiment aims to make arene exchange as irreversible as possible.

Complexes **2.18**, **5.5** and **5.6** unsurprisingly performed in a similar manner to that recorded in the previous investigation by Walton and Williams outlined in the introduction.[38] Pyridine tethered complex **5.6** was the best performing complex, reaching a conversion of 89% over 3.5 hours. The ester complex **5.5** was slightly outperformed by the non-tethered complex **2.18**, both reaching conversions of 55% and 68% respectively. The trend observed for these three functional groups matches that in the previous work by the group.

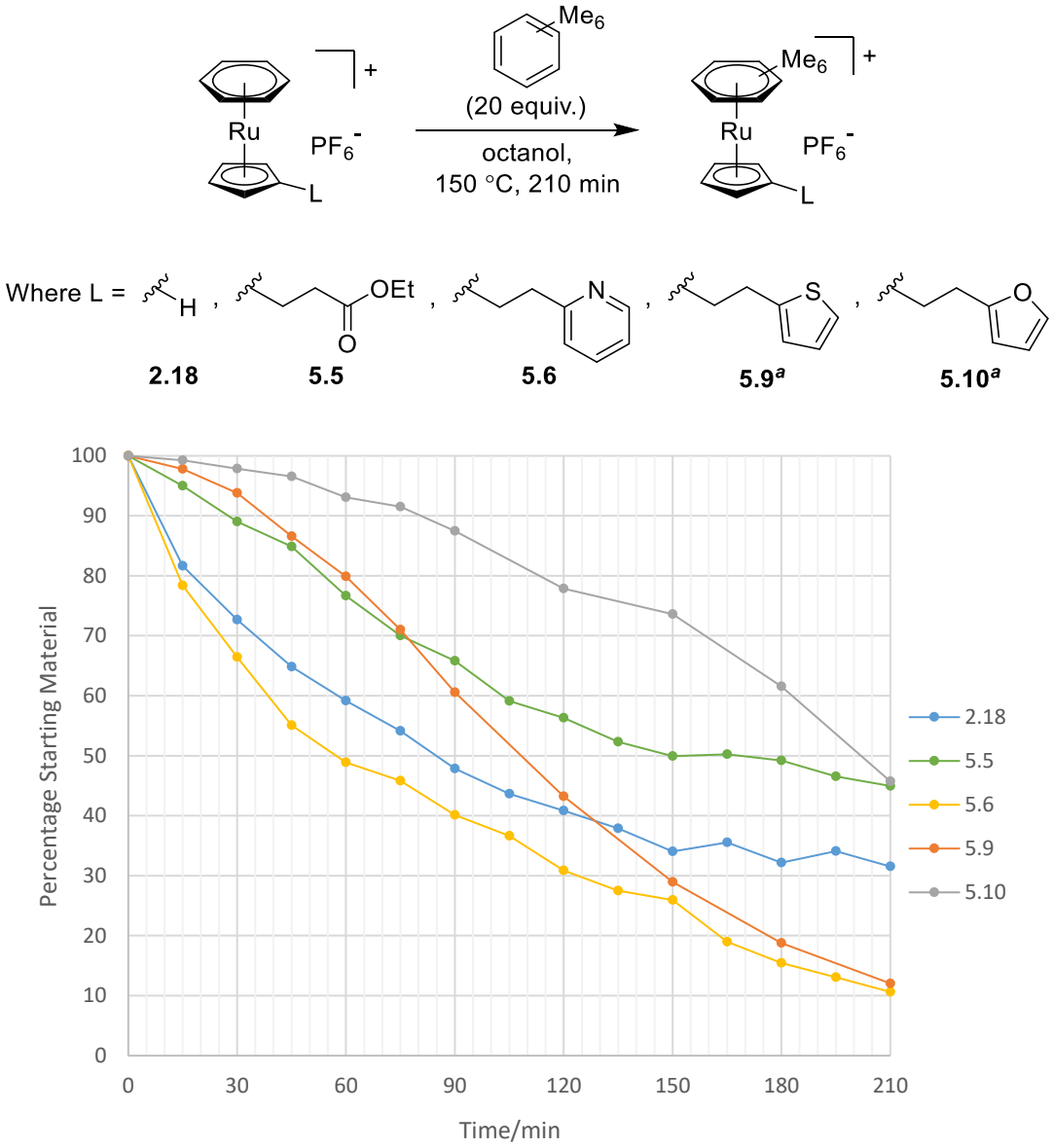

Figure 5.11 *Arene exchange of [(η⁶-benzene)RuCpL]PF₆ complexes (where L = functional group) with hexamethylbenzene.* [a] *Arene exchange experiments for complexes* ***5.9*** *and* ***5.10*** *were conducted by William Helme.*

Complexes **5.9** and **5.10** displayed an unexpected sigmoidal shaped curve as the reaction proceeded, which will be discussed in more detail later. The thiophene complex reached almost as good conversion as the pyridine complex over the three and a half hours of reaction and the furan complex showed a poor exchange rate.

On the basis that the rate determining step of this arene exchange reaction is the haptotropic shift of the bound arene from η^6 to η^4, the reaction should follow first order rate kinetics and the rate law in equation 1. Half-lives can also be calculated using equation 2, which has been derived from the rate law.

$$[A] = [A]_0 e^{-kt} \quad (1)$$

$$t_{½} = \frac{ln2}{k} \quad (2)$$

In these equations, [A] is the amount of starting material, $[A]_0$ is the initial amount of starting material, *t* is time and *k* is the rate constant for exchange.

Figure 5.12 shows the data points for complexes **2.18**, **5.5** and **5.6**, with lines of best fit plotted using least square linear regression with Microsoft Excel. Using these plots and equations 1 and 2, rate constants, *k*, and exchange half-lives were determined for these three complexes.

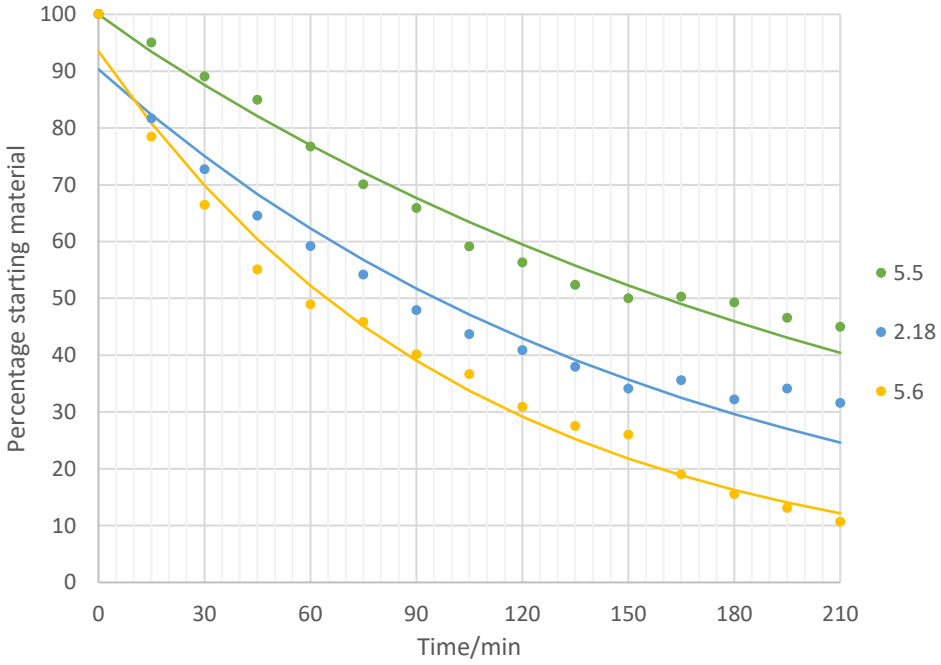

Complex	*k* / s^{-1}	$t_{½}$ / min
2.18	$6.2\times10^{-3} \pm 0.0008$	110 ± 15
5.5	$4.3\times10^{-3} \pm 0.0003$	160 ± 12
5.6	$9.7\times10^{-3} \pm 0.0009$	71 ± 6

Figure 5.12 *Lines of best fit (plot using least square linear regression) for arene exchange of complexes **2.18**, **5.5** and **5.6**, and their calculated rate constants and half-lives.*

The reaction with ester complex **5.5** is challenging to monitor, as it is expected that under the reaction conditions, octyl ester complex **5.26** can form. This has the same exact molecular weight as the product complex **5.27** which is being monitored to record conversion (Figure 5.13). The octyl ester will exchange far more slowly than the unfunctionalised Cp complex likely due to steric bulk restricting the approach of the

incoming arene. Therefore, the rate and half-life for complex **5.5** does not necessarily reflect the exchange capability of an ester functionalised Cp complex.

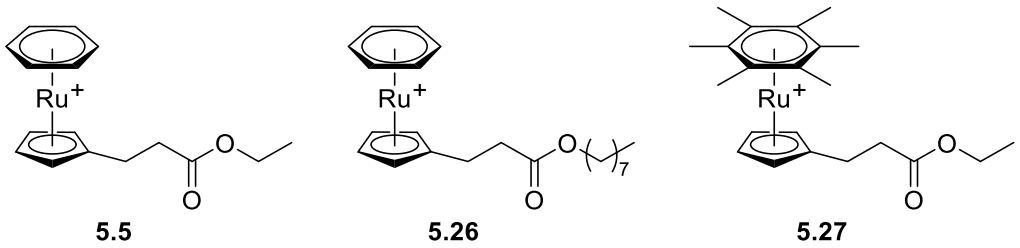

5.5 **5.26** **5.27**

Figure 5.13 *The structures of cationic complexes **5.5**, **5.26** and **2.27**, which have an exact weight of 345.043 Da, 429.137 Da and 429.137 Da respectively.*

Complexes **5.9** and **5.10** do not exhibit first order kinetics, made clear by their non-exponential decay of starting material. One explanation for the shape of the line is that the product of arene exchange further catalyses the reaction. At the beginning of the reaction, exchange is slow until the amount of product reaches a point to accelerate reaction. When a maximum rate increase is found, the reaction decays with usual first order kinetics as the materials are consumed. This could explain the observed rate of complex **5.9**, however more work is to be conducted to confirm if this is happening, and if so, what the catalysing product complex is.

5.3 Conclusions

In summary, this initial insight into these tethered complexes has suggested they could be effective at improving catalysis that proceeds *via* arene exchange. Of the complexes tested, pyridine substituted complex **5.6** has proven to produce the fastest rate of arene exchange. However, once the remaining complexes designed in the initial library have been synthesised and tested (DMAP and imidazole, complexes **5.7** and **5.8** respectively), this may not remain the case. Following kinetic testing of the entire tethered complex library, the best performing catalysis will be tested in our model reactions, including the catalytic S_NAr of aryl chlorides and the catalytic hydrodeiodination of iodoarenes. It is hypothesised that the improved efficiency of exchange should translate to greater rates of catalysis in these reactions.

6. Conclusions and Future Work

6.1 Project Conclusions

The overall aims of this project were to identify new arene transformations which could be achieved through η^6-arene-metal complexation, and to develop reactions, either new or existing, into catalytic process through these η^6-intermediates. A resurgence in the study of these complexes has prompted new inquisition into this area of catalysis, with the vast majority of catalytic cases of arene transformation being reported in the last 15 years. In order to assess the progress made over the course of three years of study, the aims of the project should be individually examined. They were as follows:

a. Develop a trifluoromethylation protocol using a nucleophilic source of CF_3 and electrophilically-activated $[(\eta^6\text{-arene})RuCp]^+$ complexes
    v. Prepare initial $[(\eta^6\text{-arene})RuCp]^+$ complex for trifluoromethylation based on literature precedent
    vi. Test complex for trifluoromethylation and optimise reaction conditions
    vii. Synthesise a library of $[(\eta^6\text{-arene})RuCp]^+$ complexes and test under optimised conditions
    viii. Develop a catalytic procedure for trifluoromethylation
b. Develop a C–H activation protocol using activated $[(\eta^6\text{-arene})RuCp]^+$ complexes
    v. Prepare initial $[(\eta^6\text{-arene})RuCp]^+$ complex for C–H activation based on literature precedent
    vi. Develop optimised conditions for C–H activation and reductive coupling of prepared complexes using Pd chemistry
    vii. Synthesise a library of $[(\eta^6\text{-arene})RuCp]^+$ complexes and test under optimised conditions
    viii. Develop a C–H activation procedure catalytic to ruthenium
c. Determine the effect of tethered catalysts on the rate of arene exchange
    iv. Prepare a library of tethered $[RuCp]^+$ complexes
    v. Measure their rates of arene exchange compared to unfunctionalised Cp
    vi. Test top performing catalysts in the groups understood catalytic reactions

The project initiated with the investigation of trifluoromethylation *via* an η^6-arene intermediate. Aided by literature precedent, nitrobenzene- and fluorobenzene-bound $[RuCp]^+$ complexes were subjected to trifluoromethylation conditions using Ruppert's reagent as the nucleophilic source of "CF_3^-". Following successful reaction, the process

was optimised and was found to proceed with a number of $[(\eta^6\text{-arene})RuCp]^+$ complexes (Figure 6.1).

Figure 6.1 *Trifluoromethylation of various Ru complexes with Me_3SiCF_3. Conditions: starting material (0.2 mmol), Me_3SiCF_3 (1.1 equiv.), KF (1.1 equiv.).*

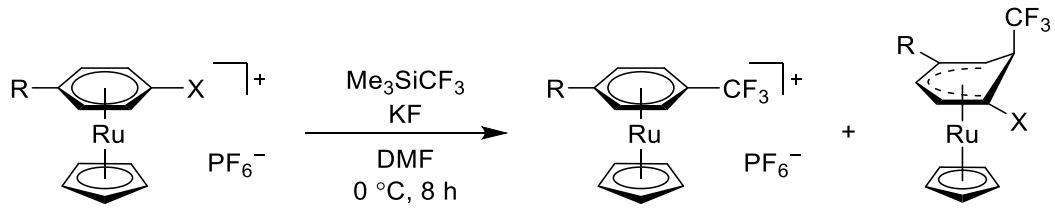

Although a novel process has been discovered, it is envisioned that a catalytic process using the current method would be very challenging. The required temperatures for the trifluoromethylation and arene exchange contradict one another and the competition between the S_NAr and *ortho*-addition reactions limits efficient catalysis. However, with further reaction optimisation *via* ligand manipulation, greater stochiometric conversions and selectivity could become feasible. The scope of this reaction is currently limited to electron deficient arenes, but incorporating more electron withdrawing ligands around the ruthenium could expand the scope to more electron rich substrates.

Running in parallel to this trifluoromethylation project was the development of a C–H activation protocol facilitated by $[RuCp]^+$. Initial investigations with *o*-fluorotoluene complex **3.3** saw great success, and once this reaction was optimised achieved a high yield of 83%. The scope of both Ru-arene complex and aryl halide were explored following optimisation, which saw conversations ranging from good to poor with a range of ruthenium-arene complexes and aryl iodides (Figure 6.2).

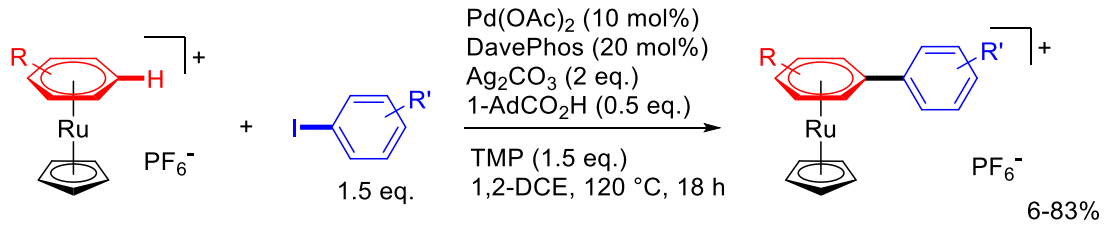

Figure 6.2 *C–H activation between various $[(\eta^6\text{-arene})RuCp]^+$ complexes and aryl halides under optimised reaction conditions.*

A promising result from both the trifluoromethylation and C–H activation protocols is the ability to regenerate the ruthenium complex following the arene transformation *via* photolysis. The quantitative conversion from the sandwich complex to the corresponding free arene and piano-stool ruthenium complex drastically improves the atom economy of this process. Despite this encouraging result, however, a reaction catalytic in ruthenium

has remained to be seen. Attempts were made by Dr Luke Wilkinson to achieve catalysis, but investigations found a strong dependence on the solvent used in order to facilitate the transformation. While 1,2-DCE was an effective solvent for the stoichiometric reaction, no conversion was observed when a catalytic amount of ruthenium was used, likely due to a lack of arene exchange. When other solvents were tested toward the catalytic C–H activation, similarly no conversion was observed. Further study of this reaction is required in order to develop a successful catalytic protocol of this manner.

In order to better understand the arene exchange process on $[RuCp]^+$ complexes and create more efficient catalysis in our group, a number of complexes with a tethered coordinating functional group were synthesised and their ability to affect the rate of exchange was studied (Figure 6.3).

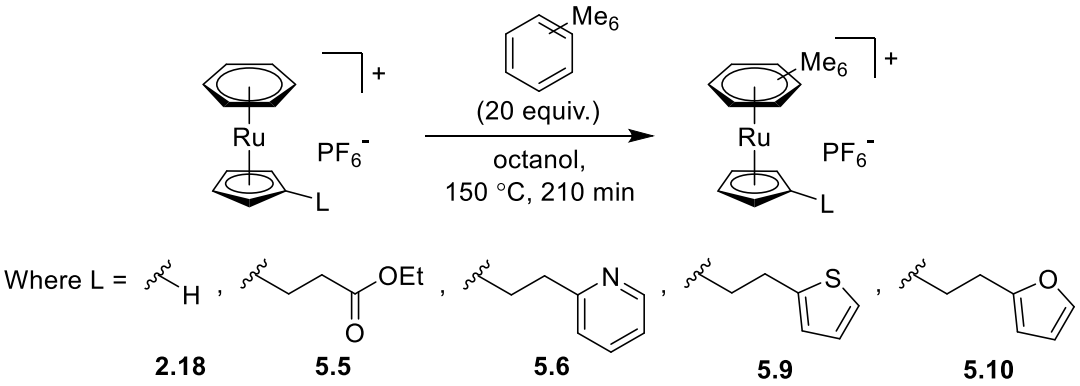

Figure 6.3 *Arene exchange of [(η^6-benzene)RuCpL]PF_6 complexes (where L = functional group) with hexamethylbenzene.*

This project is still in its infancy, firstly in terms of the complex library and secondly in evaluating their improvement on arene exchange. However, the work discussed in this chapter shows that tethers do have an effect on the rate of arene exchange, whether that be positive or negative. Future work will work on a greater selection of functional tethers to identify a complex which considerably improves rates of arene exchange in these types of systems. Additionally, the increases in rate must then translate to improved catalysis. We envision the reduced reaction times brought about by utilising microwave heating rather than conventional heating could assist the stability of these tethered complexes. However, this still needs to be tested.

Lastly, a method to hydrodeiodinate arenes catalysed by ruthenium has been developed. This project was not included in the initial aims due to its serendipitous discovery during the three years of study. Once the reaction had been optimised, this protocol became an extremely versatile and tolerant procedure, working excellently on a wide range of aryl

iodide substrates and exhibiting outstanding conversions with a variety of catalyst loadings and reaction times (Figure 6.4).

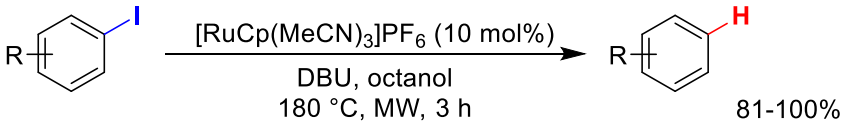

Figure 6.4 *Catalytic hydrodeiodination of aryl iodides under optimised conditions.*

Establishing the scope of this reaction was followed by rigorous investigation of the reaction mechanism. A host of experiments, utilising a range of analytical techniques, probed the nature of this transformation and helped form our conclusions regarding the radical hydrodehalogenation *via* η^6-intermediates. One can imagine further developing this reaction to achieve new transformations from the same mechanistic approach, details of which will be discussed in the next section.

6.2 Future Work

As well as the points discussed above, there are a number of areas worth exploring. Firstly, during the investigation of the scope of the deiodination reaction, it was found that when substrates bearing a nitro group were tested, they displayed some unexpected results. While the iodine was removed from the arene, analysis of the crude ^{1}H-NMR spectra suggested reduction of the nitro group had also occurred. Preliminary investigation into this transformation has begun, and the experiment described in Figure 6.5 gave a mixture of products, with the major product being aniline.

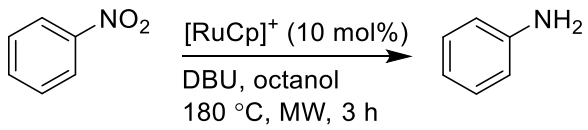

Figure 6.5 *Potential reduction of nitrobenzene catalysed by ruthenium.*

Further study is required to tune the selectivity of the reaction and to determine what mechanism may be occurring, but this result shows promise for a new catalytic nitro-group reduction and could provide an alternative to typical methods such as metal/HCl (metal = zinc, nickel, etc.).

Another project that should be explored is the potential for enantioselective radical cyclisations catalysed by ruthenium *via* η^6-arene intermediates. Data collected and discussed in *Chapter 4* demonstrates a degree of selectivity when the $[RuCp]^+$ unit binds to arenes in an η^6-fashion. Steric interaction between the arene and the metal fragment will cause this bond to form preferentially on one face over the other. With this selectivity in mind, and considering the mechanism in which the deiodination reaction is suggested to proceed, the potential to perform enantioselective cyclisation is an exciting idea. A general reaction profile is described in Figure 6.6.

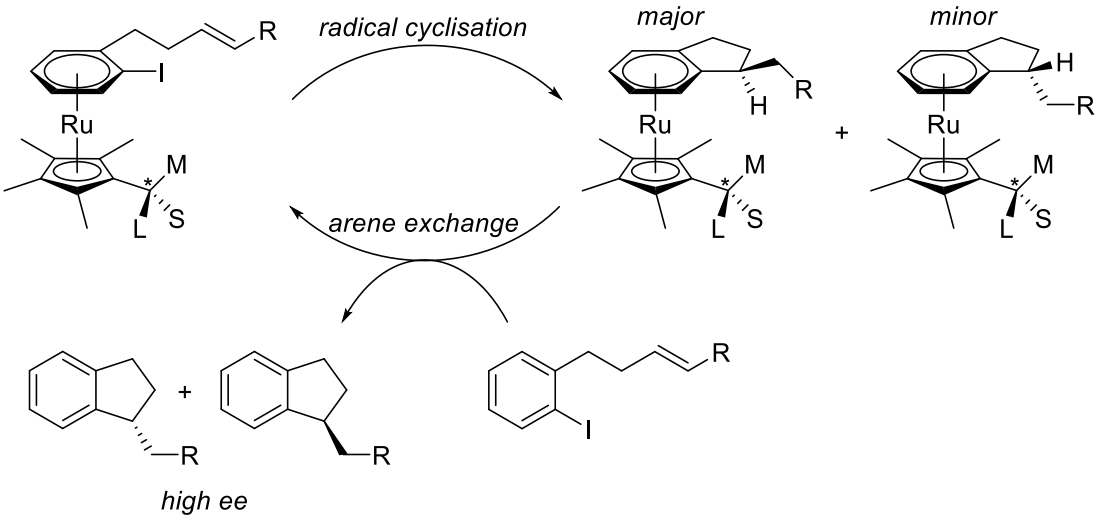

Figure 6.6 *Potential enantioselective radical cyclisation catalysed by ruthenium via η^6-arene intermediates.*

By incorporating chiral steric bulk into the Cp system, the extent of the selectivity could be enhanced and therefore could facilitate transformations with high enantiomeric excess.

Lastly, a longer-term aim for the group would be to achieve catalysis *via* η^6-arene intermediates employing photolysis to enhance arene exchange. As discussed in the introduction of this thesis (Figure 1.30), a challenge with this type of catalysis is that a strongly-withdrawing metal fragment which facilitates excellent arene transformation will have sluggish arene exchange kinetics, and vice versa. One way to circumvent this issue is by using UV light to create photocatalytic reactions (Figure 6.7).

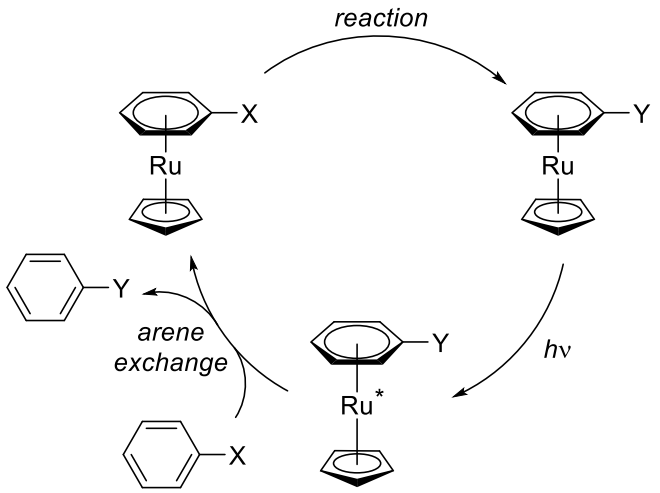

Figure 6.6 *General catalytic cycle for catalysis via arene exchange promoted by photolysis.*

By irradiating the product arene complex during reaction, significantly faster arene exchange should be possible. A potential issue with this procedure is that the irradiation will likely excite both starting and product complex. One option to negate this problem could be intermittent irradiation, which would give the system suitable time to create a build-up of product arene. We envision reactions combining photolysis and heating to achieve rapid rates of arene exchange and set a new precedent for this type of catalysis.

6.3 Final Remarks

During the three years of this project, a number of interesting transformations have been developed. Although each of these processes utilised a similar methodology, which is essentially activating the arene through a net electron-withdrawing effect of the bound metal, these studies have contributed to a wide range of fields in chemistry. The versatility and adaptability of η^6-arene activation gives it great potential as a method of organic synthesis. While the findings discussed in this thesis have broadened the understanding of this field of organometallic chemistry, large strides must be taken before this mechanism would be industrially applicable. When competing against catalysts which routinely achieve turn over numbers in the thousands, more work is required to deliver η^6-metal catalysts that can match this level of efficiency. The use of photolysis to drive catalytic conversion could be a pioneering development for improving this method. Whether these types of catalysts are used on a large scale in the near future or not, they remain to be an interesting field of organometallic chemistry.

7. Experimental

7.1 Experimental Procedures

7.1.1 General Procedures

Chemicals were purchased from Sigma Aldrich UK, Fluorochem, Merck and Fisher UK. Solvents were laboratory grade or dried by the Durham University SPS service. Dried solvents were stored over activated 3 Å molecular sieves. Reactions requiring anhydrous conditions were carried out under an atmosphere of dry argon or nitrogen using Schlenk-line techniques. Where appropriate, solvents were degassed by sparging with argon unless specified otherwise.

Thin-layer chromatography was carried out on silica plates (Merck 5554) and visualised under UV (254/365 nm) irradiation or by staining with iodine, vanillin or potassium permanganate stains. Preparative column chromatography was carried out using silica (Merck Silica Gel 60, 230400 mesh).

NMR spectra (^{1}H, ^{13}C, ^{19}F, ^{31}P) were recorded on a Varian VXR-400 spectrometer (^{1}H at 399.97 Hz, ^{13}C at 100.57 MHz, ^{19}F at 76.50 MHz, ^{31}P at 164.98 MHz) or a Varian VNMRS-700 spectrometer (^{1}H at 699.73 MHz, ^{13}C at 175.95 MHz, ^{31}P at 150.50 MHz). Spectra were recorded at 295 K in commercially available deuterated solvents and referenced internally to the residual solvent proton resonances. The number of protons (n) for a given resonance signal is indicated by nH. The multiplicity of each signal is indicated by s (singlet); d (doublet); t (triplet); q (quartet); quin (quintet) or sept (septet). Coupling constants (*J*) are quoted in Hz and are recorded to the nearest 0.5 Hz. Identical proton coupling constants (*J*) are averaged in each spectrum and reported to the nearest 0.5 Hz. The coupling constants are determined by analysis using MestReNova software. Spectra were assigned using COSY, HSQC, HMBC and NOESY experiments as necessary.

Both electrospray and high-resolution mass spectrometry were performed on a Thermo-Finnigan LTQ FT system using methanol as the carrier solvent. m/z values are reported in Daltons with specific isotopes identified.

Reverse phase HPLC analysis was performed at 298 K on an Interchim PuriFlash 4250 system, Waters XBridge Prep-C18 –19x50 mm (5 μm) column was used for complexes synthesised by C–H activation in *Chapter 3* and complex **4.32**, times varying from 2 –5

min. A solvent system of H_2O / MeCN (gradient elution) was used. The UV/Vis detector was set at appropriate wavelengths according to the species being analysed. Channel 1: UV600 SCAN – 225-600. Channel 2: UV600: SIG1 – 254 nm.

7.1.2 X-Ray Studies

The X-ray single crystal data have been collected using MoKα radiation (λ =0.71073 Å) on a Bruker D8Venture diffractometer (Photon100 CMOS detector, IμS-microsource, focusing mirrors, 1° ω-scan) equipped with a Cryostream (Oxford Cryosystems) open-flow nitrogen cryostats at the temperature 120.0(2)K. The structures were solved by direct method and refined by full-matrix least squares on F^2 for all data using SHELXTL [G.M. Sheldrick, Acta Cryst. (2008), A64, 112-122] and OLEX2 [O. V. Dolomanov, L. J. Bourhis, R. J. Gildea, J. A. K. Howard, H. Puschmann, J. Appl. Cryst. (2009), 42, 339-341.] software. All non-hydrogen atoms were refined anisotropically, the hydrogen atoms were placed in the calculated positions and refined in riding mode.

7.2 Synthetic Procedures

Stability of ruthenium compounds

All [(η^6-arene)RuCp]PF_6 complexes synthesised in this project demonstrated excellent stability. They could be stored for many months in both the solid and solution state and showed no visual or spectroscopic signs of degradation.

Compound **2.7** [RuCp$(MeCN)_3$]PF_6 used to synthesis all the sandwich complexes was moisture sensitive in the solid state, and was both moisture and air sensitive in the solution state. All reactions using this compound were carried out using degassed and anhydrous solvents under an argon atmosphere.

General procedure for C–H activation of [(η^6-arene)RuCp]PF_6 complexes

All catalysis runs were performed at high temperature in a sealed Young's Tap flask. The flask was placed in a reaction carrousel with a heating block at the bottom and a cooling block at the top. Solid reagents were weighed out and transferred to an oven dried Young's Tap flask. This was placed under an inert atmosphere, after which the dry and

deoxygenated solvent was added *via* a syringe purged with argon. The liquid reagents were then added *via* Gilson pipette under a steady stream of argon and then the reaction vessel sealed. The temperature was increased to 120 °C and the reaction was left for 18 hours. After that time, volatiles were removed via distillation and the resulting solids were re-dissolved in acetone. This mixture was filtered and the filtrate was concentrated in vacuo and dried to give a crude solid. Following column chromatography, the arylated complexes were isolated as solids.

General procedure for catalytic deiodination of aromatic substrates

A microwave vial purged under argon atmosphere was charged with $[RuCp(MeCN)_3]PF_6$ (10 mol%) and iodoarene (100 mg, see *Appendix* for amount, volumes and moles). To this, octanol (1 mL), which was degassed (3 × freeze-pump-thaw cycles) and dried over molecular sieves (3 Å), was added, followed by DBU (1.0 equiv, see *Appendix* for amount and moles). The microwave vial was then sealed and further purged with argon for 5 minutes before being heated to 180 °C and allowed to react for 3 hours. 100 µL aliquots were taken from the reaction mixture which were added to 1 mL of $CDCl_3$ containing 1 mg of DMF as internal standard. Conversions were calculated by integral comparison between product and remaining starting material, and yields were calculated by integral comparison of product and DMF. Conversions were also calculated using GC-MS by comparing amount of product arene against remaining starting material. GC-MS samples were prepared by drawing 100 µL aliquots from the reaction mixture, which were then diluted into 2.9 mL of decane. Particulates were removed *via* filtration and the remaining solution was diluted 3-fold to a concentration of approximately 1 mg/mL and analysed by GC-MS. Conversions were then calculated by Selective Ion Monitoring (SIM) GC-MS for product arene and remaining starting material (see *Appendix* for ions monitored for each given reaction).

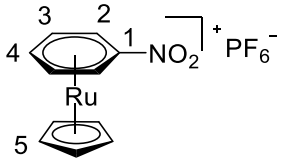

[Ru(η^6-nitrobenzene)(η^5-cyclopentadienyl)]PF_6 **2.8**

To a solution of nitrobenzene (63 mg, 53 µL, 0.507 mmol, 1.1 equiv) in degassed 1,2-dichloroethane (9 mL) at 80 °C was added $[Ru(NCMe)_3Cp]PF_6$ (200 mg, 0.461 mmol). The resulting solution was heated to reflux for 16 hours under an inert atmosphere, allowed to cool to room temperature and filtered. The filtrate was concentrated in vacuo, redissolved in a minimum of MeCN and added dropwise to Et_2O. The green solid was isolated by filtration, rinsed with ether, dissolved in MeCN, concentrated in vacuo and dried under vacuum to give the *title compound* as a light brown solid (187 mg, 93%); **δ_H** (acetone-D_6) 7.46 (2H, dt, $^3J_{H\text{-}H}$ 6.0 Hz, $^4J_{H\text{-}H}$ 2.0 Hz, H^2), 6.79 (2H, tt, $^3J_{H\text{-}H}$ 6.0 Hz, $^4J_{H\text{-}H}$ 2.0 Hz, H^3), 6.70 (1H, tt, $^3J_{H\text{-}H}$ 6.0 Hz, $^4J_{H\text{-}H}$ 2.0 Hz, H^4) 5.78 (5H, s, H^5); **δ_C** (acetone-D_6) 111.4 (1C, s, C^1), 88.5 (1C, s, C^4), 86.5 (2C, s, C^3), 83.7 (5C, s, C^5), 82.9 (2C, s, C^2); **δ_P** (acetone-D_6) -144.3 (sept., $J_{P\text{-}F}$ 707 Hz); *m/z* ($HRMS^+$) 283.9788 $[M\text{-}PF_6]^+$ ($C_{11}H_{10}NO_2{}^{96}Ru$ requires 283.9787); Anal. found (expected): C 30.47 (30.43); H 2.34 (2.32); N 3.37 (3.23).

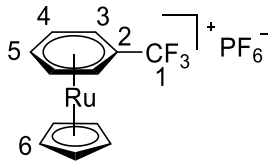

[Ru(η^6-α,α,α-trifluorotoluene)(η^5-cyclopentadienyl)]PF_6 **2.9**

[Ru(η^6-nitrobenzene)(η^5-cyclopentadiene)]PF_6 (100 mg, 0.230 mmol) was dissolved in anhydrous DMF (5 mL). Oven dried potassium fluoride (15 mg, 0.253 mmol, 1.1 equiv) and trimethyl(trifluoromethyl)silane (36 mg, 37.4 µL, 0.253 mmol, 1.1 equiv) were added. The mixture was stirred at 0 °C under argon atmosphere for 8 hours. Purification by column chromatography (silica, acetonitrile : 5% MeOH) gave the *title compound* as a brown solid (33 mg, 31%); **δ_H** (acetone-D_6) 6.86 – 6.82 (2H, m, H^3), 6.64 – 6.61 (3H, m, $H^{4\text{ and }5}$), 5.70 (5H, s, H^6); **δ_C** (acetone-D_6) 123.2 (1C, q, $^1J_{C\text{-}F}$ 274 Hz, C^1), 91.8 (1C, q, $^2J_{C\text{-}F}$ 38 Hz, C^2), 87.8 (1C, s, C^5), 86.2 (2C, s, C^4), 83.6 (2C, q, $^3J_{C\text{-}F}$ 3 Hz, C^3), 82.6 (5C, s, C^6); **δ_F** (acetone-D_6) -62.33 (3F, s, F^{arene}), -72.6 (6F, d, $^1J_{F\text{-}P}$ 707 Hz, $F^{counterion}$); *m/z* ($HRMS^+$) 306.9812 $[M\text{-}PF_6]^+$ ($C_{12}H_{10}F_3{}^{96}Ru$ requires 306.9811) R_f= 0.17 (silica, acetonitrile : 5% MeOH); Anal. found (expected): C 31.69 (31.52); H 2.21 (2.20); N 0.26 (0.00).

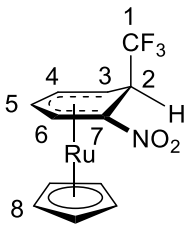

[Ru(η^5-1-nitro-2-trifluoromethylcyclohexadienyl)(η^5-cyclopentadiene)] **2.10**

[Ru(η^6-nitrobenzene)(η^5-cyclopentadiene)]PF_6 (100 mg, 0.230 mmol) was dissolved in anhydrous DMF (5 mL). Oven dried potassium fluoride (15 mg, 0.253 mmol, 1.1 equiv) and trimethyl(trifluoromethyl)silane (36 mg, 37.4 µL, 0.253 mmol, 1.1 equiv) was added. The mixture was stirred at 0 °C under argon atmosphere for 8 hours. Purification by column chromatography (silica, pet. ether : 20% EtOAc) gave the *title compound* as a yellow oil (27 mg, 32%); **δ_H** (acetone-D_6) 6.19 (1H, td, $^3J_{H\text{-}H}$ 5.5 Hz, $^4J_{H\text{-}H}$ 1.5 Hz, H^5), 6.09 (1H, ddd, $^3J_{H\text{-}H}$ 5.5 Hz, $^4J_{H\text{-}H}$ 1.5 Hz, $^4J_{H\text{-}H}$ 0.5 Hz, H^6), 5.09 (1H, t, $^3J_{H\text{-}H}$ 5.5 Hz, H^4), 4.96 (5H, s, H^8), 4.48 (1H, qdd, $^3J_{H\text{-}F}$ 8.0 Hz, $^3J_{H\text{-}H}$ 6.5 Hz, $^4J_{H\text{-}H}$ 1.5 Hz, H^2), 3.76 (1H, m, H^3); **δ_C** (acetone-D_6) 124.1 (1C, q, $^1J_{C\text{-}F}$ 287 Hz, C^1), 81.0 (1C, s, C^4), 80.6 (1C, s, C^5), 79.4 (5C, s, C^8), 75.1 (1C, s, C^6), 62.0 (1C, m, C^7), 43.4 (1C, q, $^2J_{C\text{-}F}$ 29 Hz, C^2), 28.3 (1C, q, $^1J_{C\text{-}F}$ 2 Hz, C^3); **δ_F** (acetone-D_6) -76.4 (3F, d, $^3J_{F\text{-}H}$ 8.0 Hz); IR 1569 cm^{-1} and 1378 cm^{-1} (NO_2 stretch); *m/z* (HRMS$^+$) 353.9818 $[M+H]^+$ ($C_{12}H_{11}F_3NO_2{}^{96}Ru$ requires 353.9818), 306.9811 $[M\text{-}NO_2]^+$ ($C_{12}H_{10}F_3{}^{96}Ru$ requires 306.9811), R_f= 0.28 (silica, pet. ether : 20% EtOAc).

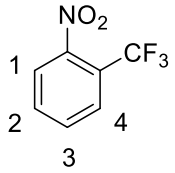

2-Trifluoromethyl-nitrobenzene **2.12**

To an oven dried Schlenk tube, [Ru(η^5-1-nitro-2-trifluoromethylcyclohexadienyl)(η^5-cyclopentadiene)] (20 mg, 55.8 µmol) was added and dissolved in anhydrous deuterated acetonitrile (1 mL). To this, 2,3-Dichloro-5,6-dicyano-1,4-benzoquinone (15 mg, 66.9 µmol, 1.2 equiv) was added and the mixture was stirred at room temperature for 24 hours. ^{1}H- and ^{19}F-NMR showed confirmation of quantitative conversion to free arene using an external standard of α,α,α-trifluorotoluene (10 mg, *quantitative*); **δ_H** (acetonitile-D_3) 8.00 (1H, m), 7.96 (1H, m), 7.89 (2H, m); **δ_F** (acetonitrile-D_3) -60.2 (3F, m).

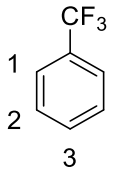

α,α,α-Trifluorotoluene **2.11**

To a quartz NMR tube, [Ru(η^6-α,α,α-trifluorotoluene)(η^5-cyclopentadienyl)]PF_6 (20 mg, 43.7 µmol) was added and dissolved in anhydrous deuterated acetonitrile (0.8 mL). The mixture was irradiated with a UV lamp (365 mn, 36 W) for 27 hours to give the *title compound* in a quantitative conversion (see Figure 2.11). **δ_H** (acetonitile-D_3) 7.73 (2H, m, H^1), 7.68 (1H, t, $^3J_{H\text{-}H}$ 7.5, H^3) 7.60 (2H, t, $^3J_{H\text{-}H}$ 7.5, H^2); **δ_F** (acetonitrile-D_3) -63.2 (3F, m).

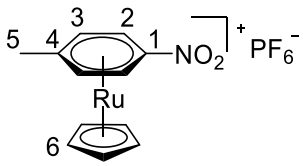

[Ru(η^6-4-nitrotoluene)(η^5-cyclopentadienyl)]PF_6 **2.13**

To a solution of 4-nitrotoluene (19 mg, 0.138 mmol, 1.1 equiv) in degassed 1,2-dichloroethane (4 mL) at 80 °C was added [Ru$(NCMe)_3$Cp]PF_6 (50 mg, 0.115 mmol). The resulting solution was heated to reflux for 16 hours, allowed to cool to room temperature and filtered. The filtrate was concentrated in vacuo, redissolved in a minimum of MeCN and added dropwise to Et_2O. The light brown precipitate was isolated by filtration, rinsed with ether, dissolved in MeCN, concentrated in vacuo and dried under vacuum to give the *title compound* as a light brown solid (56 mg, 91%). **δ_H** (acetone-D_6) 7.39 (2H, d, $^3J_{H\text{-}H}$ 6.5 Hz, H^2), 6.77 (2H, d, $^3J_{H\text{-}H}$ 6.5 Hz, H^3), 5.73 (5H, s, H^6), 2.54 (3H, s, H^5); **δ_C** (acetone-D_6) 110.5 (1C, s, C^1), 105.8 (1C, s, C^4), 88.6 (2C, s, C^3), 87.6 (1C, s, C^5), 83.3 (5C, s, C^6), 72.9 (1C, s, C^2); **δ_P** (acetone-D_6) -144.3 (sept, $^1J_{P\text{-}F}$ 713 Hz); **δ_F** (acetone-D_6) -72.2 (d, $^1J_{F\text{-}P}$ 713 Hz); *m/z* (HRMS$^+$) 263.9946 $[M - PF_6]^+$ ($C_{12}H_{12}N^{96}Ru$ requires 297.9944); Anal. found (expected): C 31.38 (32.15); H 2.71 (2.70); N 3.30 (3.12).

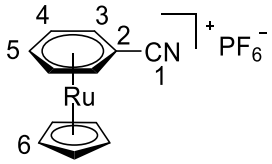

[Ru(η^6-benzonitrile)(η^5-cyclopentadienyl)]PF_6 **2.14**

To a solution of benzonitrile (26 mg, 26 µL, 0.253 mmol, 1.1 equiv) in degassed 1,2-dichloroethane (6 mL) at 80 °C was added $[Ru(NCMe)_3Cp]PF_6$ (100 mg, 0.230 mmol). The resulting solution was heated to reflux for 16 hours, allowed to cool to room temperature and filtered. The filtrate was concentrated in vacuo, redissolved in a minimum of MeCN and added dropwise to Et_2O. The light brown precipitate was isolated by filtration, rinsed with ether, dissolved in MeCN, concentrated in vacuo and dried under vacuum to give the *title compound* as a light brown solid (85 mg, 89%). **δ_H** (acetone-D_6) 6.89 (2H, dt, $^3J_{H\text{-}H}$ 6.0 Hz, $^4J_{H\text{-}H}$ 1.5 Hz, H^3), 6.65 (2H, tt, $^3J_{H\text{-}H}$ 6.0 Hz, $^4J_{H\text{-}H}$ 1.5 Hz, H^4), 6.61 (1H, $^3J_{H\text{-}H}$ 6.0 Hz, $^4J_{H\text{-}H}$ 1.5 Hz, H^5), 5.77 (5H, s, H^6); **δ_C** (acetone-D_6) 115.3 (1C, s, C^1), 88.6 (2C, s, C^3), 87.6 (1C, s, C^5), 86.7 (2C, s, C^4), 83.3 (5C, s, C^6), 72.9 (1C, s, C^2); **δ_P** (acetone-D_6) -144.3 (sept, $^1J_{P\text{-}F}$ 713 Hz); **δ_F** (acetone-D_6) -72.2 (d, $^1J_{F\text{-}P}$ 713 Hz); *m/z* (HRMS$^+$) 263.9888 $[M - PF_6]^+$ ($C_{12}H_{10}N^{96}Ru$ requires 263.9889); Anal. found (expected): C 34.85 (34.79); H 2.56 (2.43); N 3.43 (3.38).

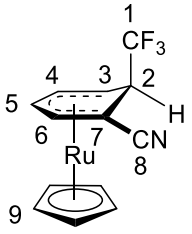

[Ru(η^5-1-cyano-2-trifluoromethylcyclohexadienyl)(η^5-cyclopentadiene)] **2.14b**

[Ru(η^6-benzonitrile)(η^5-cyclopentadiene)]PF_6 (20 mg, 48.3 µmol) was dissolved in anhydrous DMF (3 mL). Oven dried potassium fluoride (4 mg, 53.1 µmol, 1.1 equiv) and trimethyl(trifluoromethyl)silane (8 mg, 9 µL, 53.1 µmol, 1.1 equiv) was added. The mixture was stirred at 0 °C under argon atmosphere for 8 hours. Purification by column chromatography (silica, pet. ether : 20% EtOAc) gave the *title compound* as a brown oil (6 mg, 36%). **δ_H** (acetone-D_6) 6.13 (1H, td, $^3J_{H\text{-}H}$ 5.5 Hz, $^4J_{H\text{-}H}$ 1.0 Hz, H^5), 5.25 (1H, d, $^3J_{H\text{-}H}$ 5.5 Hz, H^6), 5.05 (5H, s, H^9), 4.94 (1H, t, $^3J_{H\text{-}H}$ 5.5 Hz, H^4), 3.48 (1H, qdd, $^3J_{H\text{-}F}$ 7.5 Hz, $^3J_{H\text{-}H}$ 5.5 Hz, $^4J_{H\text{-}H}$ 1.5 Hz, H^2), 3.33 (1H, t, $^3J_{H\text{-}H}$ 5.5 Hz, H^3); **δ_C** (acetone-D_6) 124.1

(1C, q, $^{1}J_{C\text{-}F}$ 286 Hz, C^{1}), 123.2 (1C, m, C^{8}), 81.9 (1C, s, C^{5}), 80.4 (1C, s, C^{4}), 79.0 (5C, s, C^{9}), 78.8 (1C, s, C^{6}), 44.2 (1C, q, $^{2}J_{C\text{-}F}$ 29 Hz, C^{2}), 24.1 (1C, q, $^{1}J_{C\text{-}F}$ 2 Hz, C^{3}), 7.07 (1C, s, C^{7}); $\boldsymbol{\delta_F}$ (acetone-D_6) -78.7 (3F, d, $^{3}J_{F\text{-}H}$ 8.0 Hz); *m/z* (HRMS^{+}) 333.9921 $[M+H]^{+}$ ($C_{13}H_{11}F_3N^{96}Ru$ requires 333.9920), R_f= 0.24 (silica, pet. ether : 20% EtOAc).

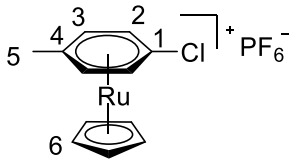

[Ru(η^{6}-4-chlorotoluene)(η^{5}-cyclopentadienyl)]PF_6 **2.15**

To a solution of 4-chlorotoluene (48 mg, 45 µL, 0.380 mmol, 1.1 equiv) in degassed 1,2-dichloroethane (8 mL) at 80 °C was added $[Ru(NCMe)_3Cp]PF_6$ (150 mg, 0.345 mmol). The resulting solution was heated to reflux for 16 hours, allowed to cool to room temperature and filtered. The filtrate was concentrated in vacuo, redissolved in a minimum of MeCN and added dropwise to Et_2O. The light brown precipitate was isolated by filtration, rinsed with ether, dissolved in MeCN, concentrated in vacuo and dried under vacuum to give the *title compound* as a light brown solid (147 mg, 97%). $\boldsymbol{\delta_H}$ (acetone-D_6) 6.81 – 6.74 (2H, m, H^{2}), 6.55 – 6.48 (2H, m, H^{3}), 5.63 (5H, s, H^{6}), 2.42 (3H, s, H^{5}); $\boldsymbol{\delta_C}$ (acetone-D_6) 104.7 (1C, s, C^{1}), 102.6 (1C, s, C^{4}), 87.2 (2C, s, $C^{2/3}$), 86.9 (2C, s, $C^{2/3}$), 83.0 (5C, s, C^{6}), 20.0 (1C, s, C^{5}); $\boldsymbol{\delta_P}$ (acetone-D_6) -144.3 (sept, $^{1}J_{P\text{-}F}$ 713 Hz); $\boldsymbol{\delta_F}$ (acetone-D_6) -72.2 (d, $^{1}J_{F\text{-}P}$ 713 Hz); *m/z* (HRMS^{+}) 286.9705 $[M - PF_6]^{+}$ ($C_{12}H_{12}{}^{35}Cl^{96}Ru$ requires 286.9704).

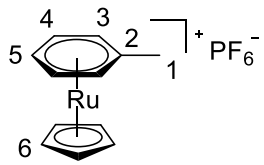

[Ru(η^6-toluene)(η^5-cyclopentadienyl)]PF_6 **2.16**

To a solution of toluene (24 mg, 27 µL, 0.253 mmol, 1.1 equiv) in degassed 1,2-dichloroethane (5 mL) at 80 °C was added $[Ru(NCMe)_3Cp]PF_6$ (100 mg, 0.230 mmol). The resulting solution was heated to reflux for 16 hours, allowed to cool to room temperature and filtered. The filtrate was concentrated in vacuo, redissolved in a minimum of MeCN and added dropwise to Et_2O. The light brown precipitate was isolated by filtration, rinsed with ether, dissolved in MeCN, concentrated in vacuo and dried under vacuum to give the *title compound* as a light brown solid (87 mg, 94%). **δ_H** (acetone-D_6) 6.35-6.38 (2H, m, H^3), 6.27-6.32 (2H, m, H^4), 6.22-6.26 (1H, m, H^5) 5.51 (5H, s, H^6), 2.39 (3H, s, H^1); **δ_C** (acetone-D_6) 102.6 (1C, s, C^2), 87.2 (2C, s, C^3), 85.4 (2C, s, C^4), 84.7 (1C, s, C^5), 80.5 (5C, s, C^6), 19.7 (1C, s, C^1); **δ_P** (acetone-D_6) -144.3 (sept, $^1J_{P\text{-}F}$ 713 Hz); **δ_F** (acetone-D_6) -72.2 (d, $^1J_{F\text{-}P}$ 713 Hz); *m/z* (ESI^+) 253.0098 $[M\text{-}PF_6]^+$ ($C_{12}H_{13}{}^{96}Ru$ requires 253.0093). Anal. found (expected): C 35.67 (35.74); H 3.36 (3.25); N 0.32 (0.00).

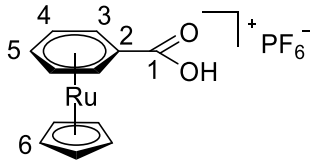

[Ru(η^6-carboxybenzene)(η^5-cyclopentadienyl)]PF_6 **2.17**

To a solution of benzoic acid (17 mg, 0.138 mmol, 1.1 equiv) in degassed 1,2-dichloroethane (6 mL) at 80 °C was added $[Ru(NCMe)_3Cp]PF_6$ (50 mg, 0.115 mmol). The resulting solution was heated to reflux for 16 hours, allowed to cool to room temperature and filtered. The filtrate was concentrated in vacuo, redissolved in a minimum of MeCN and added dropwise to Et_2O. The light brown precipitate was isolated by filtration, rinsed with ether, dissolved in MeCN, concentrated in vacuo and dried under vacuum to give the *title compound* as a light brown solid (47 mg, 94%). **δ_H** (acetone-D_6) 6.88 (2H, d, $^3J_{H\text{-}H}$ 6.0 Hz, H^3), 6.56 (2H, t, $^3J_{H\text{-}H}$ 6.0 Hz, H^4), 6.53 (1H, $^3J_{H\text{-}H}$ 6.0 Hz, H^5), 5.60 (5H, s, H^6); **δ_C** (acetone-D_6) 165.3 (1C, s, C^1), 88.5 (1C, s, C^2), 87.3 (1C, s, C^5), 86.7 (2C, s, C^4), 86.5 (2C, s, C^3), 81.8 (5C, s, C^6); **δ_P** (acetone-D_6) -144.3 (sept, $^1J_{P\text{-}F}$ 713 Hz);

δ_F (acetone-D_6) -72.2 (d, $^1J_{F\text{-}P}$ 713 Hz); *m/z* (HRMS$^+$) 282.9834 $[M - PF_6]^+$ ($C_{12}H_{11}O_2{}^{96}Ru$ requires 282.9835); Anal. found (expected) for $C_{12}H_{11}F_6O_2PRu.(MeCN)_{0.15}$: C 33.95 (33.62); H 2.70 (2.63); N 0.27 (0.48).

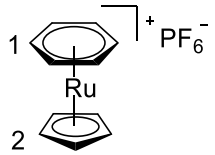

[Ru(η^6-benzene)(η^5-cyclopentadienyl)]PF_6 **2.18**

The reaction is a modification of the existing literature procedure.[37] A 100 mL oven dried round-bottom flask equipped with a stir-bar was charged with finely ground potassium carbonate (0.83 g, 6.00 mmol, 6.0 equiv) and the flask flame-dried under vacuum. After cooling to room temperature, the flask was further charged with $[(C_6H_6)RuCl_2]_2$ (0.50 g, 1.00 mmol) and a reflux condenser added. Ethanol (30 mL) was then added, followed by freshly cracked cyclopentadiene (1.5 mL, 18.0 mmol, 18 equiv). The resulting heterogeneous brown mixture was then warmed to 85 °C with rapid stirring. After approximately 16 h, the reaction mixture was cooled to room temperature and filtered through a plug of Celite, and the Celite rinsed with a further 25 mL of ethanol. The dark yellow filtrate was concentrated to 20 mL, then an aqueous solution of NH_4PF_6 (0.68 g, 4.20 mmol, 4.2 equiv, in 10 mL of H_2O) was added, resulting in the immediate formation of a tan precipitate. The remaining ethanol was removed under reduced pressure and the resulting suspension cooled for several hours. The mixture was then filtered and the tan solid dried under vacuum. The crude product was subsequently dissolved in a minimum of acetonitrile and diethyl ether added dropwise until precipitate formation was no longer observed. This mixture was cooled for several hours before being filtered to give the *title compound* as a light brown solid 0.718 g (92%). The product was spectroscopically identical as the known $[(\eta^6\text{-}C_6H_6)Ru(C_5H_5)]PF_6$[177] and was pure by ^{1}H NMR spectroscopy to the limits of detection. **δ_H** (acetone-D_6) 6.36 (6H, s, H^1), 5.56 (5H, s, H^2).

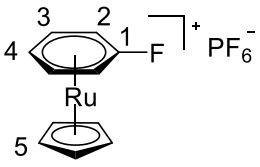

[Ru(η^6-fluorobenzene)(η^5-cyclopentadienyl)]PF_6 **2.19**

To a solution of fluorobenzene (48 mg, 47 µL, 0.507 mmol, 1.1 equiv) in degassed 1,2-dichloroethane (9 mL) at 80 °C was added [Ru(NCMe)$_3$Cp]PF_6 (200 mg, 0.461 mmol). The resulting solution was heated to reflux for 16 hours under an inert atmosphere, allowed to cool to room temperature and filtered. The filtrate was concentrated in vacuo, redissolved in a minimum of MeCN and added dropwise to Et_2O. The brown precipitate was isolated by filtration, rinsed with ether, dissolved in MeCN, concentrated in vacuo and dried under vacuum to give the *title compound* as a brown solid (153 mg, 82%); **δ_H** (acetone-D_6) 6.82 (2H, dd, $^3J_{H\text{-}H}$ 6.0 Hz, $^3J_{H\text{-}F}$ 4.5 Hz, H^2), 6.47 (2H, td, $^3J_{H\text{-}H}$ 6.0 Hz, $^4J_{H\text{-}F}$ 4.0 Hz, H^3), 6.27 (1H, td, $^3J_{H\text{-}H}$ 6.0 Hz, $^5J_{H\text{-}F}$ 3.5 Hz, H^4) 5.65 (5H, s, H^5); **δ_C** (acetone-D_6) 136.9 (1C, d, $^1J_{C\text{-}F}$ 276 Hz, C^1), 85.2 (1C, s, C^4), 84.9 (2C, d, $^3J_{C\text{-}F}$ 6 Hz, C^3), 81.6 (5C, s, C^5), 77.4 (2C, d, $^2J_{C\text{-}F}$ 21 Hz, C^2); **δ_F** (acetone-D_6) -72.6 (6F, d, $^1J_{F\text{-}P}$ 707 Hz, $F^{counterion}$), -137.5 (1F, m, F^{arene}); **δ_P** (acetone-D_6) -144.3 (sept., $J_{P\text{-}F}$ 707 Hz); *m/z* (HRMS$^+$) 256.9836 $[M\text{-}PF_6]^+$ ($C_{11}H_{10}F^{96}Ru$ requires 256.9842); Anal. found (expected): C 32.56 (32.44); H 2.52 (2.48); N 0.25 (0.00).

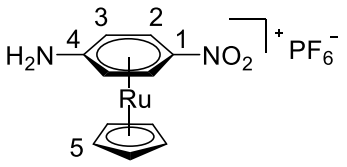

[Ru(η^6-4-nitroaniline)(η^5-cyclopentadienyl)]PF_6 **2.20**

To a solution of 4-nitroaniline (52 mg, 0.380 mmol, 1.1 equiv) in degassed 1,2-dichloroethane (9 mL) at 80 °C was added [Ru(NCMe)$_3$Cp]PF_6 (150 mg, 0.345 mmol). The resulting solution was heated to reflux for 16 hours under an inert atmosphere, allowed to cool to room temperature and filtered. The filtrate was concentrated in vacuo, redissolved in a minimum of MeCN and added dropwise to Et_2O. The brown precipitate was isolated by filtration, rinsed with ether, dissolved in MeCN, concentrated in vacuo and dried under vacuum to give the *title compound* as a brown solid (141 mg, 91%); **δ_H** (acetone-D_6) 7.20 (2H, d, $^3J_{H\text{-}H}$ 6.5 Hz, H^3), 6.37 (2H, d, $^3J_{H\text{-}H}$ 6.5 Hz, H^2), 5.51 (5H, s, H^5); **δ_C** (acetone-D_6) 130.1 (1C, s, C^4), 107.1 (1C, s, C^1), 81.7 (5C, s, C^5), 81.4 (2C, s, C^2), 69.3 (2C, s, C^3); **δ_F** (acetone-D_6) -72.6 (6F, d, $^1J_{F\text{-}P}$ 707 Hz, $F^{counterion}$); **δ_P** (acetone-D_6) -144.3 (sept., $J_{P\text{-}F}$ 707 Hz); *m/z* (HRMS$^+$) 298.9901 $[M\text{-}PF_6]^+$ ($C_{11}H_{11}N_2O_2{}^{96}Ru$ requires 298.9897).

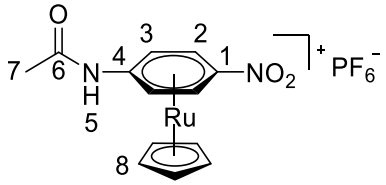

[Ru(η^6-4-nitroacetanilide)(η^5-cyclopentadienyl)]PF_6 **2.21**

To a solution of 4-nitroacetanilide (69 mg, 0.380 mmol, 1.1 equiv) in degassed 1,2-dichloroethane (9 mL) at 80 °C was added [Ru(NCMe)$_3$Cp]PF_6 (150 mg, 0.345 mmol). The resulting solution was heated to reflux for 16 hours under an inert atmosphere, allowed to cool to room temperature and filtered. The filtrate was concentrated in vacuo, redissolved in a minimum of MeCN and added dropwise to Et_2O. The brown precipitate was isolated by filtration, rinsed with ether, dissolved in MeCN, concentrated in vacuo and dried under vacuum to give the *title compound* as a brown solid (151 mg, 89%); **δ_H** (acetone-D_6) 9.63 (1H, s, H5), 7.42 (2H, d, $^3J_{H\text{-}H}$ 6.5 Hz, H^2), 7.26 (2H, dd, $^3J_{H\text{-}H}$ 6.5 Hz, $^4J_{H\text{-}H}$ 2.5 Hz, H^3), 5.69 (5H, s, H^8), 2.13 (3H, s, H^7); **δ_C** (acetone-D_6) 171.3 (1C, s, C^6), 114.2 (1C, s, C^4), 110.0 (1C, s, C^1), 84.6 (5C, s, C^8), 82.9 (2C, s, C^2), 78.3 (2C, s, C^3), 24.5 (1C, s, C^7); **δ_F** (acetone-D_6) -72.6 (6F, d, $^1J_{F\text{-}P}$ 707 Hz, $F^{counterion}$); **δ_P** (acetone-D_6) -144.3 (sept., $J_{P\text{-}F}$ 707 Hz); *m/z* (HRMS$^+$) 341.0003 $[M\text{-}PF_6]^+$ ($C_{13}H_{13}N_2O_3{}^{96}Ru$ requires 341.0002).

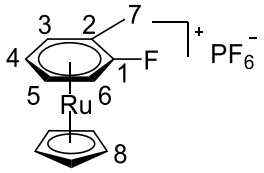

[Ru(η^6-2-fluorotoluene)(η^5-cyclopentadienyl)]PF_6 **3.3**

To a solution of 2-fluorotoluene (42 mg, 42 µL, 0.380 mmol, 1.1 equiv) in degassed 1,2-dichloroethane (9 mL) at 80 °C was added [Ru(NCMe)$_3$Cp]PF_6 (150 mg, 0.345 mmol). The resulting solution was heated to reflux for 16 hours under an inert atmosphere, allowed to cool to room temperature and filtered. The filtrate was concentrated in vacuo, redissolved in a minimum of MeCN and added dropwise to Et_2O. The brown precipitate was isolated by filtration, rinsed with ether, dissolved in MeCN, concentrated in vacuo and dried under vacuum to give the *title compound* as a brown solid (131 mg, 90%); **δ_H** (acetone-D_6) 6.77 (1H, dd, J = 6.0, 4.0 Hz, H^6), 6.51 (1H, ddd, J =

6.0, 4.0, 1.0 Hz, H^3), 6.33 (1H, tdd, *J* = 6.0, 3.0, 1.0 Hz, H^5), 6.18 (1H, td, *J* = 6.0, 3.0 Hz, H^4) 5.59 (5H, s, H^8), 2.50 (3H, d, *J* = 1.5 Hz, H^7); **δC** (acetone-D_6) 136.2 (1C, d, $^1J_{C\text{-}F}$ 274 Hz, C^1), 93.8 (1C, d, $^2J_{C\text{-}F}$ 20 Hz, C^2), 86.9 (1C, d, $^3J_{C\text{-}F}$ 6 Hz, C^3), 84.5 (1C, s, C^4), 84.1 (1C, d, $^3J_{C\text{-}F}$ 6 Hz, C^5), 81.7 (5C, s, C^8) 76.6 (1C, d, $^2J_{C\text{-}F}$ 20 Hz, C^6), 14.0 (1C, d, $^3J_{C\text{-}F}$ 6 Hz, C^7). **δF** (Acetone-D_6): -72.67 (6F, d, $^1J_{P\text{-}F}$ = 707 Hz), -142.2 (m, 1F); **δP** (acetone-D_6) -144.3 (sept., $J_{P\text{-}F}$ = 707 Hz); *m/z* (HRMS$^+$) 270.9998 $[M\text{-}PF_6]^+$ ($C_{12}H_{12}F^{96}Ru$ requires 270.9999); Anal. found (expected): C 34.15 (34.21); H 2.87 (2.87); N 0.26 (0.00).

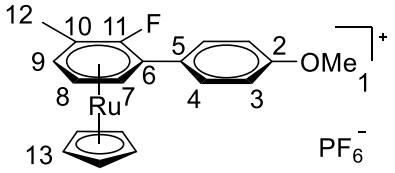

[Ru(η^6-2-methyl-6-p-methoxyphenylfluorobenzene)(η^5-cyclopentadienyl)]PF_6 **3.4**

An oven-dried Schlenk tube equipped with a stir-bar was charged with [Ru(η^6-2-fluorotoluene)(η^5-cyclopentadienyl)]PF_6 (50 mg, 0.120 mmol), 4-iodoanisole (42 mg, 0.180 mmol), 1-adamantanecarboxylic acid (11 mg, 0.060 mmol), Ag_2CO_3 (33 mg, 0.120 mmol), $Pd(OAc)_2$ (3 mg, 0.012 mmol) and DavePhos (10 mg, 0.024 mmol). The Schlenk tube was evacuate and back filled with argon gas three times. Over a flow of argon, 2,2,6,6-tetramethylpiperidine (25 mg, 30 µL, 0.180 mmol) and 1,2-dichloroethane (3 mL) was added. The resulting solution was stirred vigorously under an argon atmosphere and heated to reflux at 150 °C for 18 hours. The solution was allowed to cool to room temperature and a black solid was concentrated in vacuo and dried under vacuum. Acetone (2 mL) was added to yield a suspension, which was then filtered. The brown filtrate was concentrated in vacuo and dried under vacuum to yield a brown oil. Purification by column chromatography (silica, DCM:1.5% methanol, Rf = 0.12) gave the *title compound* as a brown oil (20.3 mg, 33%); **δH** (acetone-D_6) 7.72 (2H, m, H^4), 7.08 (2H, m, H^3), 6.56 (1H, ddd, $^3J_{H\text{-}H}$ 6 Hz, $^4J_{H\text{-}F}$ 4 Hz, $^4J_{H\text{-}H}$ 1.5 Hz, H^7), 6.50 (1H, ddd, $^3J_{H\text{-}H}$ 6 Hz, $^4J_{H\text{-}F}$ 4 Hz, $^4J_{H\text{-}H}$ 1.5 Hz, H^9), 6.28 (1H, td, $^3J_{H\text{-}H}$ 6 Hz, $^5J_{H\text{-}F}$ 2.5 Hz, H^8), 5.59 (5H, s, H^{13}), 3.89 (3H, s, H^1), 2.57 (3H, d, $^4J_{H\text{-}F}$ 2 Hz, H^{12}); **δC** (acetone-D_6)

162.1 (1C, s, C^2), 134.9 (1C, d, $^1J_{C\text{-}F}$ 273 Hz, C^{11}), 132.4 (2C, s, C^4), 123.0 (1C, s, C^5), 115.2 (2C, s, C^3), 97.6 (1C, d, $^2J_{C\text{-}F}$ 17 Hz, C^{10}) 94.1 (1C, d, $^2J_{C\text{-}F}$ 19 Hz, C^6) 87.3 (1C, s, C^9), 86.4 (1C, s, C^7), 85.0 (1C, s, C^8), 83.4 (5C, s, C^{13}), 55.9 (1C, s, C^1), 15.2 (1C, s, C^{12}); *m/z* (HRMS$^+$) 377.0421 $[M\text{-}PF_6]^+$ ($C_{19}H_{18}FO^{96}Ru$ requires 377.0418).

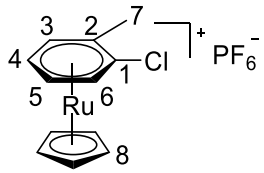

[Ru(η^6-2-chlorotoluene)(η^5-cyclopentadienyl)]PF_6 **3.16**

To a solution of 2-chlorotoluene (48 mg, 45 µL, 0.380 mmol, 1.1 equiv) in degassed 1,2-dichloroethane (9 mL) at 80 °C was added $[Ru(NCMe)_3Cp]PF_6$ (150 mg, 0.345 mmol). The resulting solution was heated to reflux for 16 hours under an inert atmosphere, allowed to cool to room temperature and filtered. The filtrate was concentrated in vacuo, redissolved in a minimum of MeCN and added dropwise to Et_2O. The brown precipitate was isolated by filtration, rinsed with ether, dissolved in MeCN, concentrated in vacuo and dried under vacuum to give the *title compound* as a brown solid (147 mg, 97%); δ_H (Acetone-D_6): 6.80 (d, J = 6.0 Hz, 1H), 6.60 (d, J = 6.0 Hz, 1H), 6.39 (td, J = 6.0, 1.0 Hz, 1H), 6.31 (t, J = 6.0 Hz, 1H), 5.59 (s, 5H, Cp), 2.60 (s, 3H); δ_C (Acetone-D_6): 106.7 (s, 1C), 102.3 (s, 1C), 87.5 (s, 1C), 87.3 (s, 1C), 85.3 (s, 1C), 85.2 (s, 1C) 82.5 (S, 5C), 18.6 (s, 1C); *m/z* (HR-ESI$^+$) 286.9703 $[M\text{-}PF_6]^+$ ($C_{12}H_{12}Cl^{96}Ru$ requires 286.9704). Anal. found (expected): C 31.69 (31.52); H 2.21 (2.20); N 0.26 (0.00).

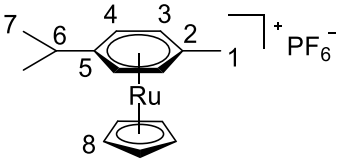

[Ru(η^6-p-cymene)(η^5-cyclopentadienyl)]PF_6 **3.17**

To a solution of *p*-cymene (18 mg, 22 µL, 0.138 mmol) in degassed 1,2-dichloroethane (3 mL) at 60°C was added $[Ru(NCMe)_3Cp]PF_6$ (50 mg, 0.115 mmol). The resulting solution was heated to reflux for 16 hours, allowed to cool to room temperature and filtered. The reaction mixture was concentrated in vacuo, redissolved in a minimum of MeCN and added dropwise to diethylether. The light brown precipitate was filtered,

rinsed with ether, dissolved in MeCN, concentrated in vacuo and dried under vacuum to give the title compound as a light brown solid (48 mg, 94%); **δ_H** (acetone-D_6) 6.30 (4H, m, $H^{3,4}$), 5.48 (5H, s, H^8), 2.81 (1H, sept., $^3J_{H\text{-}H}$ 7.0 Hz, H^6), 2.39 (3H, s, H^1), 1.29 (6H, d, $^3J_{H\text{-}H}$ 7.0 Hz, H^7); **δ_C** (acetone-D_6) 113.4 (1C, s, C^5), 102.4 (1C, s, C^2), 87.4 (2C, s, C^4), 85.2 (2C, s, C^3), 81.5 (5C, s, C^8), 32.8 (1C, s, C^6), 23.6 (2C, s, C^7), 20.2 (1C, s, C^1); Anal. Found (expected): C 40.48 (40.45); H 4.31 (4.30); N 0.20 (0.00).

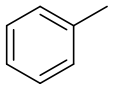

Toluene **4.3** ^{1}H NMR (400 MHz, $CDCl_3$) δ 7.25–7.18 (m, 2H), 7.17-7.11 (m, 3H), 2.35 (s, 3H); The NMR data were in agreement with literature.[178]

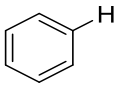

Benzene **4.4** ^{1}H NMR (400 MHz, $CDCl_3$) δ 7.36 (s, 6H); The NMR data were in agreement with literature.[179]

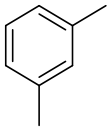

m-Xylene **4.5** ^{1}H NMR (400 MHz, $CDCl_3$) δ 7.12 ppm (t, J = 7.5 Hz, 1H), 6.99-6.92 (m, 3H), 2.29 (s, 6H); The NMR data were in agreement with literature.[180]

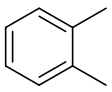

o-Xylene **4.6** ^{1}H NMR (400 MHz, $CDCl_3$) δ 7.13–7.07 (m, 4H), 2.25 (s, 6H); The NMR data were in agreement with literature.[178]

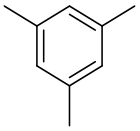

Mesitylene **4.7** ^{1}H NMR (400 MHz, $CDCl_3$) δ 6.78 (s, 3H), 2.26 (s, 9H); The NMR data were in agreement with literature.[181]

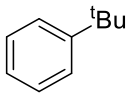

1-tert-Butylbenzene **4.8** ^{1}H NMR (400 MHz, $CDCl_3$) δ 7.40-7.35 (m, 2H), 7.32 – 7.26 (m, 2H), 7.18 – 7.12 (m, 1H), 1.31 (s, 9H); The NMR data were in agreement with literature.[182]

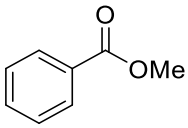

Methyl benzoate **4.10** ^{1}H NMR (400 MHz, $CDCl_3$) δ 8.06–8.00 (m, 2H), 7.53 (tt, 1H, *J* = 7.4, 1.3), 7.44–7.38 (m, 2H), 3.89 (s, 3H); The NMR data were in agreement with literature.[183]

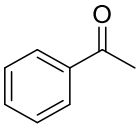

Acetophenone **4.11** ^{1}H NMR (400 MHz, $CDCl_3$) δ 7.96–7.90 (m, 2H), 7.54 (tt, 1H, *J* = 7.5, 1.5), 7.47–7.40 (m, 2H), 2.58 (s, 3H); The NMR data were in agreement with literature.[183]

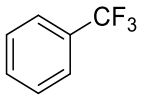

Trifluoromethylbenzene **4.12** ^{1}H NMR (400 MHz, $CDCl_3$) δ 7.60 (d, *J* = 7.5 Hz, 2H), 7.53 (t, *J* = 7.5 Hz, 1H), 7.46 (t, *J* = 7.5 Hz, 2H); The NMR data were in agreement with literature.[184]

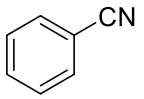

Benzonitrile **4.13** ^{1}H NMR (400 MHz, $CDCl_3$) δ 7.67–7.61 (m, 2H), 7.58 (tt, 1H, *J* = 7.5, 1.5), 7.48–7.42 (m, 2H); The NMR data were in agreement with literature.[184]

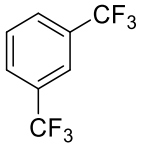

1,3-Bis(trifluoromethyl)benzene **4.14** ^{1}H NMR (400 MHz, $CDCl_3$) δ 7.86 (s, 1H), 7.82 (d, *J* = 8.0 Hz, 2H), 7.63 (t, *J* = 8.0 Hz, 1H); The NMR data were in agreement with literature.[185]

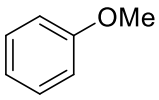

Anisole **4.15** ^{1}H NMR (400 MHz, $CDCl_3$) δ 7.26 (t, *J* = 7.5 Hz, 2H), 6.92 (t, *J* = 7.0 Hz, 1H), 6.88 (d, *J* = 9.0 Hz, 2H), 3.78 (s, 3H); The NMR data were in agreement with literature.[178]

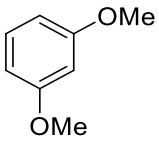

1,3-Dimethoxybenzene **4.16** ^{1}H NMR (400 MHz, $CDCl_3$) δ 7.15 (t, *J* = 8.0 Hz, 1H), 6.50–6.43 (m, 3H), 3.76 (s, 6H); The NMR data were in agreement with literature.[178]

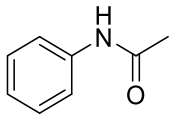

Acetanilide **4.17** ^{1}H NMR (400 MHz, $CDCl_3$) δ 7.54 (d, *J* = 7.5 Hz, 2H), 7.26 (t, *J* = 7.5 Hz, 2H), 7.04 (t, *J* = 7.5 Hz, 1H), 2.14 (s, 2H); The NMR data were in agreement with literature.[186]

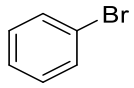

Bromobenzene **4.18** ^{1}H NMR (400 MHz, $CDCl_3$) δ 7.47 (d, *J* = 7.5 Hz, 2H), 7.27 (t, *J* = 7.5 Hz, 1H), 7.21 (t, *J* = 7.5 Hz, 2H); The NMR data were in agreement with literature.[187]

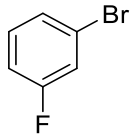

1-Bromo-3-fluorobenzene **4.19** ^{1}H NMR (400 MHz, $CDCl_3$) δ 7.28−7.15 (m, 3H), 7.02−6.95 (m, 1H); The NMR data were in agreement with literature.[188]

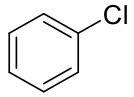

Chlorobenzene **4.20** ^{1}H NMR (400 MHz, $CDCl_3$) δ 7.42-7.23 (m, 5H); The NMR data were in agreement with literature.[189]

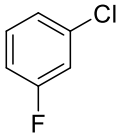

1-Chloro-3-fluorobenzene **4.21** ^{1}H NMR (400 MHz, $CDCl_3$) δ 7.28−7.21 (m, 1H), 7.14−7.09 (m, 1H), 7.09−7.04 (m, 1H), 6.98−6.90 (m, 1H); The NMR data were in agreement with literature.[190]

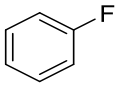

Fluorobenzene **4.22** ^{1}H NMR (400 MHz, $CDCl_3$) δ 7.32 (m, 2H), 7.10 (m, 1H), 7.02 (m, 2H); The NMR data were in agreement with literature.[178]

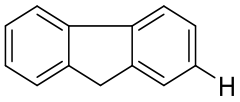

Fluorene **4.23** ^{1}H NMR (400 MHz, $CDCl_3$) δ 7.81 (d, *J* = 7.5 Hz, 2H), 7.56 (d, *J* = 7.5 Hz, 2H), 7.39 (td, *J* = 7.5, 1.0 Hz, 2H), 7.32 (td, *J* = 7.5, 1.0 Hz, 2H), 3.92 (s, 2H); The NMR data were in agreement with literature.[191]

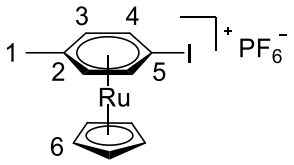

[Ru(η^6-4-iodotoluene)(η^5-cyclopentadienyl)]PF_6 **4.24**

An oven dried round bottom flask charged with $[Ru(NCMe)_3Cp]PF_6$ (100 mg, 0.231 mmol) and 4-iodotoluene (50 mg, 0.231 mmol) was purged with argon for 10 minutes. To this 1,2-dichloroethane (5 mL) was added and the resulting solution was heated to reflux for 18 hours, allowed to cool to room temperature and filtered. The reaction mixture was concentrated in vacuo, redissolved in a minimum amount of MeCN and added dropwise to diethylether. The pale brown solid was filtered, rinsed with ether, dissolved in MeCN, concentrated in vacuo and dried under vacuum to give the title compound as a pale brown solid (114 mg, 93%). $\boldsymbol{\delta_H}$ (acetone-D_6) 6.79 (2H, m, H^4), 6.36 (2H, m, H^3), 5.57 (5H, s, H^6), 2.37 (3H, s, H^1); $\boldsymbol{\delta_C}$ (acetone-D_6) 102.2 (1C, s, C^2), 94.0 (2C, s, C^4), 88.2 (2C, s, C^3), 83.0 (5C, s, C^6), 52.1 (1C, s,C^5), 19.2 (1C, s, C^1); $\boldsymbol{\delta_P}$ (acetone-D_6) -144.3 (sept., $^{1}J_{P\text{-}F}$ 707 Hz); $\boldsymbol{\delta_F}$ (acetone-D_6) -72.4 (d, $^{1}J_{F\text{-}P}$ 707 Hz); m/z (ESI^+) 378.9066 $[M\text{-}PF_6]^+$ ($C_{12}H_{12}I^{96}Ru$ requires 378.9045); Anal. Found (expected): C, 27.38 (27.24); H, 2.27 (2.29); N, 0.20 (0.00).

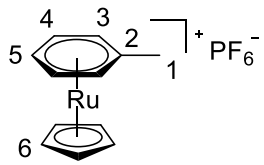

[Ru(η^6-toluene)(η^5-cyclopentadienyl)]PF_6 **4.25**

To a solution of toluene (24 mg, 27 µL, 0.253 mmol, 1.1 equiv) in degassed 1,2-dichloroethane (5 mL) at 80 °C was added $[Ru(NCMe)_3Cp]PF_6$ (100 mg, 0.230 mmol). The resulting solution was heated to reflux for 16 hours, allowed to cool to room temperature and filtered. The filtrate was concentrated in vacuo, redissolved in a minimum of MeCN and added dropwise to Et_2O. The light brown precipitate was isolated by filtration, rinsed with ether, dissolved in MeCN, concentrated in vacuo and dried under vacuum to give the *title compound* as a light brown solid (87 mg, 94%). **δ_H** (acetone-D_6) 6.35-6.38 (2H, m, H^3), 6.27-6.32 (2H, m, H^4), 6.22-6.26 (1H, m, H^5) 5.51 (5H, s, H^6), 2.39 (3H, s, H^1); **δ_C** (acetone-D_6) 102.6 (1C, s, C^2), 87.2 (2C, s, C^3), 85.4 (2C, s, C^4), 84.7 (1C, s, C^5), 80.5 (5C, s, C^6), 19.7 (1C, s, C^1); **δ_P** (acetone-D_6) -144.3 (sept, $^1J_{P\text{-}F}$ 713 Hz); **δ_F** (acetone-D_6) -72.2 (d, $^1J_{F\text{-}P}$ 713 Hz); *m/z* (ESI^+) 253.0098 $[M\text{-}PF_6]^+$ ($C_{12}H_{13}{}^{96}Ru$ requires 253.0093); Anal. Found (expected): C 35.67 (35.74); H 3.36 (3.25); N 0.32 (0.00).

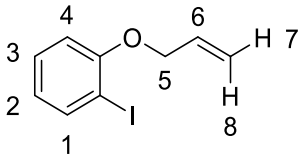

1-allyloxy-2-iodobenzene **4.26**

The *title compound* was synthesised by adapting a known literature procedure.[192] 2-Iodophenol (500 mg, 2.275 mmol), K_2CO_3 (950 mg, 6.820 mmol) and DMF (4 mL) were taken in an oven-dried Schlenk tube under argon. Allyl chloride (550 µL, 6.820 mmol) was added and the mixture was stirred at 80 °C for 16 hours. H_2O (20 mL) was added and the resulting mixture was extracted with EtOAc (3 × 20 mL). The combined organic fractions were washed with brine (15 mL), dried over $MgSO_4$ and concentrated under vacuum. The crude mixture was purified by flash column chromatography (hexane : EtOAc = 95 : 5, R_f = 0.4) to give the *title compound* as a colourless oil (519 mg, 88%).

The product is spectroscopically identical to the known compound reported and is pure by ^{1}H-NMR spectroscopy to the limits of detection.[173] **δ_H** ($CDCl_3$) 7.78 (1H, dd, $^{3}J_{H\text{-}H}$ = 7.5 Hz, $^{4}J_{H\text{-}H}$ = 1.5 Hz, H^1), 7.28 (1H, td, $^{3}J_{H\text{-}H}$ = 7.5 Hz, $^{4}J_{H\text{-}H}$ = 1.5 Hz, H^3), 6.81 (1H, dd, $^{3}J_{H\text{-}H}$ = 7.5 Hz, $^{4}J_{H\text{-}H}$ = 1.5 Hz, H^4), 6.72 (1H, td, $^{3}J_{H\text{-}H}$ = 7.5 Hz, $^{4}J_{H\text{-}H}$ = 1.5 Hz, H^2), 6.07 (1H, ddt, $^{3}J_{H\text{-}H}$ = 17.0, 10.5, 5.0 Hz, H^6), 5.53 (1H, dq, $^{3}J_{H\text{-}H}$ = 17.0 Hz, $^{2}J_{H\text{-}H}$ = $^{4}J_{H\text{-}H}$ = 1.5 Hz, H^8), 5.32 (1H, dq, $^{3}J_{H\text{-}H}$ = 10.5 Hz, $^{2}J_{H\text{-}H}$ = $^{4}J_{H\text{-}H}$ = 1.5 Hz, H^7), 4.60 (2H, dt, $^{3}J_{H\text{-}H}$ = 5.0 Hz, $^{4}J_{H\text{-}H}$ = 1.5 Hz, H^5).

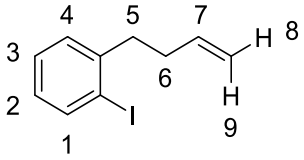

4-(2-iodobenzene)but-1-ene **4.27**

Allylmagnesium bromide (3.4 mL, 1.0 M, 3.368 mmol) was added slowly to a stirred solution of 2-iodobenzyl bromide (500 mg, 1.684 mmol) in THF (4 mL) at 0 °C. After 15 min, the reaction was allowed to warm to rt and stirred for an additional 3 h. The reaction was quenched with sat. NH_4Cl solution and extracted with Et_2O (3 × 10 mL). The combined organic fractions were washed with brine, dried of $MgSO_4$, filtered, concentrated and purified over silica gel chromatography (hexanes, R_f = 0.55) to yield the *title compound* as a colourless oil (386 mg, 89%). The product is spectroscopically identical to the known 4-(2-iodobenzene)but-1-ene.[193]

δ_H ($CDCl_3$) 7.82 (1H, dd, $^{3}J_{H\text{-}H}$ = 7.5 Hz, $^{4}J_{H\text{-}H}$ = 1.5 Hz, H^1), 7.27 (1H, td, $^{3}J_{H\text{-}H}$ = 7.5 Hz, $^{4}J_{H\text{-}H}$ = 1.5 Hz, H^3), 7.21 (1H, dd, $^{3}J_{H\text{-}H}$ = 7.5 Hz, $^{4}J_{H\text{-}H}$ = 1.5 Hz, H^4), 6.89 (1H, td, $^{3}J_{H\text{-}H}$ = 7.5 Hz, $^{4}J_{H\text{-}H}$ = 1.5 Hz, H^2), 5.90 (1H, ddt, $^{3}J_{H\text{-}H}$ = 17.0, 10.0, 6.5 Hz, H^7), 5.09 (1H, dq, $^{3}J_{H\text{-}H}$ = 17.0 Hz, $^{2}J_{H\text{-}H}$ = $^{4}J_{H\text{-}H}$ = 1.5 Hz, H^9), 5.02 (1H, m, $^{3}J_{H\text{-}H}$ = 10.0 Hz, H^8), 2.85–2.78 (2H, m, H^5), 2.40–2.32 (2H, m, H^6).

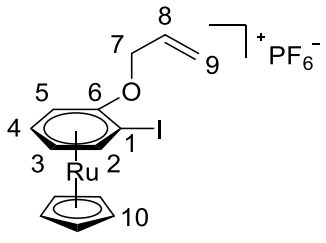

[Ru(η^6-1-allyloxy-2-iodobenzene)(η^5-cyclopentadienyl)]PF_6 **4.28**

To a solution of 1-allyloxy-2-iodobenzene (100 mg, 67 µL, 0.385 mmol) in degassed 1,2-dichloroethane (5 mL) at 80°C was added $[Ru(NCMe)_3Cp]PF_6$ (140 mg, 0.320 mmol). The resulting solution was heated to reflux for 16 hours, allowed to cool to room temperature and filtered. The reaction mixture was concentrated in vacuo, redissolved in a minimum of MeCN and added dropwise to diethylether. The precipitate was filtered, rinsed with ether, dissolved in MeCN, concentrated in vacuo and dried under vacuum to give the *title compound* as a white powder (151 mg, 83%).

δ_H (Acetone-D_6) 6.87 (1H, dd, $^3J_{H\text{-}H}$ = 5.5 Hz, $^4J_{H\text{-}H}$ = 0.5 Hz, H^5), 6.57 (1H, d, $^3J_{H\text{-}H}$ = 6.0 Hz, H^2), 6.31 (1H, td, $^3J_{H\text{-}H}$ = 6.0 Hz, $^4J_{H\text{-}H}$ = 0.5 Hz, H^3), 6.12 (1H, ddt, $^3J_{H\text{-}H}$ = 17.5, 10.5, 5.5 Hz, H^8), 6.07 (1H, td, $^3J_{H\text{-}H}$ = 5.5 Hz, $^4J_{H\text{-}H}$ = 0.5 Hz, H^4), 5.60 (1H, dq, $^3J_{H\text{-}H}$ = 17.5 Hz, $^2J_{H\text{-}H}$ = $^4J_{H\text{-}H}$ = 1.5 Hz, H^{9cis}), 5.51 (5H, s, H^{10}), 5.41 (1H, dq, $^3J_{H\text{-}H}$ = 10.5 Hz, $^2J_{H\text{-}H}$ = $^4J_{H\text{-}H}$ = 1.5 Hz, H^{9trans}), 4.90 (1H, ddt, $^2J_{H\text{-}H}$ = 13.0 Hz, $^3J_{H\text{-}H}$ = 5.5 Hz, $^4J_{H\text{-}H}$ = 1.5 Hz, $H^{7/7'}$), 4.73 (1H, ddt,$^2J_{H\text{-}H}$ = 13.0 Hz, $^3J_{H\text{-}H}$ = 5.5 Hz, $^4J_{H\text{-}H}$ = 1.5 Hz, $H^{7/7'}$); **δ_C** (acetone-D_6) 134.1 (1C, s, C^6), 132.4 (1C, s, C^8), 119.4 (1C, s, C^9), 95.3 (1C, s, C^5), 85.2 (1C, s, C^4), 85.1 (1C, s, C^3), 83.1 (5C, s, C^{10}), 72.9 (1C, s, C^2), 72.5 (1C, s, C^7), 50.3 (1C, s, C^1); *m/z* ($HRMS^+$) 420.9160 $[M\text{-}PF_6]^+$ ($C_{14}H_{14}IO^{96}Ru$ requires 420.9165); Anal. Found (expected): C 29.82 (29.44); H 2.57 (2.47); N 0.01 (0.00).

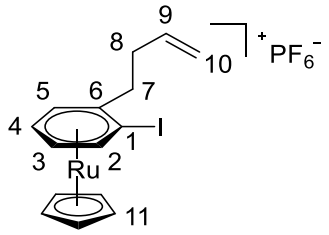

[Ru(η^6-4-(2-iodobenzene)but-1-ene)(η^5-cyclopentadienyl)]PF_6 **4.30**

To a solution of 4-(2-iodobenzene)but-1-ene (100 mg, 69 µL, 0.387 mmol) in degassed 1,2-dichloroethane (5 mL) at 80°C was added $[Ru(NCMe)_3Cp]PF_6$ (140 mg, 0.320 mmol). The resulting solution was heated to reflux for 16 hours, allowed to cool to room temperature and filtered. The reaction mixture was concentrated in vacuo, redissolved in a minimum of MeCN and added dropwise to diethylether. The precipitate was filtered, rinsed with ether, dissolved in MeCN, concentrated in vacuo and dried under vacuum to give the *title compound* as a light brown powder (162 mg, 89%).

δH (acetone-D_6) 6.89 (1H, d, $^3J_{H\text{-}H}$ = 6.0 Hz, H^2), 6.52 (1H, d, $^3J_{H\text{-}H}$ = 6.0 Hz, H^5), 6.37 (1H, t, $^3J_{H\text{-}H}$ = 6.0 Hz, H^4), 6.22 (1H, t, $^3J_{H\text{-}H}$ = 6.0 Hz, H^3), 5.94 (1H, ddt, $^3J_{H\text{-}H}$ = 17.0, 10.0, 6.5 Hz, H^9), 5.55 (5H, s, H^{11}), 5.11 (1H, dq, $^3J_{H\text{-}H}$ = 17.0, $^2J_{H\text{-}H}$ = $^4J_{H\text{-}H}$ = 1.5 Hz, H^{10cis}), 5.05 (1H, dq, $^3J_{H\text{-}H}$ = 10.0, $^2J_{H\text{-}H}$ = $^4J_{H\text{-}H}$ = 1.5 Hz, $H^{10trans}$), 2.97 (1H, ddd, $^2J_{H\text{-}H}$ = 14.0, $^3J_{H\text{-}H}$ = 9.5, 6 Hz, $H^{7/7'}$), 2.88 (1H, ddd, $^2J_{H\text{-}H}$ = 14.0, $^3J_{H\text{-}H}$ = 9.5, 6.5 Hz, $H^{7/7'}$), 2.51 (1H, m, $H^{8/8'}$), 2.39 (1H, m, $H^{8/8'}$); **δc** (acetone-D_6) 137.1 (1C, s, C^9), 116.8 (1C, s, C^{10}), 109.1 (1C, s, C^6), 96.7 (1C, s, C^2), 87.2 (1C, s, C^5), 87.1 (1C, s, C^3), 86.8 (1C, s, C^4), 83.7 (5C, s, C^{11}), 61.8 (1C, s, C^1), 38.8 (1C, s, C^7) 35.0 (1C, s, C^8); *m/z* (HRMS$^+$) 418.9379 $[M\text{-}PF_6]^+$ ($C_{15}H_{16}I^{96}Ru$ requires 418.9373); Anal. Found (expected): C 32.03 (31.65); H 2.88 (2.83); N 0.13 (0.00).

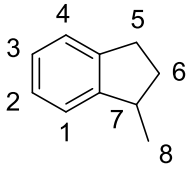

1-Methylindane **4.31**

The *title compound* was synthesised by following a known literature procedure. 3-Methyl-1-oxoindanone (500 mg, 3.42 mmol) was rapidly stirred in ethanol (20 mL) over 10%wt Pd on activated carbon (50 mg) under 3 bar of H_2 pressure. The catalyst was removed by filtration and the filtrate was concentrated in vacuo to give a yellow oil. Following flask column chromatography (hexane, R_f = 0.6) the *title compound* was isolated as a clear colourless oil (438 mg, 97%). The product is spectroscopically identical to the known compound reported and is pure by ^{1}H-NMR spectroscopy to the limits of detection. **δH** ($CDCl_3$) 7.24–7.15 (1H, m, $H^{1\text{-}4}$), 3.23–3.16 (1H, m), 2.92–2.86 (2H, m), 2.35–2.28 (1H, m), 1.65–1.57 (1H, m), 1.29 (3H, d, $^3J_{H\text{-}H}$ = 7.0 Hz, H^8).

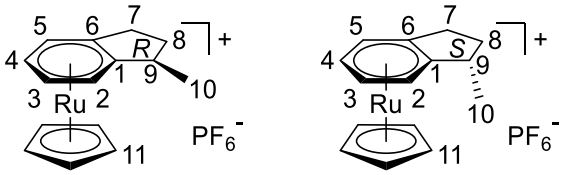

[Ru(η^6-1-methylindane)(η^5-cyclopentadienyl)]PF_6 **4.32**

To a solution of 1-methylindane (34 mg, 0.253 mmol) in degassed 1,2-dichloroethane (5 mL) at 80°C was added $[Ru(NCMe)_3Cp]PF_6$ (100 mg, 0.230 mmol). The resulting solution was heated to reflux for 16 hours, allowed to cool to room temperature and filtered. The reaction mixture was concentrated in vacuo, redissolved in a minimum of MeCN and added dropwise to diethylether. The precipitate was filtered, rinsed with ether, dissolved in MeCN, concentrated in vacuo and dried under vacuum to give the pure racemic *title compound* as an off-white powder (91 mg, 89%). A 20 mg sample was purified by reverse phase HPLC (H_2O : MeCN) to provide two pure enantiomeric pairs of complexes as an off-white solid (**(R)** 10.4 mg, **(S)** 7.2 mg).

(R) - **δ_H** (acetone-D_6) 6.48 (2H, m, $H^{2/5}$), 6.18 (2H, m, $H^{3/4}$), 5.48 (5H, s, H^{11}), 3.22 (1H, pd, $^3J_{H\text{-}H}$ = 7.5, 1.0 Hz, H^9), 3.12 (1H, m, $H^{7/7'}$), 2.81 (1H, m, $H^{7/7'}$), 2.30 (1H, m, $H^{8/8'}$), 1.87 (1H, m, $H^{8/8'}$), 1.26 (3H, d, $^3J_{H\text{-}H}$ = 7.5 Hz, H^{10}); **δ_C** (acetone-D_6) 113.4 (1C, s, C^1), 109.0 (1C, s, C^6), 85.3 (1C, s, $C^{3/4}$), 85.1 (1C, s, $C^{3/4}$), 83.7 (1C, s, $C^{2/5}$), 82.9 (1C, s, $C^{2/5}$), 81.5 (5C, s, C^{11}), 39.1 (1C, s, C^9), 32.3 (1C, s, C^8), 29.7 (1C, s, C^7), 20.9 (1C, s, C^{10}); **(S)** - **δ_H** (acetone-D_6) 6.45 (1H, d, $^3J_{H\text{-}H}$ = 5.5 Hz, H^5), 6.33 (1H, d, $^3J_{H\text{-}H}$ = 5.5 Hz, H^2), 6.21 (1H, td, $^3J_{H\text{-}H}$ = 5.5 Hz, $^4J_{H\text{-}H}$ = 1.0 Hz, H^4), 6.17 (1H, td, $^3J_{H\text{-}H}$ = 5.5 Hz, $^4J_{H\text{-}H}$ = 1.0 Hz, H^4), 5.54 (5H, s, H^{11}), 3.11 (1H, dp, $^3J_{H\text{-}H}$ = 11.0, 6.5, Hz, H^9), 2.91 (1H, m, $H^{7/7'}$), 2.74 (1H, m, $H^{7/7'}$), 2.35 (1H, m, $H^{8/8'}$), 1.55 (1H, m, $H^{8/8'}$), 1.32 (3H, d, $^3J_{H\text{-}H}$ = 6.5 Hz, H^{10}); **δ_C** (acetone-D_6) 115.9 (1C, s, C^1), 109.9 (1C, s, C^6), 84.7 (1C, s, C^4), 84.4 (1C, s, C^3), 83.0 (1C, s, C^5), 81.8 (1C, s, C^2), 80.9 (5C, s, C^{11}), 37.8 (1C, s, C^9), 34.1 (1C, s, C^8), 30.8 (1C, s, C^7), 18.2 (1C, s, C^{10}); *m/z* ($HRMS^+$) 293.0410 $[M\text{-}PF_6]^+$ ($C_{15}H_{17}{}^{96}Ru$ requires 293.0406); Anal. Found (expected): C 40.26 (40.64); H 3.77 (3.87); N 0.17 (0.00).

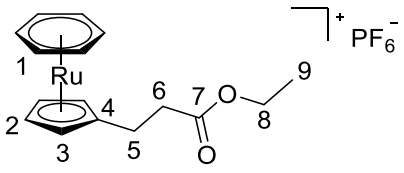

[Ru(η^6-benzene)(ethyl-3-(η^5-cyclopentadienyl)propanoate)]PF_6 **5.5**

The *title compound* was synthesised by adapting a known literature procedure.[38] A 1:1 mixture of methyl 3-(cyclopenta-1,3-dien-1-yl)propanoate and methyl 3-(cyclopenta-1,4-dien-1-yl)propanoate (400 mg, 2.630 mmol) was dissolved in anhydrous, degassed (3 x

freeze-thaw cycle) EtOH (5 mL). Na_2CO_3 (280 mg, 2.630 mmol) and [Ru(η^6-benzene)Cl_2]$_2$ (131 mg, 0.263 mmol) were added and the mixture was stirred under argon at 75 °C. After 18 h the mixture was cooled and left to stand before the supernatant was decanted from residual salts and reduced to a volume of 2.0 mL. An aqueous solution of NH_4PF_6 (105 mg, 0.32 M, 0.644 mmol) was added and the mixture was extracted with CH_2Cl_2 (5 x 5 mL). The organic fractions were combined and dried over $MgSO_4$ and the solvent removed under high vacuum to give a brown oil. The oil was triturated in Et_2O (5 x 10 mL), redissolved in CH_2Cl_2 and the solvent removed under vacuum to give the *title compound* as a brown oil (130 mg, 51%) **δ_H** ($CDCl_3$) 6.14 (6H, s, H^1), 5.43 (2H, m, H^3), 5.34 (2H, m, H^2), 4.13 (2H, q, $^3J_{H–H}$ 7.0 Hz, H^8), 2.64 (2H, t, $^3J_{H–H}$ 7.0 Hz, H^5), 2.50 (2H, t, $^3J_{H–H}$ 7.0 Hz, H^6), 1.25 (3H, t, $^3J_{H–H}$ 7.0 Hz, H^9); **δ_C** ($CDCl_3$) 172.1 (1C, s, C^7), 130.4 (1C, s, C^4), 86.5 (6C, s, C^1), 81.2 (2C, s, C^3), 80.4 (2C, s, C^2), 61.1 (1C, s, C^8), 34.9 (1C, s, C^6), 23.3 (1C, s, C^5), 14.3 (1C, s, C^9); *m/z* (HRMS$^+$) 339.0468 [M-PF_6]$^+$ ($C_{16}H_{19}O_2{}^{96}Ru$ requires 339.0461).

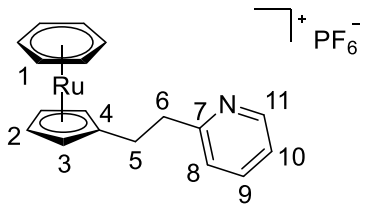

[Ru(η^6-benzene)(2-[2-(η^5-cyclopentadienyl)ethyl]pyridine)]PF_6 **5.6**

The *title compound* was synthesised by adapting a known literature procedure.[38] A 1:1 mixture of 2-[2-(cyclopenta-1,3-dien-1-yl)ethyl]pyridine and 2-[2-(cyclopenta-1,4-dien-1-yl)ethyl]pyridine (1.000 g, 5.840 mmol) was dissolved in anhydrous, degassed (3 x freeze-thaw cycle) EtOH (10 mL). Na_2CO_3 (622 mg, 5.840 mmol) and [Ru(η^6-benzene)Cl_2]$_2$ (292 mg, 0.584 mmol) were added and the mixture was stirred under argon at 75 °C. After 18 h the mixture was cooled and left to stand before the supernatant was decanted from residual salts and reduced to a volume of 2.0 mL. An aqueous solution of NH_4PF_6 (190 mg, 0.32 M, 1.168 mmol) was added and the mixture was extracted with CH_2Cl_2 (5 x 10 mL). The organic fractions were combined and dried over $MgSO_4$ and the solvent removed under high vacuum to give a brown oil. The oil was triturated in Et_2O (5 x 10 mL), redissolved in CH_2Cl_2 and the solvent removed under vacuum to give a brown oil. Flash chromatography on silica (CH_2Cl_2:EtOH 98:2, R_f = 0.2) gave the *title compound* as a brown oil (94 mg, 19%). **δ_H** (acetone-D_6) 8.52 (1H,

dd, $^{3}J_{H\text{-}H}$ 4.5 Hz, $^{4}J_{H\text{-}H}$ 2.0 Hz, H^{11}), 7.69 (1H, td, $^{3}J_{H\text{-}H}$ 7.5 Hz, $^{4}J_{H\text{-}H}$ 2.0 Hz, H^{9}), 7.26 (1H, d, $^{3}J_{H\text{-}H}$ 7.5 Hz, H^{8}), 7.21 (1H, ddd, $^{3}J_{H\text{-}H}$ 4.5, 7.5 Hz, $^{4}J_{H\text{-}H}$ 1.5 Hz, H^{10}), 6.35 (6H, s, H^{1}), 5.51 (2H, pseudo-t, $^{3}J_{\alpha,\beta}$ 2.0 Hz, H^{3}), 5.41 (2H, pseudo-t, $^{3}J_{\alpha,\beta}$ 2.0 Hz, H^{2}), 3.00 (2H, t, $^{3}J_{H\text{-}H}$ 7.5 Hz, H^{6}), 2.81 (2H, t, $^{3}J_{H\text{-}H}$ 7.5 Hz, H^{5}); **δc** (acetone-D_6) 160.9 (1C, s, C^{7}), 150.1 (1C, s, C^{11}), 137.3 (1C, s, C^{9}), 123.9 (1C, s, C^{8}), 122.4 (1C, s, C^{10}), 105.0 (1C, s, C^{4}), 87.4 (6C, s, C^{1}), 81.6 (2C, s, C^{3}), 80.5 (2C, s, C^{2}), 39.0 (1C, s, C^{6}), 28.1 (1C, s, C^{5}); *m/z* (HRMS^{+}) 350.0520 $[M\text{-}PF_6]^{+}$ ($C_{18}H_{18}ON^{96}Ru$ requires 344.0515).

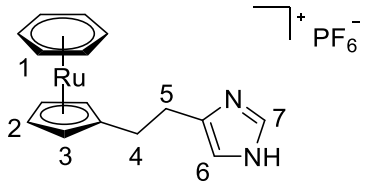

[Ru(η^{6}-benzene)(4-[2-(η^{5}-cyclopentadienyl)ethyl]imidazole)]PF_6 **5.8**

Na_2CO_3 (74 mg, 0.89 mmol) and $[Ru(benzene)Cl_2]_2$ (50 mg, 0.10 mmol) were dried in a round bottom flask fitted with a condenser. The 1:1 mixture of **2a** and **2a'** (142 mg, 0.89 mmol) was dissolved in dry, degassed (3 x freeze thaw cycle) ethanol (8 mL) and added to the solids and stirred at 75 °C under argon for 16 hr. The reaction mixture was then left to stand, and the supernatant was decanted from the residual salts and then was reduced to 2.5 mL after removing solvent under pressure. An aqueous solution of NH_4PF_6 (20 mg, .12 mmol) was added. The resulting solution was extracted with CH_2Cl_2 (4 x 15 mL) The organic fractions combined and reduced under reduced pressure leaving a brown oil. Trituration from methanol gave the *title compound* as a brown solid (17 mg, 35 %); **δH** (acetone-D_6) 7.54 (1H, d, $^{4}J_{H\text{–}H}$ 1.0 Hz, H^{7}), 6.79 (1H, d, $^{4}J_{H\text{–}H}$ 1.0 Hz, H^{6}), 6.31 (6H, s, H^{1}), 5.48 (2H, pseudo-t, $^{3}J_{\alpha,\beta}$ 2.0 Hz, H^{3}), 5.38 (2H, pseudo-t, $^{3}J_{\alpha,\beta}$ 2.0 Hz, H^{2}), 2.95 (2H, t, $^{3}J_{H\text{-}H}$ 7.5 Hz, H^{4}), 2.72 (2H, t, $^{3}J_{H\text{-}H}$ 7.5 Hz, H^{5}); *m/z* (HRMS^{+}) 333.0463 $[M\text{-}PF_6]^{+}$ ($C_{16}H_{17}N_2{}^{96}Ru^{+}$ requires 333.0468).

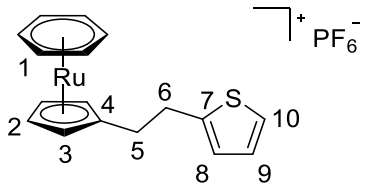

[Ru(η^{6}-benzene)(2-[2-(η^{5}-cyclopentadienyl)ethyl]thiophene)]PF_6 **5.9**

Na_2CO_3 (508 mg, 4.79 mmol, 7 equiv.) and $[Ru(benzene)Cl_2]_2$ (342 mg, 0.685 mmol, 1 equiv.) were dried in a round bottom flask fitted with a condenser. The 1:1 mixture of **2a** and **2a'** (600 mg, 3.42 mmol, 5 equiv.) was dissolved in dry, degassed (3 x freeze thaw cycle) ethanol (24 mL) and added to the solids and stirred at 75 °C under argon for 16 hr. The reaction mixture was then left to stand, and the supernatant was decanted from the residual salts and then was reduced to 2.5 mL after removing solvent under pressure. An aqueous solution of NH_4PF_6 (781 mg, 4.79 mmol, 7 equiv.) was added. The resulting solution was extracted with CH_2Cl_2 (4 x 20 mL) The organic fractions combined and reduced under reduced pressure leaving a brown oil. Trituration from methanol gave the *title compound* as a brown solid (100 mg, 15 %); **δ_H** (599 MHz, Acetone-d_6) 7.26 (1H, dd, $^3J_{H\text{-}H}$ 5.0 Hz, $^4J_{H\text{-}H}$ 1.5 Hz, H^{10}), 6.92 (1H, dd, $^3J_{H\text{-}H}$ 5.0 Hz, $^3J_{H\text{-}H}$ 3.0 Hz, H^9), 6.84 (1H, dq, $^3J_{H\text{-}H}$ 3.0 Hz, $^4J_{H\text{-}H}$ 1.5 Hz, H^8), 6.34 (6H, s, H^1), 5.52 (2H, t, $^3J_{H\text{-}H}$ 2.0 Hz, H^3), 5.42 (2H, t, $^3J_{H\text{-}H}$ 2.0 Hz, H^2), 3.07 (2H, m, H^6), 2.76 (2H, m, H^5); **δ_C** (151 MHz, Acetone-d6) 143.1 (1C, s, C^7), 126.8 (1C, s, C^9), 125.0 (1C, s, C^8), 123.6 (1C, s, C^{10}), 103.3 (1C, s, C^4), 86.5 (6C, s, C^1), 80.7 (2C, s, C^3), 79.7 (2C, s, C^2), 30.3 (1C, s, C^6), 30.0 (1C, s, C^5); *m/z* (HRMS$^+$) 349.0140 $[M\text{-}PF_6]^+$ ($C_{17}H_{17}S^{96}Ru^+$ requires 349.0127).

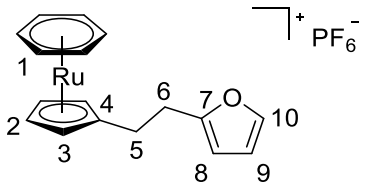

[Ru(η^6-benzene)(2-[2-(η^5-cyclopentadienyl)ethyl]furan)]PF_6 **5.10**

Na_2CO_3 (463 mg, 4.37 mmol, 7 equiv.) and $[Ru(benzene)Cl_2]_2$ (312 mg, 0.624 mmol 1 equiv.) were dried in a round bottom flask fitted with a condenser. The 1:1 mixture of **2a** and **2a'** (400 mg, 2.50 mmol, 4 equiv.) was dissolved in dry, degassed (3 x freeze thaw cycle) ethanol (24 mL) and added to the solids and stirred at 75 °C under argon for 16 hr. The reaction mixture was then left to stand, and the supernatant was decanted from the residual salts and then was reduced to 2.5 mL after removing solvent under pressure. An aqueous solution of NH_4PF_6 (712 mg, 4.38 mmol, 7 equiv.) was added. The resulting solution was extracted with CH_2Cl_2 (4 x 20 mL) The organic fractions combined and reduced under reduced pressure leaving a brown oil. Trituration from methanol gave the *title compound* as a brown solid (52 mg, 9 %); **δ_H** (700 MHz, Methanol-d_4) 7.37 (1H, dd, $^3J_{H\text{-}H}$ 2.0 Hz, $^4J_{H\text{-}H}$ 1.0 Hz, H^{10}), 6.92 (1H, dd, $^3J_{H\text{-}H}$ 2.5 Hz, $^3J_{H\text{-}H}$ 2.0 Hz, H^9), 6.06 (1H,

dq, $^{3}J_{H\text{-}H}$ 2.5 Hz, $^{4}J_{H\text{-}H}$ 1.0 Hz, H^{8}), 6.15 (6H, s, H^{1}), 5.35 (2H, m, H^{3}), 5.31 (2H, m, H^{2}), 2.83 (2H, m, H^{6}), 2.66 (2H, m, H^{5}); **δ_C** (176 MHz, Methanol-d4) 153.8 (1C, s, C^{7}), 141.2 (1C, s, C^{10}), 111.0 (1C, s, C^{9}), 105.7 (1C, s, C^{8}), 103.2 (1C, s, C^{4}), 86.1 (6C, s, C^{1}), 80.4 (2C, s, C^{3}), 79.4 (2C, s, C^{2}), 28.3 (1C, s, C^{6}), 26.35 (1C, s, C^{5}); *m/z* (HRMS^{+}) 333.0366 $[M\text{-}PF_6]^{+}$ ($C_{17}H_{17}O^{96}Ru^{+}$ requires 333.0350).

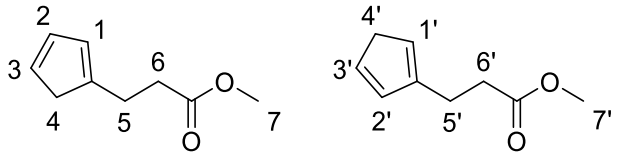

Methyl 3-(cyclopenta-1,3-dien-1-yl)propanoate and
methyl 3-(cyclopenta-1,4-dien-1-yl) propanoate **5.12a** *and* **5.12b**

The *title compounds* were synthesised following a known literature procedure and their ^{1}H-NMR spectra agree with the reported literature.[38] A solution of methyl 3-bromopropionate (685 mg,0.448 mL, 4.20 mmol) in THF (2 mL) was added dropwise to a stirred solution of sodium cyclopentadienylide (2 M in THF, 363 mg, 2.05 mL, 4.20 mmol) in THF (5 mL) at -78 °C. The mixture was then stirred for 3 h at -78 °C before CH_2Cl_2 (5 mL) was added to facilitate precipitation of NaBr, which was removed by filtration. The solvent was removed under high vacuum from the filtrate to leave a 1:1 mixture of the title compounds as a yellow oil, which was used without further purification (420 mg, 66%). **δ_H** ($CDCl_3$) 6.45 – 6.03 (6H, m, $H^{1/1',2/2',3/3'}$), 3.70 (6h, s, $H^{7,7'}$), 3.00 – 2.90 (4H, m, $H^{4/4'}$), 2.80 – 2.69 (4H, m, $H^{5/5'}$), 2.63 – 2.55 (4H, m, $H^{6/6'}$).

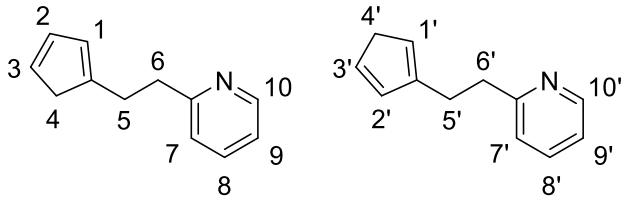

2-[2-(Cyclopenta-1,3-dien-1-yl)ethyl]pyridine and
2-[2-(cyclopenta-1,4-dien-1-yl)ethyl] pyridine **5.15a** *and* **5.15b**

The *title compounds* were synthesised by adapting a known literature procedure.[38] PPh_3 (6.98 g, 26.6 mmol) and CBr_4 (8.82 g, 26.6 mmol) were added to a solution of

2-pyridineethanol (2.00 mL, 17.8 mmol) in anhydrous THF (40 mL). The mixture was stirred at 20 °C for 24 h before excess salts were removed by filtration. The crude 2-(2-bromoethyl)pyridine solution was cooled to -78 °C and a solution of sodium cyclopentadienylide (2M in THF, 8.90 mL) was added. The mixture was stirred for 16 h under an argon atmosphere, during which time the temperature increased to 20 °C. The solvent was removed under reduced pressure to give a black residue, which was triturated with hexane (15 mL) and then Et_2O (50 mL). The organic fractions were passed through a plug of silica, which was washed with further fractions of Et_2O (100 mL). All organic fractions were combined and the solvent removed under reduced pressure to give a 1 : 1 mixture of the title compounds as a brown oil, which was used without further purification (2.85 g, 86%); $\boldsymbol{\delta_H}$ ($CDCl_3$) 8.50 (2H, m, $H^{10/10'}$), 7.54 (2H, m, $H^{8/8'}$), 7.10 (4H, m, $H^{7/7', 9/9'}$) 6.43 – 6.00 (6H, m, $H^{1/1', 2/2', 3/3'}$), 3.00 (4H, m, $H^{6/6'}$), 2.87 (4H, m, $H^{4/4'}$), 2.80 (4H, m, $H^{5/5'}$);

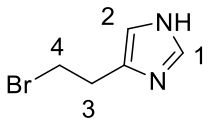

4-(2-Bromoethyl)imidazole **5.17**

The *title compound* was synthesised by adapting the known literature procedure.[194] Potassium bromide (4.80 g, 40.50 mmol) was added to a solution of histamine (1.50 g, 13.50 mmol) in sulfuric acid (16 mL, 2.5 M). The mixture was cooled to -15 °C using a salt ice bath. A saturated solution of sodium nitrite (1.25 g, 17.60 mmol) was made up in 3 mL of water. The saturated solution was added all at once to the magnetically stirred sulfuric acid/histamine solution at -15 °C. A colour change from colourless to a dark orange was observed and a gas evolved in the reaction flask immediately upon addition. After 30 min, the reaction mixture was warmed to room temperature and allowed to react for a further 3 hours until no gas evolution was observed and the mixture was a colourless solution. The mixture was cooled to -15 °C and brought to a pH of 11 with the dropwise addition of NaOH (5 M) solution. The solution was transferred to a separation funnel and quickly extracted using chloroform (5 × 15 mL). The organic layers were combined and reduce under vacuum to yield the *title compound* as a yellow oil and required no further purification (355 mg, 15%). $\boldsymbol{\delta_H}$ ($CDCl_3$) 7.64 (1H, d, $^4J_{H–H}$ 1.0 Hz, H^1), 6.92 (1H, d, $^4J_{H–}$

$_H$ 1.0 Hz, H^2), 3.65 (2H, t, $^3J_{H–H}$ 7.0 Hz, H^4), 3.20 (2H, t, $^3J_{H–H}$ 7.0 Hz, H^3); *m/z* ($HRMS^+$) 175.9868 $[M+H]^+$ ($C_{16}H_{19}O_2{}^{96}Ru$ requires 175.9865).

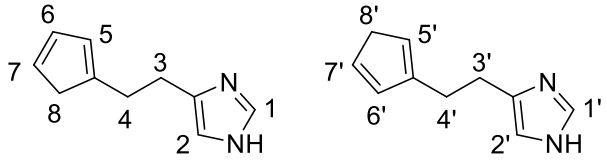

4-[2-(Cyclopenta-1,3-dien-1-yl)ethyl]imidazole and
4-[2-(cyclopenta-1,4-dien-1-yl)ethyl]imidazole **5.18a** *and* **5.18b**

The solution of crude 4-(2-bromoethyl)imidazole (355 mg, 2.02 mmol) in THF (5 mL) was cooled to -78 °C and a solution of sodium cyclopentadienylide (2M in THF, 1.01 mL) was added. The mixture was stirred for 16 h under an argon atmosphere, during which time the temperature increased to 20 °C. The solvent was removed under reduced pressure to give a black residue, which was triturated with hexane (10 mL) and then Et_2O (15 mL x 3). The organic fractions were passed through a plug of silica, which was washed with further fractions of Et_2O (100 mL). All organic fractions were combined and the solvent removed under reduced pressure to give a 1 : 1 mixture of the title compounds as a brown oil, which was used without further purification (142 mg, 44%); $\boldsymbol{\delta_H}$ ($CDCl_3$) 7.53 (2H, m, $H^{1/1'}$), 6.77 (2H, m, $H^{2/2'}$), 6.41 – 6.05 (6H, m, $H^{5/5', 6/6', 7/7'}$), 2.96 (4H, m, $H^{3/3'}$), 2.89 (4H, m, $H^{8/8'}$), 2.71 (4H, m, $H^{4/4'}$).

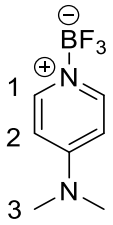

4-(Dimethylamino)pyridine·trifluoroborate **5.20**

The *title compound* was synthesised by adapting a known literature procedure.[195] $BF_3{\cdot}Et_2O$ (710 mg, 617 µL, 5.00 mmol) was added dropwise to a stirred solution of DMAP (500 mg, 4.09 mmol) in THF (5 mL) at room temperature. The reaction was allowed to stir for 3 h where a white precipitate was observed, then the addition of Et_2O

(5 mL) furthered precipitation. The precipitate was isolated by vacuum filtration and washed with more Et_2O. The *title compound* was collected as a white powder and required no further purification (771 mg, 91%). The product is spectroscopically identical to the known DMAP·BF_3[195]. **δ_H** ($CDCl_3$) 8.09 (2H, d, broad, H^1), 6.62 (2H, d, $^3J_{H–H}$ 7.0 Hz, H^2), 3.16 (6H, s, H^3).

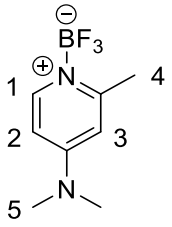

2-Methyl-4-(dimethylamino)pyridine·trifluoroborate **5.21**

The *title compound* was synthesised by adapting a known literature procedure.[196] A mixture of DMAP·BF_3 (150 mg, 0.79 mmol) in THF (4 mL) was cooled to -78 °C and *n*-BuLi (2.13 M in hexanes, 450 µL, 0.95 mmol) was added dropwise. After 15 minutes, MeI (500 µL, 7.90 mmol) was added dropwise and the resulting mixture was stirred for 30 mins. The mixture was warmed at -40 °C, quenched with water (10 mL) and then warmed to room temperature. The reaction mixture was extracted with CH_2Cl_2 (3 × 10 mL), the organic layers were combined and dried over $MgSO_4$. Evaporation and purification by flash chromatography (CH_2Cl_2-petrol, 4:1) gave the *title compound* as a white solid (154 mg, 96%). The product is spectroscopically identical to the known 2-Me-DMAP·BF_3.[196] **δ_H** ($CDCl_3$) 8.28 (1H, d, $^3J_{H-H}$ 7.5 Hz, H^1), 6.46 (1H, dd, $^3J_{H-H}$ 7.5 Hz, $^4J_{H-H}$ 2.5 Hz, H^2), 6.42 (1H, d, $^4J_{H-H}$ 2.5 Hz, H^3), 3.14 (6H, s, H^5), 2.67 (3H, s, H^4).

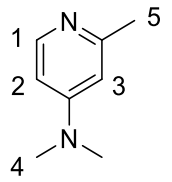

2-Methyl-4-(dimethylamino)pyridine **5.22**

A mixture of 2-bromo-4-(dimethylamino)pyridine (600 mg, 2.98 mmol) in THF (20 mL) was cooled to -78 °C and *n*-BuLi (2.20 M in hexanes, 1.63 mL, 3.58 mmol) was added dropwise. After 15 minutes, MeI (1.88 mL, 29.80 mmol) was added dropwise and the resulting mixture was stirred for 30 mins. The mixture was warmed at -40 °C, quenched with water (10 mL) and then warmed to room temperature. The reaction mixture was

extracted with CH_2Cl_2 (3 × 10 mL), the organic layers were combined and dried over $MgSO_4$. Evaporation and purification by flash chromatography (CH_2Cl_2-petrol, 4:1) gave the *title compound* as a white solid (136 mg, 87%). The product is in spectroscopic agreement to the known 2-methyl-4-(dimethylamino)pyridine.[196] $\boldsymbol{\delta_H}$ ($CDCl_3$) 8.11 (1H, d, $^3J_{H\text{-}H}$ 5.5 Hz, H^1), 6.37–6.29 (2H, m, H^{2+3}), 2.97 (6H, s, H^4), 2.43 (3H, s, H^5).

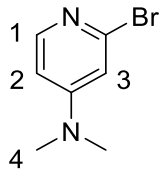

2-Bromo-4-(dimethylamino)pyridine **5.25**

The *title compound* was synthesised by adapting a known literature procedure.[197] To a suspension of sodium hydride (350 mg, 8.67 mmol, 60% dispersion in mineral oil) in THF (6 mL) at 0 °C, 2-bromo-4-aminopyridine (500 mg, 2.89mmol) was added. The reaction mixture was stirred for 30 min under an argon atmosphere at the same temperature. After methyl iodide (450 µL, 7.23 mmol) was added, the resultant mixture was stirred at room temperature for 3 h. The reaction was quench with water (10 mL) and the mixture was concentrated by removing the organic solvent *via* rotary evaporation. The organic materials were then extracted using DCM (3 × 10 mL). The combined fractions were washed with brine (15 mL) and dried over $MgSO_4$. After removal of solvents under reduced pressure, the residue was crystallised from ethanol. The *title compound* was isolated as an orange crystalline and required no further purification (512 mg, 88%). The product is spectroscopically identical to the known 2-bromo-4-N,N-dimethylaminopyridine.[197] $\boldsymbol{\delta_H}$ ($CDCl_3$) 7.93 (1H, d, $^3J_{H\text{-}H}$ 6.0 Hz, H^1), 6.63 (1H, d, $^4J_{H\text{-}H}$ 2.5 Hz, H^3), 6.43 (1H, dd, $^3J_{H\text{-}H}$ 6.0 Hz, $^4J_{H\text{-}H}$ 2.5 Hz, H^2), 2.98 (6H, s, H^4).

Appendix

Crystal Structure Data

[Ru(η^6-nitrobenzene)(η^5-cyclopentadienyl)]PF_6 **2.8**

Table 1 Crystal data and structure refinement for **2.8**.

Empirical formula	$C_{11}H_{10}NO_2Ru$ x PF_6
Formula weight	434.24
Temperature/K	120.0
Crystal system	monoclinic
Space group	$P1_1/n$
a/Å	8.17160(16)
b/Å	12.4722(2)
c/Å	13.2874(3)
α/°	90.00
β/°	91.5709(18)
γ/°	90.00
Volume/Å^3	1353.72(5)
Z	4
ρ_{calc}g/cm^3	2.131
μ/mm^{-1}	1.352
F(000)	848.0
Crystal size/mm^3	0.38 × 0.31 × 0.23
Radiation	MoKα (λ = 0.71073)
2Θ range for data collection/°	4.48 to 60
Index ranges	$-11 \leq h \leq 11$, $-17 \leq k \leq 17$, $-18 \leq l \leq 18$
Reflections collected	20965
Independent reflections	3953 [R_{int} = 0.0336, R_{sigma} = 0.0243]
Data/restraints/parameters	3953/0/199
Goodness-of-fit on F^2	1.073
Final R indexes [I>=2σ (I)]	R_1 = 0.0368, wR_2 = 0.0975
Final R indexes [all data]	R_1 = 0.0447, wR_2 = 0.1033
Largest diff. peak/hole / e Å^{-3}	1.29/-0.95

Table 2 Bond Lengths for **2.8**.

Atom		Length/Å	Atom		Length/Å
Ru1	C1	2.183(3)	C2	C3	1.419(5)
Ru1	C2	2.170(3)	C3	C4	1.419(5)
Ru1	C3	2.181(3)	C4	C5	1.419(5)
Ru1	C4	2.185(3)	C6	C7	1.409(4)
Ru1	C5	2.189(3)	C6	C11	1.407(5)
Ru1	C6	2.179(3)	C7	C8	1.410(4)
Ru1	C7	2.220(3)	C8	C9	1.423(5)
Ru1	C8	2.220(3)	C9	C10	1.412(5)
Ru1	C9	2.209(3)	C10	C11	1.417(5)
Ru1	C10	2.213(3)	P1	F1	1.604(2)
Ru1	C11	2.213(3)	P1	F2	1.592(3)
O1	N1	1.223(4)	P1	F3	1.585(2)
O2	N1	1.217(4)	P1	F4	1.599(3)
N1	C6	1.484(4)	P1	F5	1.615(2)
C1	C2	1.414(6)	P1	F6	1.590(2)
C1	C5	1.411(6)			

Table 3 Bond Angles for **2.8**.

Atom			Angle/°	Atom			Angle/°
C1	Ru1	C4	63.20(13)	O1	N1	C6	117.2(3)
C1	Ru1	C5	37.66(15)	O2	N1	O1	124.3(3)
C1	Ru1	C7	140.04(14)	O2	N1	C6	118.4(3)
C1	Ru1	C8	113.79(13)	C2	C1	Ru1	70.56(19)
C1	Ru1	C9	104.98(12)	C5	C1	Ru1	71.40(19)
C1	Ru1	C10	118.83(13)	C5	C1	C2	108.3(3)
C1	Ru1	C11	148.01(15)	C1	C2	Ru1	71.5(2)
C2	Ru1	C1	37.90(15)	C1	C2	C3	108.0(3)
C2	Ru1	C3	38.07(13)	C3	C2	Ru1	71.36(18)
C2	Ru1	C4	63.49(13)	C2	C3	Ru1	70.57(18)
C2	Ru1	C5	63.35(15)	C4	C3	Ru1	71.21(18)
C2	Ru1	C6	136.35(14)	C4	C3	C2	107.7(3)
C2	Ru1	C7	111.44(13)	C3	C4	Ru1	70.87(17)
C2	Ru1	C8	106.39(12)	C3	C4	C5	108.0(3)
C2	Ru1	C9	123.02(13)	C5	C4	Ru1	71.23(18)
C2	Ru1	C10	153.38(14)	C1	C5	Ru1	70.93(19)
C2	Ru1	C11	168.99(14)	C1	C5	C4	108.0(3)
C3	Ru1	C1	63.39(13)	C4	C5	Ru1	70.93(18)
C3	Ru1	C4	37.93(13)	N1	C6	Ru1	126.9(2)

C3	Ru1	C5	63.38(14)	C7	C6	Ru1	72.91(16)
C3	Ru1	C7	110.38(12)	C7	C6	N1	118.5(3)
C3	Ru1	C8	129.79(13)	C11	C6	Ru1	72.61(18)
C3	Ru1	C9	160.27(13)	C11	C6	N1	118.3(3)
C3	Ru1	C10	161.82(13)	C11	C6	C7	123.1(3)
C3	Ru1	C11	131.10(13)	C6	C7	Ru1	69.76(17)
C4	Ru1	C5	37.85(13)	C6	C7	C8	118.2(3)
C4	Ru1	C7	137.53(12)	C8	C7	Ru1	71.46(17)
C4	Ru1	C8	167.71(13)	C7	C8	Ru1	71.51(17)
C4	Ru1	C9	153.43(13)	C7	C8	C9	120.2(3)
C4	Ru1	C10	124.86(13)	C9	C8	Ru1	70.85(17)
C4	Ru1	C11	109.05(13)	C8	C9	Ru1	71.68(17)
C5	Ru1	C7	173.71(13)	C10	C9	Ru1	71.54(18)
C5	Ru1	C8	145.99(13)	C10	C9	C8	120.2(3)
C5	Ru1	C9	118.17(13)	C9	C10	Ru1	71.21(17)
C5	Ru1	C10	106.48(14)	C9	C10	C11	120.3(3)
C5	Ru1	C11	116.45(14)	C11	C10	Ru1	71.33(18)
C6	Ru1	C1	174.21(13)	C6	C11	Ru1	70.02(17)
C6	Ru1	C3	111.60(12)	C6	C11	C10	118.0(3)
C6	Ru1	C4	115.00(13)	C10	C11	Ru1	71.33(18)
C6	Ru1	C5	144.04(14)	F1	P1	F5	88.77(12)
C6	Ru1	C7	37.33(12)	F2	P1	F1	90.02(14)
C6	Ru1	C8	66.69(12)	F2	P1	F4	177.94(15)
C6	Ru1	C9	78.95(11)	F2	P1	F5	89.14(14)
C6	Ru1	C10	66.87(12)	F3	P1	F1	91.04(14)
C6	Ru1	C11	37.36(12)	F3	P1	F2	90.44(15)
C8	Ru1	C7	37.03(11)	F3	P1	F4	91.14(15)
C9	Ru1	C7	67.32(12)	F3	P1	F5	179.54(15)
C9	Ru1	C8	37.47(12)	F3	P1	F6	91.70(14)
C9	Ru1	C10	37.25(12)	F4	P1	F1	88.64(14)
C9	Ru1	C11	67.43(12)	F4	P1	F5	89.27(13)
C10	Ru1	C7	79.75(12)	F6	P1	F1	176.85(15)
C10	Ru1	C8	67.35(13)	F6	P1	F2	91.51(16)
C10	Ru1	C11	37.34(12)	F6	P1	F4	89.76(16)
C11	Ru1	C7	67.91(12)	F6	P1	F5	88.50(13)
C11	Ru1	C8	79.84(12)				

[Ru(η^6-1-methylindane)(η^5-cyclopentadienyl)]PF_6 **4.32**

Table 4 Crystal data and structure refinement for **4.32**.

Identification code	18srv393
Empirical formula	$C_{15}H_{17}Ru$ x PF_6
Formula weight	443.32
Temperature/K	120.0
Crystal system	monoclinic
Space group	$P2_1/c$
a/Å	15.6968(13)
b/Å	14.7127(12)
c/Å	14.1704(11)
α/°	90
β/°	106.757(3)
γ/°	90
Volume/Å^3	3133.6(4)
Z	8
ρ_{calc}g/cm^3	1.879
μ/mm^{-1}	1.160
F(000)	1760.0
Crystal size/mm^3	0.29 × 0.26 × 0.2
Radiation	MoKα (λ = 0.71073)
2Θ range for data collection/°	3.874 to 59
Index ranges	$-21 \leq h \leq 21$, $-20 \leq k \leq 20$, $-19 \leq l \leq 19$
Reflections collected	65402
Independent reflections	8722 [R_{int} = 0.0384, R_{sigma} = 0.0258]
Data/restraints/parameters	8722/28/417
Goodness-of-fit on F^2	1.048
Final R indexes [I>=2σ (I)]	R_1 = 0.0420, wR_2 = 0.1115
Final R indexes [all data]	R_1 = 0.0516, wR_2 = 0.1178
Largest diff. peak/hole / e Å^{-3}	1.90/-1.71

Table 5 Bond Lengths for **4.32**.

Atom		Length/Å	Atom		Length/Å
Ru1	C1	2.203(3)	Ru1A	C14A	2.179(3)
Ru1	C2	2.189(3)	Ru1A	C15A	2.192(3)
Ru1	C3	2.192(3)	C1A	C2A	1.421(5)
Ru1	C4	2.211(3)	C1A	C9A	1.406(4)
Ru1	C5	2.222(3)	C2A	C3A	1.414(5)
Ru1	C9	2.208(3)	C3A	C4A	1.421(5)
Ru1	C11	2.185(4)	C4A	C5A	1.407(4)
Ru1	C12	2.188(4)	C5A	C6A	1.513(4)
Ru1	C13	2.176(3)	C5A	C9A	1.419(4)
Ru1	C14	2.163(4)	C6A	C7A	1.541(5)
Ru1	C15	2.174(4)	C6A	C10A	1.526(5)
C1	C2	1.410(6)	C7A	C8A	1.545(5)
C1	C9	1.415(6)	C8A	C9A	1.504(5)
C2	C3	1.407(6)	C11A	C12A	1.414(5)
C3	C4	1.417(5)	C11A	C15A	1.412(6)
C4	C5	1.421(5)	C12A	C13A	1.417(5)
C5	C6	1.500(5)	C13A	C14A	1.425(5)
C5	C9	1.417(5)	C14A	C15A	1.419(6)
C6	C7	1.536(6)	P1	F1	1.573(3)
C6	C10	1.538(5)	P1	F2	1.604(3)
C7	C8	1.537(7)	P1	F3	1.587(3)
C8	C9	1.498(6)	P1	F4	1.552(3)
C11	C12	1.413(7)	P1	F5	1.578(3)
C11	C15	1.419(7)	P1	F6	1.582(3)
C12	C13	1.415(6)	P2	F11	1.566(3)
C13	C14	1.413(5)	P2	F12	1.590(3)
C14	C15	1.413(6)	P2	F12A	1.600(3)
Ru1A	C1A	2.215(3)	P2	F13	1.600(3)
Ru1A	C2A	2.207(3)	P2	F13A	1.597(3)
Ru1A	C3A	2.208(3)	P2	F14	1.604(3)
Ru1A	C4A	2.212(3)	P2	F14A	1.595(3)
Ru1A	C5A	2.199(3)	P2	F15	1.593(3)
Ru1A	C9A	2.210(3)	P2	F15A	1.595(3)
Ru1A	C11A	2.182(4)	P2	F16	1.585(3)
Ru1A	C12A	2.178(3)	P2	F13B	1.625(17)
Ru1A	C13A	2.178(3)			

Table 6 Bond Angles for **4.32**.

Atom			Angle/°	Atom			Angle/°
C1	Ru1	C4	80.45(14)	C11A	Ru1A	C4A	108.44(14)
C1	Ru1	C5	67.68(13)	C11A	Ru1A	C5A	126.06(13)
C1	Ru1	C9	37.43(15)	C11A	Ru1A	C9A	156.48(14)
C2	Ru1	C1	37.44(17)	C11A	Ru1A	C15A	37.65(15)
C2	Ru1	C3	37.47(16)	C12A	Ru1A	C1A	149.44(14)
C2	Ru1	C4	67.83(14)	C12A	Ru1A	C2A	172.39(13)
C2	Ru1	C5	79.65(13)	C12A	Ru1A	C3A	139.51(14)
C2	Ru1	C9	67.19(15)	C12A	Ru1A	C4A	113.09(13)
C3	Ru1	C1	67.68(15)	C12A	Ru1A	C5A	105.66(12)
C3	Ru1	C4	37.54(13)	C12A	Ru1A	C9A	120.58(13)
C3	Ru1	C5	67.27(13)	C12A	Ru1A	C11A	37.86(15)
C3	Ru1	C9	79.43(14)	C12A	Ru1A	C13A	37.97(14)
C4	Ru1	C5	37.40(13)	C12A	Ru1A	C14A	63.48(14)
C9	Ru1	C4	67.52(13)	C12A	Ru1A	C15A	63.41(14)
C9	Ru1	C5	37.32(12)	C13A	Ru1A	C1A	116.18(14)
C11	Ru1	C1	171.44(16)	C13A	Ru1A	C2A	144.37(14)
C11	Ru1	C2	147.56(18)	C13A	Ru1A	C3A	175.54(14)
C11	Ru1	C3	120.30(17)	C13A	Ru1A	C4A	143.91(13)
C11	Ru1	C4	107.75(15)	C13A	Ru1A	C5A	116.41(13)
C11	Ru1	C5	117.28(15)	C13A	Ru1A	C9A	105.46(14)
C11	Ru1	C9	142.98(17)	C13A	Ru1A	C11A	63.38(16)
C11	Ru1	C12	37.72(17)	C13A	Ru1A	C14A	38.17(14)
C12	Ru1	C1	135.34(17)	C13A	Ru1A	C15A	63.65(15)
C12	Ru1	C2	167.11(16)	C14A	Ru1A	C1A	107.08(14)
C12	Ru1	C3	154.78(16)	C14A	Ru1A	C2A	114.28(14)
C12	Ru1	C4	124.65(14)	C14A	Ru1A	C3A	139.39(14)
C12	Ru1	C5	108.28(13)	C14A	Ru1A	C4A	170.51(15)
C12	Ru1	C9	112.71(15)	C14A	Ru1A	C5A	150.93(14)
C13	Ru1	C1	108.16(15)	C14A	Ru1A	C9A	122.07(15)
C13	Ru1	C2	129.30(15)	C14A	Ru1A	C11A	63.13(16)
C13	Ru1	C3	161.59(15)	C14A	Ru1A	C15A	37.89(17)
C13	Ru1	C4	160.78(14)	C15A	Ru1A	C1A	128.32(15)
C13	Ru1	C5	129.03(13)	C15A	Ru1A	C2A	110.09(13)
C13	Ru1	C9	108.53(14)	C15A	Ru1A	C3A	112.19(14)
C13	Ru1	C11	63.28(16)	C15A	Ru1A	C4A	132.72(15)
C13	Ru1	C12	37.84(15)	C15A	Ru1A	C5A	163.31(15)
C14	Ru1	C1	109.93(15)	C15A	Ru1A	C9A	158.42(15)
C14	Ru1	C2	106.68(15)	C2A	C1A	Ru1A	70.97(19)
C14	Ru1	C3	124.89(15)	C9A	C1A	Ru1A	71.27(18)
C14	Ru1	C4	155.89(16)	C9A	C1A	C2A	119.0(3)

C14	Ru1	C5	166.59(15)	C1A	C2A	Ru1A	71.53(18)
C14	Ru1	C9	133.66(15)	C3A	C2A	Ru1A	71.36(19)
C14	Ru1	C11	63.52(16)	C3A	C2A	C1A	120.0(3)
C14	Ru1	C12	63.48(15)	C2A	C3A	Ru1A	71.28(18)
C14	Ru1	C13	38.02(15)	C2A	C3A	C4A	120.9(3)
C14	Ru1	C15	38.04(17)	C4A	C3A	Ru1A	71.40(18)
C15	Ru1	C1	139.60(17)	C3A	C4A	Ru1A	71.10(18)
C15	Ru1	C2	114.70(16)	C5A	C4A	Ru1A	70.88(17)
C15	Ru1	C3	107.22(15)	C5A	C4A	C3A	118.7(3)
C15	Ru1	C4	121.03(16)	C4A	C5A	Ru1A	71.91(18)
C15	Ru1	C5	150.01(16)	C4A	C5A	C6A	128.7(3)
C15	Ru1	C9	171.44(15)	C4A	C5A	C9A	120.5(3)
C15	Ru1	C11	38.01(18)	C6A	C5A	Ru1A	127.0(2)
C15	Ru1	C12	63.42(16)	C9A	C5A	Ru1A	71.64(18)
C15	Ru1	C13	63.53(16)	C9A	C5A	C6A	110.8(3)
C2	C1	Ru1	70.7(2)	C5A	C6A	C7A	102.7(3)
C2	C1	C9	118.9(3)	C5A	C6A	C10A	109.6(3)
C9	C1	Ru1	71.45(19)	C10A	C6A	C7A	115.1(3)
C1	C2	Ru1	71.8(2)	C6A	C7A	C8A	106.4(3)
C3	C2	Ru1	71.4(2)	C9A	C8A	C7A	103.2(3)
C3	C2	C1	120.6(3)	C1A	C9A	Ru1A	71.65(19)
C2	C3	Ru1	71.2(2)	C1A	C9A	C5A	120.8(3)
C2	C3	C4	120.8(4)	C1A	C9A	C8A	129.1(3)
C4	C3	Ru1	71.96(19)	C5A	C9A	Ru1A	70.80(17)
C3	C4	Ru1	70.5(2)	C5A	C9A	C8A	110.0(3)
C3	C4	C5	119.0(3)	C8A	C9A	Ru1A	128.4(2)
C5	C4	Ru1	71.74(18)	C12A	C11A	Ru1A	70.9(2)
C4	C5	Ru1	70.86(18)	C15A	C11A	Ru1A	71.6(2)
C4	C5	C6	129.0(3)	C15A	C11A	C12A	108.7(4)
C6	C5	Ru1	128.6(2)	C11A	C12A	Ru1A	71.2(2)
C9	C5	Ru1	70.79(19)	C11A	C12A	C13A	108.0(3)
C9	C5	C4	119.8(3)	C13A	C12A	Ru1A	71.03(19)
C9	C5	C6	111.2(3)	C12A	C13A	Ru1A	71.00(19)
C5	C6	C7	102.5(3)	C12A	C13A	C14A	107.5(4)
C5	C6	C10	109.6(3)	C14A	C13A	Ru1A	71.0(2)
C7	C6	C10	113.0(4)	C13A	C14A	Ru1A	70.88(19)
C6	C7	C8	105.9(3)	C15A	C14A	Ru1A	71.5(2)
C9	C8	C7	103.6(3)	C15A	C14A	C13A	108.3(3)
C1	C9	Ru1	71.1(2)	C11A	C15A	Ru1A	70.8(2)
C1	C9	C5	120.9(3)	C11A	C15A	C14A	107.5(3)
C1	C9	C8	129.8(4)	C14A	C15A	Ru1A	70.6(2)
C5	C9	Ru1	71.89(19)	F1	P1	F2	86.7(2)

C5	C9	C8	109.2(4)	F1	P1	F3	91.9(2)
C8	C9	Ru1	127.7(3)	F1	P1	F5	89.5(2)
C12	C11	Ru1	71.3(2)	F1	P1	F6	177.7(2)
C12	C11	C15	108.1(4)	F3	P1	F2	87.05(17)
C15	C11	Ru1	70.6(2)	F4	P1	F1	93.3(2)
C11	C12	Ru1	71.0(2)	F4	P1	F2	179.3(2)
C11	C12	C13	107.9(4)	F4	P1	F3	92.3(2)
C13	C12	Ru1	70.6(2)	F4	P1	F5	88.9(2)
C12	C13	Ru1	71.5(2)	F4	P1	F6	89.0(2)
C14	C13	Ru1	70.5(2)	F5	P1	F2	91.8(2)
C14	C13	C12	108.0(4)	F5	P1	F3	178.2(2)
C13	C14	Ru1	71.5(2)	F5	P1	F6	90.44(19)
C15	C14	Ru1	71.4(2)	F6	P1	F2	91.0(2)
C15	C14	C13	108.2(4)	F6	P1	F3	88.20(19)
C11	C15	Ru1	71.4(2)	F11	P2	F12A	97.9(3)
C14	C15	Ru1	70.5(2)	F11	P2	F13A	96.3(4)
C14	C15	C11	107.7(4)	F11	P2	F14A	83.7(4)
C2A	Ru1A	C1A	37.50(12)	F11	P2	F15A	105.2(6)
C2A	Ru1A	C3A	37.36(13)	F11	P2	F16	177.5(2)
C2A	Ru1A	C4A	67.86(13)	F12	P2	F13	93.5(3)
C2A	Ru1A	C9A	66.96(12)	F12	P2	F14	177.0(3)
C3A	Ru1A	C1A	67.44(13)	F12	P2	F15	94.7(4)
C3A	Ru1A	C4A	37.50(13)	F13	P2	F14	83.7(3)
C3A	Ru1A	C9A	79.00(12)	F13A	P2	F12A	101.6(5)
C4A	Ru1A	C1A	80.32(12)	F14A	P2	F12A	177.9(5)
C5A	Ru1A	C1A	67.68(12)	F14A	P2	F13A	76.9(5)
C5A	Ru1A	C2A	79.72(12)	F15	P2	F13	170.5(4)
C5A	Ru1A	C3A	67.01(12)	F15	P2	F14	88.3(3)
C5A	Ru1A	C4A	37.20(12)	F15A	P2	F12A	91.5(6)
C5A	Ru1A	C9A	37.56(11)	F15A	P2	F13A	153.0(7)
C9A	Ru1A	C1A	37.07(11)	F15A	P2	F14A	89.3(7)
C9A	Ru1A	C4A	67.42(12)	F16	P2	F12A	84.3(3)
C11A	Ru1A	C1A	165.77(14)	F16	P2	F13A	84.2(4)
C11A	Ru1A	C2A	134.55(14)	F16	P2	F14A	94.1(4)
C11A	Ru1A	C3A	112.43(15)	F16	P2	F15A	73.7(6)

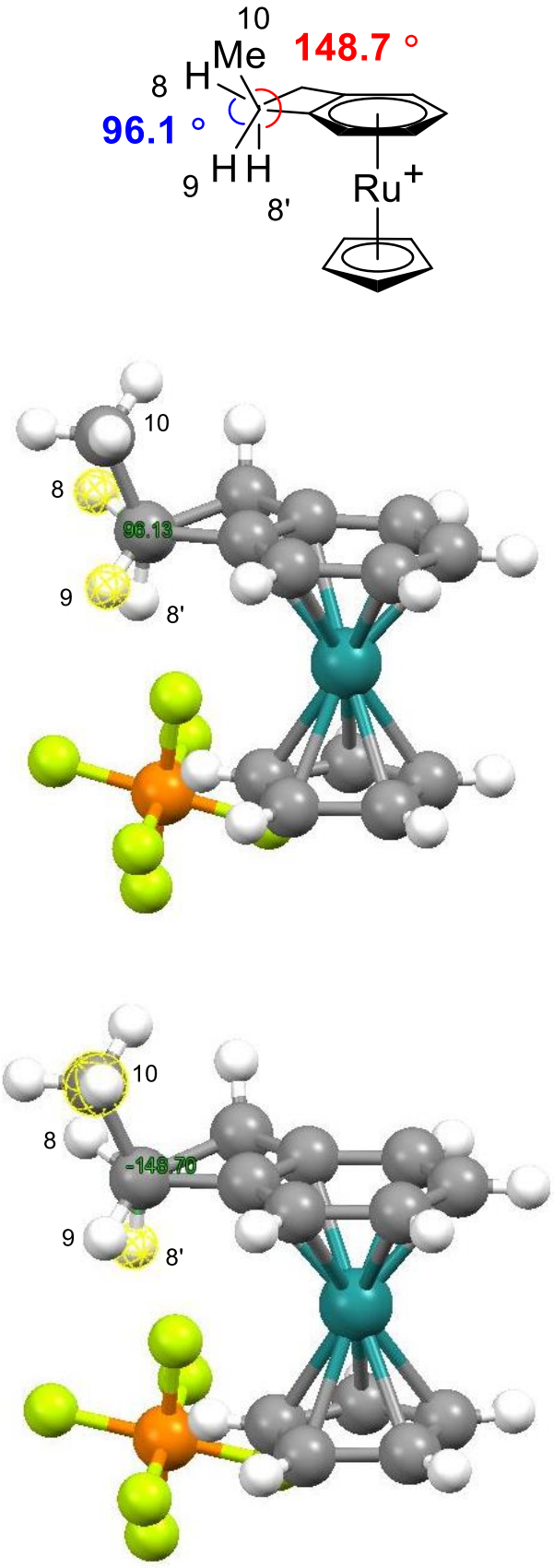

Figure 1 *Torsion angles between protons 8 and 9 and methyl group 10 and 8'. These images were creating using Mercury.*

Table 7 *Amounts of starting material (iodoarene, [RuCp(MeCN)$_3$]PF$_6$ and DBU) used for scope of catalytic deiodination.*

Run	Arene	Mr / g/mol	Mass / mg	Density / g/mL	Volume / µL	mol / mmol	mass of [Ru] / mg	mass of DBU / mg	volume of DBU / µL
1	1-Bromo-4-iodobenzene	282.906	100			0.353	15.35	53.81	52.76
2	1-Chloro-4-iodobenzene	238.45	100			0.419	18.21	63.85	62.59
3	1-Fluoro-4-iodobenzene	222.001	100	1.925	51.95	0.450	19.56	68.58	67.23
4	1-Bromo-3-iodobenzene	282.906	100	2.219	45.07	0.353	15.35	53.81	52.76
5	1-Chloro-3-iodobenzene	238.45	100	1.926	51.92	0.419	18.21	63.85	62.59
6	1-Fluoro-3-iodobenzene	222.001	100	1.89	52.91	0.450	19.56	68.58	67.23
7	1-Bromo-2-iodobenzene	282.906	100	2.203	45.39	0.353	15.35	53.81	52.76
8	1-Chloro-2-iodobenzene	238.45	100	1.952	51.23	0.419	18.21	63.85	62.59
9	1-Fluoro-2-iodobenzene	222.001	100	1.903	52.55	0.450	19.56	68.58	67.23
10	4-Chloro-2-fluoroiodobenzene	256.44	100	1.98	50.51	0.390	16.93	59.37	58.20
11	1-Bromo-3-fluoro-4-iodobenzene	300.897	100			0.332	14.43	50.60	49.60
12	2-Bromo-4-fluoro-1-iodobenzene	300.897	100	2.3	43.48	0.332	14.43	50.60	49.60
13	Iodobenzene	204.01	100	1.823	54.85	0.490	21.29	74.62	73.16
14	4-Iodotoluene	218.037	100			0.459	19.92	69.82	68.45
15	1-tert-Butyl-4-iodobenzene	260.118	100	1.468	68.12	0.384	16.70	58.53	57.38
16	2-Iodotoluene	218.037	100	1.713	58.38	0.459	19.92	69.82	68.45
17	3-Iodotoluene	218.037	100	1.698	58.89	0.459	19.92	69.82	68.45
18	2-Iodo-m-xylene	232.064	100	1.608	62.19	0.431	18.71	65.60	64.32

19	4-Iodo-o-xylene	232.064	100	1.633	61.24	0.431	18.71	65.60	64.32
20	2-Iodomesitylene	246.091	100	1.534	65.19	0.406	17.65	61.86	60.65
21	1,4-Diiodobenzene	329.907	100			0.303	13.16	46.15	45.24
22	4-Iodophenylboronic acid	247.83	100			0.404	17.52	61.43	60.22
23	4-iodobenzotrifluoride	272.009	100	1.851	54.02	0.368	15.97	55.97	54.87
24	4-iodobenzonitrile	229.02	100			0.437	18.96	66.47	65.17
25	Ethyl 4-iodobenzoate	276.073	100	1.641	60.94	0.362	15.73	55.14	54.06
26	4'-Iodoacetophenone	246.047	100			0.406	17.65	61.87	60.66
27	1-Iodo-4-nitrobenzene	249.007	100			0.402	17.44	61.14	59.94
28	1-Iodo-3-nitrobenzene	249.007	100			0.402	17.44	61.14	59.94
29	3,5-Bis(trifluoromethyl)iodobenzene	340.007	100	1.919	52.11	0.294	12.77	44.78	43.90
30	4-Iodoanisole	234.036	100			0.427	18.56	65.05	63.77
31	2-Iodo-1,3-dimethoxybenzene	264.062	100			0.379	16.45	57.65	56.52
32	4-Iodoaniline	219.025	100			0.457	19.83	69.51	68.15
33	3-Iodoaniline	219.025	100	1.821	54.91	0.457	19.83	69.51	68.15
34	3-Iodoanisole	234.036	100	1.965	50.89	0.427	18.56	65.05	63.77
35	4-Iodophenol	220.009	100			0.455	19.74	69.20	67.84
36	3-Iodophenol	220.009	100			0.455	19.74	69.20	67.84
37	2-Iodophenol	220.009	100			0.455	19.74	69.20	67.84
38	N-(4-Iodophenyl)acetamide	261.062	100			0.383	16.64	58.32	57.17

Table 8 *Selected ions monitored for calculating conversion of catalytic deiodination scope via GC-MS.*

Run	Arene starting material	Mr	precursor monoisotopic peak m/z	ion 1 m/z	ion 2 m/z	ion 3 m/z	Arene product	Mr	precursor monoisotopic peak m/z	ion 1 m/z	ion 2 m/z
1	1-Bromo-4-iodobenzene	282.91	282	155	75	50	bromobenzene	157.01	156	77	51
2	1-Chloro-4-iodobenzene	238.45	238	111	75	50	chlorobenzene	112.56	112	77	51
3	1-Fluoro-4-iodobenzene	222.00	222	95	75	50	fluorobenzene	96.10	96	70	50
4	1-Bromo-3-iodobenzene	282.91	282	155	76	50	bromobenzene	157.01	156	77	51
5	1-Chloro-3-iodobenzene	238.45	238	111	75	50	chlorobenzene	112.56	112	77	51
6	1-Fluoro-3-iodobenzene	222.00	222	95	75	50	fluorobenzene	96.10	96	70	50
7	1-Bromo-2-iodobenzene	282.91	282	155	76	50	bromobenzene	157.01	156	77	51
8	1-Chloro-2-iodobenzene	238.45	238	111	75	50	chlorobenzene	112.56	112	77	51
9	1-Fluoro-2-iodobenzene	222.00	222	95	75	50	fluorobenzene	96.10	96	70	50
10	4-Chloro-2-fluoroiodobenzene	256.44	256	129	109	94	1-Chloro-3-fluorobenzene	130.55	130	95	75
11	1-Bromo-3-fluoro-4-iodobenzene	300.90	300	173	94	50	1-bromo-3-fluorobenzene	175.00	174	95	50
12	2-Bromo-5-fluoro-1-iodobenzene	300.90	300	173	94	50	1-bromo-4-fluorobenzene	175.00	174	95	50
13	Iodobenzene	204.01	204	127	77	51	benzene	78.11	78	51	39
14	4-Iodotoluene	218.04	218	127	91	65	toluene	92.14	92	91	39
15	1-tert-Butyl-4-iodobenzene	260.12	260	245	217	118	1-tert-Butylbenzene	134.22	134	119	91
16	2-Iodotoluene	218.04	218	127	91	65	toluene	92.14	92	91	39
17	3-Iodotoluene	218.04	218	127	91	65	toluene	92.14	92	91	39
18	2-Iodo-m-xylene	232.06	232	105	79	77	m-xylene	106.17	106	91	77
19	4-Iodo-o-xylene	232.06	232	105	77		o-xylene	106.17	106	91	77
20	2-Iodomesitylene	246.09	246	119	91	77	mesitylene	120.19	120	105	77
21	1,4-Diiodobenzene	329.91	330	203	76	50	benzene	78.11	78	51	39

22	4-Iodophenylboronic acid	247.83	248				phenylboronic acid	121.93	122	78	48
23	4-iodobenzotrifluoride	272.01	272	145	95	75	trifluoromethylbenzene	146.11	146	127	96
24	4-iodobenzonitrile	229.02	229	127	102	75	benzonitrile	103.12	103	76	50
25	Methyl 4-iodobenzoate	276.07	262	231	76	50	methyl benzoate	136.15	136	105	77
26	4'-Iodoacetophenone	246.05	246	231	203	76	acetophenone	120.15	120	105	77
27	1-Iodo-4-nitrobenzene	249.01	249	219	203	76	nitrobenzene	123.11	123	77	51
28	1-Iodo-3-nitrobenzene	249.01	249	203	76	50	nitrobenzene	123.11	123	77	51
29	3,5-Bis(trifluoromethyl)iodobenzene	340.01	340	321	213	163	1,3-Bis(trifluoromethyl)benzene	214.11	214	195	164
30	4-Iodoanisole	234.04	234	107	92	77	anisole	108.14	108	78	65
31	2-Iodo-1,3-dimethoxybenzene	264.06	264	221	107	77	1,3-dimethoxybenzene	138.16	138	109	95
32	4-Iodoaniline	219.03	219	92	65	39	aniline	93.13	93	66	39
33	3-Iodoaniline	219.03	219	92	65	39	aniline	93.13	93	66	39
34	3-Iodoanisole	234.04	234	219	191	92	anisole	108.14	108	78	65
35	4-Iodophenol	220.01	220	93	65	39	phenol	94.11	94	66	39
36	3-Iodophenol	220.01	220	93	65	39	phenol	94.11	94	66	39
37	2-Iodophenol	220.01	220	93	65	39	phenol	94.11	94	66	39
38	N-(4-Iodophenyl)acetamide	261.06	261	219	92	43	Acetanilide	135.16	135	93	43

References

1 E. O. Fischer and W. Hafner, *Zeitschrift für Naturforsch.*, 1955, **10b**, 665–668.

2 J. W. Walton and L. A. Wilkinson, in *Organometallic Chemistry: Volume 42*, 2018, pp. 125–171.

3 J. H. Rigby and M. A. Kondratenko, in *Top. Organomet. Chem.*, 2004, pp. 181–204.

4 A. Meltzer, C. Präsang, C. Milsmann and M. Driess, *Angew. Chem., Int. Ed.*, 2009, **48**, 3170–3173.

5 C. Watanabe, Y. Inagawa, T. Iwamoto and M. Kira, *Dalton Trans.*, 2010, **39**, 9414–9420.

6 Y. Hoshimoto, Y. Hayashi, H. Suzuki, M. Ohashi and S. Ogoshi, *Organometallics*, 2014, **33**, 1276–1282.

7 R. G. Gastinger and K. J. Klabunde, *Transit. Met. Chem.*, 1979, **4**, 1–13.

8 A. R. O. Connor, S. A. Urbin, R. A. Moorhouse, P. S. White and M. Brookhart, *Organometallics*, 2009, **28**, 2372–2384.

9 B. Thapaliya, S. Debnath, N. Arulsamy and D. M. Roddick, *Organometallics*, 2015, **34**, 4018–4022.

10 M. Tamm, T. Bannenberg, R. Fröhlich, S. Grimme and M. Gerenkamp, *Dalton Trans.*, 2004, 482–491.

11 E. P. Kündig, C. Fabritius, G. Grossheimann and P. Romanens, *Organometallics*, 2004, 3741–3744.

12 M. F. Semmelhack, W. Seufert and L. Keller, *J. Am. Chem. Soc.*, 1980, **102**, 6586–6587.

13 R. P. Houghton, M. Voyle and R. Price, *J. Organomet. Chem.*, 1983, **259**, 183–188.

14 S. Bräse, *Tetrahedron Lett.*, 1999, **40**, 6757–6759.

15 P. Ricci, K. Kramer, X. C. Cambeiro and I. Larrosa, *J. Am. Chem. Soc.*, 2013, **135**, 13258–13261.

16 J. A. Heppert, M. A. Morgenstern, D. M. Scherubel, F. Takusagawa and M. R. Shaker, *Organometallics*, 1988, **7**, 1715–1723.

17 J. A. Heppert, M. E. Thomas-Miller, D. M. Scherubel, F. Takusagawa, M. A. Morgenstern and M. R. Shaker, *Organometallics*, 1989, **8**, 1199–1206.

18 C. D. Hoff, *J. Organomet. Chem.*, 1985, **282**, 201–214.

19 S. L. Mukerjee, R. F. Lang, T. Ju, G. Kiss, C. D. Hoff and S. P. Nolan, *Inorg. Chem.*, 1992, **31**, 4885–4889.

20 E. P. Kündig, C. H. Fabritius, G. Grossheimann, F. Robvieux, P. Romanens and G. Bernardinelli, *Angew. Chem., Int. Ed.*, 2002, **41**, 4577–4579.

21 A. J. Pearson and P. R. Bruhn, *J. Org. Chem.*, 1991, **56**, 7092–7097.

22 A. J. Pearson, J. G. Park and P. Y. Zhu, *J. Org. Chem.*, 1992, **57**, 3583–3589.

23 A. J. Pearson and H. Shin, *Tetrahedron*, 1992, **48**, 7527–7538.

24 A. J. Pearson and H. Shin, *J. Org. Chem.*, 1994, **59**, 2314–2323.

25 J. P. Collman, L. S. Hegedus, J. R. Norton and R. G. Finke, *Principles and Applications of Organotransition Metal Chemistry*, University Science Books, 1987.

26 Y. K. Chung, H. S. Choi, D. A. Sweigart and N. G. Connelly, *J. Am. Chem. Soc.*, 1982, **104**, 4245–4247.

27 N. G. Connelly and R. L. Kelly, *J. Chem. Soc., Dalton Trans.*, 1973, 2334–2337.

28 E. A. Trifonova, D. S. Perekalin, K. A. Lyssenko and A. R. Kudinov, *J. Organomet. Chem.*, 2013, **727**, 60–63.

29 G. Meola, H. Braband, D. Hernández-Valdés, C. Gotzmann, T. Fox, B. Spingler and R. Alberto, *Inorg. Chem.*, 2017, **56**, 6297–6301.

30 G. Meola, H. Braband, S. Jordi, T. Fox, O. Blacque and R. Alberto, *Dalton Trans.*, 2017, **46**, 14631–14637.

31 M. Benz, H. Braband, P. Schmutz, J. Halter and R. Alberto, *Chem. Sci.*, 2015, **6**, 165–169.

32 I. U. Khand, P. L. Pauson and W. E. Watts, *J. Chem. Soc.*, 1968, 2261–2265.

33 M.-P. Luecke, D. Porwal, A. Kostenko, Y.-P. Zhou, S. Yao, M. Keck, C. Limberg, M. Oestreichb and M. Driess, *Dalton Trans.*, 2017, **46**, 16412–16418.

34 B. M. Trost and C. M. Older, *Organometallics*, 2002, **21**, 2544–2546.

35 E. Kayahara, V. K. Patel, A. Mercier, E. P. Kündig and S. Yamago, *Angew. Chem., Int. Ed.*, 2016, **55**, 302–306.

36 J. M. Cross, T. R. Blower, N. Gallagher, J. H. Gill, K. L. Rockley and J. W. Walton, *ChemPlusChem*, 2016, **81**, 1276–1280.

37 B. M. Trost and C. M. Older, *Organometallics*, 2002, **21**, 2544–2546.

38 J. W. Walton and J. M. J. Williams, *Chem. Commun.*, 2015, **51**, 2786–2789.

39 R. C. Cambie, S. J. Janssen, P. S. Rutledge and P. D. Woodgate, *J. Organomet. Chem.*, 1991, **420**, 387–418.

40 C. N. Neumann, J. M. Hooker and T. Ritter, *Nature*, 2016, **534**, 369–373.

41 M. H. Beyzavi, D. Mandal, M. G. Strebl, C. N. Neumann, E. M. D'Amato, J. Chen, J. M. Hooker and T. Ritter, *ACS Cent. Sci.*, 2017, **3**, 944–948.

42 H. Boennemann, R. Goddard, J. Grub, R. Mynott, E. Raabe and S. Wendel, *Organometallics*, 1989, **8**, 1941–1958.

43 A. R. Kudinov, E. V. Mutseneck and D. A. Loginov, *Coord. Chem. Rev.*, 2004, **248**, 571–585.

44 S. D. Pike, A. L. Thompson, A. G. Algarra, D. C. Apperley, S. A. Macgregor and

A. S. Weller, *Science*, 2012, **337**, 1648–1651.

45 S. D. Pike, M. R. Crimmin and A. B. Chaplin, *Chem. Commun.*, 2017, **53**, 3615–3633.

46 R. P. Houghton, M. Voyle and R. Price, *J. Chem. Soc. Perkin Trans. 1*, 1984, 925–931.

47 E. M. D'Amato, C. N. Neumann and T. Ritter, *Organometallics*, 2015, **34**, 4626–4631.

48 M. F. Semmelhack, A. Chlenov and D. M. Ho, *J. Am. Chem. Soc.*, 2005, **127**, 7759–7773.

49 T. G. Traylor and K. Stewart, *Organometallics*, 1984, **3**, 325–327.

50 T. G. Traylor, K. J. Stewart and M. J. Goldberg, *J. Am. Chem. Soc.*, 1984, **106**, 4445–4454.

51 T. G. Traylor, K. J. Stewart and M. J. Goldberg, *Organometallics*, 1986, **5**, 2062–2067.

52 H. Tobita, K. Hasegawa, J. Josephus, G. Minglana, L. Luh, M. Okazaki and H. Ogino, *Organometallics*, 1999, **18**, 2058–2060.

53 A. B. Chaplin and P. J. Dyson, *J. Organomet. Chem.*, 2011, **696**, 2485–2490.

54 C. A. L. Mahaffy and P. L. Pauson, *J. Chem. Res. Synop.*, 1979, **126**, 1752–1775.

55 B. R. Jagirdar and K. J. Klabunde, *J. Coord. Chem.*, 1995, **34**, 31–43.

56 C. L. Zimmerman, S. L. Shaner, S. A. Roth and B. R. Willeford, *J. Chem. Res. Synop.*, 1980, **108**, 1289–1297.

57 E. P. Kündig, M. Kondratenko and P. Romanens, *Angew. Chem., Int. Ed.*, 1998, **37**, 3146–3148.

58 M. F. Semmelhack, A. Chlenov, L. Wu and D. Ho, *J. Am. Chem. Soc.*, 2001, **123**, 8438–8439.

59 J. W. Walton and J. M. J. Williams, *Chem. Commun.*, 2015, **51**, 2786–2789.

60 A. J. Pearson, J. G. Park, S. H. Yang and Y.-H. Chuang, *J. Chem. Soc., Chem. Commun.*, 1989, **0**, 1363–1364.

61 R. J. Lavallee and C. Kutal, *J. Organomet. Chem.*, 1998, **562**, 97–104.

62 R. C. Cambie, G. R. Clark, S. L. Coombe, S. A. Coulson, P. S. Rutledge and P. D. Woodgate, *J. Organomet. Chem.*, 1996, **507**, 1–21.

63 T. P. Gill and K. R. Mann, *Inorg. Chem.*, 1983, **22**, 1986–1991.

64 T. P. Gill and K. R. Mann, *Inorg. Chem.*, 1980, **19**, 3007–3010.

65 M. Utsunomiya and J. F. Hartwig, *J. Am. Chem. Soc.*, 2004, **126**, 2702–2703.

66 J. Takaya and J. F. Hartwig, *J. Am. Chem. Soc.*, 2005, **127**, 5756–5757.

67 M. Otsuka, H. Yokoyama, K. Endo and T. Shibata, *Org. Biomol. Chem.*, 2012, **10**, 3815–3818.

68 J. M. O'Connor, S. J. Friese and B. L. Rodgers, *J. Am. Chem. Soc.*, 2005, **127**,

16342–16343.

69 T. P. Lockhart, P. B. Comita and R. G. Bergman, *J. Am. Chem. Soc.*, 1981, **103**, 4082–4090.

70 M. Otsuka, K. Endo and T. Shibata, *Chem. Commun.*, 2010, **46**, 336–338.

71 M. Otsuka, H. Yokoyama, K. Endo and T. Shibata, *Synlett*, 2010, **17**, 2601–2606.

72 T. Tsuchimoto, M. Iwabuchi, Y. Nagase, K. Oki and H. Takahashi, *Angew. Chem., Int. Ed.*, 2011, **50**, 1375–1379.

73 K. Yonekura, Y. Yoshimura, M. Akehi and T. Tsuchimoto, *Adv. Synth. Catal.*, 2018, **360**, 1159–1181.

74 A. G. Sergeev and J. F. Hartwig, *Science*, 2011, **332**, 439–443.

75 N. I. Saper and J. F. Hartwig, *J. Am. Chem. Soc.*, 2017, **139**, 17667–17676.

76 F. Zhu and Z. X. Wang, *Adv. Synth. Catal.*, 2013, **355**, 3694–3702.

77 T. Harada, Y. Ueda, T. Iwai and M. Sawamura, *Chem. Commun.*, 2018, **54**, 1718–1721.

78 N. C. Tomson, J. Arnold and R. G. Bergman, *Dalton Trans.*, 2011, **40**, 7718–7729.

79 A. I. Konovalov, E. O. Gorbacheva, F. M. Miloserdov and V. V. Grushin, *Chem. Commun.*, 2015, **51**, 13527–13530.

80 S. Takemoto, E. Shibata, M. Nakajima, Y. Yumoto, M. Shimamoto and H. Matsuzaka, *J. Am. Chem. Soc.*, 2016, **138**, 14836–14839.

81 J. A. Pike and J. W. Walton, *Chem. Commun.*, 2017, **53**, 9858–9861.

82 L. A. Wilkinson, J. A. Pike and J. W. Walton, *Organometallics*, 2017, **36**, 4376–4381.

83 K. Müller, C. Faeh and F. Diederich, *Science*, 2007, **317**, 1881–1886.

84 S. Purser, P. R. Moore, S. Swallow and V. Gouverneur, *Chem. Soc. Rev.*, 2008, **37**, 320–330.

85 P. Jeschke, *ChemBioChem*, 2004, **5**, 570–589.

86 M.-H. Hung, W. B. Farnham, A. E. Feiring and S. Rozen, *Fluoropolymers 1 Synthesis*, Kluwer Academic Publishers, 2002.

87 D. O'Hagan, *Chem. Soc. Rev.*, 2008, **37**, 308–319.

88 G. Bott, L. D. Field and S. Sternhell, *J. Am. Chem. Soc.*, 1980, **102**, 5618–5626.

89 K. Natte, R. V. Jagadeesh, L. He, J. Rabeah, J. Chen, C. Taeschler, S. Ellinger, F. Zaragoza, H. Neumann, A. Bruckner and M. Beller, *Angew. Chem., Int. Ed.*, 2016, **55**, 2782–2786.

90 D. T. Wong, K. W. Perry and F. P. Bymaster, *Nat. Rev. Drug Discov.*, 2005, **4**, 764–774.

91 V. Reiffenrath, J. Krause, H. J. Plach and G. Weber, *Liq. Cryst.*, 1989, **5**, 159–170.

92 P. Margot, F. Huggenberger, J. Amrein and B. Weiss, *BCPC Conf.-Pests. Dis.*, 1998, **2**, 375–382.

93 L. M. Yagupolskii, N. V. Kondratenko and G. N. Timofeeva, *J. Org. Chem. USSR*, 1984, **20**, 103–106.

94 U. Teruo and I. Sumi, *Tetrahedron Lett.*, 1990, **31**, 3579–3582.

95 T. Umemoto and S. Ishihara, *J. Am. Chem. Soc.*, 1993, **115**, 2156–2164.

96 T. Umemoto, *Chem. Rev.*, 1996, **96**, 1757–1778.

97 L. M. Yagupolskii, I. I. Maletina, N. V. Kondratenko and V. Orda, *Synthesis*, 1978, 835–837.

98 T. Umemoto and Y. Kuriu, *Tetrahedron Lett.*, 1981, **22**, 5197–5200.

99 T. Umemoto and Y. Kuriu, *Chem. Lett.*, 1982, 65–66.

100 I. Kieltsch, P. Eisenberger and A. Togni, *Angew. Chem., Int. Ed.*, 2007, **46**, 754–757.

101 N. Shibata, A. Matsnev and D. Cahard, *Beilstein J. Org. Chem.*, 2010, **6**, No. 65.

102 B. R. Langlois, E. Laurent and N. Roidot, *Tetrahedron Lett.*, 1991, **32**, 7525–7528.

103 D. A. Nagib and D. W. C. MacMillan, *Nature*, 2011, **480**, 224–228.

104 Y. Ji, T. Brueckl, R. D. Baxter, Y. Fujiwara, I. B. Seiple, S. Su, D. G. Blackmond and P. S. Baran, *Proc. Natl. Acad. Sci. U. S. A.*, 2011, **108**, 14411–14415.

105 L. Li, X. Mu, W. Liu, Y. Wang, Z. Mi and C.-J. Li, *J. Am. Chem. Soc.*, 2016, **138**, 5809–5812.

106 G. K. S. Prakash and A. K. Yudin, *Chem. Rev.*, 1997, **97**, 757–786.

107 G. K. S. Prakash, R. Krishnamurti and G. A. Olah, *J. Am. Chem. Soc.*, 1989, **111**, 393–395.

108 V. V. Bardin, A. A. Kolomeitsev, G. G. Furin and Y. L. Yagupolskii, *Izv. Akad. Nauk SSSR, Ser. Khim.*, 1990, 1693.

109 H. Urata and T. Fuchikami, *Tetrahedron Lett.*, 1991, **32**, 91–94.

110 M. Oishi, H. Kondo and H. Amii, *Chem. Commun.*, 2009, 1909–1911.

111 T. Knauber, F. Arikan, G. V. Röschenthaler and L. J. Gooßen, *Chem. Eur. J.*, 2011, **17**, 2689–2697.

112 J. Morstein, H. Hou, C. Cheng and J. F. Hartwig, *Angew. Chem., Int. Ed.*, 2016, **128**, 1–5.

113 E. L. Velarde, R. A. Stephen, R. N. Mansour, L. T. Hoang and D. J. Burkey, *J. Am. Chem. Soc.*, 2003, **125**, 1188–1189.

114 M. F. Semmelhack, *J. Organomet. Chem. Libr.*, 1976, **1**, 361.

115 N. V. Kirij, A. A. Filatov, G. Y. Khrapach and Y. L. Yagupolskii, *Chem. Commun.*, 2017, **53**, 2146–2149.

116 E. P. Kündig, *Pure Appl. Chem.*, 1985, **57**, 1855–1864.

117 Y. K. Chung, P. G. Williard and D. A. Sweigart, *Organometallics*, 1982, **1**, 1053–1056.

118 W. R. Gutekunst and P. S. Baran, *Chem. Soc. Rev.*, 2011, **40**, 1976–1991.

119 H. M. L. Davies, J. Du Bois and J.-Q. Yu, *Chem. Soc. Rev.*, 2011, **40**, 1855–1856.

120 R. H. Crabtree and A. Lei, *Chem. Rev.*, 2017, **117**, 8481–8482.

121 S. Murai, F. Kakiuchi, S. Sekine, Y. Tanaka, A. Kamatani, M. Sonoda and N. Chatani, *Nature*, 1993, **366**, 529–531.

122 J. W. Walton and J. M. J. Williams, *Angew. Chem., Int. Ed.*, 2012, **51**, 12166–12168.

123 D. Zhao, S. Vásquez-Céspedes and F. Glorius, *Angew. Chem., Int. Ed.*, 2015, **54**, 1657–1661.

124 J.-Y. Cho, M. K. Tse, D. Holmes, R. E. Maleczka and M. R. Smith, *Science*, 2002, **295**, 305–308.

125 J. M. Murphy, X. Liao and J. F. Hartwig, *J. Am. Chem. Soc.*, 2007, **129**, 15434–15435.

126 O. Saidi, J. Marafie, A. E. W. Ledger, P. M. Liu, M. F. Mahon, G. Kociok-Köhn, M. K. Whittlesey and C. G. Frost, *J. Am. Chem. Soc.*, 2011, **133**, 19298–19301.

127 X. Wang, D. Leow and J.-Q. Yu, *J. Am. Chem. Soc.*, 2011, **133**, 13864–13867.

128 D. R. Stuart and K. Fagnou, *Science*, 2007, **316**, 1172–1175.

129 X. Chen, K. M. Engle, D.-H. Wang and Y. Jin-Quan, *Angew. Chem., Int. Ed.*, 2009, **48**, 5094–5115.

130 T. Nishikata, A. R. Abela, S. Huang and B. H. Lipshutz, *Beilstein J. Org. Chem.*, 2016, **12**, 1040–1064.

131 X. H. Liu, H. Park, J. H. Hu, Y. Hu, Q. L. Zhang, B. L. Wang, B. Sun, K. S. Yeung, F. L. Zhang and J. Q. Yu, *J. Am. Chem. Soc.*, 2017, **139**, 888–896.

132 P. Gandeepan and L. Ackermann, *Chem*, 2018, **4**, 199–222.

133 C. N. Iverson and M. R. Smith, *J. Am. Chem. Soc.*, 1999, **121**, 7696–7697.

134 I. V. Seregin and V. Gevorgyan, *Chem. Soc. Rev.*, 2007, **36**, 1173–1193.

135 F. Bellina, S. Cauteruccio and R. Rossi, *Curr. Org. Chem.*, 2008, **12**, 774–790.

136 J. Roger, A. L. Gottumukkala and H. Doucet, *ChemCatChem*, 2010, **2**, 20–40.

137 X. Wang, D. V. Gribkov and D. Sames, *J. Org. Chem.*, 2007, **72**, 1476–1479.

138 F. Bellina, S. Cauteruccio, A. Di Fiore and R. Rossi, *European J. Org. Chem.*, 2008, 5436–5445.

139 M. Lafrance, C. N. Rowley, T. K. Woo and K. Fagnou, *J. Am. Chem. Soc.*, 2006, **128**, 8754–8756.

140 S. I. Gorelsky, D. Lapointe and K. Fagnou, *J. Am. Chem. Soc.*, 2008, **130**, 10848–10849.

141 D. Whitaker, M. Batuecas, P. Ricci and I. Larrosa, *Chem. Eur. J.*, 2017, **23**, 12763–12766.

142 K. Vikse, T. Naka, J. S. Mcindoe, M. Besora and F. Maseras, *ChemCatChem*, 2013, **5**, 3604–3609.

143 P. Fitton and E. A. Rick, *J. Organomet. Chem.*, 1971, **28**, 287–291.

144 M. Lafrance, C. N. Rowley, T. K. Woo and K. Fagnou, *J. Am. Chem. Soc.*, 2006, **128**, 8754–8756.

145 S. Y. Lee and J. F. Hartwig, *J. Am. Chem. Soc.*, 2016, **138**, 15278–15284.

146 M. D. Lotz, N. M. Camasso, A. J. Canty and M. S. Sanford, *Organometallics*, 2017, **36**, 165–171.

147 D. Whitaker, J. Bures and I. Larrosa, *J. Am. Chem. Soc.*, 2016, **138**, 8384–8387.

148 S. Y. Lee and J. F. Hartwig, *J. Am. Chem. Soc.*, 2016, **138**, 15278–15284.

149 F. Alonso, I. P. Beletskaya and M. Yus, *Chem. Rev.*, 2002, 4009–4091.

150 C. E. Kendall, *J. Am. Med. Assoc.*, 1915, **LXIV**, 2042–2043.

151 Merck and Co: Rahway NJ, *The Merck Index, 11th ed.*, 1989.

152 R. A. Hites, *Acc. Chem. Res.*, 1990, **23**, 194–201.

153 M. Yus, *Chem. Soc. Rev.*, 1996, **25**, 155–161.

154 N. Rot and F. Bickelhaupt, *Organometallics*, 1997, **16**, 5027–5031.

155 E. Austin, C. G. Ferrayoli, R. A. Alonso and R. A. Rossi, *Tetrahedron*, 1993, **49**, 4495–4502.

156 A. A. M. Lapis, O. C. Kreutz, A. R. Pohlmann and V. E. U. Costa, *Tetrahedron: Asymmetry*, 2001, **12**, 557–561.

157 M. S. Hong, L. He, B. E. Dale and K. C. Donnelly, *Environ. Sci. Technol.*, 1995, **29**, 702–708.

158 A. M. El Massry, A. Amer and C. U. Pittman, Jr., *Synth. Commun.*, 1990, **20**, 1091–1094.

159 H. Nishiyama, K. Isaka, K. Itoh, K. Ohno, H. Nagase, K. Matsumoto and H. Yoshiwara, *J. Org. Chem.*, 1992, **57**, 407–410.

160 M. Abarbri, J. Thibonnet, L. Bérillon, F. Dehmel, M. Rottländer and P. Knochel, *J. Org. Chem.*, 2000, **65**, 4618–4634.

161 R. A. O'Brien, T. Chen and R. D. Rieke, *J. Org. Chem.*, 1992, **57**, 2667–2677.

162 H. M. Walborsky and C. Hamdouchi, *J. Org. Chem.*, 1993, **58**, 1187–1193.

163 M. Yus and D. J. Ramon, *J. Chem. Soc., Chem. Commun.*, 1991, **0**, 398–400.

164 A. Guijarro, D. J. Ramon and M. Yus, *Tetrahedron*, 1993, **49**, 469–482.

165 A. Bachki, F. Foubelo and M. Yus, *Tetrahedron Lett.*, 1994, **35**, 7643–7646.

166 A. Bachki, F. Foubelo and M. Yus, *Tetrahedron*, 1997, **53**, 4921–4934.

167 M. Yus, C. Gomez and P. Candela, *Tetrahedron Lett.*, 2001, **42**, 3977–3979.

168 N. A. Cortese and R. F. Heck, *J. Org. Chem.*, 1977, **42**, 3491–3494.

169 A. Ramanathan and L. S. Jimenez, *Synthesis*, 2010, **2**, 217–220.

170 G. Chelucci, S. Baldino and A. Ruiu, *J. Org. Chem.*, 2012, **77**, 9921–9925.

171 J. P. Djukic, P. Geysermans, F. Rose-munch and E. Rose, *Tetrahedron Lett.*, 1991, **32**, 6703–6704.

172 J.-P. Djukic, F. Rose-Munch, E. Rose, F. Simon and Y. Dromzee, *Organometallics*, 1995, **14**, 2027–2038.

173 A. Dewanji, C. Mück-Lichtenfeld and A. Studer, *Angew. Chem., Int. Ed.*, 2016, **55**, 6749–6752.

174 K. Matyjaszewski, *Macromolecules*, 1998, **31**, 4710–4717.

175 M. Sawamoto and M. Kamigaito, *J. Macromol. Sci. - Pure Appl. Chem.*, 1997, **34**, 1803–1814.

176 Y. Watanabe, H. Ishigaki, H. Okada and S. Suyama, *Polym. J.*, 1997, **29**, 366–369.

177 T. P. Gill and K. R. Mann, *Organometallics*, 1982, **1**, 485–488.

178 W. Liu and F. Hou, *Tetrahedron*, 2017, **73**, 931–937.

179 G. R. Fulmer, A. J. M. Miller, N. H. Sherden, H. E. Gottlieb, A. Nudelman, B. M. Stoltz, J. E. Bercaw and K. I. Goldberg, *Organometallics*, 2010, **29**, 2176–2179.

180 T. Krüger, K. Vorndran and T. Linker, *Chem. Eur. J.*, 2009, **15**, 12082–12091.

181 Z. Hu, Z. Dong, J. Liu, W. Liu and X. Zhu, *J. Chem. Res.*, 2005, 252–253.

182 C. Tao, L. Sun, B. Wang, Z. Liu, Y. Zhai, X. Zhang, D. Shi and W. Liu, *Tetrahedron Lett.*, 2017, **58**, 305–308.

183 S. Seo, J. B. Taylor and M. F. Greaney, *Chem. Commun.*, 2012, **48**, 8270.

184 X. Y. Wang, J. Leng, S. M. Wang, A. M. Asiri, H. M. Marwani and H. L. Qin, *Tetrahedron Lett.*, 2017, **58**, 2340–2343.

185 M. C. Haibach, B. M. Stoltz and R. H. Grubbs, *Angew. Chem., Int. Ed.*, 2017, **56**, 15123–15126.

186 S. Das, P. Natarajan and B. König, *Chem. Eur. J.*, 2017, **23**, 18161–18165.

187 B. Li, L. Gao, F. Bian and W. Yu, *Tetrahedron Lett.*, 2013, **54**, 1063–1066.

188 J. T. Reeves, D. R. Fandrick, Z. Tan, J. J. Song, S. Rodriguez, B. Qu, S. Kim, O. Niemeier, Z. Li, D. Byrne, S. Campbell, A. Chitroda, P. Decroos, T. Fachinger, V. Fuchs, N. C. Gonnella, N. Grinberg, N. Haddad, B. Jäger, H. Lee, J. C. Lorenz, S. Ma, B. A. Narayanan, L. J. Nummy, A. Premasiri, F. Roschangar, M. Sarvestani, S. Shen, E. Spinelli, X. Sun, R. J. Varsolona, N. Yee, M. Brenner and C. H. Senanayake, *J. Org. Chem.*, 2013, **78**, 3616–3635.

189 A. Bagno, *Chem. Eur. J.*, 2001, **7**, 1652–1661.

190 J. E. Loemker, J. M. Read, Jr. and J. H. Goldstein, *J. Phys. Chem.*, 1968, **72**, 991–997.

191 G. Shi, D. Chen, H. Jiang, Y. Zhang and Y. Zhang, *Org. Lett.*, 2016, **18**, 2958–2961.

192 D. P. Curran and M. J. Totleben, *J. Am. Chem. Soc.*, 1992, **114**, 6050–6058.

193 H. X. Zheng, X. H. Shan, J. P. Qu and Y. B. Kang, *Org. Lett.*, 2017, **19**, 5114–5117.

194 R. Ting, L. Lermer and D. M. Perrin, *J. Am. Chem. Soc.*, 2004, **126**, 12720–12721.

195 M. J. G. Lesley, A. Woodward, N. J. Taylor, T. B. Marder, I. Cazenobe, I. Ledoux, J. Zyss, A. Thornton, D. W. Bruce and A. K. Kakkar, *Chem. Mater.*, 1998, **10**, 1355–1365.

196 A. C. Spivey, A. Maddaford, D. P. Leese and A. J. Redgrave, *J. Chem. Soc. Perkin Trans. 1*, 2001, 1785–1794.

197 K. S. Bejoymohandas, A. Kumar, S. Varughese, E. Varathan, V. Subramanian and M. L. P. Reddy, *J. Mater. Chem. C*, 2015, **3**, 7405–7420.